LOSS OF INVERSIN CONTRIBUTES TO RENAL CYSTIC DISEASE THROUGH ALTERED CELLULAR PROCESSES AND DECREASED SODIUM TRANSPORT IN RENAL EPITHELIAL CELLS

by

Nalini H. Kulkarni

A Dissertation

Submitted to the Faculty of Purdue University

In Partial Fulfillment of the Requirements for the degree of

Doctor of Philosophy

Department of Biological Sciences

Indianapolis, Indiana

May 2017

THE PURDUE UNIVERSITY GRADUATE SCHOOL
STATEMENT OF DISSERTATION APPROVAL

Dr. Bonnie L. Blazer-Yost, Chair
Department of Biological Sciences
Dr. Cynthia V. Stauffacher
Department of Biological Sciences
Dr. Rosamund C. Smith
Department of Biological Sciences
Dr. Simon J Atkinson
Department of Biological Sciences
Dr. Nicolas F. Berbari
Department of Biological Sciences

Approved by:
Dr. Stephen K. Randall
Head of the Departmental Graduate Program

Dedication

This dissertation is dedicated to all the people in my life who have been a positive force for guidance and support during this entire process. I would like to thank my parents Hanumantha Rao and Sunanda Bai for all that they have done for me over my lifetime. You have been a constant source unconditional love and support. Thanks to my Uncle Late Narayana Kulkarni for his constant encouragement and faith in me. Most importantly, thanks to my husband, Prahalad for his love and endless support. I am very thankful for your patience and care. I want to thank my two beautiful children, Neha and Keshav for making my everyday an absolute joy.

ACKNOWLEDGMENTS

At the outset, I extend my heartfelt thanks to my mentor and committee chair, Dr. Bonnie Blazer-Yost for giving me the opportunity to work in her laboratory, providing guidance and constructive feedback during the course of this investigation. I express my sincere gratitude to my committee member Dr. Rosamund Smith for her constant encouragement, guidance and support over the years. Thanks to my committee member Dr. Cynthia Stauffacher for her valuable time and patience. I also thank my other committee members Dr. Simon Atkinson and Dr. Nicolas Berbari for their time and suggestions. I would like to thank Dr. Tao Wei for providing bioinformatics assistance and helpful discussions. My thanks to Dr. Amy Usborne for providing histology support. Finally, I would like to thank the Lilly Graduate Research Advanced Degrees program for funding, time and support.

TABLE OF CONTENTS

LIST OF TABLES

LIST OF FIGURES

ABSTRACT

Author: Kulkarni, Nalini, H. Ph.D.
Institution: Purdue University
Degree Received: May 2017
Title: Loss of Inversin Contributes to Renal Cystic Disease through Altered Cellular Processes and Decreased Sodium Transport in Renal Epithelial Cells
Major Professor: Bonnie L. Blazer-Yost

Type II nephronophthisis (NPHP2) is an autosomal recessive renal cystic disorder characterized by mutations in the inversin gene. Humans and mice with mutations in inversin have enlarged cystic kidneys. Increased kidney size in NPHP2 may involve altered cell growth, apoptosis, electrolyte transport and fluid accumulation in the cysts. To test this hypothesis, histology and transcriptome analysis were performed on one-day old wild-type and *inv/inv* mice to uncover molecular pathways altered in the mutant mice. Histology of *inv/inv* mice kidneys showed dilated cystic tubules compared to wild type. Pathway analysis of transcriptome data showed that inversin exerts its effects on kidneys, at least in part, through the transcriptional regulation of genes implicated in inflammation, immune response, cellular metabolism, cell cycle and ion transport. Genes involved in inflammation or immune response were upregulated whereas the genes involved in cell cycle progression and ion transport were downregulated. To validate the array findings from *inv/inv* mice kidneys, functional consequence of inversin loss on transepithelial ion transport was measured by electrophysiological techniques in shRNA mediated inversin-depleted renal cell type isolated from mouse cortical collecting duct (mCCD). Depletion of inversin decreased vasopressin-induced Na^+ absorption, but did not alter Cl^- secretion in mCCD cells. Addition of amiloride, a specific blocker of the

epithelial sodium channel (ENaC), abolished basal ion transport in both inversin knockdown and control cells indicating ENaC involvement. Loss of inversin decreased Na^+ absorption and this effect, in part, was mediated by transcriptional and post-translational regulation of ENaC mediators. To better understand inversin function in renal cells, transcriptome analysis was performed in control and inversin-depleted mCCD cells. Pathway analysis showed that inversin-depletion altered the genes represented in cell cycle, cellular assembly and organization, DNA replication, cell proliferation and ion transport in this isolated renal cell type. In concordance with the array data from *inv/inv* mice kidneys, a decrease in the expression of cell cycle, ion transport and apoptotic genes were observed accompanied by an upregulation of genes implicated in inflammatory or immune response indicating a direct effect of inversin on renal cells. Together, this study utilized a combination of transcriptome and functional analyses to unravel the role of inversin in renal cells. These data demonstrate that loss of inversin can cause a delay in cell cycle progression with a decrease in cell proliferation and apoptosis which in turn can perturb the development of the renal tubule. Also, a decrease in Na^+ reabsorption together with differential regulation of other ion transporters can result in altered electrolyte transport contributing to cystogenesis, cyst growth, fluid accumulation and cyst expansion in NPHP2.

CHAPTER1: INTRODUCTION

An overview of renal cystic diseases

Renal cystic disease (RCD) represents a broad spectrum of diseases that share a common feature i.e., the development of multiple renal cysts. RCDs have multiple etiologies that include developmental, acquired, unilateral and inherited (Bisceglia et al, 2006). Developmental RCD exhibits multicystic dysplastic kidneys that are thought to arise from abnormal development of metanephros (Kalyoussef et al, 2006). In acquired RCD the development of renal cysts is usually in patients who are on dialysis for end stage renal disease and is a consequence of prolonged uremia (Choyke, 2000). Unilateral RCD is characterized by the development of multiple cysts with intervening normal parenchyma in one kidney, a benign entity which is not associated with malformation or cysts in other organs (Baradhi & Abuelo, 2012). The inherited forms of RCD can be broadly classified into autosomal dominant and recessive forms. The dominant forms include autosomal dominant polycystic kidney disease (type I and type II), medullary cystic kidney disease (type I and type II), von Hippel-lindau and tuberous sclerosis. Recessive forms of renal cystic disease include autosomal recessive polycystic kidney disease, Bardet-Biedl syndrome, Meckel-Gruber syndrome and nephronophthisis (Kim et al, 2016). Characteristics and inheritance pattern of different forms of renal cystic diseases are shown in Table 1.

Table 1: Types of inherited renal cystic diseases in humans

Disease*	**Chromosome**	**Gene**	**Protein**	**Frequency**
Autosomal dominant forms				
ADPKD type I	16p13.3	*PKD1*	Polycystin-1	1:1000[a]
ADPKD type II	4q22.1	*PKD2*	Polycystin-2	
MCKD type I	1q21	*MUC1*	Mucin	Rare[b]
MCKD type II	16p12.3	*UMOD*	Uromodulin	Rare[b]
TS1	9q34.13	*TSC1*	Hamartin	1:10,000[c]
TS2	16p13.3	*TSC2*	Tuberin	
VHL	3p25-26	*VHL*	pVHL	1:35,000[d]
Autosomal recessive forms				
ARPKD	6p12.2	*PKHD1*	Fibrocystin/ polyductin	1:20,000[e]
BBS	20 genes are associated with this phenotype			1:13,500 to 1:160, 000[f]
MKS	11 genes are associated with this phenotype			1:13,000 to 140,000[g]
Familial NPHP	16 genes are associated with this phenotype (see Table 2)			1:1 million[h]

*ADPKD, autosomal dominant polycystic kidney disease; MCKD, medullary cystic kidney disease; TS, tuberous sclerosis; VHL, von Hippel-Lindau; ARPKD, autosomal recessive polycystic kidney disease; BBS, Bardet-Biedl syndrome; MKS, Meckel-Gruber syndrome; NPHP familial nephronophthisis

[a](Torres et al, 2007)
[b](Hateboer et al, 2001)
[c](Bonsib, 2009)
[d](Lonser et al, 2003)
[e](Zerres et al, 1998)
[f](Iannello et al, 2002)
[g](Salonen & Norio, 1984)
[h](Hildebrandt et al, 2009; Potter et al, 1980)

Dominant forms of inherited renal cystic diseases

***Autosomal dominant polycystic kidney disease (ADPKD)*:** Autosomal dominant polycystic kidney disease is the most common monogenic disorder in the human population (Torres et al, 2007). ADPKD is characterized by the progressive bilateral development of fluid-filled cysts derived from renal tubular epithelial cells (Chang & Ong, 2008; Torres et al, 2007). Nearly 50% of patients with ADPKD reach end stage renal failure by 60 years of age (Bardet, 1995; Harris & Torres, 2009; Ravine et al, 1992). ADPKD is caused by mutations in two genes; *PKD1* located on chromosome 16p13.3 accounts for up to 85-90% of the cases and *PKD2* located on chromosome 4q22 accounts for 10-15% of the cases (Peters & Breuning, 2001). A small number of patients exhibit ADPKD with mutations at a loci distinct from *PKD1* or *PKD2* suggesting a yet unidentified gene (Ariza et al, 1997; Daoust et al, 1995; Turco et al, 1996). *PKD1* and *PKD2* encode polycystin (PC-1and PC-2) proteins.

PC-1 is a large membrane-bound >600 kDa glycoprotein (Hughes et al, 1995). PC-2 is a 110 kD membrane protein with 6 membrane-spanning domains with both N- and the C-termini in the cytosol (Mochizuki et al, 1996). PC-1 localizes to the epithelial cells of the distal nephron and vascular endothelial cells in fetal nephrons and normal adult kidney, ductal epithelia of liver and pancreas and in smooth muscle cells (Geng et al, 1997; Geng et al, 1996; Ibraghimov-Beskrovnaya et al, 1997; Ward et al, 1996). The subcellular localization of PC-1 includes endoplasmic reticulum, plasma membrane, and membranes of the primary cilium (Boletta et al, 2001; Newby et al, 2002). PC-2 is expressed in cell membrane, pre-medial golgi and endoplasmic reticulum membranes and to the primary cilium (Cai et al, 1999; Koulen et al, 2002; Li et al, 2005; Luo et al, 2003;

Nauli et al, 2003; Yoder et al, 2002). PC-1 has multiple binding partners and links the extracellular environment to the intracellular cytoskeleton (Retailleau & Duprat, 2014). PC-2 is a non-selective cation, Ca^{++} permeable channel that interacts with PC-1 (Hanaoka et al, 2000; Mochizuki et al, 1996; Newby et al, 2002). The PC-1/PC-2 complex is thought to participate in calcium-mediated signaling. The cystic cells have been shown to have lower intracellular Ca^{++} that can affect multiple cellular processes contributing to cyst growth and expansion in ADPKD.

Medullary cystic kidney disease (MCKD): Two distinct types of autosomal dominant MCKD have been reported in humans. MCKD type I caused by mutations in *MUC1* gene localized to chromosome 1q21 that encodes mucin1 (Fuchshuber et al, 2001; Kirby et al, 2013). MCKD type II is caused by mutations in *UMOD* gene located on chromosome 16p12 that encodes uromodulin/Tamm-Horsfall mucoprotein (Hateboer et al, 2001). MCKD type I has a later onset of end stage renal failure at a median of age 62, whereas MCKD type II has an early onset at a median age 32 (Hildebrandt & Otto, 2000). MCKD is characterized by normal or shrunken kidneys and the cysts are restricted to renal medulla (Gardner, 1971; Goldman et al, 1966). Renal histology shows tubular basement membrane disruption due to thickening and attenuation, distal tubular atrophy, tubulointerstitial infiltration and cyst development (Hildebrandt & Otto, 2000).

Tuberous sclerosis (TS): TS is an autosomal-dominantly inherited systemic malformation syndrome (Bonsib, 2009). Mutations in tumor-suppressor genes, *TSC1* and *TSC2* mapped to chromosome 9q34 and 16p13 respectively, encode hamartin and tuberin

have been linked to this syndrome (van Slegtenhorst et al, 1997; Wienecke et al, 1995). TS is characterized by proliferative lesions in multiple organs, including kidneys. Approximately 50% of TS patients exhibit renal cysts and neoplasms (Kim et al, 2016). In 5% of TS2 patients, cystic kidneys are identical to ADPKD and this is referred to as contiguous gene syndrome which is a result of dual mutations of *TSC2* and *PKD1* genes which are in close proximity to each other on chromosome 16.

von Hippel-Lindau (VHL) syndrome: VHL, inherited as an autosomal dominant trait is linked to a mutation in VHL gene located on chromosome 3p25-26 (Latif et al, 1993; Lonser et al, 2003; Seizinger et al, 1988). Loss of the VHL gene causes uncontrolled cell growth, neoplastic transformation and neoangiogenesis resulting in a multisystem preneoplastic disorder. People with VHL syndrome commonly develop cysts in the kidneys, pancreas and genital tract. Renal cysts are present in approximately 75% of the VHL patients (Truong et al, 2003). VHL protein is also localized to the primary cilium analogous to other cystoproteins (Esteban et al, 2006; Lutz & Burk, 2006).

Recessive forms of inherited polycystic kidney disease

Autosomal recessive polycystic kidney disease (ARPKD): ARPKD often causes fetal or neonatal death due to bilateral enlargement of kidneys and is linked to *PKHD1* gene mapped to chromosome 6p (Zerres et al, 1994; Zerres et al, 1998). The disease is characterized by expansion and elongation of collecting ducts into multiple cysts (Adeva et al, 2006). The *PKHD1* gene encodes fibrocystin/polyductin which plays a role in terminal differentiation of collecting duct and biliary systems (Onuchic et al, 2002; Ward

et al, 2002). Fibrocystin is a 447-kD membrane-associated receptor-like protein, expressed abundantly in fetal-kidney collecting ducts but is absent in the kidneys of ARPKD patients. The protein has putative extracellular-matrix interacting domains and intracellular signaling sites (Ward et al, 2002). Similar to other proteins implicated in renal cystic diseases, fibrocystin localizes to the primary cilium of renal epithelial cells (Menezes et al, 2004).

Bardet-Biedl syndrome (BBS): BBS is one of the rare autosomal recessive disorders that are characterized by heterogenous clinical manifestations including renal abnormalities (Bardet, 1995). Renal anamolies in BBS patients are comprised of cystic tubules resulting in polyuria, polydipsia and anemia. Urine concentration defects are the major cause of morbidity and mortality in these patients (Putoux et al, 2012). This disease has been mapped to twenty genes and all of them are involved in primary cilia function and disruption in any of the genes leads to cilia impairment (Khan et al, 2016).

Meckel-Gruber syndrome (MKS): MKS is a lethal autosomal recessive disorder that shows extensive heterogeneity. Mutations in 16 genes have been shown to be causative of MKS in humans (Barker et al, 2014). The disease is characterized by bilateral renal dysplasia and cyst formation, among others (Chen, 2007). MKS1 protein has been shown to localize to the ciliary transition zone and overlap with protein complexes of other ciliary proteins implicated in Joubert syndrome and nephronophthisis (Hildebrandt & Zhou, 2007; Sang et al, 2011). MKS proteins are also found in the ciliary

membrane (Barker et al, 2014) and cells from patients with mutations in MKS genes exhibit ciliogenenesis defects (Dawe et al, 2009; Valente et al, 2010).

Nephronophthisis (NPHP): NPHP is a group of autosomal recessive kidney disorders characterized by chronic tubulointerstitial nephritis that progresses to end stage renal disease in the first three decades of life (Fanconi et al, 1951; Hildebrandt & Zhou, 2007). The prevalence of NPHP is approximately 5% of all children with end stage renal disease (Warady et al, 1997). In NPHP, renal cysts emerge at the corticomedullary junctions characterized by tubular basement membrane anomalies, tubular atrophy and interstitial fibrosis (Waldherr et al, 1982; Zollinger et al, 1980). In addition to cystic kidneys, some cases present extra-renal symptoms such as, cerebellar ataxia, congenital eye disease, polydactyly and skull abnormality. These symptoms show overlap with other ciliopathies such as, Joubert, Senior-Lokun and Meckel-Gruber syndromes and with *situs inversus* in the case of type II nephronophthisis or NPHP2 (Baala et al, 2007). Positional cloning and candidate gene approaches together with high throughput mutational analysis have led to the identification of 16 causative genes responsible for manifestation of NPHP as shown in Table 2 (Halbritter et al, 2013; Salomon et al, 2009). Three clinical variants of NPHP have been described depending on the onset of end stage renal failure; infantile, juvenile and adolescent forms (Hildebrandt & Zhou, 2007).

The current research is focused on NPHP2, the infantile form of NPHP. Interestingly, NPHP2 is different from other forms of NPHP wherein the kidneys are enlarged and it has overlapping features with ADPKD, the predominant form of renal cystic disease (Table 3). Much of the understanding of cyst growth and expansion come

from studies carried out on ADPKD. In ADPKD patients and in murine models of ADPKD, increased cell proliferation, apoptosis, electrolyte secretion and fluid accumulation in kidneys have been well documented (Ebihara et al, 1995; Gattone et al, 2002; Lee et al, 2004; Nakamura et al, 1993). The mechanism for cyst growth and expansion in NPHP2 remain unknown.

Table 2: Genetic heterogeneity and overlap of NPHP, Senior-Loken, Joubert and Meckel-Gruber syndrome

Gene	**Chromosome**	**Locus/Protein**	**Clinical manifestations***
NPHP1	2q13	*NPHP1* (nephrocystin-1)	Juvenile NPHP, (mild JBTS, mild RP
INVS	9q31	*NPHP2* (inversin)	Infantile NPHP, (RP, liver fibrosis, HT)
NPHP3	3q22	*NPHP3* (nephrocystin-3)	Juvenile NPH (liver fibrosis, RP)
NPHP4	1p36	*NPHP4* (nephroretinin)	Juvenile NPHP, RP
IQCB1	3q21	*NPHP5*/IQ containing B1	Juvenile NPHP + severe RP
CEP290	12q21	*NPHP6*/centrosomal protein 290 kDa	Juvenile NPHP + JBTS + severe RP
GLIS2	16p	*NPHP7*/GLIS family zinc finger 2	Juvenile NPHP
RGRIP1L	16q	*NPHP8*/RPGRIP1-like	Juvenile NPHP + JBTS (MKS)
NEK8	17q11	*NPHP9*/nima-related kinase 8	Juvenile and infantile NPHP
SDCCAG8	1q43	*NPHP10/serologically defined colon cancer antigen 8*	Juvenile and adolescent NPHP, RD, PCO, HM
TMEM67	8q24	*NPHP11/meckelin*	All forms of NPHP, JBTS, MKS, VSD, RD
TTC21B	2q24	*NPHP12/tetratricopeptiderepe at domain 21B*	Juvenile and infantile NPHP, HT, LF, chondrodysplasia
WDR19	4p14	*NPHP13/WD repeat domain 19*	Juvenile and infantile NPHP, hepatic cysts, RD, PD
ZNF423	16q12	*NPHP14/zinc finger protein 14*	NPHP and JBTS
CEP164	11q23	*NPHP15/centrosomal protein 164*	NPHP
ANKS6	9q22	*ANKS6/ankyrin repeat and sterile alpha motif domain containing 6*	NPHP

*****NPHP, nephronophthisis; JBTS, Joubert syndrome type B; RP, Retinitis Pigmentosa; MKS, Meckel-Gruber syndrome; HT, hypertension; PD, polydactyly; RD, retinal dystrophy; PCO, polycystic ovaries; HM, hepatomegaly; VSD, ventricular septal defect; LF, liver fibrosis

Table 3: Kidneys in NPHP2 have overlapping features with NPH and ADPKD

Features	**Other forms of NPHP***	**NPHP2***	**ADPKD***
Inheritance	autosomal recessive	autosomal recessive	autosomal dominant
Renal phenotype	cystic	cystic	cystic
Kidney size	small	enlarged	enlarged
Disease progression	rapid-slow	rapid	slow
Kidney function decline	renal failure	renal failure	renal failure
Cyst origin	cortico-medullary junction	any tubular segment	any tubular segment
Cyst growth	increased apoptosis	apoptosis and/cell proliferation ?	increased cell proliferation and apoptosis
Cyst expansion (fluid accumulation)	mechanism unknown	mechanism unknown	increased Cl^- secretion and water movement into the lumen

*ADPKD, autosomal dominant polycystic kidney disease; NPHP, nephronophthisis; NPHP2, type II NPHP

Type II nephronophthisis (NPHP2)

Clinical features, mapping and molecular genetics of NPHP2: Gagnadoux et al., in 1989 described the observations made in 7 children who presented with severe renal failure and acidosis associated with hypertension in the first months of life. A renal biopsy in all the patients showed similar features characterized by diffuse chronic tubulointerstitial nephritis and the presence of microcystic dilatation of proximal tubules and Bowman's space. Progression of the renal disease was extremely rapid and all patients reached end-stage renal failure before the age of 2 years (Gagnadoux et al, 1989).

Subsequently, a novel type of infantile nephronophthisis, later to be called NPHP2, was identified in an extended Bedouin family from Israel (Haider et al, 1998). The pedigree pattern was distinctly that of autosomal recessive inheritance with hyperechogenic kidneys, renal insufficiency, hypertension and hyperkalemia. Affected individuals showed rapid deterioration of kidney function, leading to end stage renal failure within 3 years. Histopathology of renal tissues showed variable findings, ranging from infantile polycystic kidneys to chronic tubulointerstitial nephritis, fibrosis and cortical microcysts. Linkage analysis excluded the familial juvenile nephronophthisis locus NPHP1 on 2q13 and the autosomal recessive polycystic kidney disease locus *PKHD1* on 6p21.1-p12. A homozygosity mapping strategy was employed to search for the locus causing NPHP2 and the disorder was mapped to chromosome 9q22-31 (Haider et al, 1998).

Inversin (*INVS*) located on chromosome 9q31 was identified as the gene mutated in NPHP2 with and without *situs inversus* in affected individuals (Otto et al, 2003).

Human NPHP2 gene (INVS) and mutations: The human *INVS* gene spans over 150 kb and is organized into 16 exons. There are 7 potential splice variants (Genbank, Ensemble). The full length cDNA is 3.65 kb and encodes a protein containing 1065 amino acids. Nine distinct mutations in the *INVS* gene were detected in these patients, seven of which were truncating including four non-sense and three frameshift mutations. Two of the mutations were missense mutations resulting in non-conservative exchanges of amino acids. In addition to renal cysts some of the patients had hypertension and cardiac ventricular septal defect (Otto et al, 2003). Recently, additional nonsense mutations in the *INVS* gene have been reported in two severely affected fetuses (Oud et al, 2014). Pathological examination showed enlarged cystic kidneys, liver fibrosis, oligohydraminos (deficiency of amniotic fluid) and skeletal abnormalities in the affected fetuses.

Animal models of NPHP2

Loss of inversin has been shown to recapitulate NPHP2 phenotype in Zebrafish, *Xenopus, Drosophila* and mouse animal models (Feiguin et al, 2001; Lienkamp et al, 2010; Otto et al, 2003; Yokoyama et al, 1993). The homozygous *inv/inv* mouse that carries an insertional mutation in inversin (*Invs*) gene was first discovered for its role during mammalian embryonic development. The homozygous *inv/inv* mice exhibit a complex phenotype including, reversal of left-right polarity (*situs inversus*) and significant kidney pathology with dilated tubules and abnormal glomeruli and usually die within a week of birth (Yokoyama et al, 1993). Subsequently it was shown that the mutated *Invs* gene in *inv/inv* mice is partially deleted between exons 4-12 (Morgan et al, 1998). Transgenic insertion of inversin rescued the mutant *inv* phenotype, both the *situs*

inversus and kidney pathology demonstrating that *Invs* is the causal gene in the *inv/inv* mutant mice (Mochizuki et al, 1998). Consequently, it was shown that the renal cysts of *inv/inv* mice resemble NPHP2 which is caused by mutations in *INVS* gene in humans (Phillips et al, 2004). An increase in kidney size and weight, expansion of Bowman's capsule, cysts in the collecting ducts, and a diffuse cortical and medullary region with cysts are seen in *inv/inv* mice (Phillips et al, 2004). In Zebrafish, loss of inversin resulted in development of pronephric cysts (Otto et al, 2003). Inversin knockdown, when targeted to pronephros analgen in *Xenopus*, affects the differentiation of pronephros (Lienkamp et al, 2010).

Mouse inversin

Gene structure and domain architecture: Mouse *Invs* is located on chromosome 4, spans over 150 kb and has 17 exons. The full length cDNA is 5.5 kb and encodes 1062 amino acids. The N-terminal half of the protein contains 16 ankyrin repeat regions of approximately 33 amino acids which are involved in protein-protein interactions. The C-terminal region contains "infected cell polypeptide 4" (ICP4) domain flanked by two calmodulin binding IQ domains, two destruction boxes (D-box 1 and D-box 2) and CtBP (C-terminal binding site). The C-terminus contains a ninein-homology domain required for ciliary targeting as shown in Figure 1 (Lienkamp et al, 2012; Shiba et al, 2009). The N-terminal domain of mouse and human inversin are highly conserved whereas the C-terminal end is poorly conserved. In the N-terminal region, the amino acids 1-557 are 96% and amino acids 558-604 are 100% conserved. In contrast, the C-terminal domain corresponding to amino acids 605-1062 is only 62% conserved between mouse and human inversin (Morgan et al, 2002b).

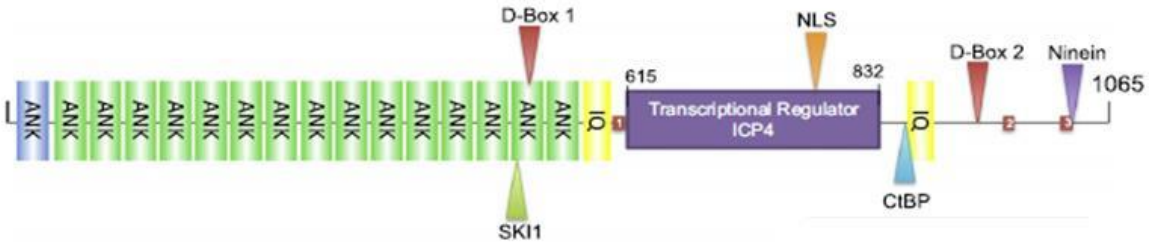

Figure 1: Domain architecture of mouse inversin. N-terminal half of inversin contains 16 ankyrin repeat domains, destruction box (D-box1), SKI1 (subtilisin/kexin isozyme-1) and C-terminal half contains ICP4 domain (transcriptional regulator, immediate early, infected cell polypeptide 4, activator and repressor of transcription), two IQ domains (calmodulin-binding), NLS (nuclear localization signal), CtBP (C-terminal binding domain site), destruction Box (D-box 2) and ninein (ninein-homology domain required for ciliary targeting) (Lienkamp et al, 2012; Shiba et al, 2009).

Inversin expression and subcellular localization: Inversin is detected as early as the 2-cell stage mouse embryo (Eley L et al., 2004). It is expressed in 9+0 cilia of the node, renal tubules, pituitary gland, retina, liver, testis, and primary fibroblast cultures (Nurnberger et al, 2006). The expected size of mouse inversin is 117 kDa, but in 14.5 dpc mouse embryo, a 165 kDa inversin protein has been detected by immunoblot and that could be due to post-translational modifications. Inversin has been shown to localize to the primary cilia in confluent cultures of MDCK-II (Madin- Darby Canine Kidney) cells (Morgan et al, 2002a). Additional isoforms, 90, 116, 125 and 140 kDa of inversin have been identified; a membrane-associated 125 kDa protein that localizes to the cell-cell junctions and complexes with N-cadherin, 90- and 140 kDa proteins that localize to nuclear and perinuclear compartments. The 90 kDa nuclear inversin forms a complex with β-catenin (Nurnberger et al, 2002). The localization of inversin to the lateral cell membrane in polarized epithelial cells suggests a role for cell-cell signaling (Nurnberger et al, 2002).

Inversin interacting proteins: Inversin has been shown to interact with several proteins with varying function (Eley et al, 2004). The ankyrin repeat region and the lysine rich central domain spanning amino acids 558-604 of the inversin protein makes it amenable to interact with other proteins (Morgan et al, 2002b). Inversin has two destruction box (D-box) motifs shown to interact with anaphase promoting complex 2 (Apc2) suggesting its role in cell cycle (Morgan et al, 2002a). Expression of inversin is dynamic throughout the cell cycle; in prophase inversin is expressed in centrosomes, in metaphase and anaphase it is expressed in spindle poles and in telophase it is expressed in

midbody, a region where microtubules overlap (Morgan et al, 2002a) and inversin has been shown to modulate the cortical actin network during mitosis (Werner et al, 2013). Inversin also interacts with Aurora A, a cell cycle kinase that promotes ciliary disassembly thereby modulating cell cycle control and proliferation (Mergen et al, 2013). Recently, inversin has been shown to interact with Akt and phosphorylation of inversin by Akt is required for proper spindle orientation during cell division (Suizu et al, 2016). Inversin contains 2 IQ (IQ-1 and IQ-2) domains that interact with calmodulin (Morgan et al, 2002b; Yasuhiko et al, 2001). Studies by Yasuhiko et al, 2001 demonstrated that calmodulin binds to IQ2 domain in a calcium-dependent manner and is essential for inversin to randomize left-right asymmetry in *Xenopus*. In proximal tubular cells, inversin is associated with nephrocystin-1 and with components of microtubule cytoskeleton (Nurnberger et al, 2004).

Inversin in development

Establishment of left-right asymmetry: Inversin is detected as early as the 2-cell stage mouse embryo (Eley et al, 2004) and is a component of node monocilia (Watanabe et al, 2003). Formation of the node occurs by E6.5 and is important for the establishment of left-right asymmetry in the mouse (Mercola, 2003). A normal body axis and left-right asymmetry is established by a leftward flow of the extra-embryonic fluid at the ventral node (Nonaka et al, 1998). In NPHP2 and in *inv/inv* mice, inversin deficiency results in *situs inversus* indicating dysfunctional cilia (Otto et al, 2003; Tory et al, 2009). In *inv/inv* mice the nodal cilia are motile but produce weak, turbulent leftward nodal flow (Okada et al, 1999). The laterality defects in the embryos were corrected by an artificial leftward flow of fluid in the node indicating that inversin is essential for the generation of the

normal nodal flow (Watanabe et al, 2003). However, the molecular mechanisms that underlie the role of inversin in modulating the nodal flow are unknown.

Planar cell polarity in kidney development: Planar cell polarity (PCP) is the coordinated orientation of tissue cells in a direction that is orthogonal to the apical/basal axis (Carroll & Das, 2011). Cell proliferation within the epithelial cell population is crucial for lengthening the tubule structures during kidney morphogenesis such that the tubules are increased in length and not in diameter. This is accomplished by cell division and that occurs along the mitotic spindle within the plane or parallel to the proximal-distal axis of the epithelium known as oriented cell division (OCD). Renal epithelial cells have planar polarity i.e., the axis of elongation is vertical to the proximal-distal axis of the tubule and this directed cell movement is known as convergent extension (CE). One of the signaling pathways in the primary cilium that is required for the proper development of the kidneys and cell polarity is the highly conserved Wnt signaling pathway.

Wnt signaling is triggered by the interaction of specific Wnt ligands and frizzled receptors. Activation of canonical Wnt signaling results in β-catenin-dependent transcription of target genes. The non-canonical Wnt/planar cell polarity (Wnt/PCP) pathway is β-catenin-independent and is stimulated by Ca^{++} influx in response to the bending of cilia. Wnt/PCP maintains the tissue architecture by controlling cell migration and function. Both OCD and CE processes are regulated by Wnt/PCP signaling associated with primary cilia (Goggolidou, 2014). During development, the primary cilia sense flow upon the start of urine production and fluid flow has been shown to increase

the expression and altered localization of inversin protein in ciliated tubular epithelial cells which results in the inhibition of canonical Wnt signaling and activation of non-canonical Wnt signaling (Simons et al, 2005).

Wnt/PCP signaling is activated by ligands such as Wnt11 and Wnt9b essential for normal development of kidney (Majumdar et al, 2003). Attenuation of Wnt9b signaling or loss of Fat4, a PCP protein, results in abnormal polarity of renal epithelia, randomized orientation of cell division and abnormal elongation of renal tubules leading to renal cysts (Karner et al, 2009; Saburi et al, 2008). Activation of Wnt signaling via Wnt ligands and frizzled receptors results in the recruitment of the cytoplasmic protein, disheveled (Dvl) to the membrane. In *Xenopus*, loss of inversin prevents the recruitment of Dvl to the plasma membrane in response to frizzled 8 (a non-canonical Wnt receptor), indicating that inversin is required for this important step in the non-canonical Wnt signaling (Lienkamp et al, 2010). However, the precise mechanism by which inversin recruits Dvl to the plasma membrane is not known. Inversin has been shown to control dorsal to ventral but not the posterior to anterior cell migration in *Xenopus* pronephros (Lienkamp et al, 2010).

Inversin role in cilia of mature renal epithelial cells

Renal primary cilia are non-motile, microtubule-based sensory organelles required for the maintenance of normal kidney architecture. (Praetorius & Spring, 2001; Praetorius & Spring, 2003). These are hair-like structures that sense fluid flow across the renal epithelial surface. Flow-induced bending of the primary cilia leads to Ca^{++} influx via PC-2. This in turn can activate the Ca^{++}-induced Ca^{++} release via ryanodine receptors in the endoplasmic reticulum and thereby increasing intracellular Ca^{++} levels (Nauli et al,

2003). Intracellular Ca^{++} homeostasis and signaling is important for regulation of variety of cellular functions such as, cell proliferation and differentiation, volume regulation, ion and fluid transport. Inversin has been shown to localize to the 'Inv compartment', a distinctive region in the proximal segment of the ciliary shaft (Shiba et al, 2009). Other NPHP proteins, NPHP3 and Nek8 (product of NPHP9) require inversin for their localization to the 'Inv compartment' (Shiba et al, 2010). Primary cell cultures derived from normal and *inv/inv* mice did not show a significant change in the number and length of primary cilia (Shiba et al, 2005). Although studies suggest that inversin is not required for ciliogenesis *in vivo*, a decrease in ciliogenesis was reported in inversin-depleted canine kidney MDCK cells *in vitro* (Mergen et al, 2013). The localization of these proteins to primary cilia of renal epithelial cells supports the unifying theory of renal cystogenesis which states that "proteins which are mutated in renal cystic diseases in humans, mice or zebrafish are expressed in primary cilia, basal bodies or centrosomes" (Hildebrandt & Zhou, 2007). Two mutant proteins other than inversin, polycystin-2 and kinesin family member 3a (Kif3a) that perturb the left-right asymmetry also localize to cilia of the renal epithelial cells (Nonaka et al, 1998; Pennekamp et al, 2002). Thus the interaction and co-localization of inversin with NPHP-1 and β-tubulin to cilia and basal bodies provides a functional link between the pathogenesis of PKD, ciliary function and left-right axis asymmetry.

Mechanism of cyst growth and expansion

Renal cystic diseases are caused by mutations in several ciliary genes, including polycystin-1, -2, the nephrocystins, inversin, among others. It is plausible that there could be a common mechanism linking the various renal cystic diseases to ciliary

function. Studies done on ADPKD provide much of the understanding of development and growth of cysts. The development and growth of cysts in ADPKD involves the proliferation of epithelial cells, changes in the extracellular matrix and fluid accumulation within the cyst cavity (Murcia et al, 1999; Sullivan et al, 1998a; Sullivan et al, 1998b). Studies have shown that renal cyst expansion in ADPKD is driven by anion secretion (Davidow et al, 1996; Grantham et al, 1995; Hanaoka et al, 1996; Mangoo-Karim et al, 1995; Ye & Grantham, 1993). Several lines of evidence suggest that the cystic fibrosis transmembrane conductance regulator (CFTR) Cl^- channel plays a major role in the accumulation of fluid and electrolytes within the lumen of ADPKD cysts. First, immunocytochemical studies have demonstrated that CFTR is located in the apical membrane of ADPKD cysts (Brill et al, 1996). Second, Cl^- currents with properties and regulation identical to those of CFTR have been identified using whole-cell patch clamp technique in ADPKD epithelial cells (Hanaoka et al, 1996). Third, CFTR antisense oligonucleotides inhibited cAMP-stimulated fluid secretion by ADPKD epithelia (Davidow et al, 1996). Furthermore, inhibitor and electrophysiological studies have shown that CFTR is one of the major Cl^- channels responsible for fluid accumulation and renal cyst growth (Li et al, 2004).

One of the common occurrences in late stage disease of ADPKD is the increased leakage of fluid from the cysts that has the ability to stimulate additional secretory activity in remaining renal epithelial cells. Lysophosphatidic acid has been identified as one of the active component in the ADPKD cyst fluid that stimulates Cl^- secretion via CFTR in mouse principal cortical collecting duct cells (Blazer-Yost et al, 2011). Taken

together, these studies suggest that Cl^- transport by CFTR is one of the key mechanisms that drive fluid accumulation in ADPKD cysts.

Other electrolyte transporters may also play roles in the fluid accumulation. For example, a decrease in epithelial sodium channel activity has been demonstrated in the principal cells of the collecting duct from the *bpk* (BALB/c polycystic kidney) autosomal recessive PKD (ARPKD) mice (Veizis et al, 2004) as well as in the cystic epithelium of PCK rats, an orthologous model of ARPKD with mutations in *PKHD1* gene (Pavlov et al, 2015). Overall, these studies suggest that ion transport is altered in both ADPKD and ARPKD, the dominant and recessive forms of polycystic kidney diseases.

Research presentation and summary

Type II nephronophthisis (NPHP2) is a renal cystic disorder that occurs in infants and progresses rapidly leading to end stage renal disease by 2-5 years of age. It is caused by mutations in the *Inversin* (*INVS)* gene that encodes inversin protein. NPHP2 has overlapping features with PKD and other forms of NPH (Table 3). In human PKD and in murine models of PKD the mechanism of cyst growth and expansion is relatively well understood compared to NPHP2. A better understanding of the role of inversin in renal function may provide insights into the mechanism of cyst growth and expansion in NPHP2. The goal of this research was to uncover the molecular mechanisms through which inversin exerts its effect on kidneys. The underlying hypothesis for this thesis work is that loss of inversin may lead to altered cell proliferation or apoptosis and fluid accumulation resulting in development and expansion of renal cysts leading to renal failure. In an effort to address this hypothesis, transcriptome analysis was initially

performed to uncover the molecular pathways that are affected in the kidneys of inversin knockout mice.

Chapter 2 describes the transcriptome analysis performed in the kidneys obtained from wild-type and *inv/inv* mice to delineate the mechanisms or pathways that are altered in the mutant mice. Gene array analysis showed that inversin exerts its effect on kidneys, at least in part through transcriptional regulation of genes involved in inflammation or immune response, cellular metabolism, cell cycle, apoptosis and ion transport.

Chapter 3 describes the functional consequences of inversin depletion on transepithelial ion transport in renal epithelial cells to validate the array findings from *inv/inv* mice kidneys. Studies from both human and animal models of NPHP2 mutant alleles suggest a key role of inversin in early development, especially the renal system. The increased kidney size in NPHP2 could be due to fluid accumulation within the cyst cavity. One mechanism by which inversin could exert its effect on renal function is by affecting electrolyte transport. Inversin siRNA and shRNA were used to generate inversin knockdown in a mouse renal epithelial cell line with the characteristics of the principal cell type of the mouse cortical collecting duct (mCCD) cells. Electrophysiological techniques along with stimulators and inhibitors of specific ions (Cl^- and Na^+) were employed to investigate ion transport in control and inversin knockdown cells. Interestingly, inversin knockdown in mCCD cells decreased Na^+ transport but did not alter Cl^- transport as compared to control cells. These results suggest that inversin may play a role in Na^+ reabsorption and its loss could lead to fluid accumulation contributing to the enlarged kidneys in NPHP2.

Chapter 4 describes the *in vitro* array findings in inversin-depleted versus control mCCD cells. Some of the key molecular and cellular functions that were affected upon inversin loss include cell cycle, cellular assembly and organization, DNA replication, recombination and repair, cellular development, cell growth and proliferation and ion transport. The control of organ size in multicellular organisms is mediated by the balance between cell proliferation, differentiation and apoptosis. In concordance with the *in vivo* array data from *inv/inv* mice kidneys, a decrease in the expression of cell cycle and apoptotic genes were also seen in the *in vitro* array data from inversin-depleted mCCD cells. The cyst formation in NPHP2 may involve altered proliferation and or apoptosis of epithelial cells. Cell proliferation was evaluated in inversin-depleted and control cells. Loss of inversin decreased cell number as function of time in renal epithelial cells indicating a decreased cell proliferation that might affect kidney development. Also, caspase 3/7 activity, a measure of apoptosis was also decreased as a function of time in inversin-depleted renal epithelial cells.

Additionally, the gene array data from inversin-depleted renal epithelial cells *in vitro* was compared with the array data from *inv/inv* mice cystic kidneys. The kidney is a complex organ comprised of multiple cell types and, in addition, circulating cells also infiltrate the renal tissue. Since *inv/inv* mice is a global knockout model of inversin loss, the gene expression changes observed in *inv/inv* kidneys alone could be a direct effect of inversin on kidney cells per se or an indirect effect of infiltrating cells, or a combination of both. The common gene expression changes observed *in vitro* in isolated renal cells that are recapitulated *in vivo* may provide insights into the direct effect of inversin loss in renal epithelial cells. Interestingly, genes that were common between *in vitro* and *in vivo*

data sets represented apoptotic, ion transport, cell cycle, inflammatory pathways suggesting that these mechanisms may be a direct effect of inversin loss contributing to cyst growth and expansion in *inv/inv* kidneys.

In summary, current research helped to further understand the role of inversin in renal epithelial cells. There are several factors that contribute to cyst growth and expansion in NPHP2. Loss of inversin may cause a delay in cell cycle progression and decrease apoptosis that can lead to perturbation in renal tubular geometry and may contribute to increased kidney size in NPHP2. In addition, a decrease in Na^+ reabsorption together with differential regulation of other transporters can result in altered ion transport. Also, activation of immune or inflammatory pathways may drive disease progression contributing to cystogenesis, cyst growth, fluid accumulation and cyst expansion in NPHP2.

CHAPTER 2: TRANSCRIPTOME ANALYSIS OF *inv/inv* MICE KIDNEYS

Introduction

The *inv/inv* mouse which carries an insertional mutation in inversin (*Invs*) gene was first discovered for its role during mammalian embryonic development (Yokoyama et al, 1993). The mice exhibit a complex phenotype including, reversal of left-right polarity (*situs inversus*) and significant kidney pathology and typically die within a week of life (Yokoyama et al, 1993). An increase in kidney size and weight, expansion of Bowman's capsule, cysts in the collecting ducts, a diffuse cortical and medullary region with cysts are seen in *inv/inv* mice. The renal cysts of *inv/inv* mice resemble NPHP2 which is caused by mutations in *INVS* gene in humans (Haider et al, 1998; Phillips et al, 2004).

Defects in primary cilia cause a broad class of human genetic diseases called "ciliopathies" (Okada et al, 1999). Mutations in ciliary proteins, including polycystin-1, -2, and nephrocystins cause renal cystic diseases (Kim et al, 2016). NPHP2 is different from other forms of NPH, because the kidney size is enlarged similar to polycystic kidney disease (PKD). In PKD patients and in murine models of PKD, increased cell proliferation, apoptosis, electrolyte secretion and fluid accumulation in kidneys have been reported (Ebihara et al, 1995; Gattone et al, 2002; Husson et al, 2004; Lee et al, 2004; Nakamura et al, 1993). However, the mechanism of renal cyst growth and expansion in NPHP2 is not well understood.

To better understand the molecular pathways through which loss of inversin affects the kidneys in *inv/inv* mice, transcriptome analyses was performed to determine gene expression changes in wild-type and *inv/inv* kidneys in one-day old mice. Previously, gene expression analysis of mouse embryonic fibroblasts from *inv/inv* mice demonstrated that inversin may play a role in fibroblast polarity and cell migration (Veland et al, 2013). To date global gene expression changes in the *inv/inv* mice kidneys have not been reported. The inversin protein contains various functional domains (Lienkamp et al, 2012) that may be involved in several cellular processes (Chapter 1, Figure 1). A study of gene expression changes may help in elucidating the mechanisms/pathways involved in enlarged cystic kidneys in *inv/inv* mice which may involve altered cell growth, apoptosis, electrolyte transport and fluid accumulation in the cysts.

Materials and methods

***Animals*:** Lack of pigmentation in albino control mice (+/+) allowed for phenotypic distinction between homozygotes (*inv/inv*) with *situs inversus* and heterozygotes (*inv*/+) with intact left-right asymmetry (Mochizuki et al, 1998; Morgan et al, 1998; Phillips et al, 2004). The inversin mouse model listed above was backcrossed onto the Balb/c background to form a unique animal model where the heterozygotes can be determined by their "dirty white" coats. Newborn homozygous animals are identified as having *situs inversus* where the milk sacs that can be identified in newborns have an opposite orientation. Kidneys from *inv/inv* and wild-type littermates were harvested from newborn mice at postpartum day 1 and flash frozen in liquid nitrogen and stored at -80^{o}C until further use. At the time of organ harvest, the phenotype of the homozygous (*inv/inv*) animals was confirmed by the notably enlarged size of the kidneys compared to wild-type littermates. Rodent use and procedures conformed to the NIH guidelines and all animal experiments were approved by the Animal Care Committee of Indiana University-Purdue University, Indianapolis (IUPUI). The Animal Care Division, School of Science, IUPUI, is a fully accredited AALAC facility.

***Histology*:** Kidneys from one-day old wild-ype and *inv/inv* mice were collected and fixed in 10% neutral buffered formalin. Histological analysis was performed using hematoxylin-eosin staining of 4μm kidney sections followed by pathogenic evaluation under light microscope.

***Total RNA isolation and real-time PCR*:** Total RNA from each sample (kidneys from wild-type and *inv/inv* mice) was isolated using RNeasy® mini kit isolation kit from Qiagen (Qiagen, Valencia, CA, USA) according to manufacturer's protocol. Briefly, the samples were homogenized in lysis buffer and the lysate was passed 5 times through a blunt 20-guage needle fitted to an RNase-free syringe. One volume of 70% ethanol was added to the sample and applied to RNeasy spin column. The samples were centrifuged and the flow-through was discarded. DNase treatment of the samples was performed using the RNase-free DNase reagent from Qiagen (Qiagen, Valencia, CA. USA) and the samples were eluted in RNase-free water. RNA quality and quantity was examined by Agilent 2100 Bioanalyzer (Agilent Technologies, Inc. Santa Clara, CA, USA) according to manufacturer's instructions. First strand cDNA was synthesized from 1µg of total RNA with random hexamer primers using the SUPERSCRIPT II first strand synthesis kit (Invitrogen). cDNA was used at a dilution of 1:50 and quantitative real-time PCR was performed using ABI Prism Sequence Detection System 5700 (Applied Biosystems). Fluorogenic primer/probe sets to detect mRNA encoding inversin and 18S RNA were obtained from Applied Biosystems as Assays on Demand^{TM} reagents (Table 4). The mRNA levels of inversin (Mm00495002_m1), were normalized to 18S ribosomal RNA that served as an internal control.

***Microarray experiments*:** Total RNA was subjected to microarray gene expression analysis. The RNA samples were processed by Asuragen Inc (Asuragen TX, USA) using Mouse Gene 230 2.0 arrays according to the company's procedures. All arrays that met the minimal recommended quality parameters as described in the

Affymetrix Data Analysis Fundamentals Guide (P/N 701190) were used for analyses. Expression signal was obtained from CEL files using MAS5 algorithm in the Affymetrix GCOS software.

***Bioinformatics and statistical analysis*:** Sequential steps were taken to identify differentially expressed genes (DEGs). First, the median signal of the entire dataset was applied as a threshold to identify genes 'Present' in comparing different groups in the study. Second, the fold changes of each 'Present' gene were computed from estimated median of comparing groups obtained in the first step. Genes with absolute fold changes equal or larger than 1.45 were kept for testing of statistical significance performed in the third step using a t-test implemented in R multtest (Resampling-based multiple hypothesis testing) package. False discovery rate (FDR) of each gene was estimated using Benjamini & Hochberg method implemented in multtest R package (Pollard et al, 2005).

The DEGs were defined as those genes with a *p*-value < 0.05 and FDR < 0.05. Principal component analysis (PCA) was performed using TIBCO Spotfire (TIBCO Spotfire, Boston, http://spotfire.tibco.com/). Enrichment analyses of Gene Ontology (GO), KEGG and Ingenuity® Pathway Analysis (IPA®, QIAGEN Redwood City, www.qiagen.com/ingenuity) were performed on the DEGs using the right tailed Fisher's exact test.

Table 4: List of primer-probe sets for validation of array findings by real-time quantitative PCR

Gene Symbol	**Gene Name**	**Primer probe set**
Invs	Inversin	Mm00495002_m1
Immune/inflammatory		
Il34	interleukin 34	Mm01243248_m1
Ccl9	chemokine (C-C motif) ligand 9	Mm00441262_g1
Tnfrsf12a	tumor necrosis factor receptor superfamily, member 12a	Mm01302476_g1
Il6ra	interleukin 6 receptor alpha	Mm00439653_m1
Osmr	oncostatin M receptor	Mm01307326_m1
C1qa	complement component 1, q subcomponent, alpha polypeptide	Mm00432142_m1
Arg2	arginase 2	Mm00477592_m1
Mrc1	mannose receptor, C type 1	Mm01329362_m1
Sphk1	sphingosine kinase 1	Mm00448841_g1
Cebpb	CCAAT/enhancer binding protein (C/EBP), beta	Mm00843434_S1
Cebpd	CCAAT/enhancer binding protein (C/EBP), delta	Mm00786711_S1
Nfil3	nuclear factor, interleukin 3	Mm00600292_S1
Junb	Jun-B oncogene	Mm04243546_S1
Cell cycle		
Anapc1	anaphase promoting complex subunit 1	Mm01336123_m1
Ccnd2	cyclin D2	Mm00438070_m1
Ccne1	cyclin E1	Mm01266311_m1
Cdkn1a	cyclin-dependent kinase inhibitor 1A (P21)	Mm00432448_m1
Skp2	S-phase kinase-associated protein 2 (p45)	Mm00449925_m1
Trp53	transformation related protein 53	Mm01731287_m1
Gadd45b	growth arrest and DNA-damage-inducible 45 beta	Mm00435123_m1
Gadd45g	growth arrest and DNA-damage-inducible 45 gamma	Mm01352550_g1
Ion transport		
Bdkrb2	bradykinin receptor, beta 2	Mm00437788_S1
Dbp	D site albumin promoter binding protein	Mm00439560_m1
Edn1	endothelin 1	Mm00438656_m1
Entpd1	ectonucleoside triphosphate diphosphohydrolase 1	Mm00515447_m1
Igf1	insulin-like growth factor 1	Mm00439560_m1

***Statistics*:** Data are represented as mean ± SD. Differences between two groups were analyzed by an unpaired Student's *t*-test. Differences were considered significant when $P<0.05$. Line or bar graphs were generated using Microsoft Excel or Sigma Plot 11.0 software.

Results

***Histology and inversin expression levels*:** As shown in Figure 2A histological assessment showed cystic changes in 1-day old kidneys of *inv/inv* mice compared to wild-type littermates consistent with a previous report (Phillips et al, 2004). The expression level of inversin as determined by quantitative PCR was absent in the kidneys of *inv/inv* mice compared to wild type controls in 1-day old mice (Figure 2B). The RNA from wild type controls and *inv/inv* mice kidneys was subjected to transcriptome analysis.

***Gene expression profiles of wild type and inv/inv mice kidneys*:** To gain insights into the mechanisms of cyst growth and expansion in *inv/inv* mice, transcriptome analysis was performed on 1-day old kidneys from *inv/inv* mice and wild-type littermates, n=5/group. Mouse genome 430 2.0 array comprises of 45,101 probe sets corresponding to over 39,000 transcripts which in turn represent 20,670 genes. A summary of the gene signal data, detection calls and gene annotations for every gene on the chip was generated using Affymetrix MAS 5.0 algorithm (GCOS, v1.3). Of the 20,670 genes present on the array, 10,572 (51%) genes were detected in the kidney samples from wild-type and *inv/inv* mouse kidneys.

***Identification of differentially expressed genes (DEGs)*:** For gene classifications and functional *in silico* analyses, the probe sets with low-grade annotations were eliminated to enable analysis of data sets with reliable annotations. The DEGs were

identified as significant if the comparisons of wild-type and *inv/inv* gene expression met the criteria of (a) $p<0.05$, (b) the median signal for all the chips in either group was larger

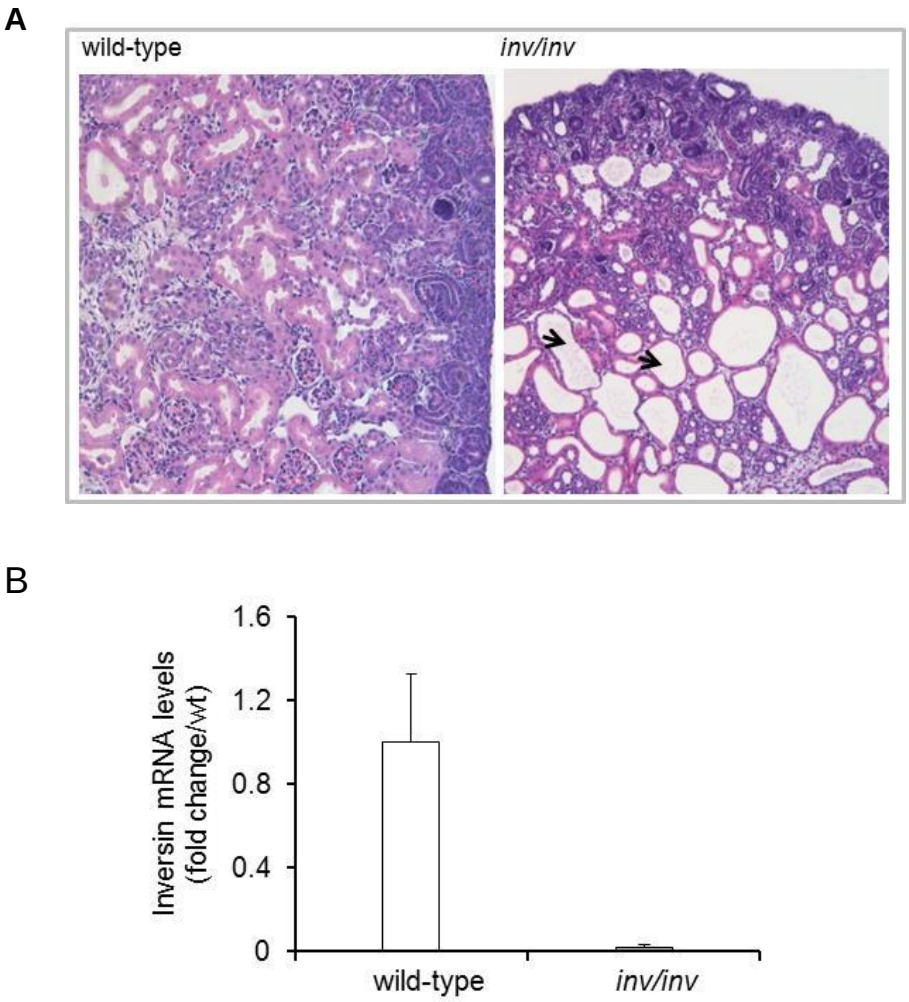

Figure 2: Histology and inversin mRNA levels in kidneys from one-day old wild-type and *inv/inv* mice. (**A**) Hematoxylin and eosin stained 4µM sections of kidneys at 10x magnification. Cystic tubules are seen in *inv/inv* mice kidneys (indicated in black arrow) (**B**) Inversin mRNA levels in wild-type and *inv/inv* mice kidneys. Total RNA was isolated from wild-type and *inv/inv* mice kidneys and the inversin mRNA levels were assessed by quantitative real- time PCR. The data was normalized to 18S RNA and expressed as fold change over wild-type littermates. Values are mean ± SD (n=5).

than 250, and (c) an absolute fold change ≥ 1.45. Of 10,572 genes expressed in kidneys, 733 genes (6.9%) were differentially expressed in *inv/inv* mice. Unannotated genes were further removed from 733 DEGs that resulting in overall 646 annotated DEGs in *inv/inv* mice kidneys. Out of 646 annotated DEGs, 274 genes were upregulated and 372 genes were downregulated in *inv/inv* mice compared to wild-type controls (Appendix, Table 31, upregulated genes; Table 32 downregulated genes). Figure 3 shows the heat map of the hierarchial clustering analysis of the DEGs in *inv/inv* mice compared to wild-type controls.

Functional classification of DEGs: To ascertain common molecular functions, DEGs were classified into the categories of the GO (Gene Ontology) terms such as, Biological Process (BP), Cellular Component (CC) and Molecular Function (MF) using DAVID (the database for annotation, visualization and integrated discovery) bioinformatics tool (Huang da et al, 2009a; Huang da et al, 2009b) and Ingenuity Pathway Analysis (IPA®). Table 5 shows the significantly enriched GO-BP categories of DEGs identified by Fisher's exact test ($P < 0.05$). As shown in Figure 4, the various biological processes identified development, macromolecule biosynthetic process, metabolic process, sterol/cholesterol transport, catabolism and biosynthetic process (carboxylic acid, amino acid, nucleotides, glycoprotein), regulation of cell death/apoptosis, cellular metabolism, protein modification (phosphorylation, ubiquitination), kinase signaling, immune response, response to wounding, acute inflammatory response, cytoskeleton organization, regulation of transcription, cellular homeostasis such as ion homeostasis and regulation of blood pressure. Thus, GO-BP

classification suggests that loss of inversin has an effect on various biological processes that may be involved in cyst formation, growth and expansion. Involvement of some of these processes such as, cell growth and differentiation, immune response, apoptosis and ion homeostasis have also been reported in ADPKD (Song et al, 2009) indicating a potential common mechanism in cyst growth and expansion between NPHP2 and PKD.

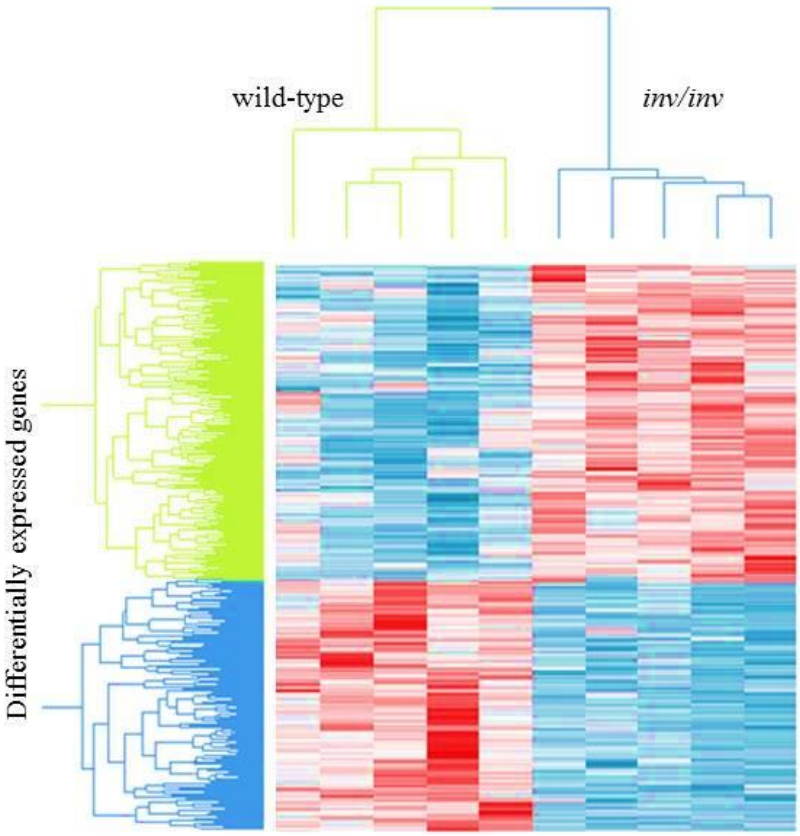

Figure 3: Heat map of hierarchial clustering analysis of 646 differentially expressed genes. Hierarchial clustering was based on genes differentiating the two groups wild-type and *inv/inv* kidneys at a significance levels of $p<0.05$, an absolute fold change ≥ 1.45 and the median signal intensity of 250. The red color indicates genes that are upregulated (274) and the light blue color indicates genes that are downregulated (372) in *inv/inv* mice kidneys compared to controls. Each column represents an individual kidney sample and each row represents a gene. The heat map is condensed and all genes are not represented in the figure. One branch of the dendrogram contained all the wild-type samples (indicated in green) and the other branch contained *inv/inv* kidney samples indicated in dark blue).

Table 5: GO biological process terms considered significantly enriched for the genes regulated in *inv/inv* mice kidneys compared to wild-type[a]

GO Level	**Count**	***P*-value**
Development		
in utero embryonic development	23	1.94E-04
embryonic development ending in birth or egg hatching	28	2.26E-03
chordate embryonic development	27	3.96E-03
blood vessel development	18	5.81E-03
vasculature development	18	7.35E-03
blood vessel morphogenesis	15	1.03E-02
embryonic organ development	15	4.60E-02
placenta development	8	3.34E-02
embryonic placenta development	7	1.99E-02
Cellular metabolism		
carboxylic acid catabolic process	11	5.29E-04
organic acid catabolic process	11	5.29E-04
cellular amino acid catabolic process	9	5.54E-04
phosphagen metabolic process	3	2.31E-02
glycoprotein metabolic process	11	3.48E-02
regulation of phosphate metabolic process	18	3.77E-02
regulation of phosphorus metabolic process	18	3.77E-02
positive regulation of macromolecule metabolic process	35	9.29E-03
amine catabolic process	9	1.92E-03
Inflammatory/immune response		
response to wounding	25	1.28E-03
acute inflammatory response	9	7.52E-03
wound healing	10	1.72E-02
inflammatory response	16	1.35E-02
acute inflammatory response	9	7.52E-03
adaptive immune response	9	9.31E-03
Transport		
transmembrane transport	26	2.09E-02
ion transport	35	4.31E-02
Circulation		
blood circulation	10	1.63E-02
circulatory system process	10	1.63E-02
Blood pressure		
regulation of blood pressure	7	2.64E-02
Apoptosis		
negative regulation of apoptosis	18	4.73E-03
negative regulation of programmed cell death	18	5.81E-03
negative regulation of cell death	18	6.05E-03
regulation of apoptosis	31	1.25E-02

Table 5 continued

regulation of cell death	31	1.58E-02
Protein modification		
protein modification by small protein conjugation	9	6.48E-03
protein ubiquitination	8	8.29E-03
protein polyubiquitination	4	2.04E-02
protein modification by small protein conjugation or removal	9	3.01E-02
biopolymer glycosylation	8	4.11E-02
protein amino acid glycosylation	8	4.11E-02
Glycosylation	8	4.11E-02
Biosynthetic process		
phosphagen biosynthetic process	3	3.62E-03
cellular amino acid biosynthetic process	6	1.85E-02
carboxylic acid biosynthetic process	11	2.72E-02
organic acid biosynthetic process	11	2.72E-02
positive regulation of cellular biosynthetic process	31	1.22E-02
positive regulation of macromolecule biosynthetic process	29	2.13E-02
positive regulation of biosynthetic process	32	7.94E-03
RNA biosynthetic process	10	3.37E-02
NAD biosynthetic process	3	3.00E-02
nitrogen compound biosynthetic process	23	1.05E-03
nucleotide biosynthetic process	12	4.37E-02
amine biosynthetic process	8	1.41E-02
Molecular function		
negative regulation of molecular function	15	2.26E-04
negative regulation of kinase activity	9	3.72E-04
negative regulation of protein kinase activity	9	3.72E-04
negative regulation of transferase activity	9	4.87E-04
negative regulation of catalytic activity	12	8.33E-04
regulation of phosphorylation	18	2.78E-02
inactivation of MAPK activity	3	3.00E-02
regulation of protein kinase activity	13	3.17E-02
regulation of kinase activity	13	3.90E-02
regulation of transferase activity	13	4.89E-02
Cell Organization		
positive regulation of cell-substrate adhesion	5	1.40E-02
positive regulation of cellular component organization	10	2.82E-02
Cell growth		
regulation of cell growth	8	4.32E-02
transcription from RNA polymerase II promoter	7	4.56E-02

[a]Genes significantly regulated were classified by GO biological process terms (GO level FAT) using DAVID 2010 online software. GO terms with values of $P<0.05$ (Fisher's exact test) are presented. Count represents the number of genes involved in each GO term.

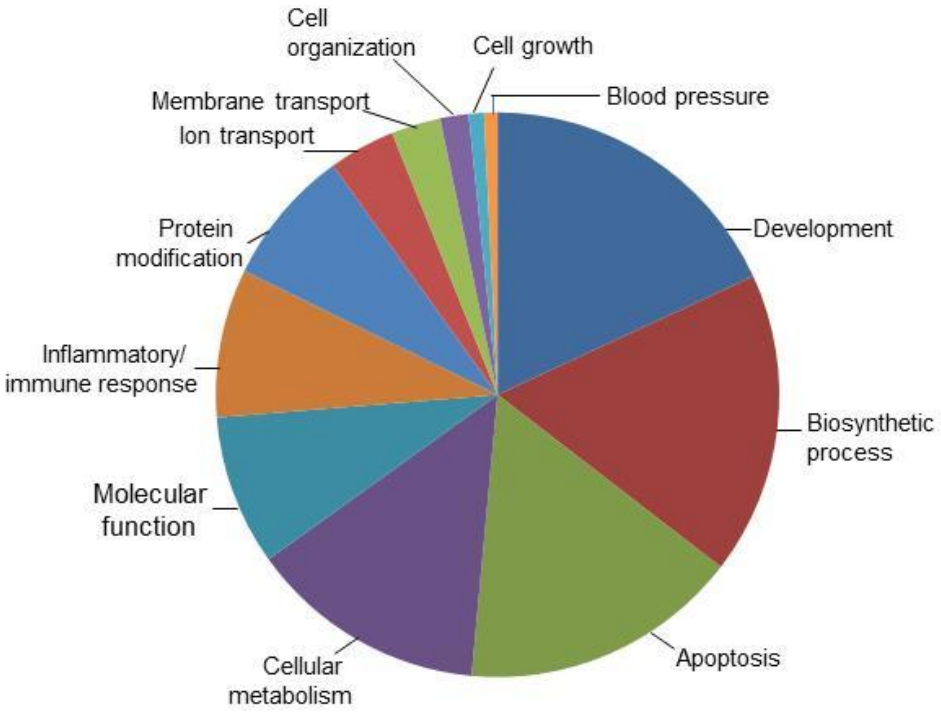

Figure 4: Overrepresented GO biological processes altered in *inv/inv* kidneys. Fisher's exact test was used to identify significant enrichment for pathway annotations. Pie chart showing the number of genes representing different categories altered in *inv/inv* mice kidneys compared to wild-type controls.

Table 6 shows the DEGs from *inv/inv* mice kidneys that were subjected to GO cellular component (CC) to obtain information about sub-cellular localization. The DEGs classified into the categories of cell-cell junction, plasma membrane, cytoplasm and interstitial matrix. These results suggest that loss of inversin may influence the expression of genes localized to various regions of the cell as well as in the interstitial matrix and hence may affect cell-cell communication and membrane integrity consistent with its localization to the cell-cell junction (Nurnberger et al, 2002) .

Finally, the DEGs from *inv/inv* mice kidneys were classified into the categories of GO molecular function (MF) (Table 7). The various categories in molecular functions that were significantly altered include, binding (cofactor, coenzyme, vitamin B6, nucleotide, nucleoside, ATP, polysachharide, glycosaminoglycan) and activity (MAP kinase, protein kinase inhibitor, tyrosine/serine/threonine phosphatase, sodium symporter, cyclin-dependent kinase regulator). These results indicate that loss of inversin may affect various molecular functions affecting ion transport, cell cycle progression, cell proliferation and apoptosis. The DEGs were further subjected to molecular and functional analysis in IPA®. The key functional categories altered were cellular development, cell growth and proliferation, cell death and survival, cell cycle, molecular transport and signaling pathways involved in inflammation/immune response consistent with GO classification.

Table 6: GO cellular component terms considered significantly enriched for the genes regulated in *inv/inv* mice kidneys compared to wild-type[a]

GO level	**GO Term**	**Count**	***P* value**
GO-CC-ALL	interstitial matrix	4	1.04E-02
GO-CC-ALL	cytosol	29	1.87E-02
GO-CC-ALL	plasma membrane	117	2.17E-02
GO-CC-ALL	plasma membrane part	70	2.62E-02
GO-CC-ALL	cell junction	25	2.75E-02
GO-CC-ALL	cyclin-dependent protein kinase holoenzyme complex	3	3.46E-02
GO-CC-ALL	cytoplasm	255	5.71E-04
GO-CC-ALL	cytoplasmic part	159	4.47E-02
GO-CC-ALL	cell-cell junction	13	1.39E-02

[a]Genes significantly regulated were classified by GO cellular component (GO level ALL) using DAVID 2010 online software. GO terms with values of $P<0.05$ (Fisher's exact test) are presented. Count represents the number of genes involved in each GO term.

Table 7: GO molecular function terms considered significantly enriched for the genes regulated in *inv/inv* mice kidneys compared to wild-type[a]

GO Level	GO Term	Count	*P* value
GO-MF-FAT	cofactor binding	28	2.88E-08
GO-MF-FAT	coenzyme binding	18	5.03E-05
GO-MF-FAT	FAD binding	10	8.39E-04
GO-MF-FAT	vitamin binding	14	3.40E-04
GO-MF-FAT	vitamin B6 binding	9	5.66E-04
GO-MF-FAT	pyridoxal phosphate binding	9	5.66E-04
GO-MF-FAT	transferase activity,	6	4.91E-03
GO-MF-FAT	protein dimerization activity	24	2.21E-03
GO-MF-FAT	identical protein binding	19	1.46E-02
GO-MF-FAT	protein homodimerization activity	14	1.95E-02
GO-MF-FAT	MAP kinase phosphatase activity	4	7.58E-03
GO-MF-FAT	MAP kinase tyrosine/serine/threonine phosphatase activity	4	7.58E-03
GO-MF-FAT	protein tyrosine phosphatase activity	10	9.33E-03
GO-MF-FAT	tyrosine/serine/threonine phosphatase activity	6	1.03E-02
GO-MF-FAT	phosphoprotein phosphatase activity	11	4.30E-02
GO-MF-FAT	adenyl nucleotide binding	74	4.61E-03
GO-MF-FAT	purine nucleoside binding	74	5.77E-03
GO-MF-FAT	nucleoside binding	74	6.75E-03
GO-MF-FAT	nucleotide binding	96	1.47E-02
GO-MF-FAT	purine nucleotide binding	84	1.48E-02
GO-MF-FAT	ATP binding	64	4.32E-02
GO-MF-FAT	protein serine/threonine kinase inhibitor activity	4	3.13E-03
GO-MF-FAT	cyclin-dependent protein kinase regulator activity	4	1.45E-02
GO-MF-FAT	protein kinase regulator activity	7	1.74E-02
GO-MF-FAT	protein kinase inhibitor activity	4	3.19E-02
GO-MF-FAT	kinase inhibitor activity	4	4.09E-02
GO-MF-FAT	kinase regulator activity	7	4.37E-02
GO-MF-FAT	peptide receptor activity	9	4.07E-02
GO-MF-FAT	peptide receptor activity, G-protein coupled	9	4.07E-02
GO-MF-FAT	carboxylic acid binding	8	3.04E-02
GO-MF-FAT	amine binding	6	6.36E-02
GO-MF-FAT	organic acid:sodium symporter activity	4	4.09E-02
GO-MF-FAT	symporter activity	10	4.41E-02
GO-MF-FAT	polysaccharide binding	10	3.74E-02
GO-MF-FAT	pattern binding	10	3.74E-02
GO-MF-FAT	glycosaminoglycan binding	9	4.86E-02

[a]Genes significantly regulated were classified by GO molecular function terms (GO level FAT) using DAVID 2010 online software. GO terms with values of $P<0.05$ (Fisher's exact test) are presented. Count represents the number of genes involved in each GO term.

***Pathway Analysis of DEGs*:** To better understand the expression patterns of functionally related proteins, the genes altered in *inv/inv* mice kidneys were subjected to Ingenuity® Pathway Analysis (IPA®). As shown in Figure 5, the top canonical pathways that were affected in *inv/inv* kidneys included upregulation of Stat3 pathway, Il-6 and Il-9 signaling, acute phase response signaling, complement system, pancreatic adenocarcinoma signaling, NFκB signaling, cell cycle (G1/S checkpoint regulation), cell cycle regulation by BTG family of antiproliferative proteins, PTEN signaling and the coagulation system. These results suggest that loss of inversin may increase cytokine signaling, acute phase response due to inflammation and also affect cell cycle progression in *inv/inv* mice kidneys.

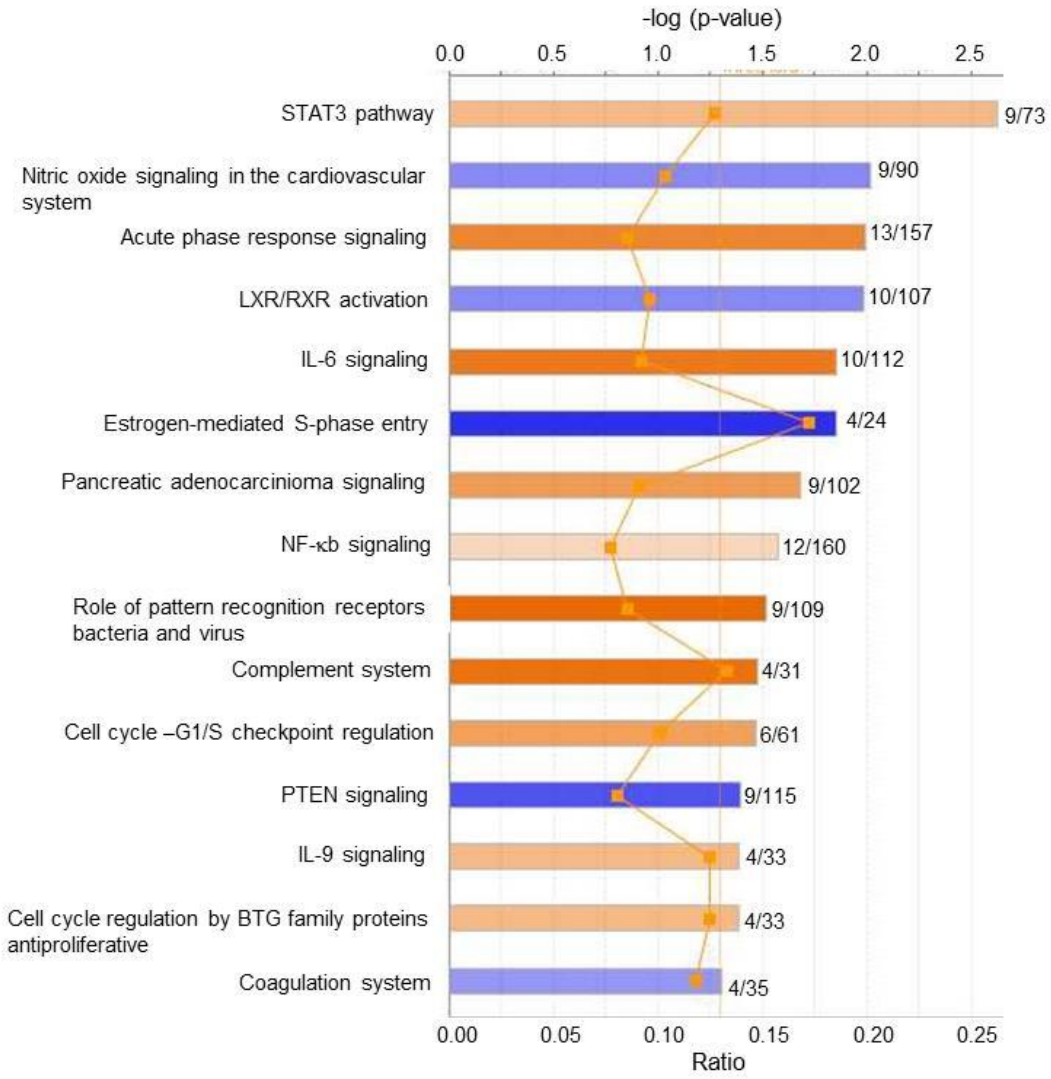

Figure 5: Canonical pathways altered in *inv/inv* mice kidneys analyzed using IPA®. The numbers to the right of each bar represents the ratio of genes regulated in *inv/inv* mice kidneys to the total number of genes implicated in the pathways indicated. The line graph that runs across each bar represents the threshold set for each pathway. Red indicates the pathways that are upregulated and blue indicates pathways that are downregulated.

***Activation of immune/inflammatory pathways in inv/inv mice kidneys*:** Several genes implicated in immune/inflammatory responses were upregulated in *inv/inv* mice kidneys compared to wild-type controls (Table 8) and validation of select genes in this category is shown in Figure 6. The upregulation of monocyte/macrophage chemoattractants, chemokine C-X-C motif like (Cxcl1) and chemokine C-C motif ligand (Ccl9) is consistent with recruitment of monocytes/macrophages to the affected *inv/inv* kidneys. CD163, a transmembrane protein exclusively expressed on macrophages (Akahori et al, 2015) was upregulated in *inv/inv* mice kidneys. Tumor necrosis factor receptor superfamily member, Tnfrsf12a/Tweak receptor that can be activated by TLR4-mediated innate immune response (Gonzalez-Guerrero et al, 2016) was also upregulated in *inv/inv* kidneys. Interestingly, among the overexpressed transcripts in *inv/inv* mice kidneys, were a subset of genes implicated in acute phase reactants such as Ambp (alphaI macroglobulin), SerpinE1 (serine peptidase inhibitor clade E), oncostatin M receptor (Osmr), interleukin receptor (Ilra). Also, the genes representing the complement system (complement component C1q1,-2, -3 and the receptor C5ar1) which links the innate and the adaptive immune pathways, and is also known to play a role in the activation of monocyte/macrophages, were upregulated in *inv/inv* mice kidneys. Additionally, transcription factors implicated in immune/inflammatory responses such as Jun-B oncogene (JunB), Cebpb (CCAAT/enhancer binding protein, beta), Cebpd (CCAAT/enhancer binding protein, delta), nuclear factor interleukin (Nfil3) and forkhead box P1 (Foxp1) were also upregulated in *inv/inv* kidneys.

Genes associated with JAK-STAT signaling pathway and its downstream targets such as Pim1, SOCS 3 and Spred2 were upregulated in the *inv/inv* mice kidneys (Table

8). Interestingly, Map4k3, an upstream regulator of Nfkb2 and Nfkbiz, induced by T cell antigen receptor was also upregulated in *inv/inv* mice kidneys. Certain upstream regulators of Osmr, the matricellular proteins, such as, connective tissue growth factor (Ctgf) and tenascin C (Tnc) and downstream signaling molecule Stat3 that can contribute to fibrosis were also upregulated in *inv/inv* kidneys suggesting that loss of inversin can result in fibrosis (Sarkozi et al, 2012; Sarkozi et al, 2011) via Ctgf/Osmr/Stat3 signaling. Additionally, the voltage-gated potassium channel Kcnc1/Kv1.3 expressed on T lymphocytes was also upregulated in *inv/inv* kidneys. K^+ channels are expressed on T lymphocytes and overexpression of Kcnc1 on lymphocytes can contribute to progression of chronic kidney disease by promoting interstitial fibrosis (Kazama, 2015). Hypoxia-inducible factor 3a (Hif3a) and its target Serpine1 and cysteine-rich protein 61 (Cyr61), an inducer of pro-inflammatory cytokines such as IL-6 were also upregulated in *inv/inv* mice kidneys. Overall, the observation of increased expression of immune/inflammatory genes in *inv/inv* kidneys is consistent with earlier reports in models of ARPKD (Mrug et al, 2008) and ADPKD (Karihaloo et al, 2011; Swenson-Fields et al, 2013) and could represent a common mechanism in cyst growth and expansion or tissue repair in these cystic disorders.

Table 8: Immune/inflammatory genes upregulated in *inv/inv* mice kidneys

Gene ID	Gene Symbol	Protein Name	Fold change (*inv*$^{-/-}$ /Wild-type)	*P*-value
Cytokine-receptor interaction				
76527	Il34	interleukin 34	1.5	7.00E-04
14825	Cxcl1	chemokine (C-X-C motif) ligand 1	1.7	1.00E-04
20308	Ccl9	chemokine (C-C motif) ligand 9	2.4	5.10E-03
16194	Il6ra	interleukin 6 receptor, alpha	2.6	0.00E+00
16177	Il1r1	interleukin 1 receptor, type I	1.7	7.80E-03
18414	Osmr	oncostatin M receptor	3.8	0.00E+00
252837	Ackr4	chemokine (C-C motif) receptor-like 1	1.6	5.80E-03
27279	Tnfrsf12a	tumor necrosis factor receptor superfamily 12a	2.3	9.00E-04
Complement System				
12259	C1qa	complement component 1q, alpha polypeptide	1.7	0.00E+00
12260	C1qb	complement component 1q, beta polypeptide	1.7	0.00E+00
12262	C1qc	complement component 1q, C chain	1.6	0.00E+00
12273	C5ar1	complement component 5a receptor 1	1.6	2.40E-03
Macrophage-associated markers/phagocytosis				
11847	Arg2	arginase type II	2.1	2.30E-03
93671	Cd163	CD163 antigen	2.2	7.00E-04
11303	Abca1	ATP-binding cassette, sub-family A (ABC1)	1.9	1.60E-03
13025	Ctla2b	cytotoxic T lymphocyte-associated protein 2 beta	1.6	4.30E-03
108664	Atp6v1h	ATPase, H+ transporting, lysosomal V1 subunit H	1.9	6.00E-04
14131	Fcgr3	Fc receptor, IgG, low affinity III	1.5	9.10E-03
17533	Mrc1	mannose receptor, C type 1	1.6	3.90E-03
20288	Msr1	macrophage scavenger receptor 1	1.6	5.70E-03
93671	Cd163	CD163 antigen	2.2	7.00E-04
Fcγr-mediated phagocytosis				
18806	Pld2	phospholipase D2	1.5	0.00E+00
20698	Sphk1	sphingosine kinase 1	1.9	0.00E+00
14131	Fcgr3	Fc receptor, IgG, low affinity III	1.5	9.10E-03

Table 8 continued

Acute phase response				
11699	Ambp	alpha 1 microglobulin/bikunin	2.4	1.02E-02
18787	Serpine1	serine (or cysteine) peptidase inhibitor, clade E, 1	5.9	0.00E+00
Transcription factors in immune/inflammatory response				
16477	Junb	Jun-B oncogene	2.1	0.00E+00
12609	Cebpd	CCAAT/enhancer binding protein (C/EBP), delta	2.9	1.30E-03
12608	Cebpb	CCAAT/enhancer binding protein (C/EBP), beta	2.6	0.00E+00
18030	Nfil3	nuclear factor, interleukin 3	1.6	4.10E-03
108655	Foxp1	forkhead box P1	1.5	1.70E-03
Jak/Stat and Nfkb signaling pathways				
13649	Egfr	epidermal growth factor receptor	1.7	2.00E-04
14254	Flt1	FMS-like tyrosine kinase 1	1.5	7.00E-04
18414	Osmr	oncostatin M receptor	3.8	0.00E+00
16337	Insr	insulin receptor	1.5	9.00E-04
338372	Map3k9	mitogen-activated protein kinase kinase kinase 9	1.6	3.00E-04
18712	Pim1	proviral integration site 1	2.1	1.00E-04
12702	Socs3	suppressor of cytokine signaling 3	2.0	0.00E+00
20848	Stat3	signal transducer and activator of transcription 3	2.0	0.00E+00
114716	Spred2	sprouty-related, EVH1 domain containing 2	2.0	3.20E-03
18034	Nfkb2	nuclear factor of kappa light polypeptide gene enhancer in B-cells 2, p49/p100	2.2	4.00E-04
80859	Nfkbiz	nuclear factor of kappa light polypeptide gene enhancer in B-cells inhibitor, zeta	1.9	0.00E+00
225028	Map4k3	mitogen-activated protein kinase kinase kinase kinase 3	1.6	8.00E-04
Fibrosis				
14219	Ctgf	connective tissue growth factor	2.8	0.00E+00
21923	Tnc	tenascin C	1.7	2.70E-03
14268	Fn1	fibronectin 1	1.5	5.00E-04
20361	Sema7a	semaphorin 7A	1.6	6.80E-03
16502	Kcnc1	potassium voltage gated channel, Shaw-related subfamily, member 1	2.2	4.50E-03
13653	Egr1	early growth response 1	2.0	0.00E+00
16007	Cyr61	cysteine rich protein 61	2.3	0.00E+00

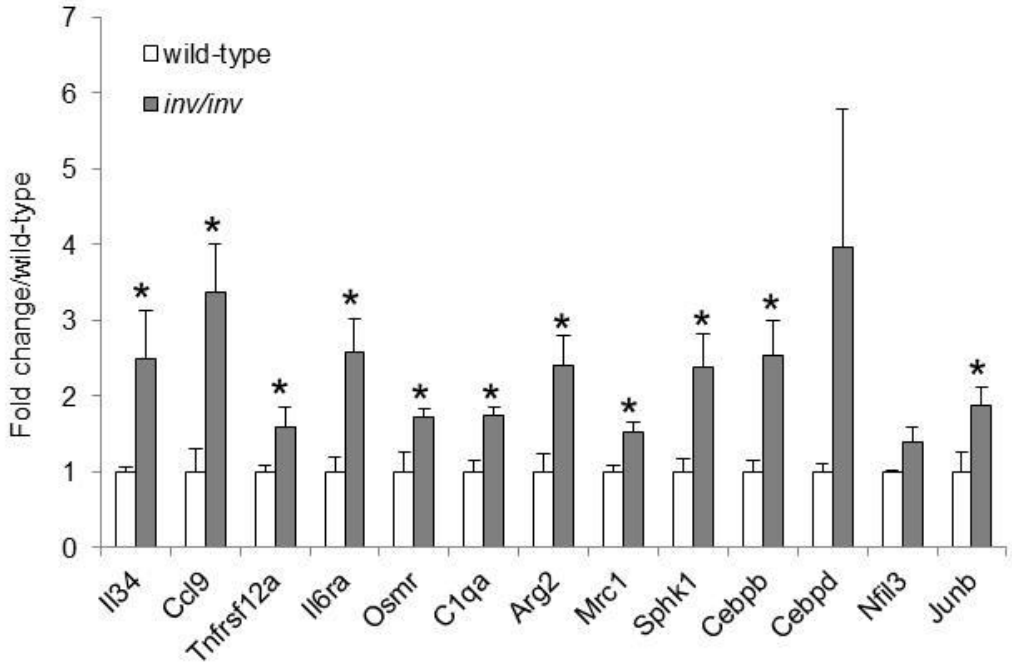

Figure 6: Validation of select immune/inflammatory genes from *in vivo* array analysis. Select genes from *in vivo* array analysis involved in inflammation/immune response were validated in one-day old wild-type and *inv/inv* mice kidneys. Total RNA was isolated and mRNA levels were assessed by quantitative real-time PCR. The data was normalized to 18S RNA and expressed as fold change over wild-type littermates. Values are mean ± SEM (n=5); *$p<0.05$ vs wild-type.

***Decreased expression of cell cycle genes in inv/inv mice kidneys*:** Some of the key cell cycle genes that were altered in *inv/inv* mice kidneys compared to the wild-type controls are shown in Table 9. Select genes implicated in cell cycle validated by real-time PCR are shown in Figure 7. Genes involved in interphase, and different stages of cell cycle (G0/G1, G1/S and G2/M phase) progression such as, anaphase promoting complex 1 (Anapc1), cyclin D2 (Ccnd2), cyclin E (Ccne1), S-phase kinase protein (Skp2) and transformation related protein (Trp53), cell cycle and neuronal differentiation (Cend1) were downregulated. Conversely, the negative regulators of cell cycle such as cyclin-dependent kinase inhibitor (Cdkn1a), growth arrest and DNA damage-inducible (Gadd45b) and Gadd45g were upregulated in *inv/inv* mice kidneys (Figure 7).

In addition, tubulin polyglutamylase complex subunit (Tpgs2) an enzyme involved in polyglutamylation of tubulin; gamma glutamylcyclotransferase (Ggct), in cell cycle arrest at G0/G1 phase (Lin et al, 2015); Bzw1 (Basic leucine zipper and 2 domains2), a conserved regulatory factor for transcription control of histone H4 gene at G1/S transition (Yu et al, 2006) were downregulated in *inv/inv* mice kidneys (Table 9). Zinc is an indispensable element vital for the functioning of several cellular processes like cell replication and growth (Pal et al, 2014). The decrease in Slc39a10, a zinc transporter (Zip-10) in *inv/inv* mice kidneys is in concordance with the decrease in various genes involved in cell cycle progression. Overall, these results suggest that loss of inversin affects several genes that can cause delay or arrest in cell cycle progression consistent with its expression during various stages of cell cycle in normal epithelial cells (Morgan et al, 2002a) and in turn can have an effect on cell proliferation.

***Decreased cell proliferation in inv/inv mice kidneys*:** Interestingly, several genes known to decrease cell proliferation were also altered in *inv/inv* mice kidneys. For example, the expression of B-cell translocation gene (Btg1), an anti-proliferative gene was upregulated in *inv/inv* mice kidneys. On the other hand, CDK-associated, cullin domain-1 (Calcul1) which inhibits cell proliferation by G1 cell cycle arrest (Zheng et al, 2013) was downregulated in *inv/inv* mice kidneys (Table 9). Acylglycerol kinase (Agk), a lipid kinase that phosphorylates substrates such as, diacylglycerol and ceramide (Waggoner et al, 2004) and also promotes cell proliferation (Wang et al, 2014b) was downregulated in *inv/inv* mice kidneys. Agk activity is inhibited by sphingosine and sphk (sphingosine kinase) that phosphorylates sphingosine was upregulated and may contribute to decreased proliferation in *inv/inv* mice kidneys. Csrnp1 (Axud1), a tumor suppressor gene induced by axin (a regulator of β-catenin) was upregulated in *inv/inv* mice kidneys. Together, these data suggest a decrease in the expression of cell cycle genes upon loss of inversin could affect or delay cell cycle progression that may result in decreased cell proliferation in *inv/inv* mice kidneys (Table 9).

Table 9: Regulation of genes affecting cell cycle progression and proliferation in *inv/inv* mice kidney

Gene ID	Gene Symbol	Protein Name	Fold change (*inv*$^{-/-}$ /wild-type)	*P*-value	Cell cycle phase
Delay in cell cycle progression					
235320	Zbtb16	zinc finger and BTB domain containing 16	7.7	2.30E-03	G1-S
23882	Gadd45g	growth arrest and DNA-damage-inducible 45 gamma	2.3	0.00E+00	S
17873	Gadd45b	growth arrest and DNA-damage-inducible 45 beta	1.9	3.00E-04	S
12575	Cdkn1a	cyclin-dependent kinase inhibitor 1A (P21)	1.6	7.90E-03	G1
14852	Gspt1	G1 to S phase transition 1	1.6	1.40E-03	G1-S
17222	Anapc	anaphase promoting complex subunit 1	1.7	0.00E+00	M
27401	Skp2	S-phase kinase-associated protein 2 (p45)	1.9	7.00E-04	G1
12444	Ccnd2	cyclin D2	1.5	1.10E-03	G1
12447	Ccne1	cyclin E1	1.5	8.50E-03	G1
22059	Trp53	transformation related protein 53	1.5	1.40E-03	S
209456	Trp53bp2	transformation related protein 53 binding protein 2	1.6	1.40E-03	S
110175	Ggct	gamma-glutamyl cyclotransferase	1.6	0.00E+00	G0-G1
66882	Bzw1	basic leucine zipper and W2 domains 1	1.5	3.10E-03	G1-S
227059	Slc39a10	solute carrier family 39 (Zinc transporter), 10	1.7	2.00E-03	
12567	Cdk4	cyclin-dependent kinase 4	1.5	4.30E-03	G1
66648	Tpgs2	tubulin polyglutamylase complex subunit 2	1.6	5.30E-03	
Decreased Cell proliferation					
215418	Csrnp1	cysteine-serine-rich nuclear protein 1	3.1	0.00E+00	
78832	Cacul1	CDK2 associated, cullin domain 1	-1.9	1.00E-04	
69923	Agk	acylglycerol kinase	-2.1	7.00E-04	
12226	Btg1	B-cell translocation gene 1, anti-proliferative	1.6	5.80E-03	
12227	Btg2	B-cell translocation gene 2, anti-proliferative	1.5	0.00E+00	

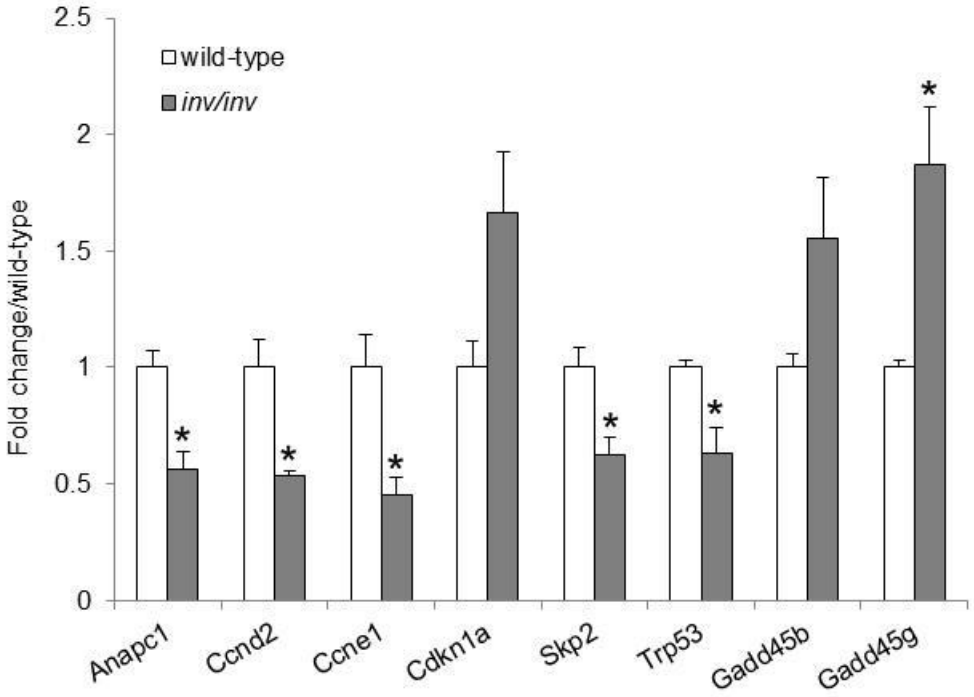

Figure 7: Validation of select cell cycle genes from *in vivo* array analysis. Select genes from *in vivo* array analysis involved in cell cycle progression were validated in one-day old wild-type and *inv/inv* mice kidneys. Total RNA was isolated and mRNA levels were assessed by quantitative real-time PCR. The data was normalized to 18S RNA and expressed as fold change over wild-type littermates. Values are mean ± SEM (n=5); *$p<0.05$ vs wild-type.

***Decrease in apoptosis and increase in cell survival gene expression in inv/inv mice kidneys*:** Control of organ size is mediated by the balance of cell proliferation, differentiation and apoptosis in multicellular organisms (Yang & Xu, 2011). Certain activators of apoptosis such as caspase (Casp3) were downregulated whereas the inhibitors of apoptosis such as baculoviral IAP-containing (Birc6), B-translocation gene (Btg-1), nicotinamide N-methyltransferase (Nnmt), serine incorporator (Serinc3), Fam129a/Niban were upegulated in *inv/inv* mice kidneys (Table 10). Kruppel-like (Klf) family of transcription factors such as, Klf-3, Klf-6 and Klf-9 implicated in cell survival/inhibition of apoptosis (Lebrun et al, 2013; Mallipattu et al, 2017) were upregulated in *inv/inv* mice (Table 10). Overall, these data suggest that loss of inversin may decrease apoptosis and increase cell survival in *inv/inv* kidneys.

Table 10: Regulation of genes representing a decrease in apoptosis and increase in cell survival in *inv/inv* mice kidneys

Gene ID	**Gene Symbol**	**Protein Name**	**Fold change (*inv*$^{-/-}$/wild-type)**	***P*-value**
Decrease in apoptosis				
2367	Casp3	caspase 3	1.6	4.90E-03
52864	Dusp15	dual specificity phosphatase-like 15	1.5	3.00E-04
2059	Trp53	transformation related protein 53	1.5	1.40E-03
8035	Nfkbia	nuclear factor of kappa light polypeptide gene enhancer in B-cells inhibitor, alpha	1.6	0.00E+00
2259	C1qa	complement component 1, q subcomponent, alpha polypeptide	1.7	0.00E+00
84783	Irs2	insulin receptor substrate 2	2.8	1.00E-04
2211	Birc6	baculoviral IAP repeat-containing 6	1.8	1.00E-04
2226	Btg1	B-cell translocation gene-1, anti-proliferative	1.6	5.80E-03
63913	Fam129a	family with sequence similarity 129, member A	3.0	2.60E-03
80890	Trim2	tripartite motif-containing 2	2.8	1.00E-04
8113	Nnmt	nicotinamide N-methyltransferase	2.2	3.80E-03
6943	Serinc3	serine incorporator 3	2.2	2.50E-03
4579	Gem	GTP binding protein (gene overexpressed in skeletal muscle)	2.3	8.50E-03
6305	Pitpnb	phosphatidylinositol transfer protein, beta	-1.5	2.80E-03
1789	Tfpi2	tissue factor pathway inhibitor 2	-1.6	1.40E-03
24454	Zdhhc14	zinc finger, DHHC domain containing 14	-1.7	1.70E-03
Increase in cell survival				
3849	Klf6	Kruppel-like factor 6	2.2	2.00E-04
6601	Klf9	Kruppel-like factor 9	2.1	6.80E-03
0794	Klf13	Kruppel-like factor 13	1.6	0.00E+00
6599	Klf3	Kruppel-like factor 3	1.5	3.00E-03
2865	Cox7a1	cytochrome c oxidase,VIIa 1	-1.8	0.00E+00

***Development*:** Genes involved in early development including certain transcription factors, ligands, regulators of chromatin and proteoglycans were differentially regulated in *inv/inv* mice kidneys (Table 11). Loss of inversin decreased the expression of Wnt 11 and impairment in Wnt11 function may lead to kidney tubular abnormalities in *inv/inv* kidneys (Nagy et al, 2016). Certain transcription factors such as Prdm16, a member of the PR domain-containing protein known to be a regulator of cell differentiation is expressed in kidneys at E14.5 (Horn et al, 2011) and was upregulated in *inv/inv* mice kidneys. General transcription factor 2i (Gtf2i) known to activate developmental genes during differentiation of mESCs (Chimge et al, 2012) was downregulated in *inv/inv* kidneys. Micro RNAs (miRNA) are known to play a key role in development and Dgcr8, a miRNA processing enzyme was downregulated in *inv/inv* mice kidneys. Nepn (Nephrocan), a small leucine-rich repeat proteoglycan which is expressed during early stages of embryogenesis (Mochida et al, 2006) was downregulated in *inv/inv* kidneys suggesting its role during kidney development. Proline 4-hydroxylase, alpha 1 polypeptide (P4ha1), a catalytic subunit of collagen prolyl 4-hydroxylase in collagen synthesis was downregulated in *inv/inv* kidneys and may contribute to basement membrane malformation. Swi/snf related, matrix-associated actin-dependent regulator of chromatin (Smarcad1/Etl1), an early developmental gene (Schoor et al, 1999) was downregulated in *inv/inv* kidneys. Zfpm2/Fog2, a cofactor for GATA3, a transcription factor involved in vertebrate embryonic development was also downregulated in *inv/inv* kidneys.

Table 11: Genes associated with development altered in *inv/inv* mice kidneys

Gene ID	**Gene Symbol**	**Protein Name**	**Fold change (*inv*$^{-/-}$/wild-type)**	***P*-value**
22411	Wnt11	wingless-related MMTV integration site 11	-1.8	3.60E-03
70673	Prdm16	PR domain containing 16	7.9	2.00E-04
14886	Gtf2i	general transcription factor II I	-1.5	6.90E-03
94223	Dgcr8	DiGeorge syndrome critical region gene 8	-2.6	1.00E-04
66650	Nepn	Nephrocan	-1.6	0.00E+00
18451	P4ha1	proline 4-hydroxylase, alpha 1 polypeptide	-2.0	9.30E-03
13990	Smarcad1	SWI/SNF-related, matrix-associated actin-dependent regulator of chromatin, subfamily a, containing DEAD/H box 1	-1.5	3.00E-04
22762	Zfpm2	zinc finger protein, multitype 2	-1.5	3.20E-03
14048	Eya1	eyes absent 1 homolog (Drosophila)	-2.4	6.00E-04

***Regulation of cell migration and trafficking in inv/inv mice kidneys*:** Genes associated with cell migration and trafficking were downregulated in *inv/inv* mice kidneys (Table 12). Extracellular matrix genes such as collagen14a1 and hyaluronan and proteoglycan link protein (Hapln1) were also downregulated in *inv/inv* mice kidneys. In polarized renal epithelial cells, membrane trafficking events are facilitated by microtubules and actin microfilaments (Brown & Stow, 1996; Hamm-Alvarez & Sheetz, 1998). Interestingly, genes involved in axon guidance that included semaphorin-3a (Sema 3a), ephrin A3 (Efna3) and its receptor Epha3 were downregulated in the kidneys of *inv/inv* mice. In addition, microtubule-associate protein, Tau (Mapt) and PDZ containing 1 (Pdzk1) that guides specific motors for trafficking of certain transporters like organic anion transporter 1a1 (Oatp1a1) (Wang et al, 2014a) and sodium-dependent inorganic phosphate (Na/P(i) (Giral et al, 2011) were also downregulated in *inv/inv* kidneys. Kinesin light chain 1 (Klc1), a motor protein and Gephyrin (Gphn), a tubulin-binding protein involved in trafficking of glycine receptors (Hanus et al, 2004) to the cell surface were downregulated. Angiomotin 1 (Amot1), involved in endothelial cell migration (Troyanovsky et al, 2001) was also downregulated in *inv/inv* kidneys. These results suggest that loss of inversin may affect the genes involved in cytoskeletal changes, trafficking and migration and is consistent with the previous observation on the role of inversin in cell migration (Veland et al, 2013). Overall, these data suggest that loss of inversin may result in impaired transcriptional regulation of genes involved in early development, differentiation and migration thus affecting the normal renal tubular geometry.

Table 12: Downregulation of genes that affect migration and trafficking in *inv/inv* mice kidneys

Gene ID	**Gene Symbol**	**Protein Name**	**Fold change (*inv*$^{-/-}$/wild-type)**	***P*-value**
12818	Col14a1	Collagen, type XIV, alpha 1	-1.6	8.00E-03
12950	Hapln1	hyaluronan and proteoglycan link protein 1	-2.0	0.00E+00
13638	Efna3	ephrin A3	-1.6	5.30E-03
13837	Epha3	Eph receptor A3	-2.8	0.00E+00
241226	Itga8	integrin alpha 8	-1.7	4.80E-03
20346	Sema3a	semaphorin 3A	-1.8	3.70E-03
17762	Mapt	microtubule-associated protein tau	-1.8	3.00E-03
16593	Klc1	kinesin light chain 1; similar to kinesin light chain 1	-1.6	8.40E-03
268566	Gphn	Gephyrin	-1.5	6.00E-04
66648	Tpgs2	tubulin polyglutamylase complex subunit 2	-1.6	5.30E-03
108100	Baiap2	brain-specific angiogenesis inhibitor 1-associated protein 2	-1.6	1.80E-03
59020	Pdzk1	PDZ domain containing 1	-1.8	1.60E-03
27494	Amot	Angiomotin	-1.5	7.70E-03
50490	Nox4	NADPH oxidase 4	-2.2	6.90E-03
109246	Tspan9	tetraspanin 9	-2.8	2.40E-03

***Decreased expression of sodium reabsorption and sodium-dependent co-transporter genes in inv/inv mice kidneys*:** The major effect of arginine vasopressin (AVP) is water reabsorption; however AVP, to a lesser extent can also stimulate Na^+ absorption in the principal cells of collecting duct (Hasler et al, 2009; Hawk et al, 1996). The stimulatory effect of AVP is due to increased intracellular cAMP via arginine vasopressin receptor 2 (Avpr2). Interestingly, several mediators that negatively modulate the AVP action by altering the intracellular levels of cAMP either at the level of production or degradation, such as, α2 adrenergic agonists, endothelin (Edn1) or bradykinin (Feraille & Doucet, 2001) were altered in *inv/inv* mice kidneys. While Avpr2 expression levels was not changed in the current array data, there was an increase in the expression levels of Edn1, bradykinin receptor (Bdkrb2), adrenergic receptor alpha 2a (Adra2a) in *inv/inv* mice kidneys. In addition, expression levels of phosphodiesterase 4d (Pde4d), a cAMP degrading enzyme was upregulated in *inv/inv* kidneys. AVP can also stimulate the kallikrein-kinin system that can be counteracted by bradykinin (Fejes-Toth et al, 1980). Interestingly, kallikrein was also downregulated in *inv/inv* mice kidneys (Table 13). Angiotensin II type receptor 1b (Agtr1b) and its associated protein (Agtrap) which affects sodium handling and blood pressure (Wakui et al, 2015) were downregulated. Taken together, these data suggest that Na^+ transport was affected in *inv/inv* kidneys resulting in overall decreased Na^+ reabsorption. Select genes implicated in Na^+ reabsorption (Bdkrb2, Dbp, Edn1, Entpd1, Igf1) were validated by real-time PCR (Figure 8).

Several Na^+-dependent co-transporters were also downregulated in *inv/inv* mice kidneys (Table 13). For example, Slc6A20b, a Na^+-dependent amino acid transporter,

Slc10a1, a sodium/taurocholate co-transporting polypeptide (Ntcp), Slc8a1, a Na^+-dependent Ca^{++} exchanger (Ncx1), Slc17a3, a Na^+-dependent phosphate transporter (Npt4) and Slc34a1, also a Na^+-dependent phosphate co-transporter (Npt2a), and Slc5a8, a Na^+- coupled transporter for short chain fatty acids (Takebe et al, 2005), were downregulated in *inv/inv* mice kidneys. Additionally, genes known to decrease Na^+ wasting, such as neurotensin (Nts), a peptide hormone (Bloom et al, 1983) were downregulated in *inv/inv* kidneys. Taken together, these results suggest that loss of inversin not only contributes to decreased Na^+ reabsorption, it also affects the Na^+-dependent transporters resulting in overall increase Na^+ wasting/natriuresis. A decrease in Na^+ reabsorption can contribute to a decrease in blood pressure. Interestingly, some of the genes implicated in regulation of blood pressure, such as, zinc finger protein 260 (Zfp260), a regulator of alpha 1 adrenergic signaling, succinate receptor (Sucnr1)/Gpr91, kidney androgen-regulated protein (Kap), Slc22a8, a organic anion transporter (Oat3) (Debrus et al, 2005; Sadagopan et al, 2007; Tornavaca et al, 2009; Vallon et al, 2008) were downregulated in *inv/inv* mice kidneys indicating that loss of inversin may decrease blood pressure in *inv/inv* mice (Table 13). Interestingly, Slc23a1, a Na^+-dependent vitamin C/ascorbate transporter (Svct1) that plays a key role in perinatal survival (Corpe et al, 2010) was downregulated in *inv/inv* mice kidneys. Overall, these data suggest that loss of inversin may decrease Na^+ reabsorption that in turn can alter some of the Na^+-dependent transporters affecting, amino acid, fatty acid, calcium and phosphate transport, blood pressure as well as perinatal survival in *inv/inv* mice.

Table 13: Regulation of genes affecting Na^+ reabsorption and Na^+-dependent transporters in *inv/inv* mice kidneys

Gene ID	Gene Symbol	Protein Name	Fold change (*inv*$^{-/-}$ /wild-type)	*P*-value
Decreased Na^+ reabsorption				
12062	Bdkrb2	bradykinin receptor, beta 2	4.0	0.00E+00
13614	Edn1	endothelin 1	2.2	0.00E+00
11551	Adra2a	adrenergic receptor, alpha 2a	1.8	3.20E-03
12495	Entpd1	ectonucleoside triphosphate diphosphohydrolase 1	1.7	3.00E-04
16612	Klk1	kallikrein 1	-4.3	1.40E-03
13170	Dbp	D site albumin promoter binding protein	-1.5	5.00E-04
16000	Igf1	insulin-like growth factor 1	-1.6	7.30E-03
11610	Agtrap	angiotensin II, type I receptor-associated protein	-1.5	3.40E-03
67405	Nts	Neurotensin	-1.5	2.70E-03
238871	Pde4d	phosphodiesterase 4d, cAMP specific	2.0	0.00E+00
11608	Agtr1b	angiotensin II receptor, type 1b	-1.6	4.70E-03
83814	Nedd4l	neural precursor cell expressed, developmentally down-regulated gene 4-like	1.7	0.00E+00
Blood pressure				
64652	Nisch	Nischarin	1.5	7.60E-03
268782	Agxt2	alanine-glyoxylate aminotransferase 2	-2.9	0.00E+00
84112	Sucnr1	succinate receptor 1	-2.4	5.60E-03
26466	Zfp260	zinc finger protein 260	-1.5	9.10E-03
54140	Avpr1a	arginine vasopressin receptor 1A	-1.6	7.30E-03
60596	Gucy1a3	guanylate cyclase 1, soluble, alpha 3	-1.6	6.20E-03
11441	Chrna7	cholinergic receptor, nicotinic, alpha polypeptide 7	-1.5	3.90E-03
19879	Slc22a8	solute carrier family 22, member 8	-3.4	3.60E-03
16483	Kap	kidney androgen regulated protein	-2.8	3.90E-03
Na^+ dependent cotransporters and exchangers				
22599	Slc6a20 b	solute carrier family 6 (neurotransmitter transporter), member 20B	-2.5	8.20E-03
20493	Slc10a1	solute carrier family 10, bile acid cotransporter,1	-2.4	1.60E-03
75750	Slc10a6	solute carrier family 10, bile acid cotransporter,6	2.2	5.30E-03
105355	Slc17a3	solute carrier family 17, phosphate cotransporter,3	-2.6	2.60E-03
20505	Slc34a1	solute carrier family 34, phosphate cotransporter,1	-2.8	9.30E-03
109342	Slc5a10	solute carrier family 5, glucose cotransporter,10	-2.6	2.30E-03
20541	Slc8a1	solute carrier family 8 ,calcium exchanger,1	-1.6	1.40E-03
75750	Slc10a6	solute carrier family 10, member 6	2.2	5.30E-03
20522	Slc23a1	solute carrier family 23 (nucleobase transporters),1	-2.3	5.90E-03
216225	Slc5a8	solute carrier family 5, member 8	-3.0	6.50E-03

***Decreased expression levels of organic anion, cations and small molecule transporters in inv/inv mice kidneys*:** The members of the solute carrier 22 (Slc22) family represent organic anion or cationic transporters (Table 14). Slc22a22, Slc22a12, Slc22a13 were downregulated in *inv/inv* mice kidneys. Slc22a22, a kidney-specific organic anion transporter that transports prostaglandins (PG) and is localized on the basolateral membrane of the proximal tubule was downregulated 12-fold. Slc22a22 is proposed to be involved in the local PGE2 clearance and metabolism for the inactivation of PG signals in the kidney cortex (Shiraya et al, 2010). Slc22a12, an anion urate transporter (Urat1), (Hosoyamada et al, 2010) was downregulated in this study indicating attenuated urate reabsorption in *inv/inv* kidneys. Slc22a6, an organic anion transporter (Oat1) involved in the clearance of endogenous toxins (Wikoff et al, 2011) was downregulated in *inv/inv* mice kidneys. These results suggest that loss of inversin alters the expression levels of genes associated with renal failure and uremia. Slc22a7, an organic anion transporter (Oat2) is involved in the transport of short chain fatty acid propionate (Islam et al, 2008), a potent glucogenic compound, was decreased by 2.5-fold in this study. Downregulation of Slc22a7 in *inv/inv* mice kidneys suggests that inversin may play a role in the regulation of cellular metabolism through transport of metabolites via Slc22a7. Slc7a13/Agt1, a cystine, aspartate and glutamate transporter (Nagamori et al, 2016) expressed in the S3 segment of the proximal tubule was also downregulated in *inv/inv* kidneys.

***Acid-base balance**:* Glutaryl-CoA dehydrogenase (Gcdh) deficiency results in accumulation of glutaric acid and 3-hydroxyglutaric acid (3OH-GA) (Stellmer et al,

2007). Slc13a3 (NaDC3), expressed in the proximal tubules, is a Na^+-dependent dicarboxylate transporter that translocates 3-hydroxyglutaric acid to the membrane (Stellmer et al, 2007). Interestingly, Gcdh and Slc13a3 were downregulated in *inv/inv* mice kidneys (Table 14). Gcdh deficiency can also result in downregulation of Slc22a2/Oct2, an ion transporter involved in renal secretion of organic cations and toxic waste. Car12 (Carbonic anhydrase-12), expressed in basolateral plasma membrane of S1 and S2 proximal tubule segments as well as in both cortical and medullary collecting ducts has a crucial role in renal bicarbonate absorption (Kyllonen et al, 2003). Car12 was downregulated in *inv/inv* mice kidneys and may have effects on bicarbonate absorption. Bicarbonate is the biological buffer that maintains acid-base balance in cells (Allen et al, 1993). Overall, these data suggest that loss of inversin may affect acid-base balance in *inv/inv* mice kidneys.

***Genes involved in cellular metabolism were affected in inv/inv mice kidneys*:** Severely affected kidneys underexpress genes associated with major metabolic pathways involved in the generation of precursor metabolites and energy compared to the normal kidneys (Zhang et al, 2004). The majority of the genes involved in purine, pyramidine, pyruvate, peroxisome, glycine, serine, threonine, arginine, proline, glutathione, and sphingolipid metabolism were downregulated in *inv/inv* mice kidneys (Table 15). Downregulation of these various metabolic genes are consistent with the reduction of functional parenchyma in *inv/inv* mice kidneys (Phillips et al, 2004).

Table 14: Regulation of genes affecting organic anion and cation transporters and acid-base balance in *inv/inv* mice kidneys

Gene ID	**Gene Symbol**	**Protein Name**	**Fold change (*inv*$^{-/-}$ /wild-type)**	***P*-value**
Organic cation transporters				
102570	Slc22a13	solute carrier family 22, member 13	-2.9	5.00E-04
74087	Slc7a13	solute carrier family 7, amino acid transporter 13	-2.5	1.60E-03
11987	Slc7a1	solute carrier family 7, member 1	1.5	0.00E+00
Organic anion transporters				
18399	Slc22a6	solute carrier family 22, member 6	-2.6	1.20E-03
108114	Slc22a7	solute carrier family 22, member 7	-2.5	4.10E-03
101488	Slco2b1	solute carrier, member 2b1	1.6	0.00E+00
319800	Slc22a30	solute carrier family 22, member 30	-2.2	1.30E-03
28254	Slco1a6	solute carrier, member 1a6	-3.3	4.10E-03
210463	Slc22a22	solute carrier family 22, member 22	-12.6	0.00E+00
20521	Slc22a12	solute carrier family 22 (urate transporter),12	-2.9	1.00E-04
Acid-base balance				
114644	Slc13a3	solute carrier family 13, dicarboxylate cotransporter,3	-3.3	5.80E-03
20518	Slc22a2	solute carrier family 22, member 2	-3.0	1.30E-03
270076	Gcdh	glutaryl-Coenzyme A dehydrogenase	-1.7	7.00E-04
76459	Car12	carbonic anyhydrase 12	-1.9	1.60E-03
Monocarboxylic acid transporters				
69309	Slc16a13	solute carrier family 16 , member 13	-1.6	1.90E-03
229699	Slc16a4	solute carrier family 16, member 4	-2.8	1.00E-03
Increased K^+ secretion				
16502	Kcnc1	potassium voltage gated channel, member 1	2.2	4.50E-03
Glucose transport				
20525	Slc2a1	solute carrier family 2 (facilitated glucose transporter),1	1.8	5.00E-04
Others				
58176	Rhbg	Rhesus blood group-associated B glycoprotein (ammonia excretion)	-2.5	1.10E-03
11416	Slc33a1	solute carrier family 33 (acetyl-CoA transporter),1	-1.5	3.40E-03
227059	Slc39a10	solute carrier family 39 (zinc transporter),10	-1.7	2.00E-03
19212	Pter	phosphotriesterase related (organphosphate transporter)	-2.4	7.70E-03
246696	Slc25a28	solute carrier family 25, member 28	1.5	8.80E-03
21366	Slc6a6	solute carrier family 6, taurine transporter,6	1.9	2.50E-03

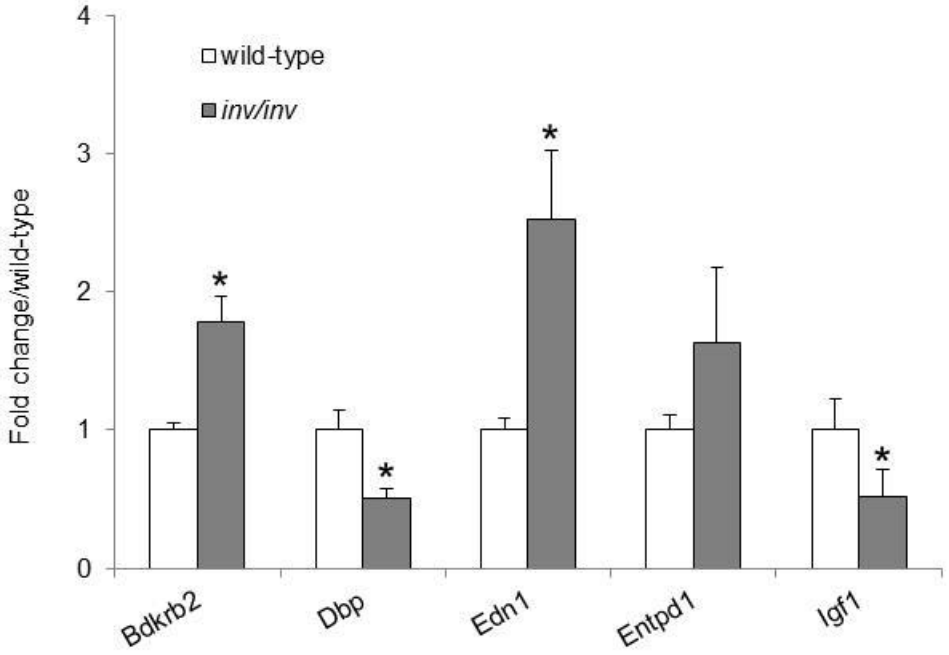

Figure 8: Validation of select Na^+ reabsorption genes from *in vivo* array analysis. Select genes from *in vivo* array analysis implicated in Na^+ reabsorption were validated in one day old wild-type and *inv/inv* mice kidneys. Total RNA from one-day old wild-type and *inv/inv* mice kidneys was isolated and mRNA levels were assessed by quantitative real-time PCR. The data was normalized to 18S RNA and expressed as fold change over wild-type littermates. Values are mean ± SEM (n=5); *$p<0.05$ vs wild-type.

Table 15: Genes associated with metabolic pathways altered in *inv/inv* mice kidneys

Gene ID	Gene Symbol	Protein Name	Fold change (*inv*$^{-/-}$ /wild-type)	*P*-value
Purine and pyramidine metabolism				
110639	Prps2	phosphoribosyl pyrophosphate synthetase 2	-1.6	4.70E-03
234889	Gucy1a2	guanylate cyclase 1, soluble, alpha 2	-1.7	4.60E-03
60596	Gucy1a3	guanylate cyclase 1, soluble, alpha 3	-1.6	6.20E-03
67005	Polr3k	polymerase (RNA) III (DNA directed) polypeptide K	-1.5	5.00E-04
19076	Prim2	DNA primase, p58 subunit	-1.5	2.50E-03
13178	Dck	deoxycytidine kinase	-1.5	4.20E-03
11639	Ak4	adenylate kinase 4	-2.3	3.00E-04
22247	Umps	uridine monophosphate synthetase	-1.7	4.30E-03
80914	Uck2	uridine-cytidine kinase 2	-1.5	6.80E-03
50493	Txnrd1	thioredoxin reductase 1	-1.5	7.00E-04
22436	Xdh	xanthine dehydrogenase	40.2	1.30E-03
238871	Pde4d	phosphodiesterase 4D, cAMP specific	2.0	0.00E+00
242202	Pde5a	Phosphodiesterase 5A	2.0	1.03E-02
12495	Entpd1	ectonucleoside triphosphate diphosphohydrolase 1	1.7	3.00E-04
18583	Pde7a	phosphodiesterase 7A	1.5	1.20E-03
Pyuruvate metabolism				
66204	Acyp1	acylphosphatase 1	-1.5	0.00E+00
621603	Aldh3b2	aldehyde dehydrogenase 3 family	-1.5	9.90E-03
76238	Grhpr	glyoxylate reductase/hydroxypyruvate reductase	-1.6	0.00E+00
75572	Acyp2	acylphosphatase 2, muscle type	-1.6	6.30E-03
18563	Pcx	pyruvate carboxylase	-2.4	3.80E-03
60525	Acss2	acyl-CoA synthetase short-chain family, 2	-1.8	4.30E-03
Amino acid metabolism				
67092	Gatm	glycine amidinotransferase	-3.9	2.00E-04
74129	Dmgdh	dimethylglycine dehydrogenase precursor	-3.5	4.50E-03
14431	Gamt	guanidinoacetate methyltransferase	-1.7	0.00E+00
27364	Srr	serine racemase	-1.5	7.00E-04
268782	Agxt2	alanine-glyoxylate aminotransferase 2	-2.9	0.00E+00
12715	Ckm	creatine kinase, muscle	-1.5	2.00E-04
18451	P4ha1	proline 4-hydroxylase, alpha 1 polypeptide	-2.0	9.30E-03
621603	Aldh3b2	aldehyde dehydrogenase 3 family	-1.5	9.90E-03
58865	Tdh	L-threonine dehydrogenase	1.8	4.60E-03

Table 15 continued

Glutathione metabolism				
110175	Ggct	gamma-glutamyl cyclotransferase	-1.6	0.00E+00
14782	Gsr	glutathione reductase	-1.8	0.00E+00
Fatty acid oxidation				
111175	Pecr	peroxisomal trans-2-enoyl-CoA reductase	-1.5	1.00E-04
235674	Acaa1b	acetyl-Coenzyme A acyltransferase 1A	-2.0	3.90E-03
17117	Amacr	alpha-methylacyl-CoA racemase	-1.8	2.00E-03
56794	Hacl1	2-hydroxyacyl-CoA lyase 1	-1.9	1.00E-04
Sphingolipid metabolism				
22239	Ugt8a	UDP galactosyltransferase 8A	-2.3	9.60E-03
20773	Sptlc2	serine palmitoyltransferase, long chain base subunit 2	4.5	0.00E+00
11847	Arg2	arginase type II	2.1	2.30E-03
20698	Sphk1	sphingosine kinase 1	1.9	0.00E+00
56386	B4galt6	UDP-Gal:betaGlcNAc beta 1,4-galactosyltransferase, polypeptide 6	1.7	0.00E+00

Discussion

Mutations in inversin gene cause renal cysts in NPHP2 patients as well as in *inv/inv* mice (Morgan et al, 1998; Otto et al, 2003). The molecular basis of cyst growth and expansion in NPHP2 is not well understood. To elucidate the molecular pathways that modulate renal cysts in *inv/inv* mice transcriptome analysis was performed on the kidneys of mutant and the wild-type littermates. This study provides for the first time a comprehensive map of the key pathways that are associated with cystic kidneys of *inv/inv* mice. The main transcriptional profiles that were altered include activation of immune/inflammatory cascades, cell proliferation (decrease in cell cycle progression), extracellular matrix deposition, fibrosis, apoptosis and electrolyte or ion transport.

Hypoxia or inflammation associated with disease or injury can induce the expression of certain members of the classic complement pathway such as, C1qa, C1qb and C1qc involved with innate immune system that were upregulated in the kidneys of *inv/inv* mice. These findings are consistent with the previous reports on the activation of the C1qa and C1qb in *cpk* mouse, a model of ARPKD (Mrug, 2008). Additionally, activation of C1qa, C1qb and C1qc been shown to mediate renal injury in models of diabetic nephropathy (Kelly et al, 2015). Macrophages play an important role in promoting inflammation (M1 macrophages) and its resolution (M2 macrophages) in response to injury (Gordon, 2003; Lambert et al, 2008). Interestingly, CD163, a receptor expressed on M2 macrophages (Kristiansen et al, 2001) that promotes tissue remodeling was upregulated in *inv/inv* mice kidneys. Activation of Tnfrsf12a/TweakR/Fn14 shown to have pro-inflammatory effects on podocytes (Sanchez-Nino et al, 2013) was also upregulated in *inv/inv* mice kidneys. Endothelial adhesion molecule Icam known to play

a role in the neutrophil migration (Sligh et al, 1993) was upregulated in *inv/inv* kidneys. Upregulation of hypoxia inducible factor (Hif3α) following ischemic injury has been suggested to play a role protective role in kidney (Heidbreder et al, 2003) and was also increased in our array analysis of *inv/inv* kidneys. Together, it is possible that inflammatory responses associated with both tissue damage and repair may co-exist in *inv/inv* kidneys.

Cytokines or growth factors that are released in response to inflammation can activate Janus kinase/signal transduction and activator of transcription (Jak/Stat) signaling (Leonard & O'Shea, 1998) which was one of the pathways altered in *inv/inv* mice kidneys. Certain cytokines, chemokines (IL34, Cxcl1 and Ccl9) and receptors (Il1ra, Il6ra, and Tnfrsf12a) among others showed increased expression in *inv/inv* mice kidneys that can result in the activation of Jak/Stat signaling cascade and its downstream effectors. Stat3, a component of Jak/Stat that mediates the expression of a variety of genes involved in cell processes such as cell growth, apoptosis and differentiation (Yang et al, 2007; Yuan et al, 2004). Activation of Jak/Stat pathway has been shown to upregulate p21/Cdkn1a, an inhibitor of cyclin D2 activity thereby inducing cell cycle arrest in G0/G1 phase in canine kidney cells (Bhunia et al, 2002). An increase in the expression of Stat3 in this study accompanied by an increase in p21/Cdkn1a indicates a possible delay in cell cycle progression in *inv/inv* mice kidneys. Furthermore, additional cell cycle genes altered in *inv/inv* mice kidneys is consistent with the role of inversin during different stages of cell cycle in renal epithelial cells (Morgan et al, 2002a). Overall, a possible delay in cycle progression or cell cycle arrest may affect cell proliferation for proper renal tubule formation in *inv/inv* kidneys. Interestingly, genes

implicated in cell proliferation such as gammaglutamytransferase (Ggct), and Cdk2-associated cullin domain-1 (Calcul) were downregulated in *inv/inv* mice kidneys. Knockdown of Ggct in lung cancer cell lines have been shown to decrease cell proliferation (Lin et al, 2015). Silencing of Cacul1 in gastric cell line resulted in decreased cell growth by cell cycle arrest (Zheng et al, 2013). Additionally, acylglycerol kinase (Agk), a kinase that phosphorylates a-acylglycerol has been shown to promote cell proliferation in breast cancer lines (Wang et al, 2014b) was also downregulated in *inv/inv* mice kidneys. Overall, a decrease in the expression of cell cycle and proliferation genes were seen in one-day old *inv/inv* mice kidneys.

Extracellular matrix proteins such as connective tissue growth factor (Ctgf) and tenascin C (Tnc) have been shown to play a crucial role in many fibrotic conditions including renal fibrosis (Fu et al, 2016; Phanish et al, 2010; Toba et al, 2016). Ctgf is expressed in glomerular podocytes, mesangial cells and proximal tubular epithelial cells and acts synergistically with TGF-β1 to promote tissue fibrosis (Mori et al, 1999). In proximal tubular cells, TGF-β1has been shown to induce Ctgf and tenascin C mRNA levels (Sarkozi et al, 2011). The increase in TGF-β1-induced Ctgf expression can be inhibited by Oncostatin M (Osm) via Osm receptor (Osmr)-activated Stat3 (Sarkozi et al, 2012; Sarkozi et al, 2011). The upregulation of both Ctgf and Tnc, Osmr as well as Stat3 in this study suggest that signaling via Ctgf/Osmr/Stat3 axis may promote fibrosis in *inv/inv* kidneys consistent with interstitial fibrosis reported in NPHP2 patients (Gagnadoux et al, 1989; Haider et al, 1998).

Apoptosis or programmed cell death is a fundamental and complex biologic process that enables an organism to remove unwanted cells during development, normal

homeostasis and disease (Jacobson et al, 1997; Thompson, 1995). Caspases are crucial mediators of apoptosis (Porter & Janicke, 1999) Caspase-3, a frequently activated death protease was downregulated in *inv/inv* mice kidneys; whereas certain inhibitors of apoptosis (Nnmt, Btg-1, Serinc3) were upregulated. Overexpression of Nnmt (nicotinamide N-methyl transferase), has been shown to inhibit lipotoxicity-induced oxidative stress and cell death in kidney proximal tubule cells (Tanaka et al, 2015). Oxidative stress upregulates B-cell translocation gene (Btg-1) mRNA and Btg1 activation represses NF-kb activity, an inducer of apoptosis in macrophages (Cho et al, 2005). Serinc (serine incorporator3/TDE1), a carrier protein that incorporates serine residue into cell membranes has been shown to inhibit apoptosis and stimulate tumorigenesis in Rat-1 fibroblasts (Bossolasco et al, 2006) was upregulated in *inv/inv* kidneys. Since loss of Niban/Fam129A, an endoplasmic reticulum stress-inducible protein was shown to increase apoptosis in He La cells (Sun et al, 2007), an increased expression of Niban in this study may hinder apoptosis in *inv/inv* kidneys. Members of the Kruppel-like transcription factors implicated in cell survival and inhibition of apoptosis were upregulated in *inv/inv* mice kidneys. Overexpression of Klf6, an essential regulator of mitochondrial function prevented podocyte apoptosis (Mallipattu et al, 2015). Overexpression of Klf9 has been shown to increase the Purkinje cell survival (Lebrun et al, 2013). Overall, an increase in the expression of cell survival genes and a decrease in the expression of apoptotic genes may contribute to enlarged cystic kidneys in *inv/inv* mice.

Inversin plays a role in non-canonical Wnt/planar cell polarity pathway (Lienkamp et al, 2010). Wnt 11, a ligand for non-canonical signaling that has been

shown to control early steps in ureteric bud branching was downregulated in *inv/inv* mice kidneys. Interestingly, impairment of Wnt11 function in $Wnt11^{-/-}$ mice leads to kidney tubular abnormalities and glomerular cysts (Nagy et al, 2016). Prdm16, a transcription regulator of cell differentiation has been shown to be expressed in kidneys at E14.5 (Horn et al, 2011). Upregulation of Prdm16 in this study may have differentiation effects during early stages of developing *inv/inv* kidneys. Gtf2i encoding TFII-I family of transcription and known to activate developmental genes during differentiation of mESCs (Chimge et al, 2012) was downregulated in *inv/inv* kidneys suggesting a possible role of Gtf2i in differentiation.

Micro RNAs (miRNA) are known to play a key role in tissue development (Ambros, 2004). Dgrc8, a miRNA processing enzyme was downregulated in *inv/inv* mice kidneys indicating its role in renal development. Conditional deletion of Dgcr8 in the developing renal tubule results in hydronephrosis, renal cysts, progressive renal failure and premature death within first two months consistent with *inv/inv* mice and NPHP2 phenotype (Bartram et al, 2015). Nepn (nephrocan), a small leucine-rich repeat proteoglycan which is expressed during early stages of embryogenesis was downregulated in *inv/inv* kidneys suggesting its role during kidney development (Mochida et al, 2006). P4ha1 (proline 4-hydroxylase, alpha 1 polypeptide), a catalytic subunit of collagen prolyl 4-hydroxylase involved in collagen synthesis was downregulated in *inv/inv* kidneys that may have effects on basement membrane integrity (Pietila et al, 2016). Smarcad1/Etl1 (Swi/snf related, matrix-associated actin-dependent regulator of chromatin), is expressed at 2-cell stage during development and loss of this gene has been implicated in skeletal dysplasia, growth retardation and reduced postnatal

survival in mice (Schoor et al, 1999). Downregulation of Smarcad1 in this study is consistent with short life-span and growth retardation observed with *inv/inv* mice and short life-span and skeletal dysplasia in NPHP2 phenotype (Oud et al, 2014). Overall, changes in several early developmental genes observed in this study may affect kidney development in *inv/inv* mice.

Fluid accumulation is a hallmark of renal cystic diseases and defective ion transport has been shown to play a role in this process (Terryn et al, 2011). One of the significantly altered categories in the array analysis of *inv/inv* mice kidneys was molecular transport. Genes involved in Na^+ transport, Na^+-dependent co-transporters and exchangers, acid-base balance, organic anion and cation transporters were downregulated *inv/inv* mice kidneys. The antidiuretic hormone (ADH) or AVP (arginine vasopressin) can stimulate Na^+ absorption in distal nephron epithelium (Reif et al, 1986; Tomita et al, 1985). The stimulatory effect of AVP on Na^+ transport is due to increased intracellular cAMP via AVP receptor 2 (Marunaka & Eaton, 1991). Expression levels of several mediators (endothelin, bradykinin receptor, adrenergic receptor alpha 2a) that negatively modulate cAMP (Feraille & Doucet, 2001) were increased in *inv/inv* mice kidneys. The increased expression of the negative modulators of cAMP may contribute to decreased Na^+ reabsorption in *inv/inv* mice kidneys. A decrease in Na^+ reabsorption in the AVP-sensitive segments of the kidneys could have an effect on blood pressure.

Blood pressure associated genes such as, Zinc finger protein (Zfp260), kidney androgen-regulated protein (Kap), Slc22a8, an organic anion transporter and succinate receptor (Sucnr1/Gpr91) were downregulated in *inv/inv* mice kidneys. Knockdown of Zfp260, a nuclear effector of alpha-1-adrenergic signaling in cardiac cells, decreases the

atrial natriuretic factor (Anf) (Debrus et al, 2005) and decreases blood pressure. Kap transgenic mice have been shown to exhibit hypertension (Tornavaca et al, 2009). Mice lacking Slc22a8 exhibit lower blood pressure compared to wild-type controls (Vallon et al, 2008). In addition, succinate receptor (Sucnr1/Gpr91) activation has been shown to induce hypertension in mice (Sadagopan et al, 2007). Overall, the regulation of genes involved in Na^+ reabsorption and hypertension indicates that loss of inversin may have an effect on blood pressure in *inv/inv* mice.

Several sodium-dependent transporters were also downregulated in *inv/inv* mice kidneys. Slc34a1/Npt2, a Na^+-dependent phosphate transporter expressed in the brush border membrane of proximal tubular cells was downregulated in *inv/inv* kidneys. $Npt2^{-/-}$ mice show decreased Na^+/Pi cotransport (Hoag et al, 1999). The decreased expression of Npt2 in *inv/inv* mice kidneys suggest a possible decrease in Na^+/Pi cotransport.

Glutaryl-CoA dehydrogenase (Gcdh) was downregulated in *inv/inv* mice kidneys. Gcdh deficiency results in accumulation of glutaric acid and 3-hydroxyglutaric acid (3OH-GA). Slc13a3/NaDC3, a Na^+-dependent dicarboxylate transporter that mediates the translocation of 3OH-GA through membranes was also downregulated *inv/inv* mice kidneys (Stellmer et al, 2007). The decrease in the expression levels of Gcdh and Slc13a3 may result in accumulation of organic acids in *inv/inv* mice kidneys. Carbonic anhydrase (Car12), a bicarbonate transporter was downregulated in *inv/inv* mice kidneys. Car12 expressed in basolateral membrane of S1 and S2 segment of proximal tubule, cortical and medullary collecting ducts is important for bicarbonate absorption and acid-base balance (Kyllonen et al, 2003). Together, the downregulation of Gcdh, Slc13a3, and Car12 may affect acid-base balance in *inv/inv* mice kidneys.

Slc23a1, an ascorbate transporter was downregulated in *inv/inv* mice mice kidneys. Slc23a1$^{-/-}$ mice exhibited increased ascorbate excretion and increased perinatal mortality (Corpe et al, 2010). The decrease in Slc23a1 in *inv/inv* mice kidneys may contribute to short life span observed in these mice (Yokoyama et al, 1993).

Slc22a6/Oat1, an organic anion transporter expressed in the proximal renal tubule was downregulated in *inv/inv* mice kidneys. Slc22a6$^{-/-}$ mice showed accumulation of endogenous toxins such as urate, and certain metabolites (indoxyl sulfate, xanthurenic acid) in the plasma associated with renal failure and uremia (Eraly et al, 2006; Wikoff et al, 2011). The decreased expression of Slc22a6 suggests that clearance of endogenous toxins might be affected in *inv/inv* mice kidneys. Slc22a12/Urat1, a urate transporter was downregulated in *inv/inv* mice kidneys. Slc22a12$^{-/-}$ mice show higher urinary urate/creatinine ratio indicating decreased urate reabsorption (Hosoyamada et al, 2010). The decrease in Slc22a12 in this study suggests urate reabsorption may be affected in the kidneys of *inv/inv* mice. Overall, several gene implicated in ion transport were regulated *inv/inv* mice. In particular, genes involved in Na^+ transport, Na^+-dependent co-transporters and exchangers, acid-base balance, organic anion and cation transporters may contribute to enlarged kidneys in *inv/inv* mice.

In summary, this study generated a comprehensive gene expression profile of one-day old wild-type and *inv/inv* mice kidneys. The genes identified categorized into functional pathways that were altered included cell proliferation, apoptosis, inflammation and ion transport. It appears that decreased cell proliferation and apoptosis accompanied by changes in Na^+ reabsorption and other genes associated with ion transport may contribute to cyst growth and expansion in *inv/inv* mice kidneys. The *inv/inv* mouse is a

global knockout model of inversin loss and the gene expression changes observed in kidneys could be a direct or an indirect effect of inversin. The changes in gene expression observed in this study is a snap shot in time, and will not capture all the gene changes that may occur during development. In addition, some of the gene regulation that occurs by protein-protein interactions may not be captured in the transcriptome analysis. The array findings on ion transport and cell proliferation were validated in an *in vitro* model of inversin loss in renal epithelial cells and are separately dealt in subsequent chapters.

CHAPTER 3: LOSS OF INVERSIN DECREASES TRANSEPITHELIAL SODIUM TRANSPORT IN MURINE RENAL CELLS OF THE CORTICAL COLLECTING DUCT

Introduction

Gene array analysis of *inv/inv* mice kidneys showed that inversin can have effects on ion transport through transcriptional regulation of genes. The array findings regarding ion transport were further validated in an *in vitro* model of inversin loss in a mouse renal epithelial cell line. Studies from both human and animal models containing NPHP2 mutant alleles suggest a key role of inversin in early development and in renal cyst formation. The increased kidney size in NPHP2 could be due to increased electrolyte secretion or decreased absorption resulting in fluid accumulation within the cyst cavity. One mechanism by which inversin could exert its effect on renal function is by directly affecting electrolyte transport. In a *Xenopus* model, loss of inversin has been shown to result in edema (Lienkamp et al, 2010). Although these data support the premise of fluid accumulation it does not address specific regulation of electrolytes and ion transport in renal epithelial cells. The intentional depletion of inversin in a well characterized epithelial cell line will help determine the function of inversin in transepithelial ion transport processes.

The cystic enlargement of kidneys is one of the features observed in the more common forms of polycystic kidney disease (PKD) arising from mutations in polycystin 1 or 2 or fibrocystin (Bergmann et al, 2003; Mochizuki et al, 1996; Ravine et al, 1992). In autosomal dominant PKD patients and animal models, increased Cl^- secretion across

the cyst-lining epithelial cells has been implicated as a mechanism for fluid accumulation in kidneys (Mangoo-Karim et al, 1995; Wallace et al, 1996). The cystic fibrosis transmembrane conductance regulator (CFTR) is the major Cl^- channel responsible for secretion into renal cysts (Davidow et al, 1996; Hanaoka et al, 1996). However, the mechanism of fluid accumulation and cyst expansion in kidneys of NPHP2 is not well understood. A better understanding of the role of inversin in normal renal function may provide additional insights into the mechanism of cyst growth and expansion in NPHP2.

Homeostasis of body fluids is maintained by the reabsorptive and secretory processes in the kidney tubules (Summa et al, 2001). The tubular reabsorption of filtered sodium (Na^+) in the kidney is tightly controlled to maintain whole body fluid volume homeostasis which together with stored Na^+ in the skin and the skeletal muscle is central for long-term regulation of blood pressure (Titze, 2015). Over 99% of the filtered Na^+ reabsorbed in the kidneys by the epithelia of the renal tubules occurs via ion transport processes (Marunaka, 1997). The majority of the Na^+ reabsorption in the proximal nephron occurs by a constitutively active Na^+ co-transport system but the amount of Na^+ reabsorbed in the distal nephron is under hormonal control (Alvarez de la Rosa et al, 2002; Blazer-Yost et al, 1998; Loffing & Korbmacher, 2009). The principal cells of the distal nephron and cortical collecting duct (CCD) are the site of hormonally controlled Na^+ and water reabsorption and are influenced by the action of aldosterone, insulin and arginine vasopressin (AVP) (Blazer-Yost et al, 1998; Loffing et al, 2006; Loffing & Korbmacher, 2009). Stimulation of Na^+ reabsorption by AVP occurs by coordinated activation of epithelial sodium channel (ENaC) and Na^+, K^+ ATPase (Feraille & Doucet, 2001; Hasler et al, 2009; Hawk et al, 1996). Luminal Na^+ crosses the apical plasma

membrane along its electrochemical gradient through ENaC. The ENaC-derived intracellular sodium is then actively extruded into the interstitial space by the Na^+, K^+-ATPase located on the basolateral membrane (Feraille & Doucet, 2001).

The extrinsic factors that regulate ENaC activity include hormonal, mechanical, cytoskeletal activity and proteolytic cleavage (Bhalla & Hallows, 2008). Intrinsic factors comprise ENaC trafficking and its phosphorylation, Na^+ self- and feedback inhibition, as well as neural precursor cell-expressed developmentally downregulated-like (Nedd4l/Nedd4-2) mediated ubiquitination of ENaC (Bhalla & Hallows, 2008; Staub et al, 1996). Nedd4-2 ubiquitinates ENaC leading to its endocytosis and degradation (Zhou et al, 2007). Serum/glucocorticoid kinase 1 (Sgk1), an aldosterone-regulated gene, stimulates ENaC-mediated Na^+ transport in part by phosphorylating Nedd4l (Snyder et al, 2002). Phosphorylation of Nedd4l prevents the interaction of Nedd4l with ENaC, resulting in increased number of active ENaC subunits at the apical surface (Debonneville et al, 2001). Sgk1 is, in turn, regulated by creb-regulated transcription coactivator (Crtc2), a kinase that phosphorylates Sgk1 (Lu et al, 2010). Overall, the Crtc2, Sgk1 and Nedd4l appear to play a role in Na^+ transport in epithelial cells.

The goal of this study was to provide functional validation of array findings from *inv/inv* mice kidney to determine whether inversin plays a role in transepithelial ion transport in renal cells. The underlying hypothesis is that loss of inversin leads to abnormal fluid accumulation resulting in growth and expansion of renal cysts leading to kidney failure. This study utilized two different methods of inversin knockdown to deplete inversin in a mouse cortical collecting duct (mCCD) cell line and used electrophysiological techniques to measure transepithelial ion transport.

Materials and methods

Accell™ SMART pool *INVS* siRNA (E-061511) was obtained from GE Dharmacon, Inc. (Lafayette, CO), *INVS* MISSION® shRNA lentiviral transduction particles in pLKO-puro vector, TRCN0000086438 (construct 438), TRCN0000086440 (construct 440), TRCN0000086441 (construct 441), TRCN0000086442 (construct 442), TRCN0000331571 (construct 571), arginine vasopressin (AVP) and amiloride were obtained from Sigma-Aldrich (St. Louis, MO). CFTR inhibitor (GlyH 101, 5485) was purchased from Tocris, Minnaepolis, MN. Fluorogenic primer/probe set to detect mRNA encoding inversin (Mm00495002_m1), sodium channel non-neuronal (Scnn1α, Mm00803386_m1), (Scnn1β, Mm00441215_m1), (Scnn1γ Mm00441228_m1), ATP1a1 (Na^+/K^+ transporting, alpha1 polypeptide Mm00523255_m1), Nedd4l (Mm00459584_m1), Sgk1 (Mm00441380_m1), Crtc2 (Mm01219960_m1) and 18S RNA (Mm03928990_g1) were obtained from Applied Biosystems as Assays on Demand™ reagents. Rabbit anti-Nedd4l, (ab131167) was purchased from Abcam (Cambridge, MA). Rabbit anti-Sgk1 (PA5-21147) and rabbit anti-Crtc2 (PA5-34547) were procured from Thermo Fisher (Rockford, IL). Rabbit anti-Phospho Nedd4l (S342; 12146S), rabbit anti-GAPDH, secondary antibodies for Western blotting analysis (anti-rabbit IgG conjugated to horse-radish peroxidase; #7074S) and biotinylated protein ladder (#7727) were from Cell Signaling Technology, Beverly, MA.

***Cell culture*:** The mouse cortical collecting duct (mCCD) cell line expressing the characteristics of the principal cell type in the collecting duct of the kidneys was obtained from Edith Hummler, University of Lausanne (Gaeggeler et al, 2005). The mCCD cells

are high resistance, Na^+ reabsorbing epithelial cells that respond to various hormones (vasopressin, aldosterone, insulin) with an increase in transepithelial movement of electrolytes (Gaeggeler et al, 2005). The mCCD cells were cultured in 75 cm^2 flask and grown in a humidified chamber at 37^oC, 5% CO_2. Cell culture medium comprised of DMEM/F12 (1:1) supplemented with 2% FBS, 80U/ml penicillin, 80µg/ml streptomycin, epidermal growth factor (10ng/ml), 5ml per liter of insulin-transferrin-selenium (100x) to a final concentration of 0.172 mM insulin, 6µM transferrin, 3.87µM sodium selenite, dexamethasone ($5x10^{-8}$M), 10^{-9} M 3,3',5-triiodo-L-thyronine. The medium was replaced three times per week and the cells were passaged weekly.

***Establishment of inversin knockdown in mCCD cells by Accell™ inversin siRNA*:** Long term inversin knockdown in mCCD cells was done using Accell™ technology according to the manufacturer's instructions. Briefly, confluent mCCD cells in a 6-well plate were transfected with Accell™ siRNA targeting inversin at a concentration of 1µM. The sequences of siRNAs targeting the inversin mRNA is shown in Table 16**.** The cells received 1-5 treatments (ranging between 1-5 µM siRNA) during the course of 2 weeks. The medium was replaced three times per week. At the end of 2 weeks, the cells were collected and the inversin mRNA level was assessed by quantitative real-time PCR and the transepithelial ion transport was measured by electrophysiology.

Table 16: Sequences of siRNA targeting mouse *Invs*

siRNA	**Target sequence**	***INVS* gene**	**Inversin protein sequence**
1	5'CCGTGAAGTTATTATTGGA-3'	Exon 8	VKLLLD
2	5'-CCTTGATTATGCATTGCTT-3'	Exon 11	PLDYQLL
3	5'-GCTGAAGCAGTAATGTAA-3'	3'-UTR[a]	
4	5'-GTATGTACCCTTAGGAGTA-3'	3'-UTR	

[a]UTR, untranslated region

***Establishment of transgenic cell lines*:** The use of lentiviral plasmid vector for stable transfection conformed to the Biosafety level 2 (BL2) protocol 1170 approved by the Biosafety committee at Indiana University-Purdue University, Indianapolis. The mCCD cells were stably transduced with a lentiviral plasmid vector (pLKO-puro) encoding a shRNA mediating inversin knockdown and carrying a puromycin resistance gene for selection of transduced clones. A total of 5 shRNAs targeting different regions of the inversin mRNA were transfected separately into mCCD cells to determine efficiency of knockdown. The sequences of shRNAs targeting the inversin gene are shown in Table 17. Following initial transduction with 2, 10 and 20 MOI (multiplicity of infection) of the lentiviral particles for 48 h, stable pools were generated by placing the cells in media containing 2µg/ml of puromycin for selection of transduced cells containing inversin shRNA. The puromycin concentration was optimized in the mCCD cells. For clonal selection of the transduced cells, single cells from the stable pools from 20 MOI were sorted by BDFACS Aria II flow cytometer according to manufacturer's protocol and plated in a 96-well plate. The cells were allowed to grow in the puromycin-containing selection media. The clones were expanded, aliquoted and stored in liquid nitrogen for further use. MISSION® TRC2-pLKO-puro control vector containing an insert that does not target mouse or human sequence was used as non-targeting control

(NTC). The levels of inversin knockdown in stable pools and individual clones were determined by quantitative real-time PCR using inversin primers.

Table 17: Sequences of shRNA constructs targeting mouse *Invs*

Construct	**Target sequence**	***INVS* gene**
441	5'CGGAGGGTACATCAACTGTAT-3'	Exon 9
440	5'-CCTAATCAGATGGAGAACAAT-3'	Exon 10
442	5'-GCAGTCTATACATCTTGACAAC-3'	Exon 16
432	5'-CGCTTTACTATTTGCACCTAA-3'	3'-UTR[a]
571	5'-GCGCTTTACTATTTGCACCTAACT-3'	3'-UTR

[a]UTR, untranslated region

***Total RNA isolation and real-time PCR*:** Total RNA from each sample was isolated using RNeasy® mini kit isolation kit (Qiagen, Valencia, CA) according to manufacturer's protocol. Briefly, the samples were homogenized in lysis buffer and the lysate was passed five times through a blunt 20-guage needle fitted to an RNase-free syringe. One volume of 70% ethanol was added to the sample which was then applied to RNeasy spin column. The samples were centrifuged and the flow through was discarded. DNase treatment of the samples was performed using the RNase-free DNase set from Qiagen (Valencia, CA) and the samples were eluted in RNase-free water. RNA quality and quantity were determined by Agilent 2100 Bioanalyzer (Agilent Technologies, Inc. Santa Clara, CA, USA) according to manufacturer's instructions. First strand cDNA was synthesized from 1.5µg of total RNA with random hexamer primers using the SUPERSCRIPT II first strand synthesis kit (Invitrogen). The mRNA levels were determined by quantitative real-time PCR using ABI Prism Sequence Detection System

5700 (Applied Biosystems). The mRNA levels were normalized to 18S ribosomal RNA that served as an internal control.

***Immunodetection*:** Cells were lysed in lysis buffer (M-PER® mammalian protein extraction reagent, Thermo Fisher Scientific Inc. Waltham, MA) supplemented with complete protease inhibitor cocktail (Roche Diagnostics, Indianapolis, IN) and HALT™ phosphatase inhibitor cocktail (Thermo Fisher Scientific Inc, Waltham, MA). The protein concentrations were measured using Pierce™ Protein assay kit. Equal amounts of protein were separated by SDS-PAGE (sodium dodecyl sulfate polyacrylamide gel electrophoresis) on 4-20% Tris-glycine gels (Invitrogen™, Thermo Fisher Scientific, Waltham, MA). The proteins were transferred to nitrocellulose membranes using iBlot® gel transfer system. The membranes were blocked in 5% non-fat dry milk in TBS-T (Tris-buffered saline containing 0.05% Tween™-20) for 1 h at room temperature. The blocking reagent was removed and appropriate primary antibodies at a dilution of 1:1000 were added to the membranes and incubated for 2 h at room temperature. The membranes were washed with TBS-T for 15 min at room temperature by agitation. The wash step was repeated three times to reduce the background. The membranes were incubated with secondary antibodies (anti-rabbit IgG-HRP) at a dilution of 1:2000 in 1% milk-TBS-T for 1 h at room temperature with gentle agitation. The membranes were washed three times with TBS-T for 15 min at room temperature by agitation. The proteins were visualized using SuperSignal® West Pico Chemiluminescent substrate (Thermo Fisher Scientific, Waltham, MA). GAPDH was used as internal control.

***Electrophysiological analyses*:** siRNA or stably transfected mCCD cells with shRNA-mediated inversin knockdown (as determined by quantitative RT-PCR) or non-targeting control were used for measuring transepithelial ion transport. Electrophysiological techniques were employed to monitor changes in ion flux across the cellular monolayers as described previously (Shane et al, 2006). Briefly, transwell permeable membranes containing the confluent monolayers (14-16 days post-seeding) of mCCD cells were mounted onto Ussing chambers and connected to a DVC-1000 voltage/current clamp (World Precision Instruments) with voltage and current electrodes on either side of the membrane. The cells were bathed in serum-free medium maintained at 37^{o}C via water-jacketed buffer chambers on either side of the filter. Media were circulated and kept at constant pH using a 5% CO_2/95% O_2 gas lift. The spontaneous transepithelial potential difference was clamped to zero, and the resultant short circuit current (SCC) was monitored continuously. Under these conditions, SCC is a measure of net transepithelial ion flux. Basal SCC was measured for 30 min prior to the addition of arginine vasopressin (AVP), a stimulator of Cl^- and Na^+ transport at time=0. AVP (100 mU/ml) was added to the serosal (basolateral side) bathing medium and the SCC were monitored for 30 min. Amiloride ($1x10^{-5}$ M), a specific inhibitor of ENaC was added to the apical bathing medium 30 min following the addition of AVP to determine if the changes observed in SCC were due to Na^+ transport via ENaC.

***Statistics*:** Data are represented as means ± standard deviation or standard error of mean. Differences between two groups were analyzed by an unpaired Student's *t*-test. Differences were considered significant when $P<0.05$.

Results

The mCCD cell line exhibits the characteristics of the distal tubule cortical collecting duct principal cell type including high transepithelial resistance ($\geq$1,000Ω.cm^2), expression of ion transporters and responsiveness to hormones such as AVP and aldosterone (Gaeggeler et al, 2005; Gaeggeler et al, 2011). These features together with endogenous expression of inversin make the mCCD cell line an ideal model to examine the role of inversin in ion transport. For ion transport measurements the cells were grown in culture for two weeks to develop a fully polarized high resistant phenotype. Long-term gene silencing of endogenous inversin was performed using two approaches in mCCD cells, (1) Accell™ technology that utilizes a passive delivery of siRNA (2) stable knockdown of inversin by lentiviral delivery of inversin shRNA. The inversin-depleted mCCD cells from both approaches were used to measure transepithelial ion transport by electrophysiology.

***Inversin knockdown in mCCD cell line by Accell™ siRNA technology*:** Initially, inversin siRNA was used to test the feasibility of inversin knockdown in mCCD cells. As shown in Figure 9, treatment with different concentrations (1-4µM) of siRNA resulted in 12-43% decrease in inversin mRNA levels following 2 weeks in culture. Surprisingly, the least concentration of siRNA (1µM-1 treatment) resulted in the highest knockdown (43%) in this experiment. The increase in siRNA concentration did not correlate with the reduction in inversin expression. This effect could be the result of inefficient siRNA uptake due to cell growth as the cells were in culture for 2 weeks. Nevertheless, the

siRNA treatments did result in different levels of inversin knockdown in mCCD cells that were useful in preliminary experiments on ion transport.

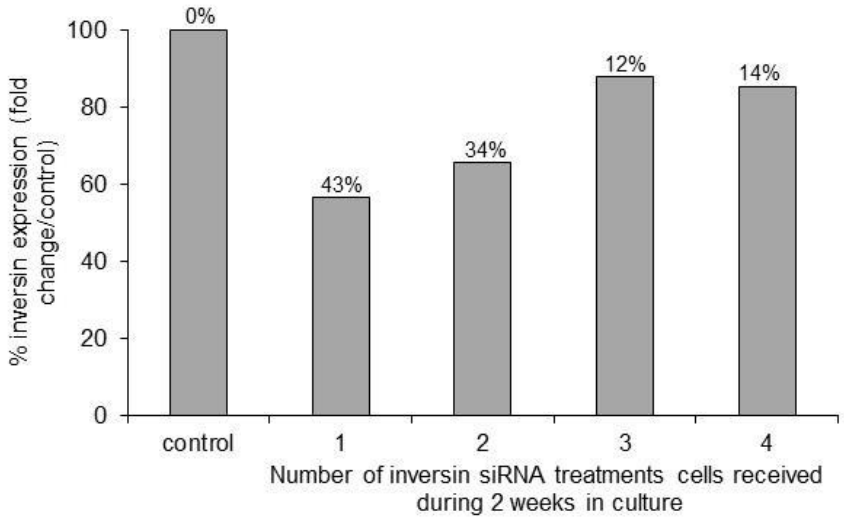

Figure 9: Long-term gene silencing in mCCD cells using inversin Accell™ siRNA. Following initial plating in the growth medium the cells were treated with 1µM of inversin siRNA resuspended in Accell delivery media. After 24 h of siRNA treatment the Accell delivery media was replaced with the growth medium. The treatment with siRNA was repeated for a total of 1-4 times for 2 weeks. At the end of the treatment mRNA levels were assessed by quantitative real-time PCR. The data were normalized to 18S RNA and expressed as fold-change over untreated control. Value above each bar represents the % inversin knockdown with siRNA treatment.

***Inversin modulates transepithelial ion transport in inversin-depleted mCCD cells obtained using Accell™ siRNA technology*:** Initially, the functional effect of inversin loss was measured as changes in net transepithelial ion transport across high resistance epithelia formed by the mCCD cell line. Confluent cell layers grown on permeable supports were mounted onto Ussing chambers and short circuit current (SCC) was used to measure electrogenic ion flux. By convention, a change in SCC in epithelial cells could be due to an anion moving from basolateral to apical media (secretory) or a cation moving from apical to basolateral media (absorptive). Following the equilibration of basal SCC for 30 min, AVP (100 mU/ml) was added at time=0 to the serosal (basolateral side) bathing medium and the SCC was monitored for additional 30 min. As shown in Figure 10A, AVP stimulation showed a biphasic response in these cells, a rapid transient anion secretory response peak possibly via CFTR (Cl^- secretion) followed by a delayed cation absorptive response via ENaC (Na^+ absorption). Interestingly, inversin knockdown did not alter the AVP-induced anion secretory peak but decreased the cation absorptive peak compared to control cells. Addition of amiloride, a specific blocker of epithelial sodium channel (ENaC) to the apical side decreased the net ion transport to zero in both inversin knockdown and control cells, indicating ENaC involvement (Figure 10A).

The majority of the basal SCC in principal cells is due to the flux of Na^+ in an absorptive direction (Shane et al, 2006). As shown in Figure 10A, loss of inversin had a profound negative effect on the basal SCC in inversin knockdown cells as compared to control. As indicated in Figure 10B, the magnitude of basal SCC correlates with inversin mRNA levels in control and inversin knockdown mCCD cells.

The changes in basal SCC associated with net transepithelial ion transport in inversin knockdown compared to control cells appear to be due to an amiloride-sensitive absorptive Na^+ flux. However, multiple ion channels may be activated in response to stimulation with hormones that are known to be active in renal principal cells. The predominate channels previously shown to be present in canine collecting duct cells (Lahr et al, 2000) indicate that the transport changes could be due to an anion (Cl^- or HCO_3^-) secretion and/or cation (Na^+, K^+) reabsorption. Arginine vasopressin (AVP), an anti-diuretic hormone regulates the activities of water channels and ion channels in the collecting duct. The two ion channels that are positively regulated by AVP are cystic fibrosis transmembrane regulator (CFTR), a Cl^- channel and ENaC (Nofziger et al, 2009).

Although Accell™ siRNA technology provided inversin knockdown for proof of concept studies on ion transport, siRNA technique had limitations for long term gene silencing in mCCD cells. Since ion transport studies require cells to be grown in culture for 2 weeks, the addition of siRNA with every media change may interfere with consistency between experiments. Additionally, there was no positive correlation with dose of siRNA and the inversin knockdown levels in this study. Alternatively, further experiments on ion transport were conducted in mCCD cells carrying a shRNA-mediated stable inversin knockdown. shRNAs can be stably integrated through virus-mediated integration into the nucleus that provide prolonged stable gene silencing.

A

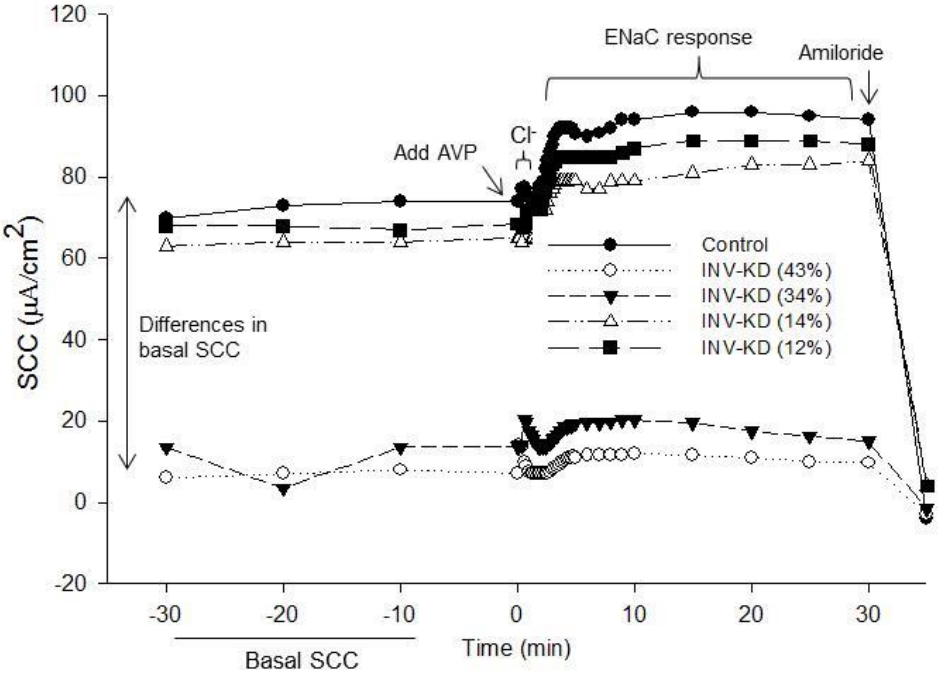

B

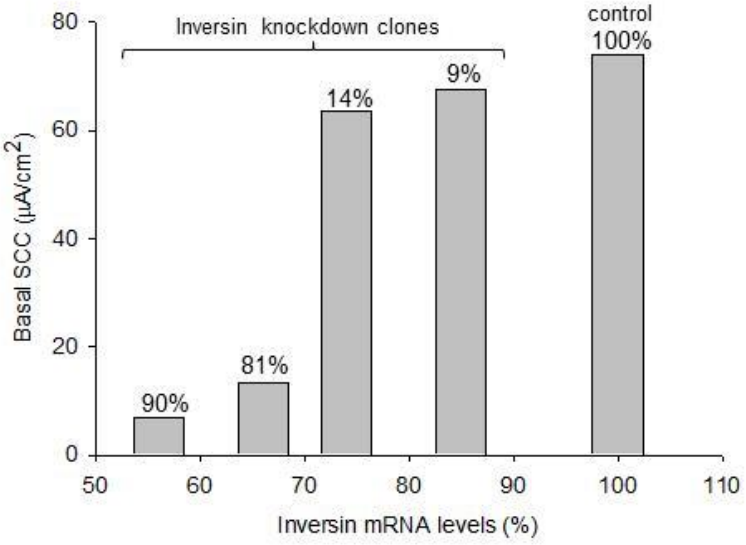

Figure 10: Transepithelial ion transport in inversin knockdown mCCD cells obtained from Accell™ siRNA technology. The cells with inversin knockdown and the control were grown to confluence on permeable Transwell supports for two weeks and the net ion transport was measured as short circuit current (SCC) using Ussing-chamber electrophysiological techniques. Basal SCC was measured for approximately 30 min. (**A**) Electrophysiological tracings show changes in basal SCC with 12, 14, 34 and 43 %

respectively in inversin knockdown compared to control cells as indicated by the arrow. Following the measurement of basal SCC for 30 minutes, the cells were stimulated with arginine vasopressin (AVP) at a concentration of 100mU/ml at time=0 and the SCC were recorded for 30 minutes. Electrophysiologic traces show no change in the initial chloride secretory peak but a decrease in the delayed sodium absorptive peak in an inversin-level dependent manner. (**B**) Basal SCC correlates with inversin mRNA levels. Value above each bar represents the % change in basal SCC.

***Stable inversin knockdown using shRNA in mCCD cells*:** Since gene silencing with Accell™ technology had limitations for long term knockdown of inversin in mCCD cells as shown above, it was crucial to generate a cell line with stable inversin knockdown. To induce inversin depletion, mCCD cells were stably transduced with a lentivirus encoding inversin shRNA. A total of 5 different shRNAs sequences (Table 17) targeting different regions of the inversin mRNA were used to determine efficiency of inversin knockdown as determined by quantitative RT-PCR. Multiplicity of infection (MOI) corresponding to 2 and 10 transducing lentiviral particles/mCCD cell were tested with each construct to determine the optimal transduction efficiency. As shown in Table 18, out of five inversin shRNA constructs tested, two constructs (440 and 441) showed the highest levels of inversin knockdown. The levels of inversin knockdown with construct 440 were 17, and 45% and construct 441 were 7, and 31% respectively, with 2, and 10 MOI. For the remaining three constructs (438, 442 and 571) the inversin knockdown levels ranged between 0 to 21% knockdown with 2 and 10 MOI compared to NTC. The higher levels of inversin knockdown in shRNA constructs 440 and 441 compared to the other 3 constructs could be due to the targeting of exon 9 and 10 versus the rest of the constructs that targeted exon 16 and 3'UTR (Table 17). Constructs 440 and 441 were further tested at 20 MOI to determine if increased levels of transduction

particles would result in even higher levels of inversin knockdown. Construct 440 at 20 MOI showed a 62% reduction in inversin levels compared to 45% at 10 MOI. Construct 441 at 20 MOI showed a 32% reduction in inversin levels compared to 31% at 10 MOI. Therefore, construct 440 was selected for further experimentation based on the dose-dependent increase (17, 45 and 62%) in inversin knockdown levels observed with 2, 10 and 20 MOI.

Table 18: Percent levels of inversin knockdown with different doses of inversin shRNA lentiviral particles in mCCD cells compared to NTC [a]

Construct ID	**Multiplicity of infection**		
	2	**10**	**20**
440	17	45	62
441	7	31	32
442	5	13	ND[b]
438	0	17	ND
571	6	-1	ND

[a]mCCD cells were treated with different doses of lentiviral particles carrying inversin shRNA. Total RNA was isolated following 48 hours infection and levels of inversin were assessed by quantitative RT-PCR. The levels of inversin were normalized to 18S ribosomal RNA and the data are expressed as fold change over NTC. Each dilution of lentiviral particles was plated in triplicate and the samples were pooled for gene expression analysis. NTC when compared to untransfected control cells showed a 10%, 4% and 0% change in inversin expression level at 2, 10 and 20 MOI. NTC, non-targeting control; [b]ND, not determined

Following clonal selection, 11 stable clones were obtained from shRNA construct 440. As shown in Table 19, the levels of inversin knockdown ranged between 18-81% compared to NTC in clones obtained from construct 440 and this could be due to differences in the sites of integration of the construct in the genome. Clones with 81% (clone 440-2) and 18% (clone 440-9) inversin knockdown was used for electrophysiological experiments. Since electrophysiology requires the cells be grown in culture for 2 weeks for formation of tight junctions, inversin mRNA levels were measured in cells from clones 440-2 and 440-9 following 2 weeks in culture. As shown in Figure 11, clone 440-2 showed 75% inversin knockdown, whereas in clone 440-9 the inversin knockdown levels increased from 18 to 38% compared to NTC. This increased inversin knockdown in (clone 440-9) cells with prolonged culture (2 weeks) perhaps could be attributed to an increased transcription of shRNA over time in culture.

Table 19: Percent inversin knockdown in stable clones and non-targeting control[a]

Clone #	**Percent inversin knockdown versus NTC-11**
NTC-11	0
440-2[b]	81
440-3	53
440-4	62
440-9[b]	18
440-10	79
440-12	61
440-13	52
440-15	71
440-19	56
440-20	63
440-22	59

[a]Stable clones carrying inversin shRNA from construct ID 440 were selected in puromycin containing selection media. Total RNA was isolated from the clones and levels of inversin were assessed by quantitative RT-PCR. The levels of inversin were normalized to 18S ribosomal RNA and the data are expressed as fold change over NTC. NTC when compared to untransfected control cells showed 6% knockdown. NTC, non-targeting control; [b]clones used for subsequent experiments

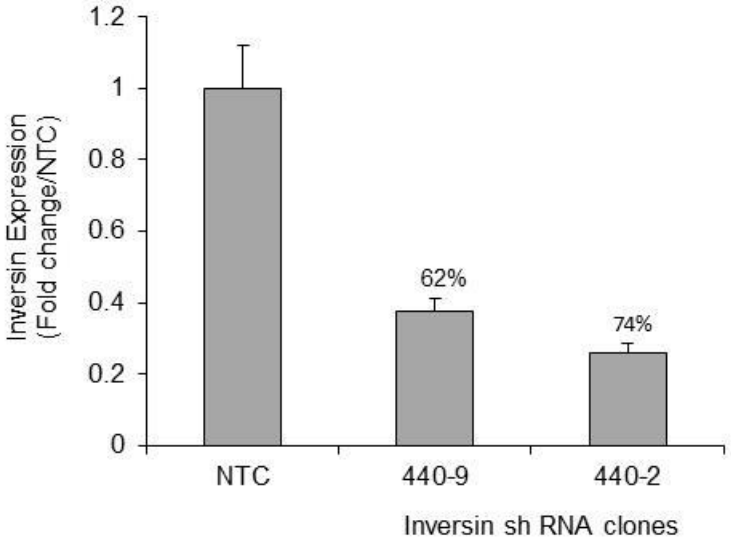

Figure 11: Expression levels of inversin in stable inversin knockdown using shRNA and untransfected mCCD cells. Cells were transduced with shRNA (construct 440) or non-targeting control (NTC). NTC is the control vector containing an insert that does not target the mouse or human sequence. Inversin mRNA levels in the confluent cells were assessed by quantitative real-time PCR. The data were normalized to 18S RNA and expressed as fold change over NTC. Inversin mRNA levels in cells from untransfected control, NTC, clone 440-9 and 440-2 following 3 days in culture. Values are mean ± SD; n=5.

***Loss of inversin decreases basal and AVP-stimulated Na^+ transport in mCCD cells*:** Confluent 440-9 and 440-2 cell layers grown on permeable supports were mounted onto Ussing chambers and short circuit current (SCC) was used to measure electrogenic ion flux. Following the equilibration of basal SCC for 30 min, arginine vasopressin (AVP) was added to the basolateral side of the cell monolayer. Addition of AVP resulted in a rapid, transient (0-4 min) anion Cl^- secretory response and delayed (4-30 min) cation Na^+ absorptive response in control and inversin knockdown cells (Figure 12A). A significant decrease in basal SCC was observed in both 440-9 and 440-2 clones indicating an altered ion flux with inversin loss. Interestingly, the basal SCC paralleled the inversin mRNA levels as shown in Figure 12B.

AVP stimulation did not show a significant change in the Cl^- secretory response but decreased cation (Na^+) flux in both 440-9 and 440-2 inversin-depleted clones compared to the control cells. Furthermore, addition of amiloride, a specific inhibitor of ENaC decreased the net ion transport to zero indicating ENaC involvement (Figure 12A). The magnitude of Na^+ absorptive response of the control and inversin knockdown clones was calculated as a mean change in SCC from baseline to the maximal response at 30 min following addition of AVP. The Na^+ flux was significantly decreased in both inversin-depleted (440-2 and 440-9) clones compared to the control cells (Figure 12C)**.** The magnitude of Cl^- secretion was calculated as the mean change in SCC from baseline to maximal response on the Cl^- peak from all the replicates. As shown in Figure 12D the magnitude of Cl^- secretion was not statistically significant between control and inversin knockdown cells. Furthermore, the transepithelial resistances of cells measured were not

statistically different between NTC and inversin knockdown clones. These results suggest that inversin plays a role in Na^+ transport via ENaC.

A

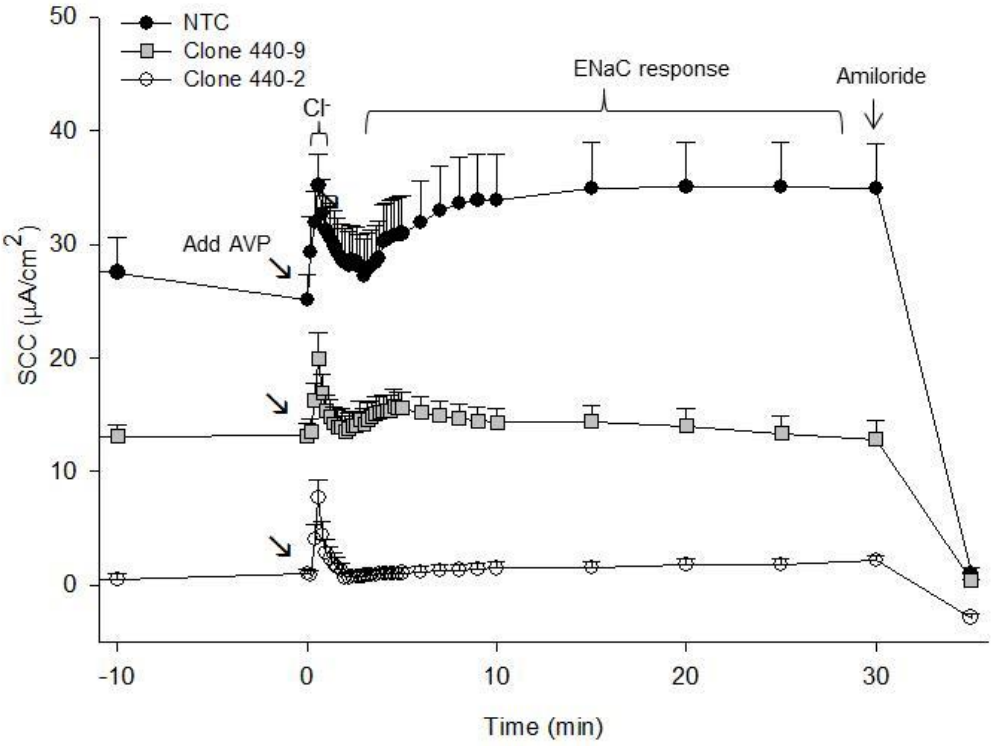

B

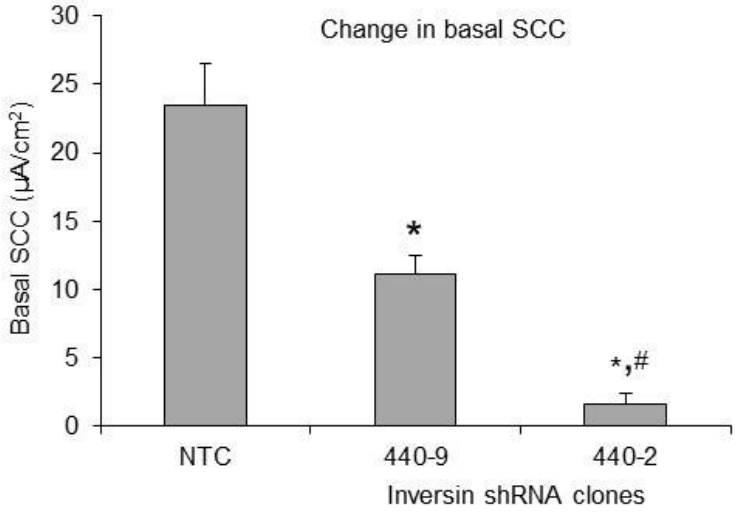

Figure 12: Transepithelial ion transport in stably transduced inversin knockdown in mCCD cells.

C

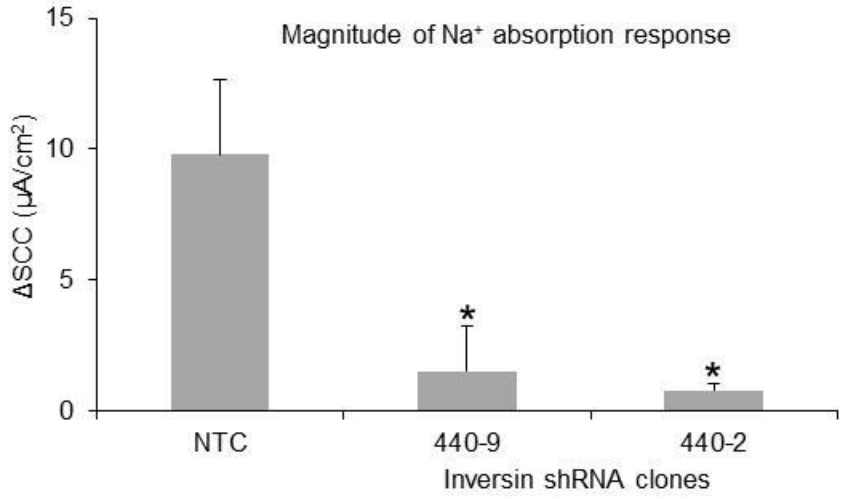

D

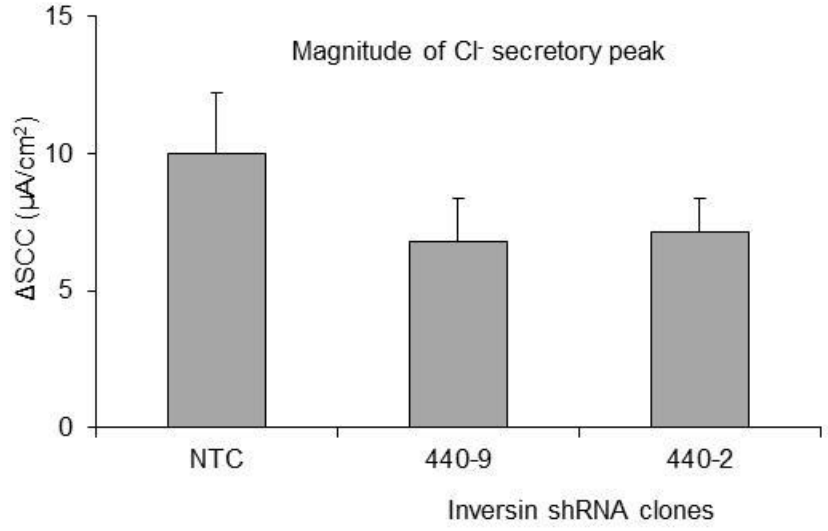

Figure 12 continued

Figure 12: Transepithelial ion transport in stably transduced inversin knockdown in mCCD cells. The inversin knockdown (clones 440-9 and 440-2) and control (NTC) cells were grown to confluence on permeable Transwell supports for two weeks and the basal ion transport was measured as short circuit current (SCC) using Ussing-chamber

electrophysiological techniques. Basal SCC was measured for approximately 30 min (shown 10 min) and the cells were stimulated with arginine vasopressin (AVP) at a concentration of 100mU/ml at time=0 and SCC was recorded for additional 30 min. Amiloride (a specific inhibitor of ENaC; $1x10^{-5}$M) added at the end of 30 min. (**A)** Electrophysiological tracings of control and inversin knockdown clones (440-9 and 440-2). (**B)** Quantitation of basal SCC in control and inversin knockdown cells correlates with inversin mRNA levels as shown. Values are mean ± SEM; n=19 for NTC; n=17 for clones 440-9 and 440-2 inversin knockdown samples; *$p<0.05$ vs NTC, # vs 440-9 clone. (**C**) SCC representing the amiloride-sensitive response showing a decreased Na^+ transport in inversin knockdown clones compared to control. **(D)** Magnitude of Cl^- secretory peak showing no significant change in inversin-depleted cells compared to control. Values are mean ± SEM; n=9 for NTC; n=6 for clone 440-9; n=8 for 440-2.

To further confirm that the effect of inversin knockdown on the AVP-induced delayed cation flux response was due to Na^+, the cells were pre-treated with amiloride. As shown in Figure 13A, addition of amiloride caused an immediate decrease in the basal SCC in both control and inversin knockdown cells from clones 440-2 and 440-9 demonstrating that the basal ion flux is primarily due to Na^+ transport consistent with an earlier report in a collecting duct cell line (Shane et al, 2006). Subsequent stimulation of the cells with AVP showed a rapid transient anion secretory response but, as expected, not the delayed Na^+ flux in either control or inversin knockdown cells (clones 440-2 and 440-9). As in the previous experiment, the changes in Cl^- secretion (Figure 13B) were not statistically different between control and inversin-depleted cells from clones 440-2 and 440-9. These data suggest that loss of inversin decreases Na^+ transport from apical to basolateral side (reflecting decreased Na^+ reabsorption *in vivo*) in mCCD cells via ENaC.

To validate if the arginine vasopressin-stimulated Cl^- secretory response is via CFTR, the control cells were stimulated with 100µM GlyH-101, a CFTR inhibitor prior to addition of vasopressin. As shown in Figure 13C, addition of CFTR inhibitor significantly inhibited the Cl^- secretory response stimulated by vasopressin indicating that Cl^- secretion is occurring via CFTR.

A

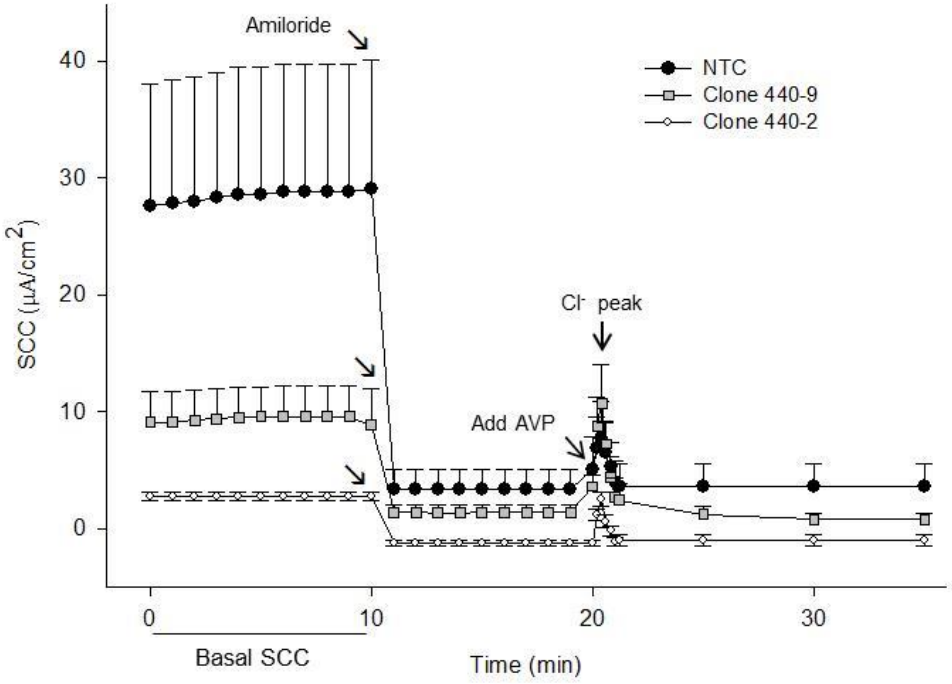

B

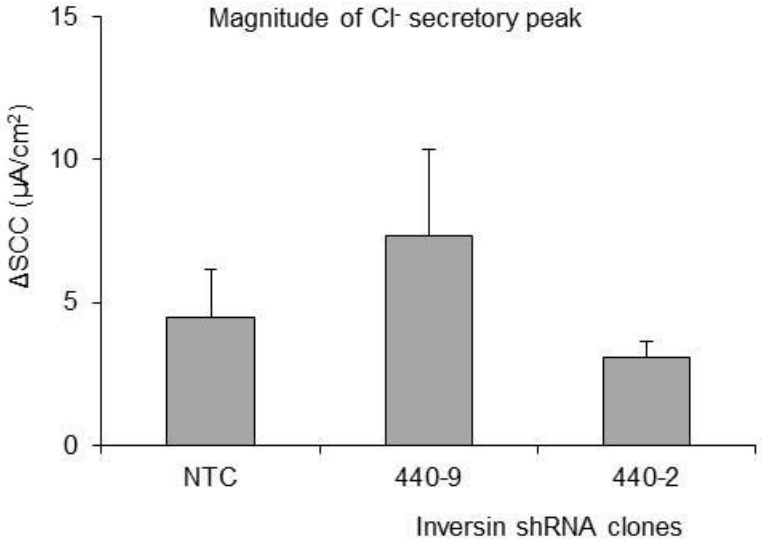

Figure 13: Loss of inversin decreases transepitihelial sodium transport.

C

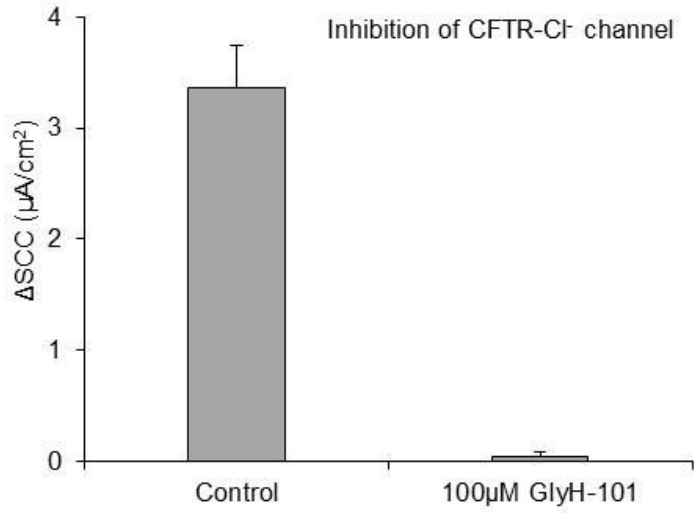

Figure 13 continued

Figure 13: Loss of inversin decreases transepithelial sodium transport. To confirm the delayed Na^+ absorptive response is via ENaC, following stabilization of SCC, the cells were pre-treated with amiloride (a specific inhibitor of ENaC; $1x10^{-5}$ M) and the SCC was recorded for 10 min. The cells were then treated with arginine vasopressin (AVP) at a concentration of 100mU/ml and the SCC was recorded for additional 30 min. (**A)** Amiloride treatment decreased the basal ion transport to zero and stimulation with AVP showed a rapid anion secretory (Cl^- peak) but not the delayed Na^+ absorptive response in inversin knockdown compared to control cells. (**B)** Magnitude of Cl^- secretion showing no significant change in inversin-depleted cells compared to controls. Values are mean ± SEM; n=5. (**C**) Addition of CFTR inhibitor GlyH-101 significantly decreased the vasopressin-stimulated Cl^- secretory peak. Values are mean ± SEM; n=4 for control group and n=5 for GlyH-101group

***Loss of Inversin modulates the expression of ENaC and its upstream regulators*:** Mechanisms for regulation of ion transport include transcriptional and post-translational modifications such as, phosphorylation, ubiquitinylation and enzymatic cleavage (Bhalla & Hallows, 2008). These processes together determine the abundance and activity of ion transporters at the plasma membrane. ENaC is a heteromeric protein made up of three homologous subunits; Scnn1 (sodium channel non neuronal1) alpha (α), Scnn1 beta (β) and Scnn1 gamma (γ) that form the channel (Canessa et al, 1994). To elucidate the mechanism of inversin knockdown on ENaC-mediated Na^+ transport, transcript levels encoding the Scnn1α, Scnn1β, Scnn1γ subunits of ENaC were measured. As shown in Figure 14 there was a significant increase in Scnn1α (1.4-fold) in clone 440-2 but not in clone 440-9 compared to control cells; Scnn1β expression was significantly decreased in both clones (440-9 and 440-2) in inversin-depleted cells compared to controls. In addition, a decrease in Scnn1γ mRNA (2-fold) was observed in clone 440-9 compared to the control cells. To examine potential regulatory components, expression levels of Nedd4l, an ubiquitin ligase that has been to shown to target ENaC for degradation and two of the upstream regulators of Nedd4l, Sgk1 and Crtc2 were also evaluated in inversin-depleted renal epithelial cells. As shown in Figure 16, an increase in the expression levels of the Nedd4l and a decrease in Sgk1 and Crtc2 would be expected to accompany a reduced ENaC activity. However, as shown in Figure 14, the transcript levels of Nedd4l was not significantly altered upon loss of inversin but a significant increase in the mRNA levels of Sgk1 (~ 6-fold) were accompanied by a significant decrease in Crtc2 (1.3-fold) in both inversin-depleted clones (440-9 and 440-2) compared to the control cells. Since stimulation of Na^+ absorption occurs by

coordinated activation of epithelial sodium channel (ENaC) and Na^+, K^+ ATPase, the expression level of Atp1a1, a subunit of Na^+, K^+ ATPase was evaluated in inversin-depleted renal epithelial cells. Interestingly, there was a significant increase in Atp1a1 subunit in clone 440-2 (1.5-fold). These results suggest that inversin modulates the transcription of ENaC subunits and its upstream regulators involved in Na^+ transport in mCCD cells either directly or via a complex interplay of factor involved in ENaC synthesis and membrane targeting.

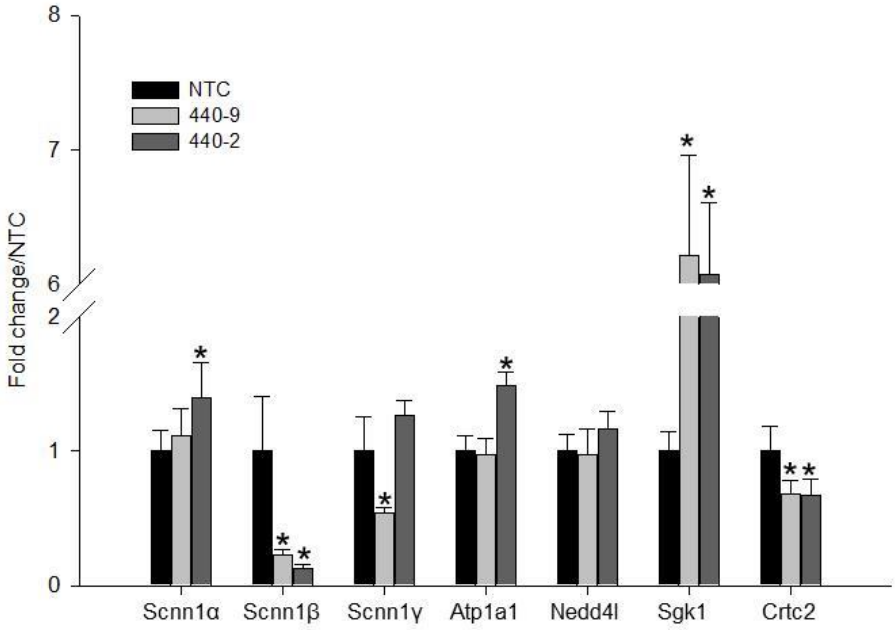

Figure 14: Expression levels of epithelial sodium channel (ENaC) subunits and genes that regulate ENaC in inversin knockdown mCCD cells. Total RNA was isolated from control (NTC) and inversin knockdown cells (clones 440-9 and 440-2) and gene expression changes were determined by quantitative real-time PCR. The mRNA levels were normalized to 18S ribosomal RNA that served as an internal control. The changes in gene expression of (Scnn) 1α (sodium channel non neuronal 1α), Scnn1β (sodium channel non neuronal 1β) Scnn1γ (sodium channel non neuronal 1γ), Nedd4l (neural precursor cell expressed, developmentally downregulated 4 like), Atp1a1 (Na^+/K^+ ATPase transporting subunit alpha 1), Sgk1 (serum glucocorticoid-inducible kinase1) and Crtc2 (creb-regulated transcription coactivator) are expressed as fold change over NTC (non-targeting control). Values are mean ± SEM. (n=5), *$p<0.05$ vs NTC

***Loss of Inversin decreases the phosphorylated form of Nedd4l*:** Since phosphorylation regulates the activity of Nedd4l, both phosphorylated and total forms of this enzyme was measured. As shown in Figure 15A, Nedd4l is phosphorylated by Sgk1 which in turn is activated by phosphorylation by Crtc2 kinase within the C-terminal hydrophobic motif (Ser422). The phosphorylated form of Nedd4l which renders Nedd4l inactive was decreased in inversin-depleted cells compared to the control cells (Figure 15B) with no change in the total Nedd4l levels (Figure 15C) consistent with RNA levels. The decrease in phosphorylated form of Nedd4l would result in a relative increase in the active Nedd4l. Since Nedd4l is a negative regulator of ENaC (Snyder et al, 2002) (Wilson, 2004)an increase in its active form would be expected to result in decreased ENaC activity. Unfortunately, validated reagents are not available to measure phosphorylated Sgk1 but levels of total Sgk1 were slightly increased at the protein level (Figure 15D) although the transcript levels were significantly increased as compared to control. However, Crtc2 protein levels were decreased in clone 440-2 (highest knockdown) but not in 440-9 inversin-depleted mCCD clones (Figure 15E). These results suggest that reduced ENaC activity upon inversin loss is mediated in part via the post-translational regulation of Crtc2/Sgk1/Nedd4l axis in addition to transcriptional effects.

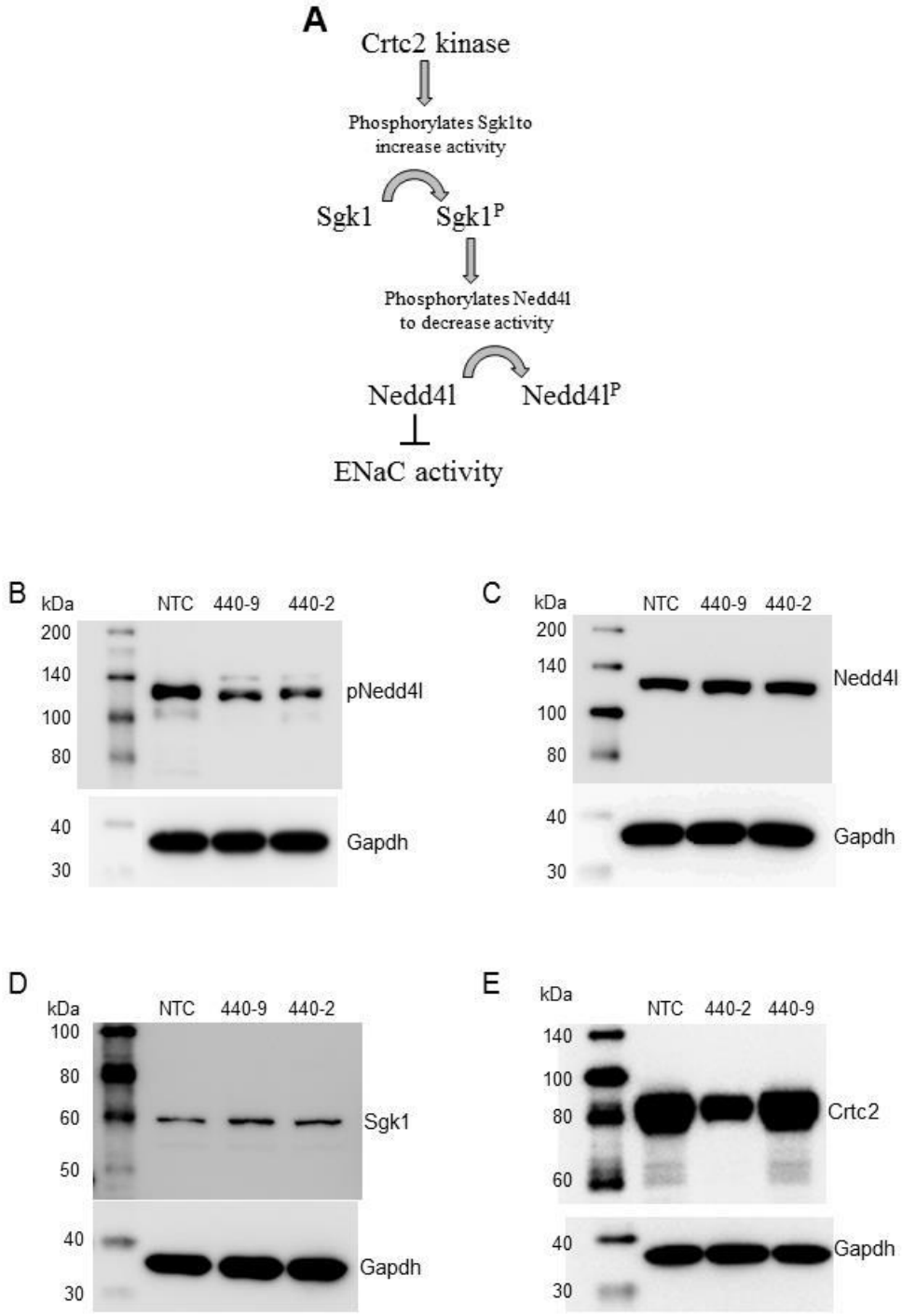

Figure 15: Regulation of Crtc2, Sgk1 and Nedd4l protein expression in inversin knockdown mCCD cells. (**A)** Diagram depicting the regulation of epithelial sodium channel activity via Crtc2/Sgk1/Nedd4l. **(B-E)** Western blot analysis of Crtc2 (creb-regulated transcription coactivator 2), Sgk1 (serum and glucocorticoid-inducible kinase1) and Nedd4l (neural precursor cell expressed, developmentally downregulated 4 like) in

control and inversin knockdown mCCD cells. Whole cell lysates were prepared as described in Materials and Methods. The proteins were separated by SDS-PAGE and transferred to nitrocellulose membranes. The blots were immunostained using antibodies directed against (**B**) Total Nedd4l (**C)** phosphorylated Nedd4l (**D)** total Sgk1, (**E)**: Crct2 at 1:1000 dilution. Anti-GAPDH was used as internal control. NTC, (non-targeting control)

Discussion

NPHP2 is an infantile form of autosomal recessive disease caused by mutations in the *Invs* (inversin) gene that causes microcystic dilatations within tubules, as well as in the Bowman's space, glomerulus and collecting ducts at the corticomedullary junctions of the kidney (Gagnadoux et al, 1989). This study validates the gene array findings of *inv/inv* mice kidneys on ion transport mechanism to understand inversin function in renal cyst growth and expansion associated with NPHP2. Using stable clones of inversin knockdown in mouse cortical collecting duct (mCCD) cells, together with arginine vasopressin (AVP), a stimulator of cation reabsorption and anion secretion, this study demonstrates that depletion of inversin results in a dose-responsive reduction in Na^+ transport. There have been some previous findings that support a role of inversin in ion transport. For example, in a *Xenopus* model, loss of inversin has been shown to result in edema (Lienkamp, 2010). Also, in mouse embryonic fibroblasts obtained from *inv*$^{-/-}$ mice aberrant expression and targeting of the Na^+/H^+ exchanger NHE, an antiporter involved in volume and pH regulation have been reported (Veland et al, 2013). Although these data support the premise of fluid accumulation and abnormal ion transport upon inversin loss, they do not address the regulation of specific ion transport in the kidney.

In this study, the reduced AVP-induced cation response seen in inversin-depleted cells was amiloride-sensitive demonstrating reduced ENaC activity and hence suggesting that Na^+ transport contributes to the reduced cation transport seen in inversin-depleted mCCD cells. Decreased ENaC activity has also been demonstrated in the principal cells of the collecting duct from the *bpk* (BALB/c polycystic kidney) autosomal recessive PKD (ARPKD) mice (Veizis et al, 2004) as well as in the cystic epithelium of PCK rats, an

orthologous model of autosomal recessive PKD (ARPKD) with mutations in *PKHD1* gene (Pavlov et al, 2015; Ward et al, 2002). This form of ARPKD also causes fetal or neonatal death but is characterized by the expansion and elongation of collecting ducts into multiple small cysts (Adeva et al, 2006). A decrease in Na^+ reabsorption via ENaC upon loss of inversin in renal epithelial cells may be a common mechanism in autosomal recessive kidney disorders. Since fine tuning of Na^+ reabsorption occurs in the collecting ducts and ENaC activity is a rate-limiting step, a minor decrease in ENaC activity could have an impact on Na^+ transport and over time contribute to fluid accumulation in renal cysts.

AVP can also stimulate Cl^- secretion via CFTR, a chloride channel expressed in renal epithelial cells. This activity was not altered in inversin knockdown cells. The observation on the lack of effect of inversin knockdown on Cl^- secretion is in contrast to that observed in autosomal dominant polycystic kidney disease (ADPKD). In ADPKD, fluid accumulation in renal cysts is primarily driven by increased Cl^- secretion together with increased channel-mediated water permeability via aquaporins (Terryn et al, 2011). The results of this study lead to the conclusion that despite overall phenotypic similarities in terms of enlarged cystic kidneys with both recessive and dominant forms of PKD, different mechanisms of ion transport control cyst growth and expansion. This may relate in part to the different mechanisms of cyst formation in these two disease states. In contrast to tubular dilatations in NPHP2 or ARPKD, in ADPKD the renal cysts bud off from the nephron and no longer communicate with the tubule from which they originate (Wilson, 2004).

ENaC plays an important role in the regulation of Na^+ homeostasis (Bhalla & Hallows, 2008; Rossier et al, 2002). To understand how loss of inversin may lead to reduced ENaC activity in mCCD cells, the expression levels of ENaC subunits and its upstream regulator Nedd4l were examined on inversin knockdown in renal epithelial cells. Direct evidence of the importance of ENaC in salt homeostasis has come from the molecular analysis of genetic diseases disturbing salt reabsorption leading to hypo- or hypertensive phenotypes (Warnock, 1998). Liddle syndrome is an autosomal form of salt-sensitive hypertension due to abnormal sodium reabsorption by the renal tubule (Warnock, 1998). Patients with Liddle syndrome carry mutations in β or γ subunit of ENaC that results in increased ENaC numbers and activity resulting in increased Na^+ reabsorption (Schild et al, 1995; Shimkets et al, 1994). This is in part due to the inability of Nedd4l binding to ENaC (Kamynina et al, 2001; Staub et al, 1996). Nedd4l, an ubiquitin protein ligase, modulates ENaC surface expression (Kabra et al, 2008). Unphosphorylated Nedd4l represses epithelial Na^+ flux by ubiquitination, endocytosis and degradation of ENaC (Snyder et al, 2002). Interestingly, mice deficient in β subunit of ENaC exhibit increased natriuresis and die within 2 days after birth (McDonald et al, 1999). The observed decrease in phosphorylated Nedd4l (which renders Nedd4l inactive) together with a decrease in the RNA levels of Scnn1β upon loss of inversin may explain the reduced ENaC activity observed in this study.

Sgk1 has been established as a convergence point for multiple regulators of Na^+ transport and dysfunctions of Sgk1 in the kidneys has been linked to altered renal Na^+ transport (Faletti et al, 2002; Loffing et al, 2006). $Sgk1^{-/-}$ mice display significant loss in renal NaCl and body weight under dietary Na^+ restriction (Wulff et al, 2002). In

addition, *ex vivo* experiments on collecting ducts showed a decreased transepithelial amiloride-sensitive potential that is consistent with reduced Na^+ transport in the cortical collecting duct (Wulff et al, 2002). The mineralocorticoid aldosterone, a principal regulator of Na^+ homeostasis is central to the control of extracellular fluid volume and blood pressure (Pearce, 2003). Sgk1 expression is induced by aldosterone and its catalytic activation is stimulated by phosphorylation (Pearce, 2003). In this study, loss of inversin increased the transcript levels of Sgk1 but did not alter total Sgk1 protein. Although the phosphorylated form of Sgk1could not be assayed in this study (due to lack of reagents), the levels of Crtc2, a kinase that is essential for Sgk1 activity and required for ENaC-dependent Na^+ reabsorption were decreased (Lu et al, 2010). Interestingly, Crtc2 has previously been shown to regulate renal tubule Na^+ homeostasis through Sgk1-dependent modulation of ENaC activity (Gleason et al, 2015). A possible model of the effects of inversin loss on ENaC via the Crtc2/Sgk1/Nedd4l axis is shown in Figure 16. Further studies will be needed to determine if inversin has a direct or indirect effect on this axis. It is also possible that the effects of inversin loss on Na^+ transport via ENaC could be due to changes in cytoskeletal activity (Veland et al, 2013). In addition, this study does not exclude the contribution of other transporters such as K^+ secretion to fluid accumulation in NPHP2.

In summary, the data demonstrate for the first time that inversin plays a role in transepithelial ion transport in renal epithelial cells. The findings suggest that loss of inversin leads to decreased Na^+ reabsorption via ENaC and this effect is in part mediated by transcriptional and post-translational regulation of the Crtc2/Sgk1/Nedd4l axis. A

defective Na^+ absorption in renal epithelial cells as observed in this study may contribute to fluid accumulation in NPHP2.

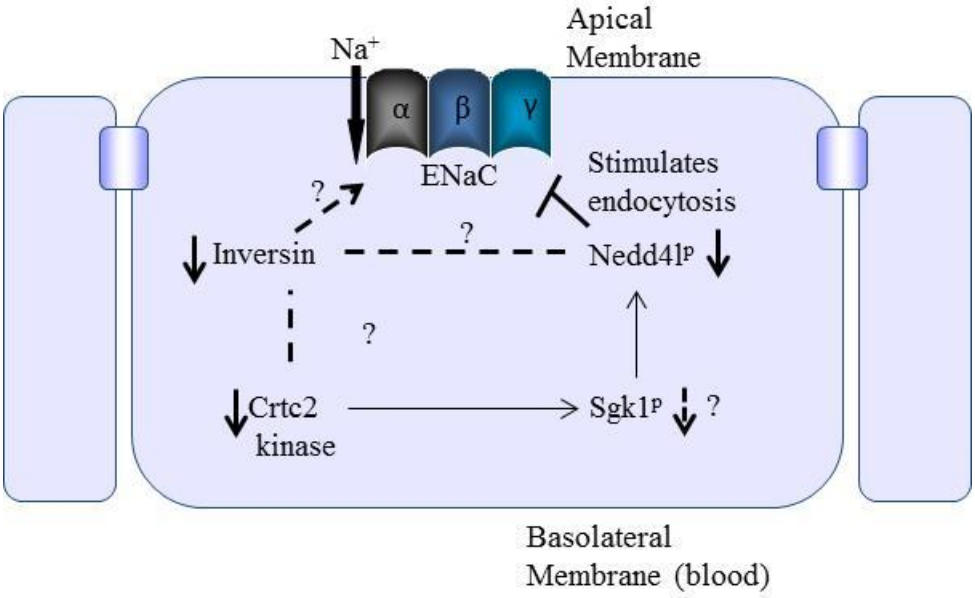

Figure 16: Proposed model for epithelial sodium channel (ENaC) regulation upon inversin loss in renal epithelial cells. Loss of inversin may reduce Crtc2 (creb-regulated transcription coactivator 2) levels that may result in decreased phosphorylation of Sgk1 (serum and glucocorticoid-inducible kinase) which in turn can cause decreased phosphorylation of Nedd4l (neural precursor cell expressed, developmentally downregulated 4 like) leading to increased degradation of ENaC by Nedd4l. Thus reduced ENaC activity can result in decreased Na^+ transport in inversin-depleted mCCD cells.

CHAPTER 4: TRANSCRIPTOME ANALYSIS OF INVERSIN-DEPLETED RENAL EPITHELIAL CELLS: COMPARSION OF *IN VITRO* WITH *IN VIVO* ARRAY DATA

Introduction

Gene array data on *inv/inv* mice cystic kidneys showed that inversin effects on kidneys are attributed, at least, in part through transcriptional regulation of genes implicated in inflammation, immune response, cellular metabolism, cell cycle and ion transport. The kidney is a complex organ comprising of multiple cell types and in addition, circulating immune cells also infiltrate the renal tissue (Mattson, 2014). Since *inv/inv* mice is a global knockout model of inversin loss, the gene expression changes observed in *inv/inv* kidneys alone could be a direct effect of inversin on kidney cells per se or an indirect effect of infiltrating cells, or a combination of both.

Renal histology of *inv/inv* mice kidneys shows cysts in the collecting ducts in addition to other nephron segments (Phillips et al, 2004). Transcriptome analysis in inversin-depleted mouse cortical collecting (mCCD) cell line expressing the characteristics of the principal cell type of the collecting duct may provide additional insights into inversin function in this isolated cell type. For example, a decrease in Na^+ transport in collecting duct cells can have an effect on cell proliferation and apoptosis (Hu et al, 2012; O'Donnell et al, 1983). To decipher additional similarities in the molecular and functional pathways affected in mouse cystic kidneys due to inversin loss, the transcriptome data from *inv/inv* mice cystic kidneys was compared to the gene array data from inversin-depleted renal epithelial cells, specifically a cell line with the

characteristics of the principal cells of the distal nephron and cortical collecting duct. The common gene expression changes observed *in vitro* in isolated renal cells that are recapitulated *in vivo* may provide insights into the direct effect of inversin loss in renal epithelial cells.

Materials and Methods

Cell culture: Inversin-depleted clone 440-2 with 80% knockdown (Table 19) and control mCCD cells transfected with NTC (non-targeting control) were used in this experiment. The cells were cultured in 6-well plates and grown in a humidified chamber at 37^{o}C, 5% CO_2. Cell culture medium comprised of DMEM/F12 (1:1) supplemented with 2% FBS, 80U/ml penicillin, 80µg/ml streptomycin, epidermal growth factor (10ng/ml), 5ml per liter of insulin-transferrin-selenium (100x) to a final concentration of 0.172 mM insulin, 6µM transferrin, 3.87µM sodium selenite, dexamethasone ($5x10^{-8}$M), 10^{-9} M 3,3',5-triiodo-L-thyronine. The medium was replaced three times per week and the cells were passaged weekly. Confluent cultures grown for two weeks were collected for gene expression analysis.

***Total RNA isolation and real-time PCR*:** Total RNA from each sample was isolated using RNeasy® mini isolation kit (Qiagen, Valencia, CA) according to manufacturer's protocol. Briefly, the samples were homogenized in lysis buffer and the lysate was passed five times through a blunt 20-guage needle fitted to an RNase-free syringe. One volume of 70% ethanol was added to the sample which was then applied to RNeasy spin column. The samples were centrifuged and the flow through was discarded. DNase treatment of the samples was performed using the RNase-free DNase set from Qiagen (Valencia, CA) and the samples were eluted in RNase-free water. RNA quality and quantity were determined by Agilent 2100 Bioanalyzer (Agilent Technologies, Inc. Santa Clara, CA, USA) according to manufacturer's instructions. First strand cDNA was synthesized from 1.5µg of total RNA with random hexamer primers using the

SUPERSCRIPT II first strand synthesis kit (Invitrogen). The mRNA levels were determined by quantitative real-time PCR using ABI Prism Sequence Detection System 5700 (Applied Biosystems). The mRNA levels were normalized to 18S ribosomal RNA that served as an internal control.

***Microarray experiments*:** Total RNA was subjected to microarray gene expression analysis. The RNA samples were processed by Asuragen Inc (Asuragen TX, USA) using Mouse Gene 230 2.0 arrays according to the company's procedures. All arrays that met the minimal recommended quality parameters as described in the Affymetrix Data Analysis Fundamentals Guide (P/N 701190) were used for analyses. Expression signal was obtained from CEL files using MAS5 algorithm in the Affymetrix GCOS software. The criteria and the potential outcome as described in Table 20 were employed to obtain genes that were differentially regulated upon inversin knockdown in renal epithelial cells in confluent cultures grown for 2 weeks. A stringent criterion was used to further remove potential NTC effects. The genes that were common to comparisons 1 and 2 and altered in the same direction of change were considered as genes altered by inversin knockdown. These genes were subjected to bioinformatics and pathway analysis.

***Bioinformatics and statistical analysis*:** Sequential steps were taken to identify differentially expressed genes (DEGs). First, the median signal of the entire dataset was applied as a threshold to identify genes 'Present' in comparing different groups in the study. Second, the fold changes of each 'Present' gene were computed from estimated

median of comparing groups obtained in the first step. Genes with absolute fold changes larger or equal to 1.45 were kept for testing of statistical significance performed in the third step using a t-test implemented in R multtest (Resampling-based multiple hypothesis testing) package (Dudoit and Ge, 2005). False discovery rate (FDR) of each gene was estimated using Benjamini & Hochberg method implemented in multtest R package (Pollard et al, 2005).

The DEGs were defined as those genes with a *p*-value < 0.05 and FDR < 0.05. Principal component analysis (PCA) was performed using TIBCO Spotfire (TIBCO Spotfire, Boston, http://spotfire.tibco.com/). Enrichment analyses of Gene Ontology (GO), KEGG and Ingenuity® Pathway Analysis (IPA®, QIAGEN Redwood City, www.qiagen.com/ingenuity) were performed on the DEGs using the right tailed Fisher's exact test.

Table 20: Criteria for gene array analysis and potential outcome in inversin-depleted renal epithelial cells *in vitro*

Comparisons	**Groups**	**Potential Outcome**
1	Untransfected control vs Inv-KD[a]	Genes alteres by Inv-KD but may include non-targeting effects
2	NTC[b] vs Inv-KD	Genes altered by Inv-KD, controlled for NTC effects
3	Genes altered in the same direction from comparison 1 and 2	Genes altered by Inv-KD

[a]Inv-KD, inversin knockdown; [b]NTC, non-targeting control

Cell proliferation: Cells with 80% inversin knockdown (clone 440-2) and the non-targeting control were plated in a 96-well plate at a density of $3x10^3$ cells per well. Cells were collected at different time points 2, 6, 20, 30, 45, and 48h after plating and fixed in PREFER fixative (Anatech Ltd, Battle Creek, MI). The cells were stained with Hoechst (2mg/ml) at a dilution of 1:5000. To each well 50 µl of diluted Hoechst reagent was added and incubated at room temperature for one hour. Cells were washed with PBS and the cell counts were determined using the CellInsight NXT High Content Imager. Scan limits were set at maximum of 15 fields or 1000 total cells per well. Data were normalized within the analysis software by dividing the total number of cells by the number of fields counted.

***Comparison of in vitro and in vivo gene array data of inversin-depleted renal epithelial cells and inv/inv mice kidneys*:** The *in vitro* array data from confluent cultures of inversin-depleted mCCD cells were compared with the array data from *inv/inv* mice cystic kidneys. Pathway analysis was performed on the common genes derived from these two data sets in IPA®.

Measurement of caspase 3/7 activity: Cells with 80% inversin knockdown (clone 440-2) and the non-targeting control were plated in a 96-well plate at a density of $2x10^4$ cells per well. Caspase 3/7 activity was measured at 6, 18, 24, 48 and 72h after plating using Caspase-Glo®3/7 assay kit (Promega) according to manufacturer's instructions.

***Statistics*:** Data are represented as mean ± SD. Differences between two groups were analyzed by an unpaired Student's *t*-test. Differences were considered significant if $P<0.05$. Line or bar graphs were generated using Microsoft Excel or Sigma Plot 11.0 software.

Results

***Gene expression profiles of inversin-depleted renal epithelial cells*:** To gain insights into inversin function, transcriptome analysis was performed on inversin-depleted mouse renal epithelial cells. Untransfected mCCD control cells, cells transfected with non-targeting control (NTC) and inversin-depleted clone 440-2 with 80% knockdown were grown in culture for 2 weeks. Replicates of 5 per group were used for this experiment. Mouse genome 430 2.0 array comprises of 45,101 probe sets corresponding to over 39,000 transcripts which in turn correspond to 20,670 genes. A summary of the gene signal data, detection calls and gene annotations for every gene on the chip was generated using Affymetrix MAS 5.0 algorithm (GCOS, v1.3). Of the 20,670 genes on the chip, 11,275 (54.5%) genes were detected in the untransfected control mCCD cells, 11,414 (55.2%) genes in cells transfected with NTC and 11, 616 (56.2%) in inversin-depleted cells. Genes altered by the stringent criteria set to remove non-targeting control effects are shown in Table 21. Number of genes altered in inversin-depleted cells when compared with the untransfected control (comparison 1) was higher compared to the number of genes altered when compared to NTC (comparison 2), potentially indicating the effects of NTC. A total of 992 genes that were altered in the same direction of change from comparison 1 and 2 were considered as genes altered by inversin knockdown and were used for further analysis.

***Identification of differentially expressed genes (DEGs) in inversin-depleted renal epithelial cells*:** For gene classifications and functional *in silico* analyses, the probe sets with low-grade annotations were eliminated to enable analysis of data sets with

reliable annotations. The DEGs were identified as significant if the comparisons of control and inversin-depleted cells gene expression met the criteria of (a) $p<0.05$, (b) the median signal for all the chips in either group was larger than 250 (c) an absolute fold change ≥ 1.45. Of 11,616 genes expressed in inversin-depleted cells, 738 genes (6.4%) were differentially expressed in inversin-depleted renal epithelial cells compared to control cells. Out of 738 annotated DEGs, 400 genes were upregulated and 338 genes were downregulated in inversin-depleted renal epithelial cells compared to controls controls (Appendix, upregulated genes, Table 33; downregulated genes, Table 34).

Table 21: Number of genes altered in control and inversin-depleted renal epithelial cells *in vitro*

Comparisons	**Groups**	**Number of genes altered in Inv-KD[a] clone**	**Potential Outcome**
1	Untransfected control vs Inv-KD	4219	Genes altered by Inv-KD but may include non-targeting effects
2	NTC[b] vs Inv-KD	3542	Genes altered by Inv-KD, controlled for NTC effects
3	Genes altered in the same direction from comparison 1 and 2	992	Genes altered by Inv-KD with stringent criterion

[a]Inv-KD, inversin-knockdown; [b]NTC, non-targeting control

***Functional classification of DEGs in inversin-depleted renal epithelial cells*:** To find common molecular functions of DEGs derived from inversin-depleted renal epithelial cells, the DEGs were classified into the categories of the GO (Gene Ontology) terms such as, Biological Process (BP), Cellular Component (CC) and Molecular Function (MF) using DAVID (the database for annotation, visualization and integrated

discovery) bioinformatics tool (Huang da et al, 2009a; Huang da et al, 2009b) and Ingenuity Pathway Analysis (IPA®). Table 22 shows the significantly enriched GO-BP categories of DEGs identified by Fisher's exact test ($P < 0.05$) and an enrichment score of 1.45 and above. As shown in Figure 17, the various biological processes altered in inversin-depleted renal epithelial cells compared to control, included regulation of transcription, cell migration, chromatid separation and cell cycle, biosynthetic processes, morphogenesis, metabolic processes, apoptosis and ion transport. The majority of these genes classified under biological processes that represented increased transcription and regulation of RNA biosynthetic process suggesting that loss of inversin may overall impact the transcription machinery (Table 22). Another enriched category that was altered in inversin knockdown cells was regulation of apoptosis. Overall, the findings on regulation of transcription, apoptosis, cell cycle and ion transport are consistent with the gene expression changes observed in *inv/inv* mice cystic kidneys as described in Chapter 2. Interestingly, the genes associated with negative regulation of sodium transport category are also consistent with the decreased sodium ion transport observed in inversin-depleted cells by electrophysiology. Thus, GO-BP classification suggests that loss of inversin *in vitro* in isolated renal cells impact various biological processes that may be involved in cyst formation, growth and expansion observed in NPHP2. Involvement of some of these processes such as, cell growth and differentiation, immune response, apoptosis and ion homeostasis have also been reported in ADPKD (Song et al, 2009), ARPKD (Mrug et al, 2008) and in mouse embryonic fibroblasts derived from *inv/inv* mice (Veland et al, 2013) indicating a potential common mechanism in cyst growth and expansion in renal diseases between NPHP2, ADPKD and ARPKD.

Table 22: GO biological process terms considered significantly enriched for the genes regulated in inversin-depleted renal epithelial cells[a]

Category	Term	Count	*P*-Value
Regulation of transcription			
GO-BP-FAT	positive regulation of transcription, DNA-templated	84	2.29E-04
GO-BP-FAT	positive regulation of nucleic acid-templated transcription	84	2.29E-04
GO-BP-FAT	positive regulation of RNA biosynthetic process	84	2.52E-04
GO-BP-FAT	regulation of nucleic acid-templated transcription	171	1.24E-02
GO-BP-FAT	regulation of transcription, DNA-templated	171	1.22E-02
Cell migration			
GO-BP-FAT	epithelial cell migration	22	9.82E-04
GO-BP-FAT	epithelium migration	22	1.15E-03
GO-BP-FAT	substrate-dependent cerebral cortex tangential migration	4	1.35E-03
GO-BP-FAT	cerebral cortex tangential migration	4	7.14E-03
GO-BP-FAT	tissue migration	22	1.58E-03
Chromatid separation and cell cycle			
GO-BP-FAT	regulation of mitotic sister chromatid separation	9	1.06E-03
GO-BP-FAT	metaphase/anaphase transition of cell cycle	9	1.22E-03
GO-BP-FAT	mitotic sister chromatid separation	9	1.38E-03
GO-BP-FAT	regulation of mitotic sister chromatid segregation	9	2.26E-03
GO-BP-FAT	negative regulation of mitotic metaphase/anaphase transition	6	1.32E-02
GO-BP-FAT	negative regulation of mitotic sister chromatid separation	6	1.32E-02
GO-BP-FAT	mitotic spindle checkpoint	6	1.32E-02
GO-BP-FAT	negative regulation of mitotic sister chromatid segregation	6	1.67E-02
GO-BP-FAT	negative regulation of metaphase/anaphase transition of cell cycle	6	1.67E-02
GO-BP-FAT	negative regulation of sister chromatid segregation	6	2.07E-02
GO-BP-FAT	negative regulation of chromosome segregation	6	2.79E-02
Biosynthetic process			
GO-BP-FAT	nucleobase-containing compound biosynthetic process	200	2.30E-03
GO-BP-FAT	regulation of RNA biosynthetic process	172	1.04E-02
GO-BP-FAT	aromatic compound biosynthetic process	201	4.24E-03
GO-BP-FAT	heterocycle biosynthetic process	200	4.62E-03
Transport of nucleic acids			
GO-BP-FAT	nucleic acid transport	15	1.56E-03
GO-BP-FAT	RNA transport	15	1.56E-03
GO-BP-FAT	establishment of RNA localization	15	1.92E-03
GO-BP-FAT	RNA localization	15	1.11E-02
Ion transport			
GO-BP-FAT	negative regulation of sodium ion transmembrane transporter activity	4	9.51E-03
GO-BP-FAT	negative regulation of sodium ion transmembrane transport	4	1.23E-02
GO-BP-FAT	negative regulation of sodium ion transport	4	2.32E-02

Table 22: continued

Morphogenesis			
GO-BP-FAT	negative regulation of angiogenesis	10	9.39E-03
GO-BP-FAT	negative regulation of blood vessel morphogenesis	10	1.17E-02
GO-BP-FAT	negative regulation of vasculature development	10	1.63E-02
Peptidase activity			
GO-BP-FAT	positive regulation of cysteine-type endopeptidase activity	12	1.17E-02
GO-BP-FAT	positive regulation of endopeptidase activity	12	1.65E-02
GO-BP-FAT	positive regulation of peptidase activity	12	2.03E-02
Axon guidance			
GO-BP-FAT	branchiomotor neuron axon guidance	4	9.51E-03
GO-BP-FAT	semaphorin-plexin signaling pathway involved in axon guidance	4	1.55E-02
GO-BP-FAT	semaphorin-plexin signaling pathway involved in neuron projection guidance	4	1.55E-02
Catabolic process			
GO-BP-FAT	ubiquitin-dependent protein catabolic process	32	2.83E-02
GO-BP-FAT	modification-dependent protein catabolic process	32	3.51E-02
GO-BP-FAT	modification-dependent macromolecule catabolic process	32	4.15E-02
Apoptosis			
GO-BP-FAT	positive regulation of cysteine-type endopeptidase activity involved in apoptotic process	12	6.20E-03
GO-BP-FAT	apoptotic process	116	4.61E-06
GO-BP-FAT	regulation of apoptotic process	98	1.70E-05
GO-BP-FAT	regulation of programmed cell death	98	2.72E-05
GO-BP-FAT	programmed cell death	116	4.29E-05
GO-BP-FAT	regulation of cell death	102	7.82E-05
GO-BP-FAT	cell death	121	9.14E-05
GO-BP-FAT	negative regulation of apoptotic process	66	8.78E-05
GO-BP-FAT	negative regulation of programmed cell death	66	1.36E-04
GO-BP-FAT	negative regulation of cell death	68	6.12E-04
Hypoxia			
GO-BP-FAT	response to hypoxia	23	8.14E-03
GO-BP-FAT	response to decreased oxygen levels	23	1.13E-02

[a]Genes significantly regulated were classified by GO biological process terms (GO level FAT) using DAVID 2010 online software. GO terms with values of $P<0.05$ (Fisher's exact test) are presented. Count represents the number of genes involved in each GO term.

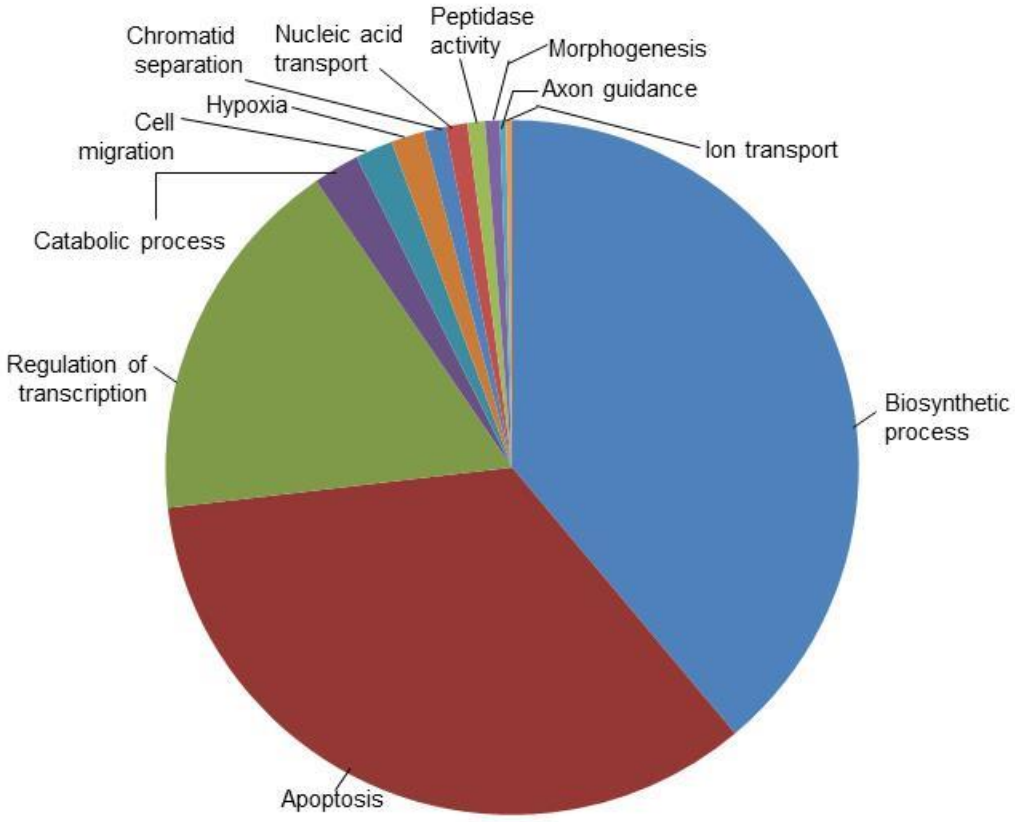

Figure 17: Overrepresented GO biological processes altered in inversin-depleted renal epithelial cells. Fisher's exact test was used to identify significant enrichment for pathway annotations. Pie chart showing the percent of genes representing different categories altered in inversin-depleted renal epithelial cells compared to controls.

Table 23 shows the DEGs from inversin-depleted renal epithelial cells that were subjected to GO cellular component (CC) analyses to obtain information about sub-cellular localization. The DEGs classified into the categories of CC include chromosome, mitotic spindle, microtubule cytoskeleton and condensed chromosome (Table 23). These results suggest that loss of inversin may influence the expression of genes localized to various regions during different stages of cell cycle consistent with its localization during cell cycle (Morgan et al, 2002a; Werner et al, 2013). Additionally, genes also classified into organelle outer membrane category, that include nuclear outer membrane consistent with the localization of 140 kDa inversin isoform to perinuclear compartment (Nurnberger et al, 2002).

Finally, the DEGs from inversin-depleted renal epithelial cells were classified into the categories of GO molecular function (MF) (Table 24). The various categories in MF that were significantly altered due to inversin loss in renal epithelial cells include, binding (nucleotide, nucleoside, GTPase, ATP, lipoprotein, L-ascorbic acid, cell adhesion molecule), cytoskeletal protein binding (tubulin), ion binding, and activity (protein dimerization, phosphatase, kinase, helicase, ligase) and microtubule motor activity. These results indicate that loss of inversin may affect various molecular functions in this isolated renal epithelial cell type associated with ion transport, trafficking, cell cycle progression, cell proliferation and apoptosis. The DEGs from inversin-depleted renal epithelial cells were further subjected to molecular and functional analysis in IPA®. The key functional categories altered were cell cycle, cellular assembly and organization, DNA replication, recombination and repair, cellular growth and proliferation and cell death and survival consistent with GO classification.

Table 23: GO cellular component terms considered significantly enriched for the genes regulated in inversin-depleted renal epithelial cells compared to controls[a]

Category	**Term**	**Count**	***P*-value**
GO-CC-FAT	Chromosome	104	1.47E-14
GO-CC-FAT	mitotic spindle or spindle pole	43	3.86E-10
GO-CC-FAT	microtubule cytoskeleton	101	4.36E-10
GO-CC-FAT	condensed nuclear chromosome, centromeric region	9	1.42E-05
GO-CC-FAT	cell cortex	26	7.59E-04
GO-CC-FAT	organelle outer membrane	17	0.0199
GO-CC-FAT	secretory granule membrane	12	0.00265

[a]Genes significantly regulated were classified by GO Cellular Component (GO level-FAT) using DAVID 2010 online software. GO terms with values of $P<0.05$ (Fisher's exact test) are presented. Count represents the number of genes involved in each GO term

Table 24: GO molecular function terms considered significantly enriched for the genes regulated in inversin-depleted renal epithelial cells compared to controls[a]

Category	Term	Count	*P*-Value
Binding			
GO-MF-FAT	nucleotide binding	159	6.58E-09
GO-MF-FAT	nucleoside phosphate binding	159	6.58E-09
GO-MF-FAT	ATP binding	109	1.87E-08
GO-MF-FAT	carbohydrate derivative binding	147	5.75E-08
GO-MF-FAT	GTPase binding	23	0.01418
GO-MF-FAT	lipoprotein particle binding	5	0.01675
GO-MF-FAT	L-ascorbic acid binding	4	0.04934
GO-MF-FAT	cell adhesion molecule binding	29	0.02297
Cytoskeletal protein binding			
GO-MF-FAT	tubulin binding	35	3.46E-08
GO-MF-FAT	microtubule binding	29	4.11E-08
GO-MF-FAT	cytoskeletal protein binding	70	6.90E-08
Ion binding			
GO-MF-FAT	metal ion binding	221	9.90E-06
GO-MF-FAT	ion binding	230	1.49E-05
Protein dimerization			
GO-MF-FAT	protein homodimerization activity	62	4.28E-06
GO-MF-FAT	protein dimerization activity	82	2.88E-05
Protein activity			
GO-MF-FAT	pyrophosphatase activity	58	4.29E-05
GO-MF-FAT	hydrolase activity, acting on acid anhydrides, in phosphorus-containing anhydrides	58	4.73E-05
GO-MF-FAT	nucleoside-triphosphatase activity	55	5.79E-05
GO-MF-FAT	ATPase activity	34	5.69E-04
GO-MF-FAT	kinase activity	59	1.90E-04
GO-MF-FAT	protein serine/threonine kinase activity	36	5.67E-04
GO-MF-FAT	protein kinase activity	45	8.43E-04
GO-MF-FAT	helicase activity	15	0.00337
GO-MF-FAT	vascular endothelial growth factor-activated receptor activity	3	0.03211
GO-MF-FAT	ligase activity	35	5.00E-05
Motor activity			
GO-MF-FAT	microtubule motor activity	9	0.01417
GO-MF-FAT	ATP-dependent microtubule motor activity, plus-end-directed	4	0.01537
GO-MF-FAT	motor activity	12	0.03693

[a]Genes significantly regulated were classified by GO Molecular Function terms (GO level FAT) using DAVID 2010 online software. GO terms with values of $P<0.05$ (Fisher's exact test) are presented. Count represents the number of genes involved in each GO term.

Pathway analysis of DEGs: To understand the expression patterns of functionally related proteins, the genes altered in inversin-depleted renal epithelial cells were subjected to Ingenuity® Pathway Analysis (IPA®). As shown in Figure 18, the top canonical pathways that were affected in inversin-depleted renal epithelial cells included the upregulation of thrombin, phosphoinositide 3-kinase (PI3K), epidermal growth factor (EGF), protein kinase A, gonadotropin-releasing hormone (GnRH), AMP-activated protein kinase (AMPK), corticotropin releasing hormone and renin-angiotensin signaling. On the other hand, the pathways involving polo-like kinase in mitosis, cyclins and cell cycle regulation were downregulated in inversin-depleted cells compared to controls. These results suggest that loss of inversin may affect cell growth and differentiation, inflammation, lipid homeostasis and cell cycle progression in renal epithelial cells.

Key molecular and cellular functions that were identified by IPA® analysis in inversin-depleted renal epithelial cells included cell cycle, cellular assembly and organization, DNA replication, recombination and repair, cell death and survival and cellular development. Transcription factors such as cyclin D1 (Ccnd1) and E2f transcription factor 1 (E2f1) involved in cell proliferation, cell cycle progression and apoptosis were downregulated in inversin-depleted renal epithelial cells (Table 25). In addition, key disease categories in IPA® analysis that were altered in inversin-depleted cells included glomerulosclerosis and fibrosis of kidney.

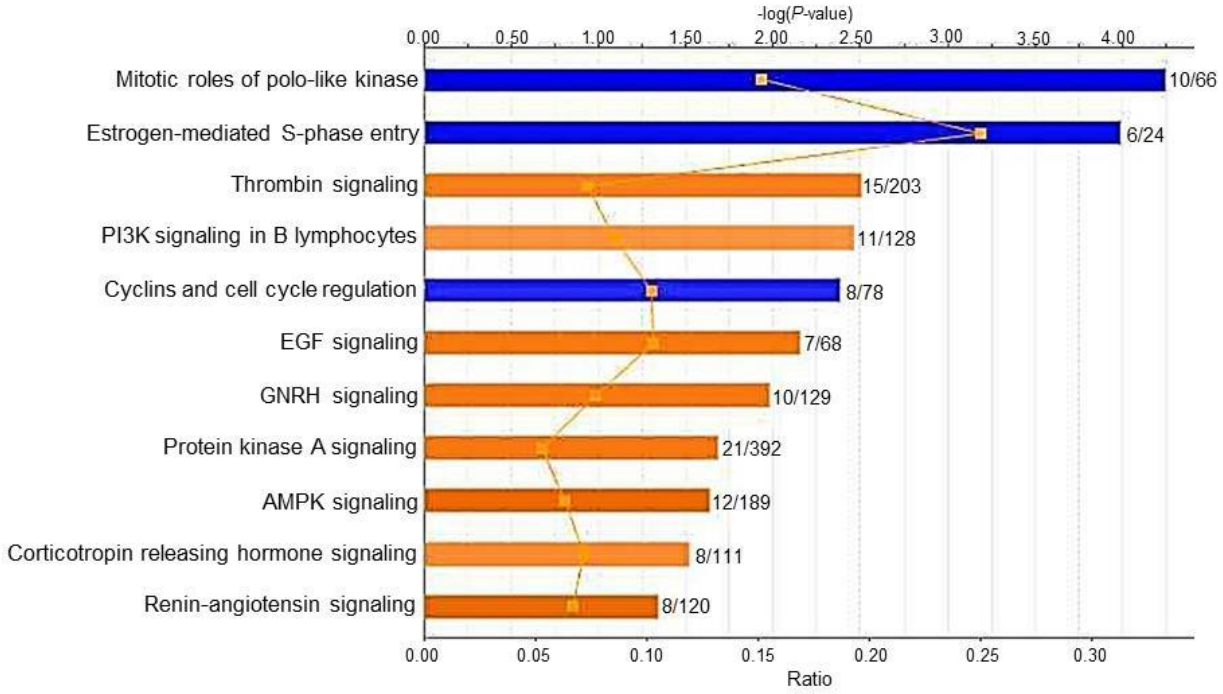

Figure 18: Canonical pathways altered in inversin-depleted renal epithelial cells analyzed using IPA®. The numbers to the right of each bar represents the ratio of genes regulated in *inv/inv* mice kidneys to the total number of genes implicated in the pathways indicated. The line graph that runs across each bar represents the threshold set for each pathway. Orange indicates the pathways that are upregulated and blue indicates pathways that are downregulated. The orange points connected by thin line represent the ratio and is calculated as number of genes in a given pathway that meets the cut-off criteria set divided by the total number of genes in the reference data set.

***Decreased expression of upstream transcription regulators in inversin-depleted renal epithelial cells*:** Upstream regulator analysis in IPA® was used to gain insights into certain observed gene expression changes in inversin-depleted renal epithelial cells. As shown in Table 25, certain transcription regulators such as, cyclin D1 (Ccnd1) and E2f transcription factor 1 (E2f1) involved in cell proliferation, cell cycle progression and apoptosis were downregulated, in inversin-depleted renal epithelial cells. Forty genes downstream of Ccnd1 and 55 genes downstream of E2f1 were altered in inversin-depleted renal epithelial cells. Together these data suggest that loss of inversin affects the expression of certain transcription factors and regulators that target downstream genes involved in cell cycle progression, apoptosis and inflammation.

***Decrease in the expression levels of cell cycle genes in inversin-depleted renal epithelial cells*:** Genes in the key canonical pathways representing cell cycle progression such as, cyclin A2 (Ccna2), cyclin D1 (Ccnd1), cyclin E2 (Ccne2), cell division cycle A (Cdc25a) and E2f1 were downregulated in inversin-depleted renal epithelial cells (Figure 19). As shown in Figure 20, Polo-like kinase (Plk1), a serine/threonine protein kinase highly expressed in mitosis, and genes downstream of Plk-1 such as Kif11 (kinesin family member11/Eg5) and Chek2 (checkpoint kinase 2/Chk2) were downregulated which may affect mitotic entry and exit, centrosome separation and maturation, and cytokinesis in inversin-depleted renal epithelial cells. Genes representing DNA synthesis, S-phase entry, alignment of chromosomes and chromosomal aberration were altered in inversin-depleted renal epithelial cells and may affect cell cycle progression (Table 26).

Table 25: Transcription regulators and the downstream targets affected in inversin-depleted renal epithelial cells

Transcription regulator	Expression fold change in clone 440-2	Predicted activation state	Activation z-score	*P*-value of overlap	Target genes in the dataset[a]	Number of genes
CCND1	-1.46	Inhibited	-4.661	1.75E-12	ATAD2,AURKA,BIRC5,BRCA1,CCNA2,CCND1,CCNE2,CDC6,CDCA2,CDCA8,CENPF,CENPH,CENPK,CEP55,DEPDC1,DNMT1,DTL,E2F1,ELOVL7,FGFR1,GAS2L3,ITGB6,KIF11,KIF20B,KIF2C,MBD5,MCM4,MELK,NCAPH,PLK1,PSRC1,RAD51,RRM2,SPC25,SPP1,STARD4,TPX2,TSC2,UHRF1,USE1	40
E2F1	-1.54	Inhibited	-4.172	1.96E-12	ABCG2,ATAD2,AURKA,AURKB,BIRC5,BRCA1,CASP3,CCNA2,CCNB2,CCND1,CCNE2,CDC20,CDC25A,CDC6,CDK1,CFLAR,CHEK1,CHEK2,DHFR,DNMT1,E2F1,FEN1,FGFR1,GINS1,GMNN,GTF2H4,HELLS,HES1,HSPD1,LTA4H,MAD2L1,MAPK14,MCM3,MCM4,MCM5,MDC1,MSH2,NRP1,NUSAP1,PKNOX1,PPP1R26,RAD51,RRM1,RRM2,SP1,TERT,THBS1,TK1,TOP2A,UCK2,UNG	51

[a]Genes indicated in red are upregulated and in blue are downregulated in inversin-depleted renal epithelial cells.

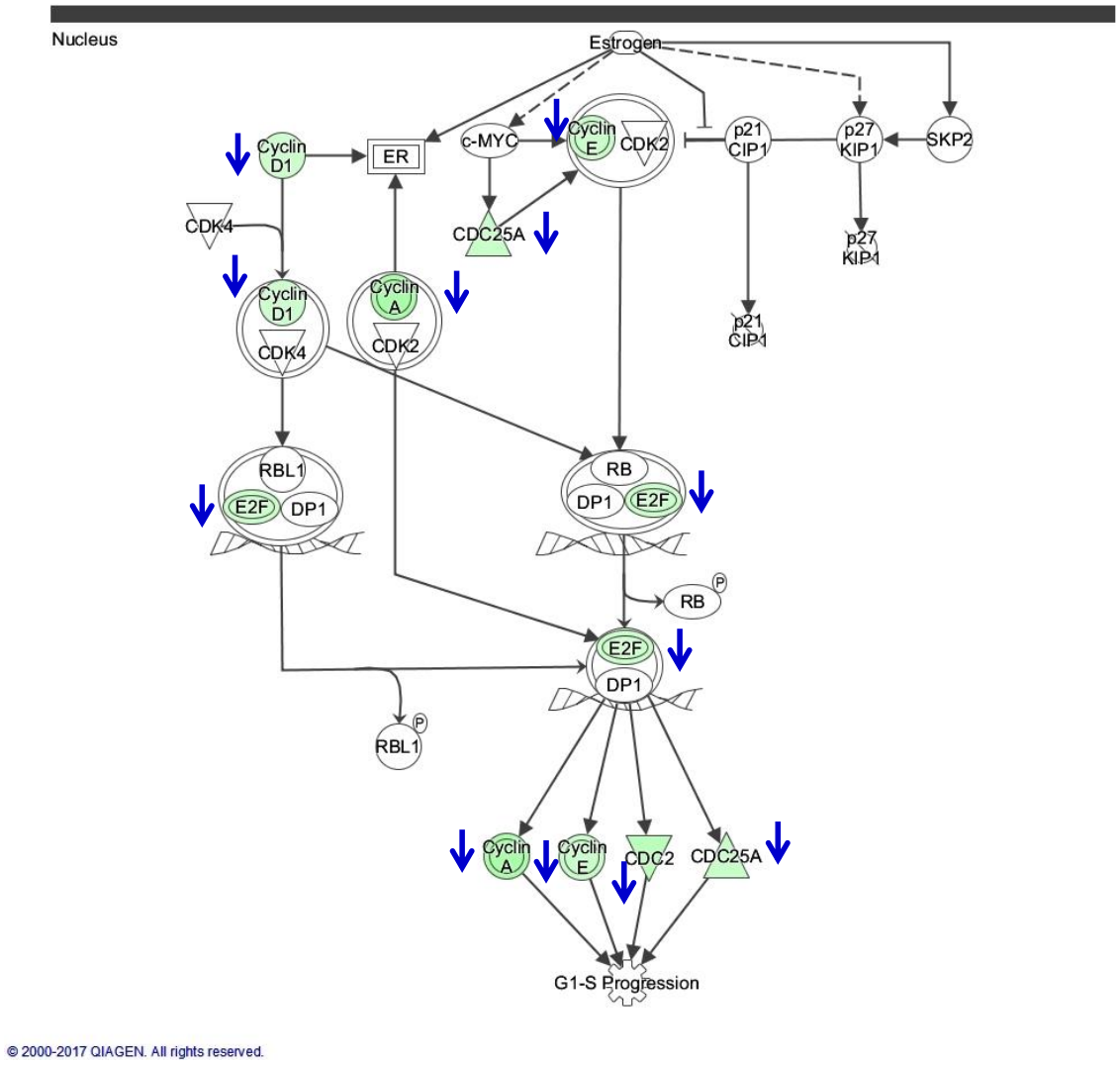

Figure 19: Network of genes represented in the estrogen-mediated S-phase entry of cell cycle identified by pathway analysis in IPA® with a Z-score of -2.5 and *P*-value 1.1E-03 in inversin-depleted renal epithelial cells. Genes shaded in green in the pathway are detected and downregulated (indicated by blue arrow) in inversin-depleted renal epithelial cells compared to controls affecting G1-S progression.

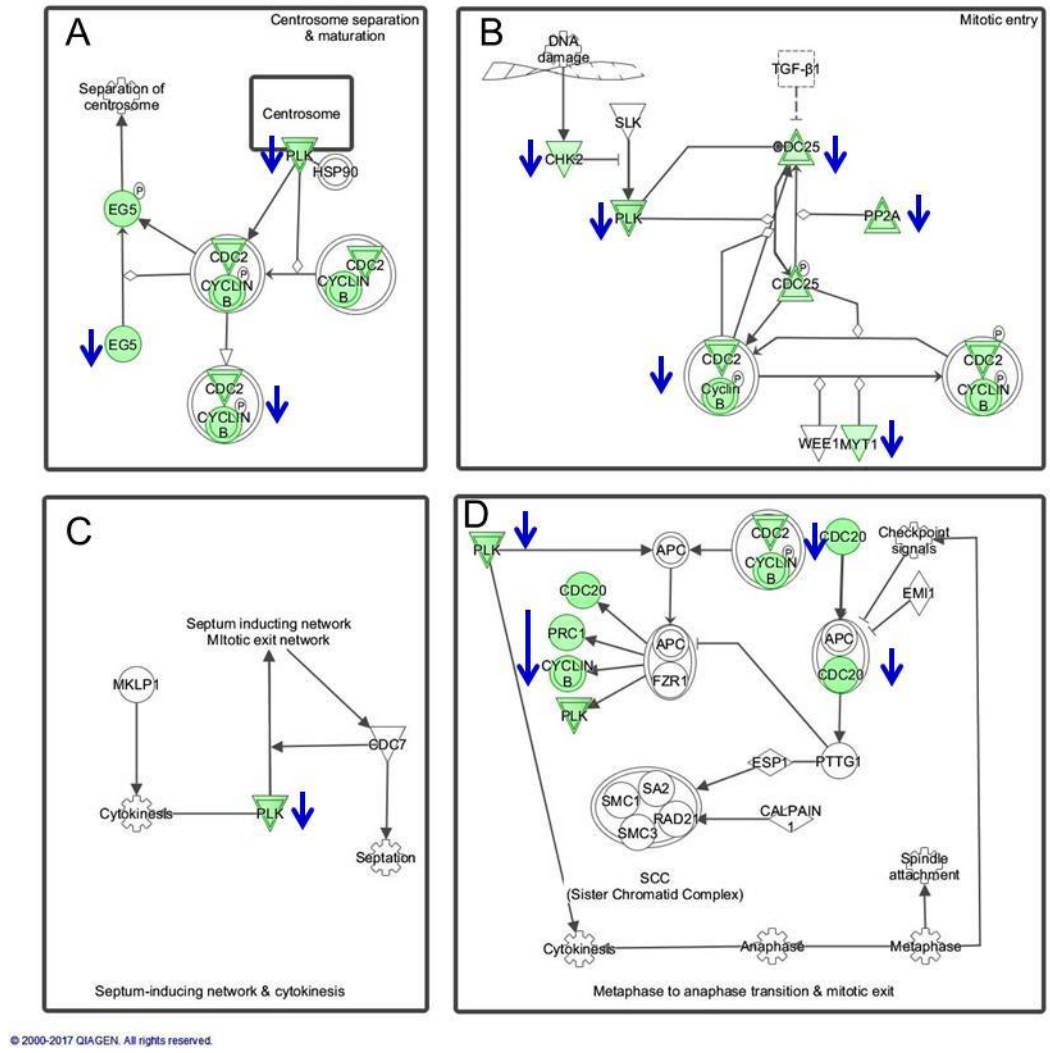

Figure 20: Network of genes represented in the mitotic roles of polo-like kinase identified by pathway analysis in IPA® with a Z-score of -2.6 and *P*-value 2.44E-04 in inversin-depleted renal epithelial cells. Genes shaded in green in the pathway are detected and downregulated (indicated by blue arrow) in inversin-depleted renal epithelial cells compared to controls affecting (**A**) centrosome separation and maturation (**B**) mitotic entry (**C**) septum-inducing network and cytokinesis (**D**) metaphase to anaphase transition and mitotic exit

Table 26: Genes affecting cell cycle progression are altered in inversin-depleted renal epithelial cells

Gene ID	Gene Symbol	Protein Name	Fold change/ NTC	*P*-value
DNA synthesis				
16598	Klf2	Kruppel-like factor 2 (lung)	2.13	0
18803	Plcg1	phospholipase C, gamma 1	1.95	0
26416	Mapk14	mitogen-activated protein kinase 14	1.53	0
15382	Hnrnpa1	heterogeneous nuclear ribonucleoprotein A1	1.49	5.00E-04
18854	Pml	promyelocytic leukemia	1.6	0.0013
22084	Tsc2	tuberous sclerosis 2	1.84	0
14083	Ptk2	PTK2 protein tyrosine kinase 2	1.48	0
18973	Pole	polymerase (DNA directed), epsilon	-11.57	0
16007	Cyr61	cysteine rich protein 61	-6.39	0
20750	Spp1	secreted phosphoprotein 1	-2.95	0
14677	Gnai1	guanine nucleotide binding protein (G protein), alpha inhibiting 1	-2.63	0
11799	Birc5	baculoviral IAP repeat-containing 5	-2.46	0.0124
21814	Tgfbr3	transforming growth factor, beta receptor III	-2.44	0
67177	Cdt1	chromatin licensing and DNA replication factor 1	-2.22	0
15901	Id1	inhibitor of DNA binding 1	-2.12	0
18817	Plk1	polo-like kinase 1	-2.19	0.006
12428	Ccna2	cyclin A2	-2.7	0
12450	Ccng1	cyclin G1	-2.06	0
18140	Uhrf1	ubiquitin-like, containing PHD and RING finger domains, 1	-1.88	0.004
15945	Cxcl10	chemokine (C-X-C motif) ligand 10	-1.87	0.0111
58186	Rad18	RAD18 homolog (S. cerevisiae)	-1.76	2.00E-04
17387	Mmp14	matrix metallopeptidase 14 (membrane-inserted)	-1.67	0
14156	Fen1	flap structure specific endonuclease 1	-1.66	0
12530	Cdc25a	cell division cycle 25A	-1.63	5.00E-04
12448	Ccne2	cyclin E2	-1.61	0.0011
13433	Dnmt1	DNA methyltransferase (cytosine-5) 1	-1.61	0.0013
21752	Tert	telomerase reverse transcriptase	-1.59	0.0113

Table 26 continued

13555	E2f1	E2F transcription factor 1	-1.54	0.0378
12443	Ccnd1	cyclin D1	-1.46	0
26909	Exo1	exonuclease 1	-1.43	0.0186
S-phase entry				
12236	Bub1b	budding uninhibited by benzimidazoles 1 homolog, beta (S. cerevisiae)	-3.13	0.0037
12235	Bub1	budding uninhibited by benzimidazoles 1 homolog (S. cerevisiae)	-3.93	0.005
107995	Cdc20	cell division cycle 20	-2.97	0.0018
56150	Mad2l1	MAD2 mitotic arrest deficient-like 1	-2.49	3.00E-04
Alignment of chromosomes				
110033	Kif22	kinesin family member 22	-3.18	0.0013
12428	Ccna2	cyclin A2	-2.7	0
11799	Birc5	baculoviral IAP repeat-containing 5	-2.46	0.0124
72415	Sgol1	shugoshin-like 1 (S. pombe)	-2.45	0.0057
73804	Kif2c	kinesin family member 2C	-2.31	0.0024
20878	Aurka	aurora kinase A	-1.87	0.0071
2E+05	Cenpe	centromere protein E	-1.77	0.0049
Chromosomal aberration				
12236	Bub1b	budding uninhibited by benzimidazoles 1 homolog, beta (S. cerevisiae)	-3.13	0.0037
11799	Birc5	baculoviral IAP repeat-containing 5	-2.46	0.0124
12443	Ccnd1	cyclin D1	-1.46	0
26909	Exo1	exonuclease 1	-1.43	0.0186
15205	Hes1	hairy and enhancer of split 1 (Drosophila)	-1.55	0
16881	Lig1	ligase I, DNA, ATP-dependent	-1.65	0
56150	Mad2l1	MAD2 mitotic arrest deficient-like 1	-2.49	3.00E-04
17762	Mapt	microtubule-associated protein tau	1.62	0
18771	Pknox1	Pbx/knotted 1 homeobox	1.47	4.00E-04
19712	Rest	RE1-silencing transcription factor	-1.52	0
21752	Tert	telomerase reverse transcriptase	-1.59	0.0113
80914	Uck2	uridine-cytidine kinase 2	-1.61	0

To determine if the changes in the expression of cell cycle genes has an effect on cell number, cell proliferation was evaluated in an *in vitro* model of inversin loss in renal epithelial cells. As shown in Figure 21, loss of inversin decreased cell number as a function of time in inversin-depleted renal epithelial (mCCD) cells compared to controls. These data suggest that loss of inversin results in decreased cell proliferation in *inv/inv* mice kidneys that may affect the development of kidneys.

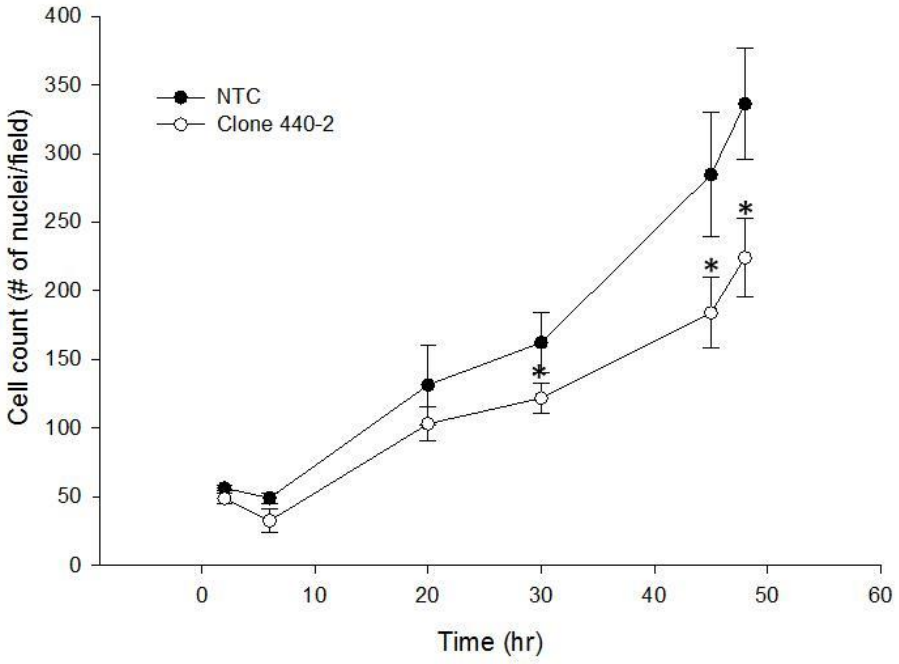

Figure 21: Assessment of cell proliferation in inversin-depleted renal epithelial (mCCD) cells. Cells with inversin knockdown (clone 440-2) and the control were plated at a density of $3x10^3$ cells/ well. Cell number was evaluated at different time points by Hoechst staining of nuclei and imaging using ArrayScan™. Values are mean ± SD; NTC n=4, Clone 440-2, n=6; $^*P < 0.05$ vs NTC; mCCD, mouse cortical collecting duct

***Upregulated pathways in inversin-depleted renal epithelial cells*:** Key upregulated signaling pathways in inversin-depleted renal epithelial cells included thrombin, phosphoinositide 3-kinase (PI3K), epidermal growth factor (EGF), protein kinase A (PKA), gonadotropin-releasing hormone (GnRH), AMP-activated protein kinase (AMPK), corticotropin releasing hormone (CRH) and renin-angiotensin signaling. Genes representing these pathways are shown in Table 27. Certain common downstream targets of the Egf signaling via Egfr, angiotensin signaling via angiotensin II receptor (Agtr1) and GnRH signaling via GnRH-1 and II receptors include, inositol 1-4-5, trisphosphate receptor 2 (Itpr2), mitogen-activated protein kinase (Mapk12), Mapk14, phospholipase C-gamma 1 (Plcg1), and Sos Ras/Rac guanine nucleotide exchange factor (Sos1) were also upregulated in inversin-depleted renal epithelial cells. GnRH signaling via GnRH-1 and II receptors has been shown to have anti-proliferative effects on ovarian cells suggesting possible involvement of GnRH in some of extra-pituitary functions (Kim et al, 2006). The results suggest that upregulation of these pathways can contribute to cell proliferation, cytoskeletal changes and cell migration.

AMPK is a master metabolic regulator which inhibits enzymes of ATP consuming pathways and is activated in response to injury, inflammation, hypoxia or ischemia (Long & Zierath, 2006). Certain downstream genes of AMPK activation such as 3-hydroxy-3-methylglutaryl CoA reductase (Hmgcr), Mapk12 and Mapk14, ribosomal protein S6 kinase 1 (Rps6kb1), sirtuin1 (Sirt1) and tuberous sclerosis complex (Tsc2) were upregulated in inversin-depleted renal epithelial cells. CRH signaling via CRH receptor, a mediator of stress response was upregulated in inversin-depleted renal epithelial cells. CRH functions through activation of several signaling pathways

including adenylate cyclase/PKA, phospholipase C/protein kinase and MAPK pathways (Subbannayya et al, 2013). Genes associated with CRH signaling such as, adenylate cyclase 6 (Adcy6), Plcg1, Mapk12 and 14 were also upregulated in inversin-depleted renal epithelial cells.

PI3 kinase signaling has been implicated in wide range of cellular processes and B-cell differentiation (Baracho et al, 2011). Downstream genes of PI3K signaling such as calcium/calmodulin dependent protein kinase 2a (Camk2a) and Camk2d, activating transcription factor 6 beta (Atf6b) and Atf, Itpr2 and malt1 paracaspase (Malt1) and Plcg1were also upregulated in inversin-depleted renal epithelial cells. Overall, the upregulation of these genes can contribute to cell proliferation or hypertrophy, increase the expression and synthesis of extracellular matix proteins or elicit immune response that can contribute to renal fibrosis resulting in renal damage.

Table 27: Genes in the upregulated canonical signaling pathways in inversin-depleted renal epithelial cells

Gene ID	Gene Symbol	Protein Name	Fold change/ NTC	*P*-value
Genes common to EGF, Thrombin and GnRH signaling				
16439	Itpr2	inositol 1,4,5-triphosphate receptor 2	2.13	0
18803	Plcg1	phospholipase C, gamma 1	1.95	0
26416	Mapk14	mitogen-activated protein kinase 14	1.53	0
29857	Mapk12	mitogen-activated protein kinase 12	1.72	0
20662	Sos1	son of sevenless homolog 1	1.63	1.00E-04
72508	Rps6kb1	ribosomal protein S6 kinase, polypeptide 1	1.54	2.00E-04
Renin-Angiotensin signaling				
16439	Itpr2	inositol 1,4,5-triphosphate receptor 2	2.13	0
18803	Plcg1	phospholipase C, gamma 1	1.95	0
29857	Mapk12	mitogen-activated protein kinase 12	1.72	0
11512	Adcy6	adenylate cyclase 6	1.66	0
20662	Sos1	son of sevenless homolog 1	1.63	1.00E-04
26416	Mapk14	mitogen-activated protein kinase 14	1.53	0
14083	Ptk2	PTK2 protein tyrosine kinase 2	1.48	0
AMPK signaling				
22084	Tsc2	tuberous sclerosis 2	1.84	0
93759	Sirt1	sirtuin 1	1.73	0
29857	Mapk12	mitogen-activated protein kinase 12	1.72	0
72508	Rps6kb1	ribosomal protein S6 kinase, 1	1.54	2.00E-04
26416	Mapk14	mitogen-activated protein kinase 14	1.53	0
15357	Hmgcr	3-hydroxy-3-methylglutaryl-Coenzyme A reductase	-1.52	0
Corticotropin releasing hormone signaling				
18803	Plcg1	phospholipase C, gamma 1	1.95	0
29857	Mapk12	mitogen-activated protein kinase 12	1.72	0
11512	Adcy6	adenylate cyclase 6	1.66	0
26416	Mapk14	mitogen-activated protein kinase 14	1.53	0
109880	Braf	Braf transforming gene	1.48	0
GnRH signaling				
12322	Camk2a	calcium/calmodulin-dependent protein kinase II alpha	1.97	0.0124
11512	Adcy6	adenylate cyclase 6	1.66	0
14083	Ptk2	PTK2 protein tyrosine kinase 2	1.48	0
108058	Camk2d	calcium/calmodulin-dependent protein kinase II, delta	1.49	2.00E-04

Table 27 continued

PI3 kinase signaling				
107503	Atf5	activating transcription factor 5	3.9	0
16439	Itpr2	inositol 1,4,5-triphosphate receptor 2	2.13	0
12322	Camk2a	calcium/calmodulin-dependent protein kinase II alpha	1.97	0.0124
18803	Plcg1	phospholipase C, gamma 1	1.95	0
223922	Atf7	activating transcription factor 7	1.71	0.0161
12915	Atf6b	activating transcription factor 6 beta	1.66	0
240354	Malt1	mucosa associated lymphoid tissue lymphoma translocation gene 1	1.58	7.00E-04
108058	Camk2d	calcium/calmodulin-dependent protein kinase II, delta	1.49	2.00E-04
PKA signaling				
16439	Itpr2	inositol 1,4,5-triphosphate receptor 2	2.13	0
12322	Camk2a	calcium/calmodulin-dependent protein kinase II alpha	1.97	0.0124
18803	Plcg1	phospholipase C, gamma 1	1.95	0
11512	Adcy6	adenylate cyclase 6	1.66	0
108058	Camk2d	calcium/calmodulin-dependent protein kinase II, delta	1.49	2.00E-04
109880	Braf	Braf transforming gene	1.48	0
14083	Ptk2	PTK2 protein tyrosine kinase 2	1.48	0
12530	Cdc25a	cell division cycle 25A	-1.63	5.00E-04
19272	Ptprk	protein tyrosine phosphatase, receptor type, K	-1.74	0
72391	Cdkn3	cyclin-dependent kinase inhibitor 3	-2.03	0.0167
14677	Gnai1	guanine nucleotide binding protein (G protein), alpha inhibiting 1	-2.63	0
19274	Ptprm	protein tyrosine phosphatase, receptor type, M	-3.52	0
Thrombin signaling				
17904	Myl6	myosin, light polypeptide 6, alkali, smooth muscle and non-muscle	2.24	0
12322	Camk2a	calcium/calmodulin-dependent protein kinase II alpha	1.97	0.0124
11512	Adcy6	adenylate cyclase 6	1.66	0
16800	Arhgef2	rho/rac guanine nucleotide exchange factor (GEF) 2	1.62	0
108058	Camk2d	calcium/calmodulin-dependent protein kinase II, delta	1.49	2.00E-04
14083	Ptk2	PTK2 protein tyrosine kinase 2	1.48	0

***Genes affecting ion transport are altered in inversin-depleted renal epithelial cells*:** Several genes that affect ion transport including sodium reabsorption were altered in inversin-depleted renal epithelial cells (Table 28). Neural precursor expressed developmentally downregulated gene 4-like (Nedd4l), a negative regulator of epithelial sodium channel (ENaC) activity was upregulated whereas, serine threonine kinase 39 (Stk39/Spak), a positive regulator of ENaC (Ahmed et al, 2015) was downregulated in inversin-depleted renal epithelial cells. Overall, these two findings suggest that loss of inversin decreased sodium transport in renal epithelial cells consistent with the findings in *inv/inv* mice kidneys and in inversin-depleted mouse cortical collecting duct cells. Calcium/calmodulin-dependent kinase 2 delta (Camk2d), one of the protein kinases that can phosphorylate aquaporin-2, a water channel in the collecting duct, was upregulated in inversin-depleted renal epithelial cells. Members of the solute carrier (Slc) family were differentially regulated in inversin-depleted renal epithelial cells that included monocarboxylic acid transporters Slc16a6 (upregulated) and Slc16a12 (downregulated); mitochondrial transport members such as Slc25a12/aralar, Slc25a27/Ucp4 (uncoupling protein 4), Slc25a53, a mitochondrial carrier triple repeat 6 (Mcart6) were upregulated. In addition, some of the upregulated solute carrier members included Slc7a5, an L-type amino acid transporter (Lat1), Slc46a1, a proton-coupled folate transporter (Pcft) and Slc30a10, a zinc transporter (Znt10). Interestingly, Slc29a2, a nucleoside transporter that mediates reabsorption of nucleosides from lumen to blood driven by Na^+ currents was upregulated in inversin-depleted renal epithelial cells. Slc4a3/Ae3 (an anion exchanger 3), a Cl^-/bicarbonate exchanger and Slc4a8, a Na^+-coupled bicarbonate co-transporter (Nbc3) were also upregulated.

Table 28: Genes involved in ion transport altered in inversin-depleted renal epithelial cells

Gene ID	Gene Symbol	Protein Name	Fold change/ NTC	*P*-value
Na^+ transport				
83814	Nedd4l	neural precursor cell expressed, developmentally down-regulated gene 4-like	2.37	0
108058	Camk2d	calcium/calmodulin-dependent protein kinase II, delta	1.49	2.00E-04
53416	Stk39	serine/threonine kinase 39	-3.61	0
59033	Slc4a8	solute carrier family 4 (anion exchanger), member 8	1.48	0.0131
Others				
104681	Slc16a6	solute carrier family 16 (monocarboxylic acid transporters), member 6	3.21	0
20539	Slc7a5	solute carrier family 7 (cationic amino acid transporter, y+ system), member 5	1.92	0
52466	Slc46a1	solute carrier family 46, member 1	1.89	0
78830	Slc25a12	solute carrier family 25 (mitochondrial carrier, Aralar), member 12	1.79	1.00E-04
74011	Slc25a27	solute carrier family 25, member 27	1.75	6.00E-04
67062	Slc25a53	solute carrier family 25, member 53	1.72	0
13340	Slc29a2	solute carrier family 29 (nucleoside transporters), member 2	1.62	1.00E-04
226781	Slc30a10	solute carrier family 30, member 10	1.55	0
73836	Slc35b2	solute carrier family 35, member B2	1.51	0.0041
242585	Slc35d1	solute carrier family 35 (UDP-glucuronic acid/UDP-N-acetylgalactosamine dual transporter), member D1	1.49	2.00E-04
20536	Slc4a3	solute carrier family 4 (anion exchanger), member 3	1.46	7.00E-04
229782	Slc35a3	solute carrier family 35 (UDP-N-acetylglucosamine (UDP-GlcNAc) transporter), member 3	-1.47	0
240638	Slc16a12	solute carrier family 16 (monocarboxylic acid transporters), member 12	-3.71	0
210027	Slc35f3	solute carrier family 35, member F3	-4.83	0

***Genes implicated in renal fibrosis were altered in inversin-depleted renal epithelial cells*:** Kidney failure, a disease category identified in IPA® analysis comprising of glomerular injury and renal fibrosis was altered in inversin-depleted renal epithelial cells. Key genes in this category included budding uninhibited by benzimidazole 1 (Bub1b), a mitotic regulator, matrix metalloproteinase 14 (Mmp14), metallothionein 2 (Mt2), a metal-binding protein, stanniocalcin1 (Stc1), tumor necrosis factor superfamily 1b (Tnfrsf1b) were downregulated in inversin-depleted renal epithelial cells compared to control. Additionally, certain genes implicated in glomerulosclerosis such as thymidine kinase (Tk1), a gene in pyrimidine nucleotide salvage pathway (Dobrovolsky et al, 2003) and secreted phosphoprotein (Spp1/osteopontin), were also downregulated in inversin-depleted renal epithelial cells (Table 29).

Table 29: Genes affecting renal fibrosis altered in inversin-depleted renal epithelial cells

Gene ID	**Gene Symbol**	**Protein Name**	**Fold change/ NTC**	***P*-value**
12236	Bub1b	budding uninhibited by benzimidazoles 1 homolog, beta (S. cerevisiae)	-3.13	0.0037
20855	Stc1	stanniocalcin 1	-1.96	3.00E-04
17750	Mt2	metallothionein 2	-1.77	2.00E-04
17387	Mmp14	matrix metallopeptidase 14 (membrane-inserted)	-1.67	0
21938	Tnfrsf1b	tumor necrosis factor receptor superfamily, member 1b	-1.97	0
21877	Tk1	thymidine kinase 1	-5.08	0.0045
20750	Spp1	secreted phosphoprotein 1	-2.95	0

Overall, some of the key biological processes that were altered in inversin-depleted renal epithelial cells included transcription, regulation of RNA biosynthetic process and apoptosis. Some of the cellular and molecular functions that were affected upon inversin loss in renal epithelial cells include cell cycle, cellular assembly and organization, DNA replication, recombination and repair, cellular development, cell growth and proliferation and ion transport. The key signaling pathways that were upregulated were EGF, AMPK, PI3K, renin-angiotensin that may contribute to mitogenesis, cytoskeletal changes or renal fibrosis. The key downregulated pathway included cell cycle regulation. Loss of inversin decreased cell number as a function of time in renal epithelial cells indicating a decreased cell proliferation.

***Comparison of transcriptome data from inv/inv mice cystic kidneys and inversin-depleted renal epithelial cells*:** Gene array data showed a total of 646 genes that were differentially expressed in *inv/inv* mice cystic kidneys compared to the wild-type controls (Appendix, Tables 31 and 32). A total of 738 genes were differentially expressed in inversin-depleted renal epithelial cells compared to control cells (Appendix, Tables 33 and 34). Comparison of the gene array from *inv/inv* mice kidneys and inversin-depleted renal epithelial cell cultures are shown in Table 30. A total of 38 genes were common to both data sets and altered in the same direction. Of the 38 common genes 28 were upregulated and 10 were downregulated. As expected, inversin was downregulated in both *inv/inv* mice kidneys as well as in inversin-depleted renal epithelial cells. Furthermore, these 38 common differentially expressed genes were further subjected to pathway analysis in IPA®. Two functional categories that were

significantly altered were a decrease in organismal death (increased survival) and the other one is increase in body size.

Out of 38 genes that were common between the two data sets 16 genes were represented in the organismal death category, of which 12 genes were upregulated and 4 were downregulated (Figure 22). Genes such as, sprouty-related EVH1 domain containing 2 (spred2), cysteine rich transmembrane BMP regulator 1 (Crim1) which is a developmentally expressed transmembrane protein, neural precursor cell expressed developmentally down-regulated 4-like (Nedd4l), an E3 ubiquitin ligase that ubiquitinates ENaC, A kinase (PRKA) anchor protein 13 (Akap13), baculoviral IAP repeat-containing 6 (Birc6), Braf transforming gene (Braf), strawberry notch homolog 2 (Sbno2) which is a DExD/H helicase family corepressor, Erbb2 interacting protein (Erbb2ip), kruppel-like factor 6 (Klf6), a zinc finger domain transcription factor, methyl-CpG binding domain protein 5 (Mbd5), muscleblind-like (Mbnl1) and nuclear receptor corepressor 1 (Ncor1), an activating subunit of chromatin modifying enzyme histone decetylase (Hdac3) were upregulated in both data sets. On the other hand, caspase 3 (Casp3), cytochrome P450 family 51a1 (Cyp51), GA binding protein beta 1 (Gabpb1) and hepatocyte growth factor activator (Hgfac) were downregulated in both data sets. Overall, the differential regulation of these genes may contribute to decreased organismal death (increased survival) as a compensatory mechanism to maintain homeostasis since the *inv/inv* mice have a short lifespan (Yokoyama et al, 1993).

Table 30: Altered genes common to inversin-depleted renal epithelial cells and *inv/inv* mice cystic kidneys

Gene ID	Gene Symbol	Protein Name	Fold change /NTC-Inversin-depleted cells	Fold change (*inv*$^{-/-}$ /wild-type)	Family
Upregulated genes					
214150	Ago3	argonaute RISC catalytic subunit 3	1.68	1.90	translational regulator
75547	Akap13	A kinase (PRKA) anchor protein 13	1.82	1.52	protein kinase scaffold
106585	Ankrd12	ankyrin repeat domain 12	1.83	1.53	other
12211	Birc6	baculoviral IAP repeat-containing 6	1.48	1.80	ubiquitin ligase
109880	Braf	Braf transforming gene	1.48	1.52	kinase
268936	Brpf3	bromodomain and PHD finger containing, 3	1.55	1.95	other
66371	Chmp4c	charged multivesicular body protein 4C	1.46	3.03	other
50766	Crim1	cysteine rich transmembrane BMP regulator 1 (chordin like)	1.79	1.60	kinase
70686	Dusp16	dual specificity phosphatase 16	1.54	1.59	phosphatase
18218	Dusp8	dual specificity phosphatase 8	1.62	1.85	phosphatase
59079	Erbb2ip	Erbb2 interacting protein	1.46	1.49	other
58180	Hic2	hypermethylated in cancer 2	2.68	2.15	other
63830	Kcnq1ot 1	KCNQ1 overlapping transcript 1	2.15	3.86	other
23849	Klf6	Kruppel-like factor 6	1.47	2.15	transcriptional regulator
14924	Magi1	membrane associated guanylate kinase, WW and PDZ domain containing 1	1.51	1.61	guanylate kinase
109241	Mbd5	methyl-CpG binding domain protein 5	1.59	1.53	other
56758	Mbnl1	muscleblind-like 1 (Drosophila)	1.49	1.79	other
20185	Ncor1	nuclear receptor co-repressor 1	1.67	1.57	transcriptional regulator
83814	Nedd4l	neural precursor cell expressed, developmentally down-regulated gene 4-like	2.37	1.68	ubiquitin ligase
71175	Nipbl	Nipped-B homolog (Drosophila)	1.48	1.50	transcriptional regulator
22038	Plscr1	phospholipid scramblase 1	1.71	2.04	enzyme
216161	Sbno2	strawberry notch homolog 2 (Drosophila)	1.46	1.45	other

Table 30: continued

59009	Sh3rf1	SH3 domain containing ring finger 1	1.45	1.59	other
114716	Spred2	sprouty-related, EVH1 domain containing 2	1.58	1.96	cytokine
75956	Srrm2	serine/arginine repetitive matrix 2	1.61	1.93	other
24132	Zfp53	zinc finger protein 53	2.02	2.04	other
69020	Zfp707	zinc finger protein 707	1.58	1.48	other
Downregulated genes					
12367	Casp3	caspase 3	-2.06	-1.55	peptidase
13121	Cyp51	cytochrome P450, family 51	-1.65	-1.49	enzyme
14391	Gabpb1	GA repeat binding protein, beta 1	-1.45	-1.64	transcriptional regulator
54426	Hgfac	hepatocyte growth factor activator	-1.52	-2.06	serine protease
110920	Hspa13	heat shock protein 70 family, member 13	-2.29	-1.45	other
16348	**Invs**	**inversin**	**-2.70**	**-3.10**	transcriptional regulator/ protein binding
18451	P4ha1	procollagen-proline, 2-oxoglutarate 4-dioxygenase (proline 4-hydroxylase), alpha 1 polypeptide	-1.61	-2.03	enzyme
225845	Pla2g16	phospholipase A2, group XVI	-1.51	-1.86	enzyme
80914	Uck2	uridine-cytidine kinase 2	-1.61	-1.53	kinase
224454	Zdhhc14	zinc finger, DHHC domain containing 14	-1.56	-1.68	enzyme

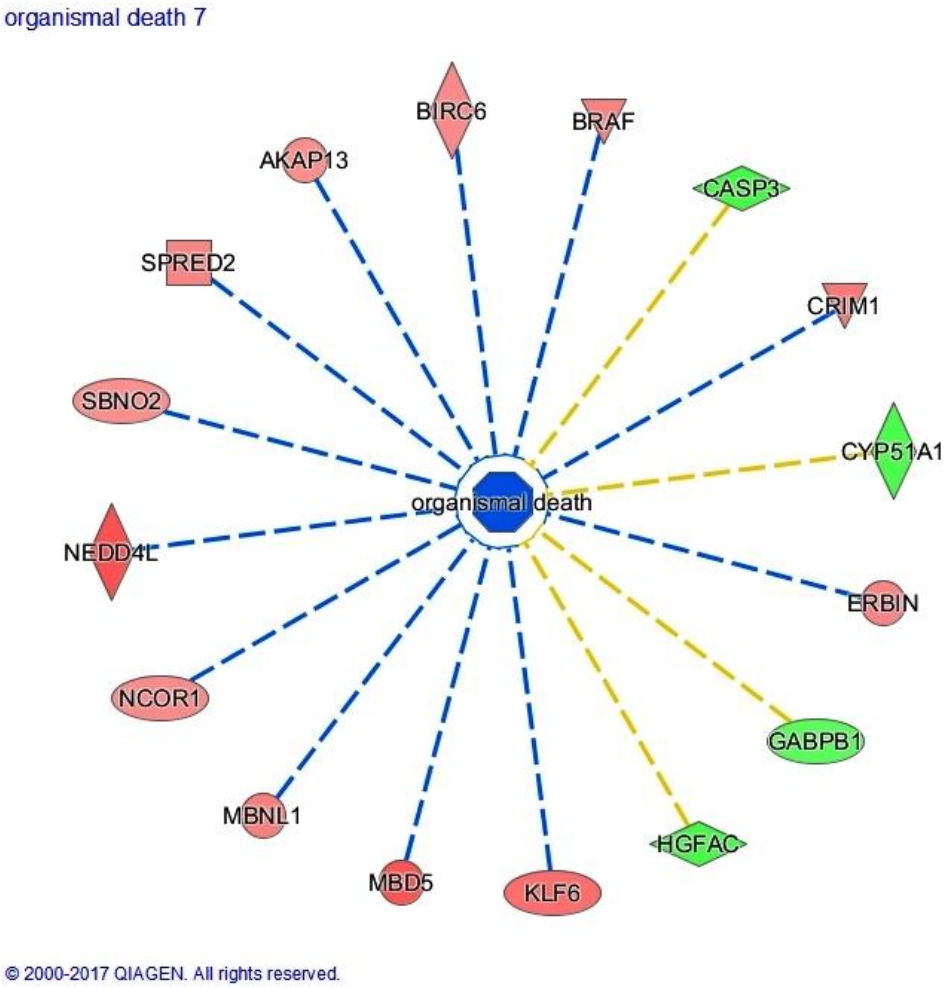

Figure 22: IPA® analysis of genes common to *inv/inv* mice cystic kidneys and inversin-depleted renal epithelial cells predicted decrease in organismal death (shaded in blue in the center) category to be increased with an activation Z score of -2.05. Shaded in red are the genes that are upregulated and shaded in green are downregulated genes in the dataset. The direction of change in the gene expression of 12 out of 16 genes in the category was predicted to increase body size. Blue dotted arrow indicates a decrease in organismal death. Yellow dotted lines indicate genes where the direction of change in gene expression (downregulation) is predicted to increase organismal death.

Interestingly, a subset of genes from the organismal death category was also represented in the body size functional category. As shown in Figure 23, genes that were predicted to affect the body size included Mbd5, Mbnl, a RNA-processing factor, Ncor1, Sbno2, KCNQ1 overlapping transcript 1 (Kcnq1ot1), an imprinting gene and Kruppel-like factor 6 (Klf6) were upregulated in both data sets. Since the gene expression data are from kidney and renal epithelial cells, these findings indicate that these genes may contribute to increased kidney size observed in *inv/inv* mice (Phillips et al, 2004; Yokoyama et al, 1993).

***Decreased caspase 3 activity in inversin-depleted renal epithelial cells*:** Caspase 3 was one of the genes common to both *inv/inv* mice cystic kidneys and inversin-depleted renal epithelial cells. To determine if the decrease in the expression of caspase 3 has an effect on its activity, caspase 3/7 activity was evaluated in inversin-depleted renal epithelial cells. As shown in Figure 24, loss of inversin decreased caspase 3/7 activity as a function of time in inversin-depleted cells compared to controls. These data suggest that loss of inversin may result in decreased apoptosis in *inv/inv* mice kidneys and in renal epithelial cells that may contribute to kidneys.

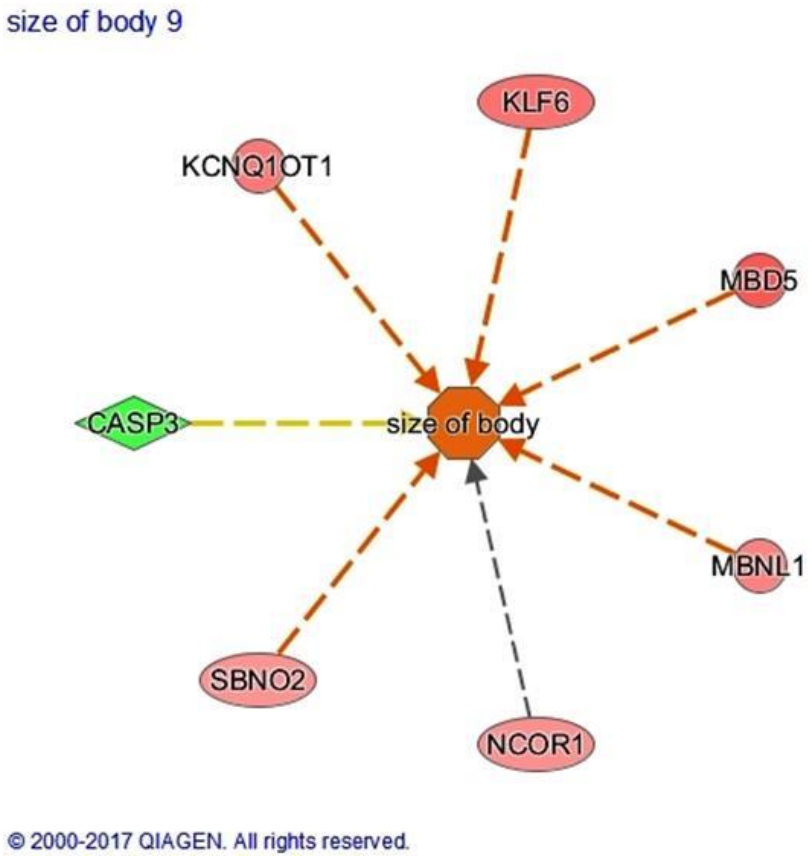

Figure 23: IPA® analysis of genes common to *inv/inv* mice cystic kidneys and inversin-depleted renal epithelial cells predicted increased body size (shaded in orange in the center) category to be increased with an activation Z score of 1.46. Shaded in red are the genes that are upregulated and shaded in green are downregulated genes in the data set. The direction of change in the gene expression of 5 out of 7 genes in the category was predicted to increase body size. Red dotted arrow indicates an increase in the size of body. Grey arrow indicates the effect of Ncor1 affects body size but the direction of change is not known. Yellow dotted lines indicate gene where the direction of change in gene expression is not consistent with findings on downstream effects.

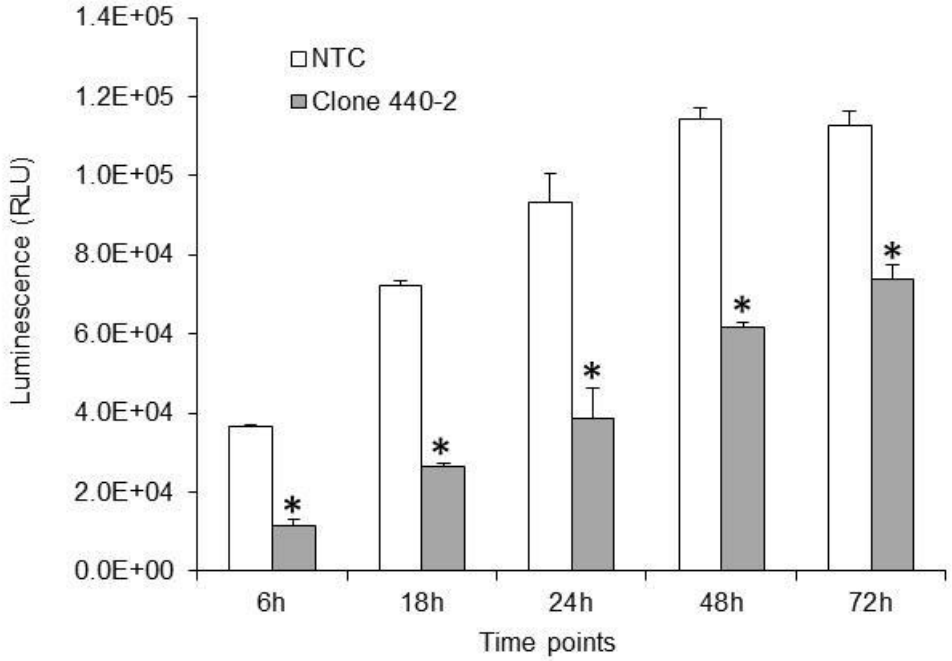

Figure 24: Assessment of caspase 3/7 activity in inversin-depleted renal epithelial cells. Cells with inversin knockdown (clone 440-2) and the control were plated at a density of $2x10^4$ cells per well in a 96-well plate. Following incubation at the indicated time points, 200 µl of the Caspase-Glo 3/7® reagent was added directly to the cells in 96-well plates, mixed well and incubated at room temperature for 90 min. Luminescence (relative light units, RLU) was recorded using Wallac Victor 2™ 1420 multilabel counter. Values are mean ± SD; n=5, $^{*}P < 0.05$ vs NTC. NTC, non-targeting control

Discussion

In kidneys, the cortical collecting duct is the final site of regulation of sodium, potassium, acid or base and water excretion. The major hormonal factors that positively control sodium reabsorption in the collecting duct are aldosterone and vasopressin (Feraille & Doucet, 2001). A decrease in vasopressin-stimulated amiloride-sensitive Na^+ transport was observed in inversin-depleted renal epithelial cells by electrophysiology. To better understand inversin function, transcriptome analysis was performed in inversin-depleted renal epithelial cells isolated from mouse collecting duct. The key transcription profiles that were altered in pathway analysis included cell cycle progression, cellular assembly and organization, DNA replication, recombination and repair, cellular development, cell growth and proliferation and ion transport.

In the collecting duct cells, main actions of vasopressin, an anti-diuretic hormone is to permeabilize the apical membrane to water through increased expression of aquaporin 2 (Aqp2), sodium reabsorption and potassium secretion (Kwon et al, 2013). Although Aqp2 was not altered in inversin-depleted renal epithelial cells, AMP kinase (AMPK), a metabolic sensor known to inhibit Aqp2 function in kidney principal cells (Al-Bataineh et al, 2016) was upregulated indicating that water reabsorption may be affected upon inversin loss. Stk39/Spak, a serine threonine kinase, participates in renal salt excretion through the regulation of NaCl and Na(+), K(+), 2Cl(-) cotransport was downregulated in inversin-depleted renal cells. Coexpression of Stk39 in ENaC expressing oocytes increased the amiloride sensitive current indicating ENaC activity (Ahmed et al, 2015). Nedd4l, an ubiquitin ligase that ubiquitinates ENaC and inhibits its activity was upregulated in inversin-depleted renal cells. Interestingly, the

downregulation of Stk39 (a positive regulator of ENaC) and upregulation of Nedd4l (a negative regulator of ENaC) decreases overall Na^+ transport in inversin-depleted renal epithelial cells. Regulation of Na^+ balance is a crucial factor to maintain blood volume and dysregulation of sodium excretion results in altered intravascular volume resulting in hypertension (Guyton, 1991) or natriuresis due to decreased reabsorption (Granger et al, 2002). Na^+ reabsorption can also occur via Na^+-dependent $Cl^-/HCO3^-$ exchanger (Slc4a8), and Na^+-independent transporters $Cl^-/HCO3^-$ exchanger (Slc26a4) in collecting duct cells (Leviel et al, 2010). Interestingly, Slc4a8 and Slc4a3, also a $Cl^-/HCO3^-$ exchangers, were upregulated in inversin-depleted renal epithelial cells suggesting a compensatory mechanism to maintain Na^+ balance in these cells.

Solute carrier 25 family of mitochondrial carriers (MC) provide a link between metabolic reactions occurring in the cytosol and mitochondrial matrix by catalyzing the translocation of solutes across the membrane and MCs are involved in many metabolic pathways (Palmieri, 2013). Upregulation of mitochondrial transporters Slc25a12/aralar (aspartate/glutamate carrier), Slc25a27/Ucp4 and Slc25a53/Mcart6 in inversin-depleted cells may increase aspartate/glutamate transport and maintain energy homeostasis. Renal handling of the nucleosides is a major determinant of their plasma levels and tissue availability (Elwi et al, 2006) and upregulation of Slc29a2, a nucleoside transporter in inversin-depleted renal epithelial cells may help in supply of nucleosides to maintain cell homeostasis.

Certain genes implicated in renal fibrosis were altered in inversin-depleted renal epithelial cells. Mice overexpressing Stanniocalcin 1 (Stc1), a connective tissue growth factor inhibits reactive oxygen species and protects from ischemia/reperfusion injury (Pan

et al, 2015) was downregulated in inversin-depleted renal epithelial cells. Thymidine kinase (Tk1) knockout mice exhibit short lifespan, develop glomerulosclerosis and have abnormal immune system (Dobrovolsky et al, 2003) too was downregulated in inversin-depleted renal cells. Bub1b /BubR1, a mitotic regulator decreases age-related interstitial fibrosis in mice (Baker et al, 2013) was also downregulated in inversin-depleted renal epithelial cells. Taken together, these data suggest that loss of inversin may contribute to fibrosis via downregulation of certain genes implicated in renal fibrosis.

To decipher similarities in the molecular and functional pathways affected in mouse cystic kidneys due to inversin loss, the transcriptome data from *inv/inv* mice cystic kidneys was compared to the gene array data from inversin-depleted renal epithelial cells. Interestingly, some of the gene expression changes observed in *inv/inv* mice cystic kidneys were recapitulated in inversin-depleted renal epithelial cells. Some of the several biological processeses common to both *inv/inv* mice cystic kidneys and inversin-depleted renal epithelial cells included, cell proliferation, apoptosis and ion transport. A decrease in Na^+ transport and cell cycle progression was evident in both data sets indicating the direct effects of inversin in *inv/inv* cystic kidneys as well as in inversin-depleted renal epithelial cells. In addition, the genes represented in the functional categories of organ size and survival were common to both *in vivo* and *in vitro* data sets of inversin loss. Genes implicated in development and postnatal growth (Mbd5, Mbnl, Ncor1 and Nedd4l) in both *in vitro* and *in vivo* model of inversin loss suggests that inversin may contribute to organ size through regulation of these genes. Mbd family of proteins has been shown to play central roles in transcriptional regulation and development (Fan & Hutnick, 2005; Razin, 1998) and Mbd5 was upregulated in both *in vitro* and *in vivo* models of inversin

loss data sets. Loss of Mbd5$^{-/-}$ mice has been shown to exhibit growth retardation, wasting and pre-weaning lethality (Du et al, 2012). Mbnl, a RNA processing factor was also upregulated in both *in vitro* and *in vivo* models of inversin loss. Enhanced expression of Mbnl can improve muscle function and increase lifespan in a *Drosophila* model of DM (Cerro-Herreros et al, 2016) whereas loss of Mbnl can cause myotonic dystrophy (DM) and reduced lifespan (Lee et al, 2013). Ncor1, a nuclear receptor corepressor was also upregulated in both the *in vitro* and *in vivo* data sets of inversin loss. Ncor1 plays crucial role in development and Ncor1$^{-/-}$ embryos exhibit decreased size compared to wild type controls (Jepsen et al, 2000). Overall, the upregulation of these various transcriptional regulators suggests that these players may contribute to enlarged kidneys in *inv/inv* mice or could play a compensatory role to maintain homeostasis and improve survival.

Transcription factor Klf-6, a zinc finger protein was upregulated in both inversin-depleted renal epithelial cells and *inv/inv* mice cystic kidneys. Klf-6 has been shown to be an essential regulator of mitochondrial function in podocyte apoptosis and increased survival (Mallipattu et al, 2015). Braf, a signaling factor and suppressor of apoptosis, and Birc6, an inhibitor of apoptosis were also upregulated in inversin-depleted renal cells. Mice with targeted disruption of Braf gene, has been shown to promote apoptotic death of differentiated endothelial cells (Wojnowski et al, 1997). Increased expression of Braf and Birc6, an inhibitor of apoptosis in inversin-depleted renal epithelial cells may contribute to decreased apoptosis. Another gene Nedd4l, an ubiquitin ligase and a negative regulator of ENaC was also upregulated in both the *in vitro* and *in vivo* data sets of inversin loss. Nedd4l$^{-/-}$ mice exhibit perinatal lethality due to increased ENaC activity

(Boase et al, 2011). Members of the cysteine aspartic acid-specific protease (caspase) family play key effector roles in apoptosis in mammalian cells. Interestingly, caspase 3 (Casp3), an inducer of apoptosis was downregulated in both *in vitro* and *in vivo* models of inversin loss. Overall, the genes common to both inversin-depleted cells and *inv/inv* mice cystic kidneys represented an increase in survival and decreased apoptosis and these mechansims may contribute to enlarged kidneys.

In summary, transcriptome analysis revealed some of the key molecular and cellular functions that were altered upon inversin-depletion in an isolated renal cell type. Pathways implicated in cell cycle, cellular assembly and organization, DNA replication, recombination and repair, cellular development, cell growth and proliferation and ion transport were altered in inversin-depleted cells as compared to controls. Loss of inversin upregulated the pathways associated with mitogenesis, cytoskeletal changes, migration and inflammation/immune response. On the other hand, pathways involved in cell cycle progression and proliferation were downregulated in inversin-depleted cells. Loss of inversin also decreased cell number as function of time in renal epithelial cells indicating a decreased cell proliferation. The *in vitro* transcriptome data showing a decrease in the expression of cell cycle and an increase in survival genes was in concordance with the *in vivo* array data from *inv/inv* mice kidneys. Additionally, the gene array data from inversin-depleted renal epithelial cells *in vitro* was compared with the array data from *inv/inv* mice cystic kidneys. The common pathways that were altered in both *inv/inv* mice cystic kidneys and inversin-depleted renal epithelial cells included survival, ion transport, cell cycle, and inflammatory/immune response suggesting that these mechanisms may be a direct effect of inversin loss. Interestingly, genes that were

common between *in vitro* and *in vivo* data sets represented categories of organism survival and organ size suggesting that the regulation of common genes may contribute to cyst growth and expansion in *inv/inv* kidneys.

CONCLUSIONS

Type II nephronophthisis (NPHP2), a renal cystic disease occurs in infants and progresses rapidly leading to end stage renal disease by 2-5 years of age. It is caused by mutations in the *Inversin* (*INVS)* gene that encodes inversin protein. NPHP2 has overlapping features with PKD and other forms of NPH. In human PKD and in murine models of PKD the mechanism of cyst growth and expansion is relatively well understood compared to NPHP2. To better understand inversin function, transcriptome analysis in the kidneys of inversin knockout mice was carried out. Pathway analysis showed that inversin exerts its effect on kidneys, at least in part through transcriptional regulation of genes involved in inflammation or immune response, cellular metabolism, cell cycle, and ion transport. A decrease in the expression of cell cycle and apoptosis genes and an increase in the expression of inflammation/immune response in this study suggest dysregulated cell proliferation that might affect proper formation of renal tubules. In addition, a decrease in the expression of ion transport genes may contribute to fluid accumulation in inversin knockout mice.

Functional consequence of inversin depletion on transepithelial ion transport was evaluated in an isolated renal cell line using electrophysiological techniques. Loss of inversin decreased vasopressin-induced Na^+ absorption but did not alter Cl^- secretion compared to control cells suggesting that inversin may play a role in Na^+ reabsorption and its loss could lead to fluid accumulation contributing to the enlarged kidneys in inversin knockout mice.

The control of organ size in multicellular organisms is mediated by the balance between cell proliferation, differentiation and apoptosis. Inversin is a complex protein with multiple functional domains that can interact with several proteins and can affect various cellular processes. To elucidate inversin function in an isolated renal cell type (mouse cortical collecting duct cells, mCCD), transcriptome analysis was performed in inversin-depleted versus control cells. Some of the key molecular and cellular functions that were affected upon inversin loss included cell cycle, cellular assembly and organization, DNA replication, recombination and repair, cellular development, cell growth and proliferation and ion transport indicating the role of inversin in various celluar processes in this isolated renal cell type. Gene expression profiling showed that loss of inversin decreased the expression of cell cycle genes indicating a delay in cell cycle progression. Additionally, cell number, a measure of cell proliferation and caspase 3/7 activity, a measure of apoptosis was decreased as a function of time in inversin-depleted cells.

The kidney is a complex organ comprising multiple cell types and in addition circulating cells also infiltrate the tissue. To ascertain the direct effects of inversin in renal cells, the gene array data from inversin-depleted renal epithelial cells *in vitro* were compared with the array data from *inv/inv* mice cystic kidneys. Gene expression changes observed *in vitro* in isolated renal cells were recapitulated *in vivo.* Interestingly, genes that were common between *in vitro* and *in vivo* data sets represented apoptotic, ion transport, cell cycle, inflammatory pathways. A decrease in the expression of cell cycle and apoptotic genes along with genes affecting Na^+ transport accompanied by an increase

in the inflammatory or immune response genes may be a direct effect of inversin loss in renal cells contributing to cyst growth and expansion in *inv/inv* kidneys.

In summary, current research helped to further understand the role of inversin in renal epithelial cells. There are several factors that contribute to cyst growth and expansion in NPHP2. Loss of inversin may cause a delay in cell cycle progression that can lead to perturbation of renal tubular geometry. Also, a decrease in Na^+ reabsorption together with differential regulation of other transporters can result in altered ion transport. Additionally, activation of immune or inflammatory pathways may drive disease progression contributing to cystogenesis, cyst growth, fluid accumulation and cyst expansion in NPHP2 (Figure 25).

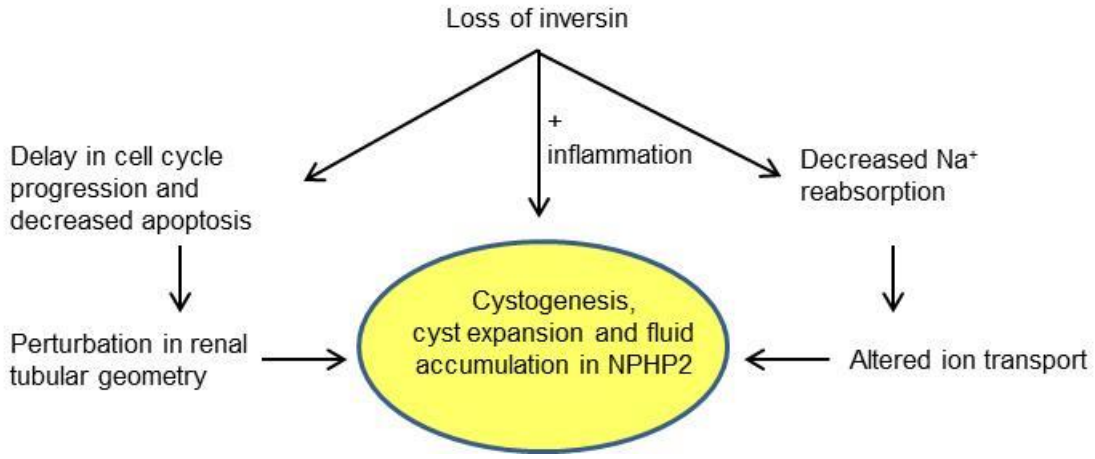

Figure 25: Proposed model of cyst growth and expansion in NPHP2

REFERENCES

Adeva M, El-Youssef M, Rossetti S, Kamath PS, Kubly V, Consugar MB, Milliner DM, King BF, Torres VE, Harris PC (2006) Clinical and molecular characterization defines a broadened spectrum of autosomal recessive polycystic kidney disease (ARPKD). *Medicine* **85:** 1-21

Ahmed M, Salker MS, Elvira B, Umbach AT, Fakhri H, Saeed AM, Shumilina E, Hosseinzadeh Z, Lang F (2015) SPAK Sensitive Regulation of the Epithelial Na Channel ENaC. *Kidney & blood pressure research* **40:** 335-343

Akahori H, Karmali V, Polavarapu R, Lyle AN, Weiss D, Shin E, Husain A, Naqvi N, Van Dam R, Habib A, Choi CU, King AL, Pachura K, Taylor WR, Lefer DJ, Finn AV (2015) CD163 interacts with TWEAK to regulate tissue regeneration after ischaemic injury. *Nature communications* **6:** 7792

Al-Bataineh MM, Li H, Ohmi K, Gong F, Marciszyn AL, Naveed S, Zhu X, Neumann D, Wu Q, Cheng L, Fenton RA, Pastor-Soler NM, Hallows KR (2016) Activation of the metabolic sensor AMP-activated protein kinase inhibits aquaporin-2 function in kidney principal cells. *American journal of physiology renal physiology* **311:** F890-F900

Allen A, Flemstrom G, Garner A, Kivilaakso E (1993) Gastroduodenal mucosal protection. *Physiological reviews* **73:** 823-857

Alvarez de la Rosa D, Li H, Canessa CM (2002) Effects of aldosterone on biosynthesis, traffic, and functional expression of epithelial sodium channels in A6 cells. *The journal of general physiology* **119:** 427-442

Ambros V (2004) The functions of animal microRNAs. *Nature* **431:** 350-355

Ariza M, Alvarez V, Marin R, Aguado S, Lopez-Larrea C, Alvarez J, Menendez MJ, Coto E (1997) A family with a milder form of adult dominant polycystic kidney disease not linked to the PKD1 (16p) or PKD2 (4q) genes. *Journal of medical genetics* **34:** 587-589

Baala L, Romano S, Khaddour R, Saunier S, Smith UM, Audollent S, Ozilou C, Faivre L, Laurent N, Foliguet B, Munnich A, Lyonnet S, Salomon R, Encha-Razavi F, Gubler MC, Boddaert N, de Lonlay P, Johnson CA, Vekemans M, Antignac C, Attie-Bitach T (2007) The Meckel-Gruber syndrome gene, MKS3, is mutated in Joubert syndrome. *American journal of human genetics* **80:** 186-194

Baker DJ, Dawlaty MM, Wijshake T, Jeganathan KB, Malureanu L, van Ree JH, Crespo-Diaz R, Reyes S, Seaburg L, Shapiro V, Behfar A, Terzic A, van de Sluis B, van Deursen JM (2013) Increased expression of BubR1 protects against aneuploidy and cancer and extends healthy lifespan. *Nature cell biology* **15:** 96-102

Baracho GV, Miletic AV, Omori SA, Cato MH, Rickert RC (2011) Emergence of the PI3-kinase pathway as a central modulator of normal and aberrant B cell differentiation. *Current opinion in immunology* **23:** 178-183

Baradhi KM, Abuelo GJ (2012) Unilateral renal cystic disease. *Kidney international* **81:** 220

Bardet G (1995) On congenital obesity syndrome with polydactyly and retinitis pigmentosa (a contribution to the study of clinical forms of hypophyseal obesity). 1920. *Obesity research* **3:** 387-399

Barker AR, Thomas R, Dawe HR (2014) Meckel-Gruber syndrome and the role of primary cilia in kidney, skeleton, and central nervous system development. *Organogenesis* **10:** 96-107

Bartram MP, Dafinger C, Habbig S, Benzing T, Schermer B, Muller RU (2015) Loss of Dgcr8-mediated microRNA expression in the kidney results in hydronephrosis and renal malformation. *BMC nephrology* **16:** 55

Bergmann C, Senderek J, Sedlacek B, Pegiazoglou I, Puglia P, Eggermann T, Rudnik-Schoneborn S, Furu L, Onuchic LF, De Baca M, Germino GG, Guay-Woodford L, Somlo S, Moser M, Buttner R, Zerres K (2003) Spectrum of mutations in the gene for autosomal recessive polycystic kidney disease (ARPKD/PKHD1). *Journal of the american society of nephrology : JASN* **14:** 76-89

Bhalla V, Hallows KR (2008) Mechanisms of ENaC regulation and clinical implications. *Journal of the american society of nephrology : JASN* **19:** 1845-1854

Bhunia AK, Piontek K, Boletta A, Liu L, Qian F, Xu PN, Germino FJ, Germino GG (2002) PKD1 induces p21(waf1) and regulation of the cell cycle via direct activation of the JAK-STAT signaling pathway in a process requiring PKD2. *Cell* **109:** 157-168

Bisceglia M, Galliani CA, Senger C, Stallone C, Sessa A (2006) Renal cystic diseases: a review. *Advances in anatomic pathology* **13:** 26-56

Blazer-Yost BL, Blacklock BJ, Flaig S, Bacallao RL, Gattone VH (2011) Lysophosphatidic acid is a modulator of cyst growth in autosomal dominant polycystic kidney disease. *Cellular physiology and biochemistry : international journal of experimental cellular physiology, biochemistry, and pharmacology* **28:** 1255-1264

Blazer-Yost BL, Liu X, Helman SI (1998) Hormonal regulation of ENaCs: insulin and aldosterone. *The American journal of physiology* **274:** C1373-1379

Bloom SR, Peart WS, Unwin RJ (1983) Neurotensin and antinatriuresis in the conscious rabbit. *British journal of pharmacology* **79:** 15-18

Boase NA, Rychkov GY, Townley SL, Dinudom A, Candi E, Voss AK, Tsoutsman T, Semsarian C, Melino G, Koentgen F, Cook DI, Kumar S (2011) Respiratory distress and perinatal lethality in Nedd4-2-deficient mice. *Nature communications* **2:** 287

Boletta A, Qian F, Onuchic LF, Bragonzi A, Cortese M, Deen PM, Courtoy PJ, Soria MR, Devuyst O, Monaco L, Germino GG (2001) Biochemical characterization of bona fide polycystin-1 in vitro and in vivo. *American journal of kidney diseases : the official journal of the National Kidney Foundation* **38:** 1421-1429

Bonsib SM (2009) Renal cystic diseases and renal neoplasms: a mini-review. *Clinical journal of the american society of nephrology : CJASN* **4:** 1998-2007

Bossolasco M, Veillette F, Bertrand R, Mes-Masson AM (2006) Human TDE1, a TDE1/TMS family member, inhibits apoptosis in vitro and stimulates in vivo tumorigenesis. *Oncogene* **25:** 4549-4558

Brill SR, Ross KE, Davidow CJ, Ye M, Grantham JJ, Caplan MJ (1996) Immunolocalization of ion transport proteins in human autosomal dominant polycystic kidney epithelial cells. *Proceedings of the national academy of sciences of the United States of America* **93:** 10206-10211

Brown D, Stow JL (1996) Protein trafficking and polarity in kidney epithelium: from cell biology to physiology. *Physiological reviews* **76:** 245-297

Cai Y, Maeda Y, Cedzich A, Torres VE, Wu G, Hayashi T, Mochizuki T, Park JH, Witzgall R, Somlo S (1999) Identification and characterization of polycystin-2, the PKD2 gene product. *The Journal of biological chemistry* **274:** 28557-28565

Canessa CM, Schild L, Buell G, Thorens B, Gautschi I, Horisberger JD, Rossier BC (1994) Amiloride-sensitive epithelial Na+ channel is made of three homologous subunits. *Nature* **367:** 463-467

Carroll TJ, Das A (2011) Planar cell polarity in kidney development and disease. *Organogenesis* **7:** 180-190

Cerro-Herreros E, Fernandez-Costa JM, Sabater-Arcis M, Llamusi B, Artero R (2016) Derepressing muscleblind expression by miRNA sponges ameliorates myotonic dystrophy-like phenotypes in Drosophila. *Scientific reports* **6:** 36230

Chang MY, Ong AC (2008) Autosomal dominant polycystic kidney disease: recent advances in pathogenesis and treatment. *Nephron physiology* **108:** p1-7

Chen CP (2007) Meckel syndrome: genetics, perinatal findings, and differential diagnosis. *Taiwanese journal of obstetrics & gynecology* **46:** 9-14

Chimge NO, Makeyev AV, Waigel SJ, Enkhmandakh B, Bayarsaihan D (2012) PI3K/Akt-dependent functions of TFII-I transcription factors in mouse embryonic stem cells. *Journal of cellular biochemistry* **113:** 1122-1131

Cho IJ, Lee AK, Lee SJ, Lee MG, Kim SG (2005) Repression by oxidative stress of iNOS and cytokine gene induction in macrophages results from AP-1 and NF-kappaB inhibition mediated by B cell translocation gene-1 activation. *Free radical biology & medicine* **39:** 1523-1536

Choyke PL (2000) Acquired cystic kidney disease. *European radiology* **10:** 1716-1721

Corpe CP, Tu H, Eck P, Wang J, Faulhaber-Walter R, Schnermann J, Margolis S, Padayatty S, Sun H, Wang Y, Nussbaum RL, Espey MG, Levine M (2010) Vitamin C transporter Slc23a1 links renal reabsorption, vitamin C tissue accumulation, and perinatal survival in mice. *The journal of clinical investigation* **120:** 1069-1083

Daoust MC, Reynolds DM, Bichet DG, Somlo S (1995) Evidence for a third genetic locus for autosomal dominant polycystic kidney disease. *Genomics* **25:** 733-736

Davidow CJ, Maser RL, Rome LA, Calvet JP, Grantham JJ (1996) The cystic fibrosis transmembrane conductance regulator mediates transepithelial fluid secretion by human autosomal dominant polycystic kidney disease epithelium in vitro. *Kidney international* **50:** 208-218

Dawe HR, Adams M, Wheway G, Szymanska K, Logan CV, Noegel AA, Gull K, Johnson CA (2009) Nesprin-2 interacts with meckelin and mediates ciliogenesis via remodelling of the actin cytoskeleton. *Journal of cell science* **122:** 2716-2726

Debonneville C, Flores SY, Kamynina E, Plant PJ, Tauxe C, Thomas MA, Munster C, Chraibi A, Pratt JH, Horisberger JD, Pearce D, Loffing J, Staub O (2001) Phosphorylation of Nedd4-2 by Sgk1 regulates epithelial Na(+) channel cell surface expression. *The EMBO journal* **20:** 7052-7059

Debrus S, Rahbani L, Marttila M, Delorme B, Paradis P, Nemer M (2005) The zinc finger-only protein Zfp260 is a novel cardiac regulator and a nuclear effector of alpha1-adrenergic signaling. *Molecular and cellular biology* **25:** 8669-8682

Dobrovolsky VN, Bucci T, Heflich RH, Desjardins J, Richardson FC (2003) Mice deficient for cytosolic thymidine kinase gene develop fatal kidney disease. *Molecular genetics and metabolism* **78:** 1-10

Du Y, Liu B, Guo F, Xu G, Ding Y, Liu Y, Sun X (2012) The essential role of Mbd5 in the regulation of somatic growth and glucose homeostasis in mice. *PloS one* **7:** e47358

Ebihara I, Nakamura T, Takahashi T, Yamamoto M, Tomino Y, Nagao S, Takahashi H, Koide H (1995) Altered extracellular matrix component gene expression in murine polycystic kidney. *Renal physiology and biochemistry* **18:** 73-80

Eley L, Turnpenny L, Yates LM, Craighead AS, Morgan D, Whistler C, Goodship JA, Strachan T (2004) A perspective on inversin. *Cell biology international* **28:** 119-124

Elwi AN, Damaraju VL, Baldwin SA, Young JD, Sawyer MB, Cass CE (2006) Renal nucleoside transporters: physiological and clinical implications. *Biochemistry and cell biology = Biochimie et biologie cellulaire* **84:** 844-858

Eraly SA, Vallon V, Vaughn DA, Gangoiti JA, Richter K, Nagle M, Monte JC, Rieg T, Truong DM, Long JM, Barshop BA, Kaler G, Nigam SK (2006) Decreased renal organic anion secretion and plasma accumulation of endogenous organic anions in OAT1 knock-out mice. *The journal of biological chemistry* **281:** 5072-5083

Esteban MA, Harten SK, Tran MG, Maxwell PH (2006) Formation of primary cilia in the renal epithelium is regulated by the von Hippel-Lindau tumor suppressor protein. *Journal of the american society of nephrology : JASN* **17:** 1801-1806

Faletti CJ, Perrotti N, Taylor SI, Blazer-Yost BL (2002) sgk: an essential convergence point for peptide and steroid hormone regulation of ENaC-mediated Na+ transport. *American journal of physiology cell physiology* **282:** C494-500

Fan G, Hutnick L (2005) Methyl-CpG binding proteins in the nervous system. *Cell research* **15:** 255-261

Fanconi G, Hanhart E, von AA, Uhlinger E, Dolivo G, Prader A (1951) [Familial, juvenile nephronophthisis (idiopathic parenchymal contracted kidney)]. *Helvetica paediatrica acta* **6:** 1-49

Feiguin F, Hannus M, Mlodzik M, Eaton S (2001) The ankyrin repeat protein Diego mediates Frizzled-dependent planar polarization. *Developmental cell* **1:** 93-101

Fejes-Toth G, Zahajszky T, Filep J (1980) Effect of vasopressin on renal kallikrein excretion. *The American journal of physiology* **239:** F388-F392

Feraille E, Doucet A (2001) Sodium-potassium-adenosinetriphosphatase-dependent sodium transport in the kidney: hormonal control. *Physiological reviews* **81:** 345-418

Fu H, Tian Y, Zhou L, Zhou D, Tan RJ, Stolz DB, Liu Y (2017) Tenascin-C Is a Major Component of the Fibrogenic Niche in Kidney Fibrosis. *Journal of the american society of nephrology : JASN* **28**: 785-801

Fuchshuber A, Kroiss S, Karle S, Berthold S, Huck K, Burton C, Rahman N, Koptides M, Deltas C, Otto E, Ruschendorf F, Feest T, Hildebrandt F (2001) Refinement of the gene locus for autosomal dominant medullary cystic kidney disease type 1 (MCKD1) and construction of a physical and partial transcriptional map of the region. *Genomics* **72:** 278-284

Gaeggeler HP, Gonzalez-Rodriguez E, Jaeger NF, Loffing-Cueni D, Norregaard R, Loffing J, Horisberger JD, Rossier BC (2005) Mineralocorticoid versus glucocorticoid receptor occupancy mediating aldosterone-stimulated sodium transport in a novel renal cell line. *Journal of the american society of nephrology : JASN* **16:** 878-891

Gaeggeler HP, Guillod Y, Loffing-Cueni D, Loffing J, Rossier BC (2011) Vasopressin-dependent coupling between sodium transport and water flow in a mouse cortical collecting duct cell line. *Kidney international* **79:** 843-852

Gagnadoux MF, Bacri JL, Broyer M, Habib R (1989) Infantile chronic tubulo-interstitial nephritis with cortical microcysts: variant of nephronophthisis or new disease entity? *Pediatr nephrol* **3:** 50-55

Gardner KD, Jr. (1971) Evolution of clinical signs in adult-onset cystic disease of the renal medulla. *Annals of internal medicine* **74:** 47-54

Gattone VH, Ricker JL, Trambaugh CM, Klein RM (2002) Multiorgan mRNA misexpression in murine autosomal recessive polycystic kidney disease. *Kidney international* **62:** 1560-1569

Geng L, Segal Y, Pavlova A, Barros EJ, Lohning C, Lu W, Nigam SK, Frischauf AM, Reeders ST, Zhou J (1997) Distribution and developmentally regulated expression of murine polycystin. *The american journal of physiology* **272:** F451-459

Geng L, Segal Y, Peissel B, Deng N, Pei Y, Carone F, Rennke HG, Glucksmann-Kuis AM, Schneider MC, Ericsson M, Reeders ST, Zhou J (1996) Identification and localization of polycystin, the PKD1 gene product. *The journal of clinical investigation* **98:** 2674-2682

Giral H, Lanzano L, Caldas Y, Blaine J, Verlander JW, Lei T, Gratton E, Levi M (2011) Role of PDZK1 protein in apical membrane expression of renal sodium-coupled phosphate transporters. *The journal of biological chemistry* **286:** 15032-15042

Gleason CE, Frindt G, Cheng CJ, Ng M, Kidwai A, Rashmi P, Lang F, Baum M, Palmer LG, Pearce D (2015) mTORC2 regulates renal tubule sodium uptake by promoting ENaC activity. *The journal of clinical investigation* **125:** 117-128

Goggolidou P (2014) Wnt and planar cell polarity signaling in cystic renal disease. *Organogenesis* **10:** 86-95

Goldman SH, Walker SR, Merigan TC, Jr., Gardner KD, Jr., Bull JM (1966) Hereditary occurrence of cystic disease of the renal medulla. *The New England journal of medicine* **274:** 984-992

Gonzalez-Guerrero C, Cannata-Ortiz P, Guerri C, Egido J, Ortiz A, Ramos AM (2016) TLR4-mediated inflammation is a key pathogenic event leading to kidney damage and fibrosis in cyclosporine nephrotoxicity. *Archives of toxicology*

Gordon S (2003) Alternative activation of macrophages. *Nature reviews Immunology* **3:** 23-35

Granger JP, Alexander BT, Llinas M (2002) Mechanisms of pressure natriuresis. *Current hypertension reports* **4:** 152-159

Grantham JJ, Ye M, Gattone VH, 2nd, Sullivan LP (1995) In vitro fluid secretion by epithelium from polycystic kidneys. *The Journal of clinical investigation* **95:** 195-202

Guyton AC (1991) Blood pressure control--special role of the kidneys and body fluids. *Science* **252:** 1813-1816

Haider NB, Carmi R, Shalev H, Sheffield VC, Landau D (1998) A Bedouin kindred with infantile nephronophthisis demonstrates linkage to chromosome 9 by homozygosity mapping. *American journal of human genetics* **63:** 1404-1410

Halbritter J, Porath JD, Diaz KA, Braun DA, Kohl S, Chaki M, Allen SJ, Soliman NA, Hildebrandt F, Otto EA (2013) Identification of 99 novel mutations in a worldwide cohort of 1,056 patients with a nephronophthisis-related ciliopathy. *Human genetics* **132:** 865-884

Hamm-Alvarez SF, Sheetz MP (1998) Microtubule-dependent vesicle transport: modulation of channel and transporter activity in liver and kidney. *Physiological reviews* **78:** 1109-1129

Hanaoka K, Devuyst O, Schwiebert EM, Wilson PD, Guggino WB (1996) A role for CFTR in human autosomal dominant polycystic kidney disease. *The american journal of physiology* **270:** C389-399

Hanaoka K, Qian F, Boletta A, Bhunia AK, Piontek K, Tsiokas L, Sukhatme VP, Guggino WB, Germino GG (2000) Co-assembly of polycystin-1 and -2 produces unique cation-permeable currents. *Nature* **408:** 990-994

Hanus C, Vannier C, Triller A (2004) Intracellular association of glycine receptor with gephyrin increases its plasma membrane accumulation rate. *The journal of neuroscience : the official journal of the society for neuroscience* **24:** 1119-1128

Harris PC, Torres VE (2009) Polycystic kidney disease. *Annual review of medicine* **60:** 321-337

Hasler U, Leroy V, Martin PY, Feraille E (2009) Aquaporin-2 abundance in the renal collecting duct: new insights from cultured cell models. *American journal of physiology renal physiology* **297:** F10-18

Hateboer N, Gumbs C, Teare MD, Coles GA, Griffiths D, Ravine D, Futreal PA, Rahman N (2001) Confirmation of a gene locus for medullary cystic kidney disease (MCKD2) on chromosome 16p12. *Kidney international* **60:** 1233-1239

Hawk CT, Li L, Schafer JA (1996) AVP and aldosterone at physiological concentrations have synergistic effects on Na+ transport in rat CCD. *Kidney international supplement* **57:** S35-41

Heidbreder M, Frohlich F, Johren O, Dendorfer A, Qadri F, Dominiak P (2003) Hypoxia rapidly activates HIF-3alpha mRNA expression. *FASEB journal : official publication of the federation of american societies for experimental biology* **17:** 1541-1543

Hildebrandt F, Attanasio M, Otto E (2009) Nephronophthisis: disease mechanisms of a ciliopathy. *Journal of the american society of nephrology : JASN* **20:** 23-35

Hildebrandt F, Otto E (2000) Molecular genetics of nephronophthisis and medullary cystic kidney disease. *Journal of the american society of nephrology : JASN* **11:** 1753-1761

Hildebrandt F, Zhou W (2007) Nephronophthisis-associated ciliopathies. *Journal of the american society of nephrology : JASN* **18:** 1855-1871

Hoag HM, Martel J, Gauthier C, Tenenhouse HS (1999) Effects of Npt2 gene ablation and low-phosphate diet on renal Na(+)/phosphate cotransport and cotransporter gene expression. *The journal of clinical investigation* **104:** 679-686

Horn KH, Warner DR, Pisano M, Greene RM (2011) PRDM16 expression in the developing mouse embryo. *Acta histochemica* **113:** 150-155

Hosoyamada M, Takiue Y, Morisaki H, Cheng J, Ikawa M, Okabe M, Morisaki T, Ichida K, Hosoya T, Shibasaki T (2010) Establishment and analysis of SLC22A12 (URAT1) knockout mouse. *Nucleosides, nucleotides & nucleic acids* **29:** 314-320

Hu W, Chen FH, Yuan FL, Zhang TY, Wu FR, Rong C, Jiang S, Tang J, Zhang CC, Lin MY (2012) Blockade of acid-sensing ion channels protects articular chondrocytes from acid-induced apoptotic injury. *Inflammation research : official journal of the european histamine research society [et al]* **61:** 327-335

Huang da W, Sherman BT, Lempicki RA (2009a) Bioinformatics enrichment tools: paths toward the comprehensive functional analysis of large gene lists. *Nucleic acids research* **37:** 1-13

Huang da W, Sherman BT, Lempicki RA (2009b) Systematic and integrative analysis of large gene lists using DAVID bioinformatics resources. *Nature protocols* **4:** 44-57

Hughes J, Ward CJ, Peral B, Aspinwall R, Clark K, San Millan JL, Gamble V, Harris PC (1995) The polycystic kidney disease 1 (PKD1) gene encodes a novel protein with multiple cell recognition domains. *Nature genetics* **10:** 151-160

Husson H, Manavalan P, Akmaev VR, Russo RJ, Cook B, Richards B, Barberio D, Liu D, Cao X, Landes GM, Wang CJ, Roberts BL, Klinger KW, Grubman SA, Jefferson DM, Ibraghimov-Beskrovnaya O (2004) New insights into ADPKD molecular pathways using combination of SAGE and microarray technologies. *Genomics* **84:** 497-510

Iannello S, Bosco P, Cavaleri A, Camuto M, Milazzo P, Belfiore F (2002) A review of the literature of Bardet-Biedl disease and report of three cases associated with metabolic syndrome and diagnosed after the age of fifty. *Obesity reviews : an official journal of the international association for the study of obesity* **3:** 123-135

Ibraghimov-Beskrovnaya O, Dackowski WR, Foggensteiner L, Coleman N, Thiru S, Petry LR, Burn TC, Connors TD, Van Raay T, Bradley J, Qian F, Onuchic LF, Watnick TJ, Piontek K, Hakim RM, Landes GM, Germino GG, Sandford R, Klinger KW (1997) Polycystin: in vitro synthesis, in vivo tissue expression, and subcellular localization identifies a large membrane-associated protein. *Proceedings of the national academy of sciences of the United States of America* **94:** 6397-6402

Islam R, Anzai N, Ahmed N, Ellapan B, Jin CJ, Srivastava S, Miura D, Fukutomi T, Kanai Y, Endou H (2008) Mouse organic anion transporter 2 (mOat2) mediates the transport of short chain fatty acid propionate. *Journal of pharmacological sciences* **106:** 525-528

Jacobson MD, Weil M, Raff MC (1997) Programmed cell death in animal development. *Cell* **88:** 347-354

Jepsen K, Hermanson O, Onami TM, Gleiberman AS, Lunyak V, McEvilly RJ, Kurokawa R, Kumar V, Liu F, Seto E, Hedrick SM, Mandel G, Glass CK, Rose DW, Rosenfeld MG (2000) Combinatorial roles of the nuclear receptor corepressor in transcription and development. *Cell* **102:** 753-763

Kabra R, Knight KK, Zhou R, Snyder PM (2008) Nedd4-2 induces endocytosis and degradation of proteolytically cleaved epithelial Na+ channels. *The journal of biological chemistry* **283:** 6033-6039

Kalyoussef E, Hwang J, Prasad V, Barone J (2006) Segmental multicystic dysplastic kidney in children. *Urology* **68:** 1121 e1129-1111

Kamynina E, Debonneville C, Bens M, Vandewalle A, Staub O (2001) A novel mouse Nedd4 protein suppresses the activity of the epithelial Na+ channel. *FASEB journal : official publication of the federation of american societies for experimental biology* **15:** 204-214

Karihaloo A, Koraishy F, Huen SC, Lee Y, Merrick D, Caplan MJ, Somlo S, Cantley LG (2011) Macrophages promote cyst growth in polycystic kidney disease. *Journal of the american society of nephrology : JASN* **22:** 1809-1814

Karner CM, Chirumamilla R, Aoki S, Igarashi P, Wallingford JB, Carroll TJ (2009) Wnt9b signaling regulates planar cell polarity and kidney tubule morphogenesis. *Nature genetics* **41:** 793-799

Kazama I (2015) Physiological significance of delayed rectifier K(+) channels (Kv1.3) expressed in T lymphocytes and their pathological significance in chronic kidney disease. *The journal of physiological sciences : JPS* **65:** 25-35

Kelly KJ, Liu Y, Zhang J, Dominguez JH (2015) Renal C3 complement component: feed forward to diabetic kidney disease. *American journal of nephrology* **41:** 48-56

Khan SA, Muhammad N, Khan MA, Kamal A, Rehman ZU, Khan S (2016) Genetics of human Bardet-Biedl syndrome, an updates. *Clinical genetics* **90:** 3-15

Kim B, King BF, Jr., Vrtiska TJ, Irazabal MV, Torres VE, Harris PC (2016) Inherited renal cystic diseases. *Abdom radiol (NY)* **41:** 1035-1051

Kim KY, Choi KC, Auersperg N, Leung PCK (2006) Mechanism of gonadotropin-releasing hormone GnRH-I and II induced cell growth inhibition in ovarian cancer cells: role of the GnRH-1 receptor and protein kinase C pathway. *Endocrine-related cancer* **13:** 211-220

Kirby A, Gnirke A, Jaffe DB, Baresova V, Pochet N, Blumenstiel B, Ye C, Aird D, Stevens C, Robinson JT, Cabili MN, Gat-Viks I, Kelliher E, Daza R, DeFelice M, Hulkova H, Sovova J, Vylet'al P, Antignac C, Guttman M, Handsaker RE, Perrin D, Steelman S, Sigurdsson S, Scheinman SJ, Sougnez C, Cibulskis K, Parkin M, Green T, Rossin E, Zody MC, Xavier RJ, Pollak MR, Alper SL, Lindblad-Toh K, Gabriel S, Hart PS, Regev A, Nusbaum C, Kmoch S, Bleyer AJ, Lander ES, Daly MJ (2013) Mutations causing medullary cystic kidney disease type 1 lie in a large VNTR in MUC1 missed by massively parallel sequencing. *Nature genetics* **45:** 299-303

Koulen P, Cai Y, Geng L, Maeda Y, Nishimura S, Witzgall R, Ehrlich BE, Somlo S (2002) Polycystin-2 is an intracellular calcium release channel. *Nature cell biology* **4:** 191-197

Kristiansen M, Graversen JH, Jacobsen C, Sonne O, Hoffman HJ, Law SK, Moestrup SK (2001) Identification of the haemoglobin scavenger receptor. *Nature* **409:** 198-201

Kwon TH, Frokiaer J, Nielsen S (2013) Regulation of aquaporin-2 in the kidney: A molecular mechanism of body-water homeostasis. *Kidney research and clinical practice* **32:** 96-102

Kyllonen MS, Parkkila S, Rajaniemi H, Waheed A, Grubb JH, Shah GN, Sly WS, Kaunisto K (2003) Localization of carbonic anhydrase XII to the basolateral membrane of H+-secreting cells of mouse and rat kidney. *The journal of histochemistry and cytochemistry : official journal of the histochemistry society* **51:** 1217-1224

Lahr TF, Record RD, Hoover DK, Hughes CL, Blazer-Yost BL (2000) Characterization of the ion transport responses to ADH in the MDCK-C7 cell line. *Pflugers archiv : European journal of physiology* **439:** 610-617

Lambert JM, Lopez EF, Lindsey ML (2008) Macrophage roles following myocardial infarction. *International journal of cardiology* **130:** 147-158

Latif F, Tory K, Gnarra J, Yao M, Duh FM, Orcutt ML, Stackhouse T, Kuzmin I, Modi W, Geil L, et al. (1993) Identification of the von Hippel-Lindau disease tumor suppressor gene. *Science* **260:** 1317-1320

Lebrun C, Avci HX, Wehrle R, Doulazmi M, Jaudon F, Morel MP, Rivals I, Ema M, Schmidt S, Sotelo C, Vodjdani G, Dusart I (2013) Klf9 is necessary and sufficient for Purkinje cell survival in organotypic culture. *Molecular and cellular neurosciences* **54:** 9-21

Lee JE, Park MH, Park JH (2004) The gene expression profile of cyst epithelial cells in autosomal dominant polycystic kidney disease patients. *Journal of biochemistry and molecular biology* **37:** 612-617

Lee KY, Li M, Manchanda M, Batra R, Charizanis K, Mohan A, Warren SA, Chamberlain CM, Finn D, Hong H, Ashraf H, Kasahara H, Ranum LP, Swanson MS (2013) Compound loss of muscleblind-like function in myotonic dystrophy. *EMBO molecular medicine* **5:** 1887-1900

Leonard WJ, O'Shea JJ (1998) Jaks and STATs: biological implications. *Annual review of immunology* **16:** 293-322

Leviel F, Hubner CA, Houillier P, Morla L, El Moghrabi S, Brideau G, Hassan H, Parker MD, Kurth I, Kougioumtzes A, Sinning A, Pech V, Riemondy KA, Miller RL, Hummler E, Shull GE, Aronson PS, Doucet A, Wall SM, Chambrey R, Eladari D (2010) The Na+-dependent chloride-bicarbonate exchanger SLC4A8 mediates an electroneutral Na+ reabsorption process in the renal cortical collecting ducts of mice. *The journal of clinical investigation* **120:** 1627-1635

Li H, Findlay IA, Sheppard DN (2004) The relationship between cell proliferation, Cl- secretion, and renal cyst growth: a study using CFTR inhibitors. *Kidney international* **66:** 1926-1938

Li Y, Wright JM, Qian F, Germino GG, Guggino WB (2005) Polycystin 2 interacts with type I inositol 1,4,5-trisphosphate receptor to modulate intracellular Ca2+ signaling. *The journal of biological chemistry* **280:** 41298-41306

Lienkamp S, Ganner A, Boehlke C, Schmidt T, Arnold SJ, Schafer T, Romaker D, Schuler J, Hoff S, Powelske C, Eifler A, Kronig C, Bullerkotte A, Nitschke R, Kuehn EW, Kim E, Burkhardt H, Brox T, Ronneberger O, Gloy J, Walz G (2010) Inversin relays Frizzled-8 signals to promote proximal pronephros development. *Proceedings of the national academy of sciences of the United States of America* **107:** 20388-20393

Lienkamp S, Ganner A, Walz G (2012) Inversin, Wnt signaling and primary cilia. *Differentiation; research in biological diversity* **83:** S49-55

Lin Z, Xiong L, Zhou J, Wang J, Li Z, Hu H, Lin Q (2015) gamma-Glutamylcyclotransferase Knockdown Inhibits Growth of Lung Cancer Cells Through G0/G1 Phase Arrest. *Cancer biotherapy & radiopharmaceuticals* **30:** 211-216

Loffing J, Flores SY, Staub O (2006) Sgk kinases and their role in epithelial transport. *Annual review of physiology* **68:** 461-490

Loffing J, Korbmacher C (2009) Regulated sodium transport in the renal connecting tubule (CNT) via the epithelial sodium channel (ENaC). *Pflugers archiv : European journal of physiology* **458:** 111-135

Long YC, Zierath JR (2006) AMP-activated protein kinase signaling in metabolic regulation. *The journal of clinical investigation* **116:** 1776-1783

Lonser RR, Glenn GM, Walther M, Chew EY, Libutti SK, Linehan WM, Oldfield EH (2003) von Hippel-Lindau disease. *Lancet* **361:** 2059-2067

Lu M, Wang J, Jones KT, Ives HE, Feldman ME, Yao LJ, Shokat KM, Ashrafi K, Pearce D (2010) mTOR complex-2 activates ENaC by phosphorylating SGK1. *Journal of the american society of nephrology : JASN* **21:** 811-818

Luo Y, Vassilev PM, Li X, Kawanabe Y, Zhou J (2003) Native polycystin 2 functions as a plasma membrane Ca2+-permeable cation channel in renal epithelia. *Molecular and cellular biology* **23:** 2600-2607

Lutz MS, Burk RD (2006) Primary cilium formation requires von hippel-lindau gene function in renal-derived cells. *Cancer research* **66:** 6903-6907

Majumdar A, Vainio S, Kispert A, McMahon J, McMahon AP (2003) Wnt11 and Ret/Gdnf pathways cooperate in regulating ureteric branching during metanephric kidney development. *Development* **130:** 3175-3185

Mallipattu SK, Estrada CC, He JC (2017) The critical role of Kruppel-like factors in kidney disease. *American journal of physiology renal physiology* **312:** F259-F265

Mallipattu SK, Horne SJ, D'Agati V, Narla G, Liu R, Frohman MA, Dickman K, Chen EY, Ma'ayan A, Bialkowska AB, Ghaleb AM, Nandan MO, Jain MK, Daehn I, Chuang PY, Yang VW, He JC (2015) Kruppel-like factor 6 regulates mitochondrial function in the kidney. *The journal of clinical investigation* **125:** 1347-1361

Mangoo-Karim R, Ye M, Wallace DP, Grantham JJ, Sullivan LP (1995) Anion secretion drives fluid secretion by monolayers of cultured human polycystic cells. *The American journal of physiology* **269:** F381-388

Marunaka Y (1997) Hormonal and osmotic regulation of NaCl transport in renal distal nephron epithelium. *The Japanese journal of physiology* **47:** 499-511

Marunaka Y, Eaton DC (1991) Effects of vasopressin and cAMP on single amiloride-blockable Na channels. *The American journal of physiology* **260:** C1071-1084

Mattson DL (2014) Infiltrating immune cells in the kidney in salt-sensitive hypertension and renal injury. *American journal of physiology renal physiology* **307:** F499-508

McDonald FJ, Yang B, Hrstka RF, Drummond HA, Tarr DE, McCray PB, Jr., Stokes JB, Welsh MJ, Williamson RA (1999) Disruption of the beta subunit of the epithelial Na+ channel in mice: hyperkalemia and neonatal death associated with a pseudohypoaldosteronism phenotype. *Proceedings of the national academy of sciences of the United States of America* **96:** 1727-1731

Menezes LF, Cai Y, Nagasawa Y, Silva AM, Watkins ML, Da Silva AM, Somlo S, Guay-Woodford LM, Germino GG, Onuchic LF (2004) Polyductin, the PKHD1 gene product, comprises isoforms expressed in plasma membrane, primary cilium, and cytoplasm. *Kidney international* **66:** 1345-1355

Mercola M (2003) Left-right asymmetry: nodal points. *Journal of cell science* **116:** 3251-3257

Mergen M, Engel C, Muller B, Follo M, Schafer T, Jung M, Walz G (2013) The nephronophthisis gene product NPHP2/Inversin interacts with Aurora A and interferes with HDAC6-mediated cilia disassembly. *Nephrology, dialysis, transplantation : official publication of the european dialysis and transplant association - European renal association* **28:** 2744-2753

Mochida Y, Parisuthiman D, Kaku M, Hanai J, Sukhatme VP, Yamauchi M (2006) Nephrocan, a novel member of the small leucine-rich repeat protein family, is an inhibitor of transforming growth factor-beta signaling. *The journal of biological chemistry* **281:** 36044-36051

Mochizuki T, Saijoh Y, Tsuchiya K, Shirayoshi Y, Takai S, Taya C, Yonekawa H, Yamada K, Nihei H, Nakatsuji N, Overbeek PA, Hamada H, Yokoyama T (1998) Cloning of inv, a gene that controls left/right asymmetry and kidney development. *Nature* **395:** 177-181

Mochizuki T, Wu G, Hayashi T, Xenophontos SL, Veldhuisen B, Saris JJ, Reynolds DM, Cai Y, Gabow PA, Pierides A, Kimberling WJ, Breuning MH, Deltas CC, Peters DJ, Somlo S (1996) PKD2, a gene for polycystic kidney disease that encodes an integral membrane protein. *Science* **272:** 1339-1342

Morgan D, Eley L, Sayer J, Strachan T, Yates LM, Craighead AS, Goodship JA (2002a) Expression analyses and interaction with the anaphase promoting complex protein Apc2 suggest a role for inversin in primary cilia and involvement in the cell cycle. *Human molecular genetics* **11:** 3345-3350

Morgan D, Goodship J, Essner JJ, Vogan KJ, Turnpenny L, Yost HJ, Tabin CJ, Strachan T (2002b) The left-right determinant inversin has highly conserved ankyrin repeat and IQ domains and interacts with calmodulin. *Human genetics* **110:** 377-384

Morgan D, Turnpenny L, Goodship J, Dai W, Majumder K, Matthews L, Gardner A, Schuster G, Vien L, Harrison W, Elder FF, Penman-Splitt M, Overbeek P, Strachan T (1998) Inversin, a novel gene in the vertebrate left-right axis pathway, is partially deleted in the inv mouse. *Nature genetics* **20:** 149-156

Mori T, Kawara S, Shinozaki M, Hayashi N, Kakinuma T, Igarashi A, Takigawa M, Nakanishi T, Takehara K (1999) Role and interaction of connective tissue growth factor with transforming growth factor-beta in persistent fibrosis: A mouse fibrosis model. *Journal of cellular physiology* **181:** 153-159

Mrug M, Zhou J, Woo Y, Cui X, Szalai AJ, Novak J, Churchill GA, Guay-Woodford LM (2008) Overexpression of innate immune response genes in a model of recessive polycystic kidney disease. *Kidney international* **73:** 63-76

Murcia NS, Sweeney WE, Jr., Avner ED (1999) New insights into the molecular pathophysiology of polycystic kidney disease. *Kidney international* **55:** 1187-1197

Nagamori S, Wiriyasermkul P, Guarch ME, Okuyama H, Nakagomi S, Tadagaki K, Nishinaka Y, Bodoy S, Takafuji K, Okuda S, Kurokawa J, Ohgaki R, Nunes V, Palacin M, Kanai Y (2016) Novel cystine transporter in renal proximal tubule identified as a missing partner of cystinuria-related plasma membrane protein rBAT/SLC3A1. *Proceedings of the national academy of sciences of the United States of America* **113:** 775-780

Nagy, II, Xu Q, Naillat F, Ali N, Miinalainen I, Samoylenko A, Vainio SJ (2016) Impairment of Wnt11 function leads to kidney tubular abnormalities and secondary glomerular cystogenesis. *BMC developmental biology* **16:** 30

Nakamura T, Ebihara I, Nagaoka I, Tomino Y, Nagao S, Takahashi H, Koide H (1993) Growth factor gene expression in kidney of murine polycystic kidney disease. *Journal of the american society of nephrology : JASN* **3:** 1378-1386

Nauli SM, Alenghat FJ, Luo Y, Williams E, Vassilev P, Li X, Elia AE, Lu W, Brown EM, Quinn SJ, Ingber DE, Zhou J (2003) Polycystins 1 and 2 mediate mechanosensation in the primary cilium of kidney cells. *Nature genetics* **33:** 129-137

Newby LJ, Streets AJ, Zhao Y, Harris PC, Ward CJ, Ong AC (2002) Identification, characterization, and localization of a novel kidney polycystin-1-polycystin-2 complex. *The journal of biological chemistry* **277:** 20763-20773

Nofziger C, Brown KK, Smith CD, Harrington W, Murray D, Bisi J, Ashton TT, Maurio FP, Kalsi K, West TA, Baines D, Blazer-Yost BL (2009) PPARgamma agonists inhibit vasopressin-mediated anion transport in the MDCK-C7 cell line. *American journal of physiology renal physiology* **297:** F55-62

Nonaka S, Tanaka Y, Okada Y, Takeda S, Harada A, Kanai Y, Kido M, Hirokawa N (1998) Randomization of left-right asymmetry due to loss of nodal cilia generating leftward flow of extraembryonic fluid in mice lacking KIF3B motor protein. *Cell* **95:** 829-837

Nurnberger J, Bacallao RL, Phillips CL (2002) Inversin forms a complex with catenins and N-cadherin in polarized epithelial cells. *Molecular biology of the cell* **13:** 3096-3106

Nurnberger J, Kavapurackal R, Zhang SJ, Opazo Saez A, Heusch G, Philipp T, Pietruck F, Kribben A (2006) Differential tissue distribution of the Invs gene product inversin. *Cell and tissue research* **323:** 147-155

Nurnberger J, Kribben A, Opazo Saez A, Heusch G, Philipp T, Phillips CL (2004) The Invs gene encodes a microtubule-associated protein. *Journal of the american society of nephrology : JASN* **15:** 1700-1710

O'Donnell ME, Cragoe E, Jr., Villereal ML (1983) Inhibition of Na+ influx and DNA synthesis in human fibroblasts and neuroblastoma-glioma hybrid cells by amiloride analogs. *The Journal of pharmacology and experimental therapeutics* **226:** 368-372

Okada Y, Nonaka S, Tanaka Y, Saijoh Y, Hamada H, Hirokawa N (1999) Abnormal nodal flow precedes situs inversus in iv and inv mice. *Molecular cell* **4:** 459-468

Onuchic LF, Furu L, Nagasawa Y, Hou X, Eggermann T, Ren Z, Bergmann C, Senderek J, Esquivel E, Zeltner R, Rudnik-Schoneborn S, Mrug M, Sweeney W, Avner ED, Zerres K, Guay-Woodford LM, Somlo S, Germino GG (2002) PKHD1, the polycystic kidney and hepatic disease 1 gene, encodes a novel large protein containing multiple immunoglobulin-like plexin-transcription-factor domains and parallel beta-helix 1 repeats. *American journal of human genetics* **70:** 1305-1317

Otto EA, Schermer B, Obara T, O'Toole JF, Hiller KS, Mueller AM, Ruf RG, Hoefele J, Beekmann F, Landau D, Foreman JW, Goodship JA, Strachan T, Kispert A, Wolf MT, Gagnadoux MF, Nivet H, Antignac C, Walz G, Drummond IA, Benzing T, Hildebrandt F (2003) Mutations in INVS encoding inversin cause nephronophthisis type 2, linking renal cystic disease to the function of primary cilia and left-right axis determination. *Nature genetics* **34:** 413-420

Oud MM, van Bon BW, Bongers EM, Hoischen A, Marcelis CL, de Leeuw N, Mol SJ, Mortier G, Knoers NV, Brunner HG, Roepman R, Arts HH (2014) Early presentation of cystic kidneys in a family with a homozygous INVS mutation. *American journal of medical genetics Part A* **164A:** 1627-1634

Pal D, Sharma U, Singh SK, Prasad R (2014) Association between ZIP10 gene expression and tumor aggressiveness in renal cell carcinoma. *Gene* **552:** 195-198

Palmieri F (2013) The mitochondrial transporter family SLC25: identification, properties and physiopathology. *Molecular aspects of medicine* **34:** 465-484

Pan JS, Huang L, Belousova T, Lu L, Yang Y, Reddel R, Chang A, Ju H, DiMattia G, Tong Q, Sheikh-Hamad D (2015) Stanniocalcin-1 inhibits renal ischemia/reperfusion injury via an AMP-activated protein kinase-dependent pathway. *Journal of the american society of nephrology : JASN* **26:** 364-378

Pavlov TS, Levchenko V, Ilatovskaya DV, Palygin O, Staruschenko A (2015) Impaired epithelial Na+ channel activity contributes to cystogenesis and development of autosomal recessive polycystic kidney disease in PCK rats. *Pediatric research* **77:** 64-69

Pearce D (2003) SGK1 regulation of epithelial sodium transport. *Cellular physiology and biochemistry : international journal of experimental cellular physiology, biochemistry, and pharmacology* **13:** 13-20

Pennekamp P, Karcher C, Fischer A, Schweickert A, Skryabin B, Horst J, Blum M, Dworniczak B (2002) The ion channel polycystin-2 is required for left-right axis determination in mice. *Current biology : CB* **12:** 938-943

Peters DJ, Breuning MH (2001) Autosomal dominant polycystic kidney disease: modification of disease progression. *Lancet* **358:** 1439-1444

Phanish MK, Winn SK, Dockrell ME (2010) Connective tissue growth factor-(CTGF, CCN2)--a marker, mediator and therapeutic target for renal fibrosis. *Nephron experimental nephrology* **114:** e83-92

Phillips CL, Miller KJ, Filson AJ, Nurnberger J, Clendenon JL, Cook GW, Dunn KW, Overbeek PA, Gattone VH, 2nd, Bacallao RL (2004) Renal cysts of inv/inv mice resemble early infantile nephronophthisis. *Journal of the american society of nephrology : JASN* **15:** 1744-1755

Pietila I, Prunskaite-Hyyrylainen R, Kaisto S, Tika E, van Eerde AM, Salo AM, Garma L, Miinalainen I, Feitz WF, Bongers EM, Juffer A, Knoers NV, Renkema KY, Myllyharju J, Vainio SJ (2016) Wnt5a Deficiency Leads to Anomalies in Ureteric Tree Development, Tubular Epithelial Cell Organization and Basement Membrane Integrity Pointing to a Role in Kidney Collecting Duct Patterning. *PloS one* **11:** e0147171

Pollard K, Dudoit S, Laan M (2005) Multiple testing procedures: the multtest package and applications to genomics. *Bioinformatics and computational biology solutions using R and bioconductor***:** 249-271

Porter AG, Janicke RU (1999) Emerging roles of caspase-3 in apoptosis. *Cell death and differentiation* **6:** 99-104

Potter DE, Holliday MA, Piel CF, Feduska NJ, Belzer FO, Salvatierra O, Jr. (1980) Treatment of end-stage renal disease in children: a 15-year experience. *Kidney international* **18:** 103-109

Praetorius HA, Spring KR (2001) Bending the MDCK cell primary cilium increases intracellular calcium. *The journal of membrane biology* **184:** 71-79

Praetorius HA, Spring KR (2003) The renal cell primary cilium functions as a flow sensor. *Current opinion in nephrology and hypertension* **12:** 517-520

Putoux A, Attie-Bitach T, Martinovic J, Gubler MC (2012) Phenotypic variability of Bardet-Biedl syndrome: focusing on the kidney. *Pediatr nephrol* **27:** 7-15

Ravine D, Walker RG, Gibson RN, Forrest SM, Richards RI, Friend K, Sheffield LJ, Kincaid-Smith P, Danks DM (1992) Phenotype and genotype heterogeneity in autosomal dominant polycystic kidney disease. *Lancet* **340:** 1330-1333

Razin A (1998) CpG methylation, chromatin structure and gene silencing-a three-way connection. *The EMBO journal* **17:** 4905-4908

Reif MC, Troutman SL, Schafer JA (1986) Sodium transport by rat cortical collecting tubule. Effects of vasopressin and desoxycorticosterone. *The journal of clinical investigation* **77:** 1291-1298

Retailleau K, Duprat F (2014) Polycystins and partners: proposed role in mechanosensitivity. *The journal of physiology* **592:** 2453-2471

Rossier BC, Pradervand S, Schild L, Hummler E (2002) Epithelial sodium channel and the control of sodium balance: interaction between genetic and environmental factors. *Annual review of physiology* **64:** 877-897

Saburi S, Hester I, Fischer E, Pontoglio M, Eremina V, Gessler M, Quaggin SE, Harrison R, Mount R, McNeill H (2008) Loss of Fat4 disrupts PCP signaling and oriented cell division and leads to cystic kidney disease. *Nature genetics* **40:** 1010-1015

Sadagopan N, Li W, Roberds SL, Major T, Preston GM, Yu Y, Tones MA (2007) Circulating succinate is elevated in rodent models of hypertension and metabolic disease. *American journal of hypertension* **20:** 1209-1215

Salomon R, Saunier S, Niaudet P (2009) Nephronophthisis. *Pediatr nephrol* **24:** 2333-2344

Salonen R, Norio R (1984) The Meckel syndrome in Finland: epidemiologic and genetic aspects. *American journal of medical genetics* **18:** 691-698

Sanchez-Nino MD, Poveda J, Sanz AB, Mezzano S, Carrasco S, Fernandez-Fernandez B, Burkly LC, Nair V, Kretzler M, Hodgin JB, Ruiz-Ortega M, Selgas R, Egido J, Ortiz A (2013) Fn14 in podocytes and proteinuric kidney disease. *Biochimica et biophysica acta* **1832:** 2232-2243

Sang L, Miller JJ, Corbit KC, Giles RH, Brauer MJ, Otto EA, Baye LM, Wen X, Scales SJ, Kwong M, Huntzicker EG, Sfakianos MK, Sandoval W, Bazan JF, Kulkarni P, Garcia-Gonzalo FR, Seol AD, O'Toole JF, Held S, Reutter HM, Lane WS, Rafiq MA, Noor A, Ansar M, Devi AR, Sheffield VC, Slusarski DC, Vincent JB, Doherty DA, Hildebrandt F, Reiter JF, Jackson PK (2011) Mapping the NPHP-JBTS-MKS protein network reveals ciliopathy disease genes and pathways. *Cell* **145:** 513-528

Sarkozi R, Flucher K, Haller VM, Pirklbauer M, Mayer G, Schramek H (2012) Oncostatin M inhibits TGF-beta1-induced CTGF expression via STAT3 in human proximal tubular cells. *Biochemical and biophysical research communications* **424:** 801-806

Sarkozi R, Hauser C, Noppert SJ, Kronbichler A, Pirklbauer M, Haller VM, Grillari J, Grillari-Voglauer R, Mayer G, Schramek H (2011) Oncostatin M is a novel inhibitor of TGF-beta1-induced matricellular protein expression. *American journal of physiology renal physiology* **301:** F1014-1025

Schild L, Canessa CM, Shimkets RA, Gautschi I, Lifton RP, Rossier BC (1995) A mutation in the epithelial sodium channel causing Liddle disease increases channel activity in the Xenopus laevis oocyte expression system. *Proceedings of the national academy of sciences of the United States of America* **92:** 5699-5703

Schoor M, Schuster-Gossler K, Roopenian D, Gossler A (1999) Skeletal dysplasias, growth retardation, reduced postnatal survival, and impaired fertility in mice lacking the SNF2/SWI2 family member ETL1. *Mechanisms of development* **85:** 73-83

Seizinger BR, Rouleau GA, Ozelius LJ, Lane AH, Farmer GE, Lamiell JM, Haines J, Yuen JW, Collins D, Majoor-Krakauer D, et al. (1988) Von Hippel-Lindau disease maps to the region of chromosome 3 associated with renal cell carcinoma. *Nature* **332:** 268-269

Shane MA, Nofziger C, Blazer-Yost BL (2006) Hormonal regulation of the epithelial Na+ channel: from amphibians to mammals. *General and comparative endocrinology* **147:** 85-92

Shiba D, Manning DK, Koga H, Beier DR, Yokoyama T (2010) Inv acts as a molecular anchor for Nphp3 and Nek8 in the proximal segment of primary cilia. *Cytoskeleton (Hoboken)* **67:** 112-119

Shiba D, Takamatsu T, Yokoyama T (2005) Primary cilia of inv/inv mouse renal epithelial cells sense physiological fluid flow: bending of primary cilia and Ca2+ influx. *Cell structure and function* **30:** 93-100

Shiba D, Yamaoka Y, Hagiwara H, Takamatsu T, Hamada H, Yokoyama T (2009) Localization of Inv in a distinctive intraciliary compartment requires the C-terminal ninein-homolog-containing region. *Journal of cell science* **122:** 44-54

Shimkets RA, Warnock DG, Bositis CM, Nelson-Williams C, Hansson JH, Schambelan M, Gill JR, Jr., Ulick S, Milora RV, Findling JW, et al. (1994) Liddle's syndrome: heritable human hypertension caused by mutations in the beta subunit of the epithelial sodium channel. *Cell* **79:** 407-414

Shiraya K, Hirata T, Hatano R, Nagamori S, Wiriyasermkul P, Jutabha P, Matsubara M, Muto S, Tanaka H, Asano S, Anzai N, Endou H, Yamada A, Sakurai H, Kanai Y (2010) A novel transporter of SLC22 family specifically transports prostaglandins and co-localizes with 15-hydroxyprostaglandin dehydrogenase in renal proximal tubules. *The journal of biological chemistry* **285:** 22141-22151

Simons M, Gloy J, Ganner A, Bullerkotte A, Bashkurov M, Kronig C, Schermer B, Benzing T, Cabello OA, Jenny A, Mlodzik M, Polok B, Driever W, Obara T, Walz G (2005) Inversin, the gene product mutated in nephronophthisis type II, functions as a molecular switch between Wnt signaling pathways. *Nature genetics* **37:** 537-543

Sligh JE, Jr., Ballantyne CM, Rich SS, Hawkins HK, Smith CW, Bradley A, Beaudet AL (1993) Inflammatory and immune responses are impaired in mice deficient in intercellular adhesion molecule 1. *Proceedings of the national academy of sciences of the United States of America* **90:** 8529-8533

Snyder PM, Olson DR, Thomas BC (2002) Serum and glucocorticoid-regulated kinase modulates Nedd4-2-mediated inhibition of the epithelial Na+ channel. *The journal of biological chemistry* **277:** 5-8

Song X, Di Giovanni V, He N, Wang K, Ingram A, Rosenblum ND, Pei Y (2009) Systems biology of autosomal dominant polycystic kidney disease (ADPKD): computational identification of gene expression pathways and integrated regulatory networks. *Human molecular genetics* **18:** 2328-2343

Staub O, Dho S, Henry P, Correa J, Ishikawa T, McGlade J, Rotin D (1996) WW domains of Nedd4 bind to the proline-rich PY motifs in the epithelial Na+ channel deleted in Liddle's syndrome. *The EMBO journal* **15:** 2371-2380

Stellmer F, Keyser B, Burckhardt BC, Koepsell H, Streichert T, Glatzel M, Jabs S, Thiem J, Herdering W, Koeller DM, Goodman SI, Lukacs Z, Ullrich K, Burckhardt G, Braulke T, Muhlhausen C (2007) 3-Hydroxyglutaric acid is transported via the sodium-dependent dicarboxylate transporter NaDC3. *J mol med (Berl)* **85:** 763-770

Subbannayya T, Balakrishnan L, Sudarshan G, Advani J, Kumar S, Mahmood R, Nair B, Sirdeshmukh R, Mukherjee KK, Umathe SN, Raju R, Prasad TSK (2013) An integrated map of corticotropin-releasing hormone signaling pathway. *J cell commun signal* **7:** 295-300

Suizu F, Hirata N, Kimura K, Edamura T, Tanaka T, Ishigaki S, Donia T, Noguchi H, Iwanaga T, Noguchi M (2016) Phosphorylation-dependent Akt-Inversin interaction at the basal body of primary cilia. *The EMBO journal* **35:** 1346-1363

Sullivan LP, Wallace DP, Grantham JJ (1998a) Chloride and fluid secretion in polycystic kidney disease. *Journal of the american society of nephrology : JASN* **9:** 903-916

Sullivan LP, Wallace DP, Grantham JJ (1998b) Epithelial transport in polycystic kidney disease. *Physiological reviews* **78:** 1165-1191

Summa V, Mordasini D, Roger F, Bens M, Martin PY, Vandewalle A, Verrey F, Feraille E (2001) Short term effect of aldosterone on Na,K-ATPase cell surface expression in kidney collecting duct cells. *The journal of biological chemistry* **276:** 47087-47093

Sun GD, Kobayashi T, Abe M, Tada N, Adachi H, Shiota A, Totsuka Y, Hino O (2007) The endoplasmic reticulum stress-inducible protein Niban regulates eIF2alpha and S6K1/4E-BP1 phosphorylation. *Biochemical and biophysical research communications* **360:** 181-187

Swenson-Fields KI, Vivian CJ, Salah SM, Peda JD, Davis BM, van Rooijen N, Wallace DP, Fields TA (2013) Macrophages promote polycystic kidney disease progression. *Kidney international* **83:** 855-864

Takebe K, Nio J, Morimatsu M, Karaki S, Kuwahara A, Kato I, Iwanaga T (2005) Histochemical demonstration of a Na(+)-coupled transporter for short-chain fatty acids (slc5a8) in the intestine and kidney of the mouse. *Biomed res* **26:** 213-221

Tanaka Y, Kume S, Araki H, Nakazawa J, Chin-Kanasaki M, Araki S, Nakagawa F, Koya D, Haneda M, Maegawa H, Uzu T (2015) 1-Methylnicotinamide ameliorates lipotoxicity-induced oxidative stress and cell death in kidney proximal tubular cells. *Free radical biology & medicine* **89:** 831-841

Terryn S, Ho A, Beauwens R, Devuyst O (2011) Fluid transport and cystogenesis in autosomal dominant polycystic kidney disease. *Biochimica et biophysica acta* **1812:** 1314-1321

Thompson CB (1995) Apoptosis in the pathogenesis and treatment of disease. *Science* **267:** 1456-1462

Titze J (2015) A different view on sodium balance. *Current opinion in nephrology and hypertension* **24:** 14-20

Toba H, Cannon PL, Yabluchanskiy A, Iyer RP, D'Armiento JM, Lindsey ML (2016) Transgenic overexpression of macrophage matrix metalloproteinase-9 exacerbates age-related cardiac hypertrophy, vessel rarefaction, inflammation, and fibrosis. *American journal of physiology heart and circulatory physiology***:** ajpheart 00633 02016

Tomita K, Pisano JJ, Knepper MA (1985) Control of sodium and potassium transport in the cortical collecting duct of the rat. Effects of bradykinin, vasopressin, and deoxycorticosterone. *The journal of clinical investigation* **76:** 132-136

Tornavaca O, Pascual G, Barreiro ML, Grande MT, Carretero A, Riera M, Garcia-Arumi E, Bardaji B, Gonzalez-Nunez M, Montero MA, Lopez-Novoa JM, Meseguer A (2009) Kidney androgen-regulated protein transgenic mice show hypertension and renal alterations mediated by oxidative stress. *Circulation* **119:** 1908-1917

Torres VE, Harris PC, Pirson Y (2007) Autosomal dominant polycystic kidney disease. *Lancet* **369:** 1287-1301

Tory K, Rousset-Rouviere C, Gubler MC, Moriniere V, Pawtowski A, Becker C, Guyot C, Gie S, Frishberg Y, Nivet H, Deschenes G, Cochat P, Gagnadoux MF, Saunier S, Antignac C, Salomon R (2009) Mutations of NPHP2 and NPHP3 in infantile nephronophthisis. *Kidney international* **75:** 839-847

Troyanovsky B, Levchenko T, Mansson G, Matvijenko O, Holmgren L (2001) Angiomotin: an angiostatin binding protein that regulates endothelial cell migration and tube formation. *The journal of cell biology* **152:** 1247-1254

Truong LD, Choi YJ, Shen SS, Ayala G, Amato R, Krishnan B (2003) Renal cystic neoplasms and renal neoplasms associated with cystic renal diseases: pathogenetic and molecular links. *Advances in anatomic pathology* **10:** 135-159

Turco AE, Clementi M, Rossetti S, Tenconi R, Pignatti PF (1996) An Italian family with autosomal dominant polycystic kidney disease unlinked to either the PKD1 or PKD2 gene. *American journal of kidney diseases : the official journal of the National Kidney Foundation* **28:** 759-761

Valente EM, Logan CV, Mougou-Zerelli S, Lee JH, Silhavy JL, Brancati F, Iannicelli M, Travaglini L, Romani S, Illi B, Adams M, Szymanska K, Mazzotta A, Lee JE, Tolentino JC, Swistun D, Salpietro CD, Fede C, Gabriel S, Russ C, Cibulskis K, Sougnez C, Hildebrandt F, Otto EA, Held S, Diplas BH, Davis EE, Mikula M, Strom CM, Ben-Zeev B, Lev D, Sagie TL, Michelson M, Yaron Y, Krause A, Boltshauser E, Elkhartoufi N, Roume J, Shalev S, Munnich A, Saunier S, Inglehearn C, Saad A, Alkindy A, Thomas S, Vekemans M, Dallapiccola B, Katsanis N, Johnson CA, Attie-Bitach T, Gleeson JG (2010) Mutations in TMEM216 perturb ciliogenesis and cause Joubert, Meckel and related syndromes. *Nature genetics* **42:** 619-625

Vallon V, Eraly SA, Wikoff WR, Rieg T, Kaler G, Truong DM, Ahn SY, Mahapatra NR, Mahata SK, Gangoiti JA, Wu W, Barshop BA, Siuzdak G, Nigam SK (2008) Organic anion transporter 3 contributes to the regulation of blood pressure. *Journal of the american society of nephrology : JASN* **19:** 1732-1740

van Slegtenhorst M, de Hoogt R, Hermans C, Nellist M, Janssen B, Verhoef S, Lindhout D, van den Ouweland A, Halley D, Young J, Burley M, Jeremiah S, Woodward K, Nahmias J, Fox M, Ekong R, Osborne J, Wolfe J, Povey S, Snell RG, Cheadle JP, Jones AC, Tachataki M, Ravine D, Sampson JR, Reeve MP, Richardson P, Wilmer F, Munro C, Hawkins TL, Sepp T, Ali JB, Ward S, Green AJ, Yates JR, Kwiatkowska J, Henske EP, Short MP, Haines JH, Jozwiak S, Kwiatkowski DJ (1997) Identification of the tuberous sclerosis gene TSC1 on chromosome 9q34. *Science* **277:** 805-808

Veizis EI, Carlin CR, Cotton CU (2004) Decreased amiloride-sensitive Na+ absorption in collecting duct principal cells isolated from BPK ARPKD mice. *American journal of physiology renal physiology* **286:** F244-254

Veland IR, Montjean R, Eley L, Pedersen LB, Schwab A, Goodship J, Kristiansen K, Pedersen SF, Saunier S, Christensen ST (2013) Inversin/Nephrocystin-2 is required for fibroblast polarity and directional cell migration. *PloS one* **8:** e60193

Waggoner DW, Johnson LB, Mann PC, Morris V, Guastella J, Bajjalieh SM (2004) MuLK, a eukaryotic multi-substrate lipid kinase. *The journal of biological chemistry* **279:** 38228-38235

Wakui H, Uneda K, Tamura K, Ohsawa M, Azushima K, Kobayashi R, Ohki K, Dejima T, Kanaoka T, Tsurumi-Ikeya Y, Matsuda M, Haruhara K, Nishiyama A, Yabana M, Fujikawa T, Yamashita A, Umemura S (2015) Renal tubule angiotensin II type 1 receptor-associated protein promotes natriuresis and inhibits salt-sensitive blood pressure elevation. *Journal of the american heart association* **4:** e001594

Waldherr R, Lennert T, Weber HP, Fodisch HJ, Scharer K (1982) The nephronophthisis complex. A clinicopathologic study in children. *Virchows archiv A, pathological anatomy and histology* **394:** 235-254

Wallace DP, Grantham JJ, Sullivan LP (1996) Chloride and fluid secretion by cultured human polycystic kidney cells. *Kidney international* **50:** 1327-1336

Wang WJ, Murray JW, Wolkoff AW (2014a) Oatp1a1 requires PDZK1 to traffic to the plasma membrane by selective recruitment of microtubule-based motor proteins. *Drug metabolism and disposition: the biological fate of chemicals* **42:** 62-69

Wang X, Lin C, Zhao X, Liu A, Zhu J, Li X, Song L (2014b) Acylglycerol kinase promotes cell proliferation and tumorigenicity in breast cancer via suppression of the FOXO1 transcription factor. *Molecular cancer* **13:** 106

Warady BA, Hebert D, Sullivan EK, Alexander SR, Tejani A (1997) Renal transplantation, chronic dialysis, and chronic renal insufficiency in children and adolescents. The 1995 Annual Report of the North American Pediatric Renal Transplant Cooperative Study. *Pediatr nephrol* **11:** 49-64

Ward CJ, Hogan MC, Rossetti S, Walker D, Sneddon T, Wang X, Kubly V, Cunningham JM, Bacallao R, Ishibashi M, Milliner DS, Torres VE, Harris PC (2002) The gene mutated in autosomal recessive polycystic kidney disease encodes a large, receptor-like protein. *Nature genetics* **30:** 259-269

Ward CJ, Turley H, Ong AC, Comley M, Biddolph S, Chetty R, Ratcliffe PJ, Gattner K, Harris PC (1996) Polycystin, the polycystic kidney disease 1 protein, is expressed by epithelial cells in fetal, adult, and polycystic kidney. *Proceedings of the national academy of sciences of the United States of America* **93:** 1524-1528

Warnock DG (1998) Liddle syndrome: an autosomal dominant form of human hypertension. *Kidney international* **53:** 18-24

Watanabe D, Saijoh Y, Nonaka S, Sasaki G, Ikawa Y, Yokoyama T, Hamada H (2003) The left-right determinant Inversin is a component of node monocilia and other 9+0 cilia. *Development* **130:** 1725-1734

Werner ME, Ward HH, Phillips CL, Miller C, Gattone VH, Bacallao RL (2013) Inversin modulates the cortical actin network during mitosis. *American journal of physiology cell physiology* **305:** C36-47

Wienecke R, Konig A, DeClue JE (1995) Identification of tuberin, the tuberous sclerosis-2 product. Tuberin possesses specific Rap1GAP activity. *The journal of biological chemistry* **270:** 16409-16414

Wikoff WR, Nagle MA, Kouznetsova VL, Tsigelny IF, Nigam SK (2011) Untargeted metabolomics identifies enterobiome metabolites and putative uremic toxins as substrates of organic anion transporter 1 (Oat1). *Journal of proteome research* **10:** 2842-2851

Wilson PD (2004) Polycystic kidney disease. *The New England journal of medicine* **350:** 151-164

Wojnowski L, Zimmer AM, Beck TW, Hahn H, Bernal R, Rapp UR, Zimmer A (1997) Endothelial apoptosis in Braf-deficient mice. *Nature genetics* **16:** 293-297

Wulff P, Vallon V, Huang DY, Volkl H, Yu F, Richter K, Jansen M, Schlunz M, Klingel K, Loffing J, Kauselmann G, Bosl MR, Lang F, Kuhl D (2002) Impaired renal Na(+) retention in the sgk1-knockout mouse. *The journal of clinical investigation* **110:** 1263-1268

Yang X, Xu T (2011) Molecular mechanism of size control in development and human diseases. *Cell research* **21:** 715-729

Yang XO, Panopoulos AD, Nurieva R, Chang SH, Wang D, Watowich SS, Dong C (2007) STAT3 regulates cytokine-mediated generation of inflammatory helper T cells. *The journal of biological chemistry* **282:** 9358-9363

Yasuhiko Y, Imai F, Ookubo K, Takakuwa Y, Shiokawa K, Yokoyama T (2001) Calmodulin binds to inv protein: implication for the regulation of inv function. *Development, growth & differentiation* **43:** 671-681

Ye M, Grantham JJ (1993) The secretion of fluid by renal cysts from patients with autosomal dominant polycystic kidney disease. *The New England journal of medicine* **329:** 310-313

Yoder BK, Hou X, Guay-Woodford LM (2002) The polycystic kidney disease proteins, polycystin-1, polycystin-2, polaris, and cystin, are co-localized in renal cilia. *Journal of the american society of nephrology : JASN* **13:** 2508-2516

Yokoyama T, Copeland NG, Jenkins NA, Montgomery CA, Elder FF, Overbeek PA (1993) Reversal of left-right asymmetry: a situs inversus mutation. *Science* **260:** 679-682

Yu M, Sha H, Gao Y, Zeng H, Zhu M, Gao X (2006) Alternative 3' UTR polyadenylation of Bzw1 transcripts display differential translation efficiency and tissue-specific expression. *Biochemical and biophysical research communications* **345:** 479-485

Yuan ZL, Guan YJ, Wang L, Wei W, Kane AB, Chin YE (2004) Central role of the threonine residue within the p+1 loop of receptor tyrosine kinase in STAT3 constitutive phosphorylation in metastatic cancer cells. *Molecular and cellular biology* **24:** 9390-9400

Zerres K, Mucher G, Bachner L, Deschennes G, Eggermann T, Kaariainen H, Knapp M, Lennert T, Misselwitz J, von Muhlendahl KE, et al. (1994) Mapping of the gene for autosomal recessive polycystic kidney disease (ARPKD) to chromosome 6p21-cen. *Nature genetics* **7:** 429-432

Zerres K, Mucher G, Becker J, Steinkamm C, Rudnik-Schoneborn S, Heikkila P, Rapola J, Salonen R, Germino GG, Onuchic L, Somlo S, Avner ED, Harman LA, Stockwin JM, Guay-Woodford LM (1998) Prenatal diagnosis of autosomal recessive polycystic kidney disease (ARPKD): molecular genetics, clinical experience, and fetal morphology. *American journal of medical genetics* **76:** 137-144

Zhang W, Morris QD, Chang R, Shai O, Bakowski MA, Mitsakakis N, Mohammad N, Robinson MD, Zirngibl R, Somogyi E, Laurin N, Eftekharpour E, Sat E, Grigull J, Pan Q, Peng WT, Krogan N, Greenblatt J, Fehlings M, van der Kooy D, Aubin J, Bruneau BG, Rossant J, Blencowe BJ, Frey BJ, Hughes TR (2004) The functional landscape of mouse gene expression. *Journal of biology* **3:** 21

Zheng Q, Zhao LY, Kong Y, Nan KJ, Yao Y, Liao ZJ (2013) CDK-associated Cullin 1 can promote cell proliferation and inhibit cisplatin-induced apoptosis in the AGS gastric cancer cell line. *World journal of surgical oncology* **11:** 5

Zhou R, Patel SV, Snyder PM (2007) Nedd4-2 catalyzes ubiquitination and degradation of cell surface ENaC. *The journal of biological chemistry* **282:** 20207-20212

Zollinger HU, Mihatsch MJ, Edefonti A, Gaboardi F, Imbasciati E, Lennert T (1980) Nephronophthisis (medullary cystic disease of the kidney). A study using electron microscopy, immunofluorescence, and a review of the morphological findings. *Helvetica paediatrica acta* **35:** 509-530

APPENDIX

Table 31: Upregulated genes *inv/inv* mice cystic kidneys

Gene ID	Gene Symbol	Protein Name	Fold change (*inv*$^{-/-}$/wild-type)	*P*-value
22436	Xdh	xanthine dehydrogenase	40.19	1.30E-03
70673	Prdm16	PR domain containing 16	7.91	2.00E-04
235320	Zbtb16	zinc finger and BTB domain containing 16	7.67	2.30E-03
76282	Gpt	glutamic pyruvic transaminase, soluble	6.12	9.40E-03
18787	Serpine1	serine (or cysteine) peptidase inhibitor, clade E, member 1	5.91	0.00E+00
77794	Adamtsl2	ADAMTS-like 2	5.87	1.00E-04
17133	Maff	v-maf musculoaponeurotic fibrosarcoma oncogene family, protein F (avian)	5.85	0.00E+00
12795	Plk3	polo-like kinase 3 (Drosophila)	5.67	3.00E-04
226040	Tmem252	Transmembrane protein 252	5.54	6.80E-03
18124	Nr4a3	nuclear receptor subfamily 4, group A, member 3	5	0.00E+00
240672	Dusp5	dual specificity phosphatase 5	4.67	2.90E-03
74392	Specc1l	sperm antigen with calponin homology and coiled-coil domains 1-like	4.51	2.00E-04
20773	Sptlc2	serine palmitoyltransferase, long chain base subunit 2	4.5	0.00E+00
12062	Bdkrb2	bradykinin receptor, beta 2	4.01	0.00E+00
63830	Kcnq1ot1	potassium voltage-gated channel, subfamily Q, member 1	3.86	1.10E-03
18414	Osmr	oncostatin M receptor	3.78	0.00E+00
15959	Ifit3	interferon-induced protein with tetratricopeptide repeats 3	3.61	6.00E-04
18491	Pappa	pregnancy-associated plasma protein A	3.08	0.00E+00
215418	Csrnp1	cysteine-serine-rich nuclear protein 1	3.05	0.00E+00
63913	Fam129a	family with sequence similarity 129, member A	3.04	2.60E-03
66371	Chmp4c	charged multivesicular body protein 4C	3.03	1.01E-02
239719	Mkl2	MKL/myocardin-like 2	3.02	0.00E+00
12010	B2m	beta-2 microglobulin	2.9	2.40E-03
12609	Cebpd	CCAAT/enhancer binding protein (C/EBP), delta	2.88	1.30E-03
14219	Ctgf	connective tissue growth factor	2.83	0.00E+00
80890	Trim2	tripartite motif-containing 2	2.81	1.00E-04
384783	Irs2	insulin receptor substrate 2	2.77	1.00E-04
74155	Errfi1	ERBB receptor feedback inhibitor 1	2.64	1.70E-03
74486	Osbpl10	oxysterol binding protein-like 10	2.64	9.30E-03
14313	Fst	Follistatin	2.6	2.70E-03
16194	Il6ra	interleukin 6 receptor, alpha	2.59	0.00E+00
12608	Cebpb	CCAAT/enhancer binding protein (C/EBP), beta	2.56	0.00E+00
19120	Prm3	protamine 3	2.54	8.90E-03
68774	Ms4a6d	membrane-spanning 4-domains, subfamily A, member 6D	2.47	4.00E-04
57915	Tbc1d1	TBC1 domain family, member 1	2.42	1.00E-03

Table 31 continued

20308	Ccl9	chemokine (C-C motif) ligand 9	2.41	5.10E-03
69640	Fam83g	family with sequence similarity 83, member G	2.41	6.90E-03
68354	Plekhd1os	pleckstrin homology domain containing, family D (with coiled-coil domains) member 1, opposite strand	2.41	6.20E-03
381605	Tbc1d2	similar to TBC1 domain family, member 2	2.38	1.60E-03
225372	Apbb3	amyloid beta (A4) precursor protein-binding, family B, member 3	2.37	2.00E-04
20411	Sorbs1	sorbin and SH3 domain containing 1	2.37	0.00E+00
11699	Ambp	alpha 1 microglobulin/bikunin	2.36	1.02E-02
23886	Gdf15	growth differentiation factor 15	2.33	0.00E+00
70574	Cpm	carboxypeptidase M	2.33	6.70E-03
27279	Tnfrsf12a	tumor necrosis factor receptor superfamily, member 12a	2.31	9.00E-04
14579	Gem	GTP binding protein (gene overexpressed in skeletal muscle)	2.3	8.50E-03
16007	Cyr61	cysteine rich protein 61	2.29	0.00E+00
23882	Gadd45g	growth arrest and DNA-damage-inducible 45 gamma	2.29	0.00E+00
18113	Nnmt	nicotinamide N-methyltransferase	2.24	3.80E-03
17135	Mafk	v-maf musculoaponeurotic fibrosarcoma oncogene family, protein K (avian)	2.21	8.00E-03
26943	Serinc3	serine incorporator 3	2.21	2.50E-03
74716	Wbp2nl	WBP2 N-terminal like	2.2	2.90E-03
68691	Kansl1l	KAT8 regulatory NSL complex subunit 1-like	2.2	1.00E-04
13614	Edn1	endothelin 1	2.2	0.00E+00
53417	Hif3a	hypoxia inducible factor 3, alpha subunit	2.18	2.90E-03
75750	Slc10a6	solute carrier family 10, member 6	2.17	5.30E-03
93671	Cd163	CD163 antigen	2.16	7.00E-04
107765	Ankrd1	ankyrin repeat domain 1 (cardiac muscle)	2.16	6.00E-04
18034	Nfkb2	nuclear factor of kappa light polypeptide gene enhancer in B-cells 2, p49/p100	2.16	4.00E-04
16502	Kcnc1	potassium voltage gated channel, Shaw-related subfamily, member 1	2.15	4.50E-03
23849	Klf6	Kruppel-like factor 6	2.15	2.00E-04
58180	Hic2	hypermethylated in cancer 2	2.15	1.03E-02
18626	Per1	period homolog 1 (Drosophila)	2.14	2.60E-03
16477	Junb	Jun-B oncogene	2.13	0.00E+00
18712	Pim1	proviral integration site 1	2.13	1.00E-04
14229	Fkbp5	FK506 binding protein 5	2.12	5.90E-03
11847	Arg2	arginase type II	2.1	2.30E-03
230796	Wdtc1	WD and tetratricopeptide repeats 1	2.06	2.90E-03
16601	Klf9	Kruppel-like factor 9	2.06	6.80E-03
74646	Spsb1	splA/ryanodine receptor domain and SOCS box containing 1	2.05	8.00E-04
24132	Zfp53	zinc finger protein 53	2.04	1.00E-04
12702	Socs3	suppressor of cytokine signaling 3	2.04	0.00E+00
22038	Plscr1	phospholipid scramblase 1	2.04	1.90E-03
242202	Pde5a	Phosphodiesterase 5A	2.03	1.03E-02
104831	Ptpn23	protein tyrosine phosphatase, non-receptor type 23	2.02	0.00E+00
286940	Flnb	filamin, beta	2.01	2.00E-04

Table 31 continued

20848	Stat3	signal transducer and activator of transcription 3	2	0.00E+00
433022	Plcxd2	phosphatidylinositol-specific phospholipase C, X domain containing 2	2	5.90E-03
14284	Fosl2	similar to fos-like antigen 2; fos-like antigen 2	2	0.00E+00
13653	Egr1	early growth response 1	1.96	0.00E+00
114716	Spred2	sprouty-related, EVH1 domain containing 2	1.96	3.20E-03
56620	Clec4n	C-type lectin domain family 4, member n	1.95	0.00E+00
238871	Pde4d	phosphodiesterase 4D, cAMP specific	1.95	0.00E+00
268936	Brpf3	bromodomain and PHD finger containing, 3	1.95	6.20E-03
16400	Itga3	integrin alpha 3	1.94	1.40E-03
80859	Nfkbiz	nuclear factor of kappa light polypeptide gene enhancer in B-cells inhibitor, zeta	1.93	0.00E+00
75956	Srrm2	serine/arginine repetitive matrix 2	1.93	6.00E-04
19252	Dusp1	dual specificity phosphatase 1	1.93	1.00E-04
109620	Dsp	desmoplakin	1.92	1.00E-04
17873	Gadd45b	growth arrest and DNA-damage-inducible 45 beta	1.92	3.00E-04
108664	Atp6v1h	ATPase, H+ transporting, lysosomal V1 subunit H	1.92	6.00E-04
381199	Tmem151a	transmembrane protein 151A	1.91	3.40E-03
20698	Sphk1	sphingosine kinase 1	1.91	0.00E+00
214150	Ago3	eukaryotic translation initiation factor 2C, 3	1.9	7.00E-04
338367	Myo1d	myosin ID	1.9	8.00E-04
17196	Mbp	myelin basic protein	1.88	2.00E-04
13655	Egr3	early growth response 3	1.88	0.00E+00
13198	Ddit3	DNA-damage inducible transcript 3	1.88	3.70E-03
194231	Cnksr1	connector enhancer of kinase suppressor of Ras 1	1.88	1.90E-03
26564	Ror2	expressed sequence AL024213	1.88	0.00E+00
94332	Cadm3	cell adhesion molecule 3	1.87	9.40E-03
11303	Abca1	ATP-binding cassette, sub-family A (ABC1), member 1	1.87	1.60E-03
21366	Slc6a6	solute carrier family 6 (neurotransmitter transporter, taurine), member 6	1.87	2.50E-03
18218	Dusp8	dual specificity phosphatase 8	1.85	2.50E-03
19878	Rock2	Rho-associated coiled-coil containing protein kinase 2	1.84	7.00E-04
18810	Plec	plectin 1	1.82	1.10E-03
20525	Slc2a1	solute carrier family 2 (facilitated glucose transporter), member 1	1.81	5.00E-04
23792	Adam23	a disintegrin and metallopeptidase domain 23; similar to ADAM23	1.81	2.20E-03
67072	Cdc37l1	cell division cycle 37 homolog (S. cerevisiae)-like 1	1.8	1.10E-03
12211	Birc6	baculoviral IAP repeat-containing 6	1.8	1.00E-04
19324	Rab1	RAB1, member RAS oncogene family	1.8	8.30E-03
329152	Hecw2	HECT, C2 and WW domain containing E3 ubiquitin protein ligase 2	1.8	6.20E-03
11551	Adra2a	adrenergic receptor, alpha 2a	1.79	3.20E-03
56758	Mbnl1	muscleblind-like 1 (Drosophila)	1.79	3.10E-03
18739	Pitpnm1	phosphatidylinositol transfer protein, membrane-associated 1	1.78	1.10E-03
11307	Abcg1	ATP-binding cassette, sub-family G (WHITE), member 1	1.78	5.00E-03
68112	Sdccag3	serologically defined colon cancer antigen 3	1.78	9.20E-03

Table 31 continued

12740	Cldn4	claudin 4	1.77	0.00E+00
52440	Tax1bp1	Tax1 (human T-cell leukemia virus type I) binding protein 1	1.77	0.00E+00
74173	Rab10os	RIKEN cDNA 1700012B15 gene	1.77	1.00E-04
106052	Fbxo4	F-box protein 4	1.76	0.00E+00
56417	Adar	adenosine deaminase, RNA-specific	1.76	2.00E-04
217708	Lin52	lin-52 homolog (C. elegans); predicted gene 7020	1.76	4.30E-03
63955	Cables1	CDK5 and Abl enzyme substrate 1	1.76	4.00E-04
58865	Tdh	L-threonine dehydrogenase; predicted gene 13929	1.75	4.60E-03
15370	Nr4a1	nuclear receptor subfamily 4, group A, member 1	1.74	0.00E+00
208104	Mlxip	MLX interacting protein	1.73	1.00E-04
68703	Rere	arginine glutamic acid dipeptide (RE) repeats	1.73	4.00E-04
21923	Tnc	tenascin C	1.73	2.70E-03
105732	Fam83h	family with sequence similarity 83, member H	1.72	5.60E-03
1.01E+08	Gdap10	ganglioside-induced differentiation-associated-protein 10	1.71	0.00E+00
12260	C1qb	complement component 1, q subcomponent, beta polypeptide	1.71	0.00E+00
235587	Parp3	poly (ADP-ribose) polymerase family, member 3	1.71	5.00E-04
12259	C1qa	complement component 1, q subcomponent, alpha polypeptide	1.7	0.00E+00
56386	B4galt6	UDP-Gal:betaGlcNAc beta 1,4-galactosyltransferase, polypeptide 6	1.7	0.00E+00
233011	Itpkc	inositol 1,4,5-trisphosphate 3-kinase C	1.7	1.00E-04
80981	Arl4d	ADP-ribosylation factor-like 4D; hypothetical protein LOC100044157	1.69	1.00E-04
13649	Egfr	epidermal growth factor receptor	1.69	2.00E-04
17886	Myh9	myosin, heavy polypeptide 9, non-muscle	1.69	8.00E-04
104445	Cdc42ep1	CDC42 effector protein (Rho GTPase binding) 1	1.69	6.00E-04
73569	Vgll3	vestigial like 3 (Drosophila)	1.68	2.00E-04
71738	Mamdc2	MAM domain containing 2	1.68	2.80E-03
83814	Nedd4l	neural precursor cell expressed, developmentally down-regulated gene 4-like	1.68	0.00E+00
14825	Cxcl1	chemokine (C-X-C motif) ligand 1	1.68	1.00E-04
56421	Pfkp	phosphofructokinase, platelet	1.67	3.70E-03
12817	Col13a1	collagen, type XIII, alpha 1	1.67	5.90E-03
77733	Rnf170	ring finger protein 170	1.67	0.00E+00
170638	Hpcal4	hippocalcin-like 4	1.67	0.00E+00
98496	Pid1	prior incubation determinant 1	1.67	8.90E-03
16668	Krt18	keratin 18	1.67	9.00E-04
16177	Il1r1	interleukin 1 receptor, type I	1.67	7.80E-03
108123	Napg	N-ethylmaleimide sensitive fusion protein attachment protein gamma	1.66	1.80E-03
12660	Chka	choline kinase alpha	1.66	0.00E+00
226551	Suco	expressed sequence AI848100	1.66	2.00E-03
233789	Smg1	SMG1 homolog, phosphatidylinositol 3-kinase-related kinase (C. elegans)	1.66	0.00E+00
12495	Entpd1	ectonucleoside triphosphate diphosphohydrolase 1	1.65	3.00E-04
242481	Palm2	A kinase (PRKA) anchor protein 2; paralemmin 2	1.65	5.00E-04
14066	F3	coagulation factor III	1.64	1.00E-04

Table 31 continued

77087	Ankrd11	ankyrin repeat domain 11	1.64	8.00E-03
18035	Nfkbia	nuclear factor of kappa light polypeptide gene enhancer in B-cells inhibitor, alpha	1.64	0.00E+00
18030	Nfil3	similar to NFIL3/E4BP4 transcription factor; nuclear factor, interleukin 3, regulated	1.63	4.10E-03
50794	Klf13	RIKEN cDNA 9430029L20 gene	1.63	0.00E+00
16430	Stt3a	STT3, subunit of the oligosaccharyltransferase complex, homolog A (S. cerevisiae)	1.63	1.00E-04
225028	Map4k3	mitogen-activated protein kinase kinase kinase kinase 3; similar to mitogen-activated protein kinase kinase kinase kinase 3	1.63	8.00E-04
12642	Ch25h	cholesterol 25-hydroxylase	1.63	0.00E+00
12575	Cdkn1a	cyclin-dependent kinase inhibitor 1A (P21)	1.62	7.90E-03
69562	Cdk13	cell division cycle 2-like 5 (cholinesterase-related cell division controller)	1.62	0.00E+00
73167	Arhgap8	Rho GTPase activating protein 8; proline rich 5 (renal)	1.62	0.00E+00
14538	Gcnt2	glucosaminyl (N-acetyl) transferase 2, I-branching enzyme	1.61	8.10E-03
252837	Ackr4	chemokine (C-C motif) receptor-like 1	1.61	5.80E-03
70675	Vcpip1	valosin containing protein (p97)/p47 complex interacting protein 1	1.61	2.60E-03
14063	F2rl1	coagulation factor II (thrombin) receptor-like 1	1.61	6.00E-04
14924	Magi1	membrane associated guanylate kinase, WW and PDZ domain containing 1	1.61	2.00E-04
78892	Crispld2	cysteine-rich secretory protein LCCL domain containing 2	1.61	1.00E-04
56722	Litaf	LPS-induced TN factor	1.6	2.00E-04
50766	Crim1	cysteine rich transmembrane BMP regulator 1 (chordin like)	1.6	5.00E-03
218811	Sec24c	Sec24 related gene family, member C (S. cerevisiae)	1.6	7.70E-03
230088	Fam214b	RIKEN cDNA B230312A22 gene	1.6	5.00E-04
14055	Ezh1	enhancer of zeste homolog 1 (Drosophila)	1.6	0.00E+00
17533	Mrc1	mannose receptor, C type 1	1.6	3.90E-03
338372	Map3k9	mitogen-activated protein kinase kinase kinase 9	1.6	3.00E-04
70686	Dusp16	dual specificity phosphatase 16	1.59	0.00E+00
11669	Aldh2	aldehyde dehydrogenase 2, mitochondrial	1.59	3.00E-03
72296	Rusc1	RUN and SH3 domain containing 1	1.59	5.30E-03
66713	Actr2	ARP2 actin-related protein 2 homolog (yeast); predicted gene 6828	1.59	1.00E-04
12262	C1qc	complement component 1, q subcomponent, C chain	1.59	0.00E+00
59009	Sh3rf1	SH3 domain containing ring finger 1	1.59	6.00E-04
19155	Npepps	aminopeptidase puromycin sensitive	1.58	5.40E-03
1E+08	Hrct1	histidine rich carboxyl terminus 1	1.58	1.40E-03
78797	Ndor1	NADPH dependent diflavin oxidoreductase 1	1.58	6.00E-04
319817	Rc3h2	ring finger and CCCH-type zinc finger domains 2	1.58	0.00E+00
50776	Polg2	polymerase (DNA directed), gamma 2, accessory subunit	1.58	7.00E-04
77864	Ypel2	yippee-like 2 (Drosophila)	1.58	0.00E+00

Table 31 continued

20352	Sema4b	sema domain, immunoglobulin domain (Ig), transmembrane domain (TM) and short cytoplasmic domain, (semaphorin) 4B	1.58	3.40E-03
11975	Atp6v0a1	ATPase, H+ transporting, lysosomal V0 subunit A1	1.57	1.00E-04
20185	Ncor1	nuclear receptor co-repressor 1	1.57	5.50E-03
19290	Pura	RIKEN cDNA 6330403M23 gene	1.57	1.40E-03
13025	Ctla2b	cytotoxic T lymphocyte-associated protein 2 beta	1.57	4.30E-03
66853	Pnpla2	patatin-like phospholipase domain containing 2	1.56	9.70E-03
101488	Slco2b1	solute carrier organic anion transporter family, member 2b1	1.56	0.00E+00
231207	Cpeb2	cytoplasmic polyadenylation element binding protein 2	1.56	8.60E-03
108735	Sft2d2	SFT2 domain containing 2	1.56	1.00E-04
99526	Usp53	ubiquitin specific peptidase 53	1.56	0.00E+00
20288	Msr1	macrophage scavenger receptor 1	1.56	5.70E-03
67150	Rnf141	predicted gene 10179; ring finger protein 141	1.55	4.40E-03
12273	C5ar1	complement component 5a receptor 1	1.55	2.40E-03
12226	Btg1	B-cell translocation gene 1, anti-proliferative; similar to myocardial vascular inhibition factor	1.55	5.80E-03
66053	Ppil2	peptidylprolyl isomerase (cyclophilin)-like 2	1.55	7.00E-04
76901	Jade2	PHD finger protein 15	1.55	0.00E+00
20361	Sema7a	sema domain, immunoglobulin domain (Ig), and GPI membrane anchor, (semaphorin) 7A	1.55	6.80E-03
26930	Ppnr	per-pentamer repeat gene	1.54	3.10E-03
72674	Adipor1	adiponectin receptor 1	1.54	0.00E+00
77963	Hook1	hook homolog 1 (Drosophila)	1.54	2.00E-04
66369	Dus2	dihydrouridine synthase 2-like (SMM1, S. cerevisiae)	1.54	4.20E-03
11982	Atp10a	ATPase, class V, type 10A	1.54	0.00E+00
80888	Hspb8	heat shock protein 8	1.53	0.00E+00
19106	Eif2ak2	eukaryotic translation initiation factor 2-alpha kinase 2	1.53	4.40E-03
15507	Hspb1	heat shock protein 1	1.53	5.70E-03
223649	Nrbp2	nuclear receptor binding protein 2	1.53	1.00E-04
232431	Gprc5a	G protein-coupled receptor, family C, group 5, member A	1.53	0.00E+00
109241	Mbd5	methyl-CpG binding domain protein 5	1.53	0.00E+00
106585	Ankrd12	ankyrin repeat domain 12; similar to Ankrd12 protein	1.53	8.50E-03
317717	Sec22a	SEC22 vesicle trafficking protein homologe A (S. cerevisiae)	1.53	4.40E-03
12227	Btg2	B-cell translocation gene 2, anti-proliferative	1.53	0.00E+00
66395	Ahnak	AHNAK nucleoprotein (desmoyokin)	1.53	8.50E-03
75547	Akap13	A kinase (PRKA) anchor protein 13	1.52	2.30E-03
12725	Clcn3	chloride channel 3	1.52	3.00E-04
225358	Fam13b	family with sequence similarity 13, member B	1.52	1.10E-03
69863	Ttc39b	tetratricopeptide repeat domain 39B	1.52	0.00E+00
109880	Braf	Braf transforming gene	1.52	6.00E-04
66083	Setd6	SET domain containing 6	1.52	1.40E-03
57294	Rps27	ribosomal protein S27	1.52	4.00E-03
72388	Ripk4	receptor-interacting serine-threonine kinase 4	1.51	8.70E-03
15894	Icam1	intercellular adhesion molecule 1	1.51	0.00E+00
76527	Il34	interleukin 34	1.51	7.00E-04
328365	Zmiz1	zinc finger, MIZ-type containing 1	1.51	4.10E-03

Table 31 continued

66404	Rtfdc1	Replication termination factor domain containing 1	1.51	1.00E-04
18806	Pld2	phospholipase D2	1.5	0.00E+00
226252	Fam160b1	family with sequence similarity 160, member B1	1.5	3.00E-04
263803	Pkn3	protein kinase N3	1.5	9.10E-03
71175	Nipbl	Nipped-B homolog (Drosophila)	1.5	5.60E-03
72429	Dnajc25	DnaJ (Hsp40) homolog, subfamily C, member 25	1.5	1.90E-03
217069	Trim25	tripartite motif-containing 25	1.49	2.90E-03
16396	Itch	itchy, E3 ubiquitin protein ligase	1.49	0.00E+00
16337	Insr	insulin receptor	1.49	9.00E-04
217866	Cdc42bpb	CDC42 binding protein kinase beta	1.49	0.00E+00
14268	Fn1	fibronectin 1	1.49	5.00E-04
282619	Sbsn	suprabasin	1.49	3.80E-03
59079	Erbb2ip	Erbb2 interacting protein	1.49	3.00E-04
77446	Heg1	HEG homolog 1 (zebrafish)	1.49	2.40E-03
14131	Fcgr3	Fc receptor, IgG, low affinity III	1.49	9.10E-03
72349	Dusp3	dual specificity phosphatase 3 (vaccinia virus phosphatase VH1-related)	1.49	3.00E-04
270162	Elmod1	ELMO domain containing 1	1.48	9.30E-03
76199	Med13l	mediator complex subunit 13-like	1.48	7.00E-03
69020	Zfp707	zinc finger protein 707	1.48	5.00E-04
108829	Jmjd1c	jumonji domain containing 1C	1.48	3.50E-03
14254	Flt1	FMS-like tyrosine kinase 1	1.48	7.00E-04
20239	Atxn2	similar to ataxin 2	1.48	6.00E-03
19263	Ptprb	protein tyrosine phosphatase, receptor type, B	1.47	9.00E-04
16599	Klf3	Kruppel-like factor 3 (basic); similar to BKLF	1.47	3.00E-03
12916	Crem	cAMP responsive element modulator	1.46	2.70E-03
70497	Arhgap17	Rho GTPase activating protein 17	1.46	0.00E+00
16905	Lmna	lamin A	1.45	5.00E-04
246696	Slc25a28	solute carrier family 25, member 28	1.45	8.80E-03
64652	Nisch	nischarin	1.45	7.60E-03
108655	Foxp1	forkhead box P1	1.45	1.70E-03
18583	Pde7a	phosphodiesterase 7A	1.45	1.20E-03
103537	Mbtd1	mbt domain containing 1	1.45	6.00E-04
212391	Lcor	ligand dependent nuclear receptor corepressor	1.45	2.00E-04
381290	Atp2b4	ATPase, Ca++ transporting, plasma membrane 4	1.45	8.40E-03
14718	Got1	glutamate oxaloacetate transaminase 1, soluble	1.45	3.10E-03
11987	Slc7a1	solute carrier family 7 (cationic amino acid transporter, y+ system), member 1	1.45	0.00E+00
17210	Mcl1	similar to myeloid cell leukemia sequence 1; myeloid cell leukemia sequence 1	1.45	6.00E-04
216161	Sbno2	strawberry notch homolog 2 (Drosophila)	1.45	0.00E+00

Table 32: Downregulated genes in *inv/inv* mice cystic kidneys

Gene ID	Gene Symbol	Protein Name	Fold change (*inv*$^{-/-}$/wild-type)	*P*-value
210463	Slc22a22	solute carrier family 22 (organic cation transporter), member 22	-12.58	0.00E+00
72160	Tmem163	transmembrane protein 163	-8.27	0.00E+00
56727	Miox	myo-inositol oxygenase	-8.12	1.00E-04
68352	Aspdh	aspartate dehydrogenase domain containing	-6.49	0.00E+00
246700	Defb19	defensin beta 19	-5.57	9.80E-03
18478	Pah	phenylalanine hydroxylase	-5.04	5.60E-03
16612	Klk1	kallikrein 1	-4.33	1.40E-03
192113	Atp12a	ATPase, H+/K+ transporting, nongastric, alpha polypeptide	-3.99	5.80E-03
112417	Ugt2b37	UDP glucuronosyltransferase 2 family, polypeptide B37	-3.99	3.90E-03
67092	Gatm	glycine amidinotransferase (L-arginine:glycine amidinotransferase)	-3.94	2.00E-04
14060	F13b	coagulation factor XIII, beta subunit	-3.88	4.10E-03
15186	Hdc	histidine decarboxylase	-3.67	8.00E-03
77462	Tmem116	transmembrane protein 116	-3.66	5.00E-04
12350	Car3	carbonic anhydrase 3	-3.54	0.00E+00
74129	Dmgdh	dimethylglycine dehydrogenase precursor	-3.54	4.50E-03
19879	Slc22a8	solute carrier family 22 (organic anion transporter), member 8	-3.4	3.60E-03
114644	Slc13a3	solute carrier family 13 (sodium-dependent dicarboxylate transporter), member 3	-3.3	5.80E-03
28254	Slco1a6	solute carrier organic anion transporter family, member 1a6	-3.28	4.10E-03
109901	Cela1	chymotrypsin-like elastase family, member 1	-3.21	0.00E+00
22034	Traf6	TNF receptor-associated factor 6	-3.16	0.00E+00
66116	Cml1	N-acetyltransferase 8B; camello-like 1	-3.11	0.00E+00
16348	Invs	inversin	-3.1	2.00E-03
12425	Cckar	cholecystokinin A receptor	-3.08	0.00E+00
20518	Slc22a2	solute carrier family 22 (organic cation transporter), member 2	-2.98	1.30E-03
216225	Slc5a8	solute carrier family 5 (iodide transporter), member 8	-2.95	6.50E-03
102570	Slc22a13	solute carrier family 22 (organic cation transporter), member 13	-2.94	5.00E-04
234564	Ces1f	carboxylesterase 1F	-2.94	4.10E-03
69123	Eci3	enoyl-Coenzyme A delta isomerase 3	-2.92	0.00E+00
268782	Agxt2	alanine-glyoxylate aminotransferase 2	-2.88	0.00E+00
20521	Slc22a12	solute carrier family 22 (organic anion/cation transporter), member 12	-2.87	1.00E-04
232984	B3gnt8	UDP-GlcNAc:betaGal beta-1,3-N-acetylglucosaminyltransferase 8	-2.85	4.20E-03
20505	Slc34a1	solute carrier family 34 (sodium phosphate), member 1	-2.81	9.30E-03
109246	Tspan9	tetraspanin 9	-2.8	2.40E-03

Table 32 continued

229699	Slc16a4	solute carrier family 16 (monocarboxylic acid transporters), member 4	-2.79	1.00E-03
16483	Kap	kidney androgen regulated protein	-2.77	3.90E-03
13837	Epha3	Eph receptor A3	-2.75	0.00E+00
14261	Fmo1	flavin containing monooxygenase 1	-2.73	1.40E-03
113854	Vmn1r44	vomeronasal 1 receptor, B4	-2.72	7.20E-03
64918	Bhmt2	betaine-homocysteine methyltransferase 2	-2.71	9.30E-03
68680	Fitm1	fat storage-inducing transmembrane protein 1	-2.67	6.00E-04
17229	Tpsb2	tryptase beta 2	-2.66	7.10E-03
18399	Slc22a6	solute carrier family 22 (organic anion transporter), member 6	-2.63	1.20E-03
109342	Slc5a10	solute carrier family 5 (sodium/glucose cotransporter), member 10	-2.62	2.30E-03
94223	Dgcr8	DiGeorge syndrome critical region gene 8	-2.58	1.00E-04
105355	Slc17a3	solute carrier family 17 (sodium phosphate), member 3	-2.56	2.60E-03
17071	Ly6f	lymphocyte antigen 6 complex, locus F	-2.53	0.00E+00
108114	Slc22a7	solute carrier family 22 (organic anion transporter), member 7	-2.53	4.10E-03
239133	Dleu7	deleted in lymphocytic leukemia, 7	-2.51	6.00E-04
58176	Rhbg	Rhesus blood group-associated B glycoprotein	-2.48	1.10E-03
22599	Slc6a20b	solute carrier family 6 (neurotransmitter transporter), member 20B	-2.47	8.20E-03
74087	Slc7a13	solute carrier family 7, (cationic amino acid transporter, y+ system) member 13	-2.46	1.60E-03
18008	Nes	nestin	-2.43	0.00E+00
20493	Slc10a1	solute carrier family 10 (sodium/bile acid cotransporter family), member 1	-2.42	1.60E-03
320678	Iffo1	intermediate filament family orphan 1	-2.42	2.00E-04
106389	Eaf2	ELL associated factor 2	-2.41	4.40E-03
19212	Pter	phosphotriesterase related	-2.39	7.70E-03
84112	Sucnr1	succinate receptor 1	-2.39	5.60E-03
14048	Eya1	eyes absent 1 homolog (Drosophila)	-2.39	6.00E-04
50498	Ebi3	Epstein-Barr virus induced gene 3	-2.38	2.20E-03
234267	Gpm6a	glycoprotein m6a	-2.37	3.80E-03
18563	Pcx	pyruvate carboxylase	-2.36	3.80E-03
13109	Cyp2j5	cytochrome P450, family 2, subfamily j, polypeptide 5	-2.35	9.20E-03
18080	Nin	ninein	-2.35	6.00E-04
208665	Akr1d1	aldo-keto reductase family 1, member D1	-2.35	7.40E-03
22239	Ugt8a	UDP galactosyltransferase 8A	-2.33	9.60E-03
212442	Lactb2	lactamase, beta 2	-2.32	0.00E+00
244954	Prss35	protease, serine, 35	-2.32	1.60E-03
20522	Slc23a1	solute carrier family 23 (nucleobase transporters), member 1	-2.32	5.90E-03
11639	Ak4	adenylate kinase 3-like 1	-2.25	3.00E-04
170952	Prima1	proline rich membrane anchor 1	-2.25	1.90E-03
232078	Thnsl2	threonine synthase-like 2 (bacterial)	-2.25	0.00E+00
27392	Pign	phosphatidylinositol glycan anchor biosynthesis, class N	-2.24	1.30E-03
12763	Cmah	cytidine monophospho-N-acetylneuraminic acid hydroxylase	-2.23	8.00E-04

Table 32 continued

69454	Clic3	chloride intracellular channel 3	-2.22	5.90E-03
319800	Slc22a30	solute carrier family 22, member	-2.22	1.30E-03
20377	Sfrp1	secreted frizzled-related protein 1	-2.22	6.60E-03
13482	Dpp4	dipeptidylpeptidase 4	-2.21	0.00E+00
50490	Nox4	NADPH oxidase 4	-2.21	6.90E-03
319922	Vwc2	von Willebrand factor C domain containing 2	-2.2	4.50E-03
223774	Alg12	asparagine-linked glycosylation 12 homolog	-2.19	0.00E+00
74717	Spata17	spermatogenesis associated 17	-2.19	0.00E+00
19293	Pvalb	parvalbumin	-2.16	7.50E-03
101202	Hepacam2	HEPACAM family member 2	-2.15	4.70E-03
69923	Agk	acylglycerol kinase	-2.13	7.00E-04
13822	Epb4.1l2	erythrocyte protein band 4.1-like 2	-2.12	0.00E+00
72685	Dnajc6	DnaJ (Hsp40) homolog, subfamily C, member 6	-2.12	0.00E+00
212190	Ubxn10	UBX domain protein 10	-2.11	9.00E-04
21338	Tacr3	tachykinin receptor 3	-2.1	6.60E-03
54426	Hgfac	hepatocyte growth factor activator	-2.06	4.10E-03
224079	Atp13a4	ATPase type 13A4	-2.05	2.00E-03
16508	Kcnd2	potassium voltage-gated channel, Shal-related family, member 2	-2.03	1.90E-03
18451	P4ha1	procollagen-proline, 2-oxoglutarate 4-dioxygenase (proline 4-hydroxylase), alpha 1 polypeptide	-2.03	9.30E-03
330657	Prss53	protease, serine 53	-2.03	1.00E-03
207683	Igsf11	immunoglobulin superfamily, member 11	-2.02	5.00E-04
14255	Flt3	FMS-like tyrosine kinase 3	-2.01	7.20E-03
235674	Acaa1b	acetyl-Coenzyme A acyltransferase 1A	-2.01	3.90E-03
231842	Amz1	archaelysin family metallopeptidase 1	-2.01	3.40E-03
72039	Mccc1	methylcrotonoyl-Coenzyme A carboxylase 1 (alpha)	-1.97	4.90E-03
12950	Hapln1	hyaluronan and proteoglycan link protein 1	-1.97	0.00E+00
67375	Qprt	quinolinate phosphoribosyltransferase	-1.95	1.00E-03
99543	Olfml3	olfactomedin-like 3	-1.94	8.60E-03
75578	Fggy	FGGY carbohydrate kinase domain containing	-1.94	2.70E-03
329421	Myo3b	myosin IIIB	-1.94	1.90E-03
51813	Ccnc	cyclin C	-1.93	1.00E-04
66696	Snx31	sorting nexin 31	-1.9	1.00E-02
102448	Xylb	xylulokinase homolog (H. influenzae)	-1.89	0.00E+00
76459	Car12	carbonic anyhydrase 12	-1.89	1.60E-03
20322	Sord	sorbitol dehydrogenase	-1.89	0.00E+00
217371	Rab40b	Rab40b, member RAS oncogene family	-1.88	1.20E-03
27401	Skp2	S-phase kinase-associated protein 2 (p45)	-1.87	7.00E-04
14675	Gna14	guanine nucleotide binding protein, alpha 14	-1.87	0.00E+00
66469	Fam213b	family with sequence similarity 213, member b	-1.86	1.00E-04
78832	Cacul1	CDK2 associated, cullin domain 1	-1.86	1.00E-04
225845	Pla2g16	phospholipase A2, group XVI	-1.86	3.00E-04
225913	Dak	dihydroxyacetone kinase 2 homolog (yeast)	-1.85	0.00E+00
56794	Hacl1	2-hydroxyacyl-CoA lyase 1	-1.85	1.00E-04
22411	Wnt11	wingless-related MMTV integration site 11	-1.84	3.60E-03
320840	Negr1	neuronal growth regulator 1	-1.84	1.60E-03
12865	Cox7a1	cytochrome c oxidase, subunit VIIa 1	-1.83	0.00E+00
17762	Mapt	microtubule-associated protein tau	-1.83	3.00E-03

Table 32 continued

59020	Pdzk1	PDZ domain containing 1	-1.82	1.60E-03
235386	Hykk	hydroxylysine kinase 1	-1.82	4.90E-03
20346	Sema3a	semaphorin 3A	-1.82	3.70E-03
56175	Bace2	beta-site APP-cleaving enzyme 2	-1.81	4.00E-04
76426	Fam209	family with sequence similarity 209	-1.8	3.90E-03
64074	Smoc2	SPARC related modular calcium binding 2	-1.8	0.00E+00
242667	Dlgap3	discs, large (Drosophila) homolog-associated protein 3	-1.79	1.00E-04
17117	Amacr	alpha-methylacyl-CoA racemase	-1.78	2.00E-03
16019	Ighm	immunoglobulin heavy chain 6 (heavy chain of IgM)	-1.78	1.00E-04
71974	Prmt3	protein arginine N-methyltransferase 3	-1.78	2.00E-04
20209	Saa2	serum amyloid A 2	-1.78	9.30E-03
11834	Aqr	aquarius	-1.78	3.00E-04
60525	Acss2	acyl-CoA synthetase short-chain family member 2	-1.77	4.30E-03
56403	Syncrip	synaptotagmin binding, cytoplasmic RNA interacting protein	-1.77	1.00E-04
15251	Hif1a	hypoxia inducible factor 1, alpha subunit	-1.77	1.50E-03
226791	Lyplal1	lysophospholipase-like 1	-1.77	5.00E-04
59008	Anapc5	anaphase-promoting complex subunit 5	-1.77	3.70E-03
22341	Vegfc	vascular endothelial growth factor C	-1.76	2.40E-03
73910	Arhgap18	Rho GTPase activating protein 18	-1.76	0.00E+00
100952	Emilin1	elastin microfibril interfacer 1	-1.76	1.02E-02
11484	Aspa	aspartoacylase	-1.75	6.10E-03
11489	Adam12	a disintegrin and metallopeptidase domain 12 (meltrin alpha)	-1.75	1.10E-03
14782	Gsr	similar to Glutathione reductase, mitochondrial precursor (GR) (GRase); glutathione reductase	-1.75	0.00E+00
14810	Grin1	glutamate receptor, ionotropic, NMDA1 (zeta 1)	-1.75	7.20E-03
67923	Tceb1	transcription elongation factor B (SIII), polypeptide 1	-1.75	3.80E-03
80718	Rab27b	RAB27b, member RAS oncogene family	-1.74	3.00E-04
20686	Spa17	sperm autoantigenic protein 17	-1.74	1.30E-03
12167	Bmpr1b	bone morphogenetic protein receptor, type 1B	-1.74	0.00E+00
57754	Cend1	cell cycle exit and neuronal differentiation 1	-1.74	3.70E-03
232086	Tmem150a	transmembrane protein 150	-1.74	0.00E+00
70789	Kynu	kynureninase (L-kynurenine hydrolase)	-1.74	0.00E+00
14431	Gamt	guanidinoacetate methyltransferase	-1.73	0.00E+00
227059	Slc39a10	solute carrier family 39 (zinc transporter), member 10	-1.73	2.00E-03
217449	Trappc12	tetratricopeptide repeat domain 15	-1.73	4.90E-03
23964	Tenm2	odd Oz/ten-m homolog 2 (Drosophila)	-1.73	8.00E-04
67840	Mrpl57	mitochondrial ribosomal protein 63	-1.73	3.00E-04
64934	Pes1	pescadillo homolog 1, containing BRCT domain	-1.72	5.30E-03
13132	Dab2	disabled homolog 2 (Drosophila)	-1.72	0.00E+00
280662	Afm	Afamin	-1.72	7.00E-03
75847	Ispd	isoprenoid synthase domain containing	-1.72	0.00E+00
214058	Megf11	multiple EGF-like-domains 11	-1.72	0.00E+00
13034	Ctse	cathepsin E	-1.71	2.70E-03
68044	Chac2	ChaC, cation transport regulator homolog 2 (E. coli)	-1.71	7.40E-03
58194	Sh3kbp1	SH3-domain kinase binding protein 1	-1.71	3.70E-03
108653	Rimklb	ribosomal modification protein rimK-like family member B	-1.71	0.00E+00

Table 32 continued

1.01E+08	Ccdc13	coiled-coil domain containing 13	-1.71	0.00E+00
193385	Fam65b	family with sequence similarity 65, member B	-1.71	8.30E-03
30959	Ddx25	DEAD (Asp-Glu-Ala-Asp) box polypeptide 25	-1.7	1.10E-03
22174	Tyro3	TYRO3 protein tyrosine kinase 3	-1.7	0.00E+00
104183	Chil4	chitinase 3-like 4	-1.7	1.00E-04
241226	Itga8	integrin alpha 8	-1.7	4.80E-03
224454	Zdhhc14	zinc finger, DHHC domain containing 14	-1.68	1.70E-03
270076	Gcdh	glutaryl-Coenzyme A dehydrogenase	-1.68	7.00E-04
109019	Nabp1	oligonucleotide/oligosaccharide-binding fold containing 2A	-1.67	8.90E-03
208643	Eif4g1	eukaryotic translation initiation factor 4, gamma 1	-1.67	0.00E+00
16370	Irs4	insulin receptor substrate 4	-1.66	1.60E-03
19691	Recql	RecQ protein-like	-1.66	8.00E-04
69358	Lrrc51	leucine rich repeat containing 51	-1.66	4.10E-03
234889	Gucy1a2	guanylate cyclase 1, soluble, alpha 2	-1.66	4.60E-03
67109	Zfp787	zinc finger protein 787	-1.66	2.00E-04
14802	Gria4	glutamate receptor, ionotropic, AMPA4 (alpha 4)	-1.66	7.80E-03
22247	Umps	uridine monophosphate synthetase	-1.66	4.30E-03
103136	Pwp1	PWP1 homolog (S. cerevisiae)	-1.66	6.80E-03
17222	Anapc1	anaphase promoting complex subunit 1	-1.65	0.00E+00
26879	B3galnt1	UDP-GalNAc:betaGlcNAc beta 1,3-galactosaminyltransferase, polypeptide 1	-1.65	9.00E-04
74197	Gtf2e1	general transcription factor II E, polypeptide 1 (alpha subunit)	-1.65	3.90E-03
234407	Glt25d1	glycosyltransferase 25 domain containing 1	-1.65	0.00E+00
192216	Tmem47	transmembrane protein 47	-1.65	3.80E-03
68539	Tmem109	transmembrane protein 109	-1.64	5.00E-04
14105	Srsf10	serine/arginine-rich splicing factor 10	-1.64	3.60E-03
14391	Gabpb1	GA repeat binding protein, beta 1	-1.64	1.00E-04
11608	Agtr1b	angiotensin II receptor, type 1b	-1.64	4.70E-03
71760	Etnppl	alanine-glyoxylate aminotransferase 2-like 1	-1.64	4.30E-03
69309	Slc16a13	solute carrier family 16 (monocarboxylic acid transporters), member 13	-1.64	1.90E-03
67455	Klhl13	kelch-like 13 (Drosophila)	-1.63	0.00E+00
110639	Prps2	phosphoribosyl pyrophosphate synthetase 2	-1.63	4.70E-03
99011	Pomt1	protein-O-mannosyltransferase 1	-1.63	4.60E-03
66950	Tmem206	transmembrane protein 206	-1.63	2.00E-04
17986	Ndp	Norrie disease (pseudoglioma) (human)	-1.63	7.10E-03
11602	Angpt4	angiopoietin 4	-1.63	3.00E-04
16000	Igf1	insulin-like growth factor 1	-1.63	7.30E-03
229211	Acad9	acyl-Coenzyme A dehydrogenase family, member 9	-1.63	3.70E-03
22017	Tpmt	thiopurine methyltransferase	-1.63	0.00E+00
12290	Cacna1e	calcium channel, voltage-dependent, R type, alpha 1E subunit	-1.62	7.80E-03
56189	Prodh2	proline dehydrogenase (oxidase) 2	-1.62	0.00E+00
243537	Uroc1	urocanase domain containing 1	-1.62	1.20E-03
11831	Aqp6	aquaporin 6	-1.62	6.00E-04
21391	Tbxas1	thromboxane A synthase 1, platelet	-1.61	2.00E-03
66183	Sptssb	serine palmitoyltransferase, small subunit b	-1.61	4.60E-03

Table 32 continued

19288	Ptx3	pentraxin related gene	-1.61	3.00E-04
21401	Tcea3	transcription elongation factor A (SII), 3	-1.61	0.00E+00
93961	B3galt5	UDP-Gal:betaGlcNAc beta 1,3-galactosyltransferase, polypeptide 5	-1.61	0.00E+00
14586	Gfra2	glial cell line derived neurotrophic factor family receptor alpha 2	-1.61	3.60E-03
18391	Sigmar1	sigma non-opioid intracellular receptor 1	-1.61	1.00E-04
110809	Srsf1	serine/arginine-rich splicing factor 10	-1.61	5.10E-03
18767	Pkia	protein kinase inhibitor, alpha	-1.6	1.00E-04
18768	Pkib	protein kinase inhibitor beta, cAMP dependent, testis specific	-1.6	4.40E-03
68916	Cdkal1	CDK5 regulatory subunit associated protein 1-like 1	-1.6	0.00E+00
68021	Bphl	biphenyl hydrolase-like (serine hydrolase, breast epithelial mucin-associated antigen)	-1.6	1.00E-04
22200	Uba3	ubiquitin-like modifier activating enzyme 3	-1.6	1.00E-04
75590	Dusp9	dual specificity phosphatase 9	-1.6	5.80E-03
22652	Mkrn3	makorin, ring finger protein, 3	-1.59	9.00E-03
75572	Acyp2	acylphosphatase 2, muscle type; similar to acylphosphatase 2, muscle type	-1.59	6.30E-03
56367	Scoc	short coiled-coil protein	-1.59	6.00E-04
67333	Stk35	serine/threonine kinase 35	-1.59	5.40E-03
68126	Fahd2a	fumarylacetoacetate hydrolase domain containing 2A	-1.59	2.00E-04
110175	Ggct	gamma-glutamyl cyclotransferase	-1.59	0.00E+00
170718	Idh3b	isocitrate dehydrogenase 3 (NAD+) beta	-1.59	2.70E-03
66648	Tpgs2	tubulin polyglutamylase complex subunit 2	-1.59	5.30E-03
13048	Cux2	cut-like homeobox 2	-1.59	6.00E-04
16593	Klc1	kinesin light chain 1; similar to Kinesin light chain 1	-1.59	8.40E-03
56790	Supt20	suppressor of Ty 20	-1.59	0.00E+00
108100	Baiap2	brain-specific angiogenesis inhibitor 1-associated protein 2	-1.59	1.80E-03
66106	Smpx	small muscle protein, X-linked	-1.58	0.00E+00
66650	Nepn	nephrocan	-1.58	0.00E+00
26434	Prnd	prion protein dublet	-1.58	5.20E-03
80985	Trim44	tripartite motif-containing 44	-1.58	6.00E-04
241118	Asic4	amiloride-sensitive cation channel 4, pituitary	-1.58	5.10E-03
68472	Tmem126b	transmembrane protein 126B	-1.58	3.80E-03
13638	Efna3	ephrin A3	-1.58	5.30E-03
13732	Emp3	epithelial membrane protein 3	-1.57	4.00E-04
76238	Grhpr	glyoxylate reductase/hydroxypyruvate reductase	-1.57	0.00E+00
21789	Tfpi2	tissue factor pathway inhibitor 2	-1.57	1.40E-03
14852	Gspt1	G1 to S phase transition 1	-1.57	1.40E-03
12818	Col14a1	collagen, type XIV, alpha 1	-1.57	8.00E-03
11428	Aco1	aconitase 1	-1.57	1.00E-03
20541	Slc8a1	solute carrier family 8 (sodium/calcium exchanger), member 1	-1.56	1.40E-03
60596	Gucy1a3	guanylate cyclase 1, soluble, alpha 3	-1.56	6.20E-03
68385	Tlcd1	TLC domain containing 1	-1.56	3.80E-03
209584	Tyw3	tRNA-yW synthesizing protein 3 homolog (S. cerevisiae)	-1.56	1.00E-04
14609	Gja1	gap junction protein, alpha 1	-1.55	9.90E-03

Table 32 continued

54140	Avpr1a	arginine vasopressin receptor 1A	-1.55	7.30E-03
64008	Aqp9	aquaporin 9	-1.55	9.00E-03
12367	Casp3	caspase 3	-1.55	4.90E-03
70620	Ube2v2	ubiquitin-conjugating enzyme E2 variant 2	-1.55	1.00E-04
209456	Trp53bp2	transformation related protein 53 binding protein 2	-1.55	1.40E-03
239435	Aard	alanine and arginine rich domain containing protein	-1.55	2.90E-03
23831	Car14	carbonic anhydrase 14	-1.55	4.90E-03
268670	Zfp759	zinc finger protein 759	-1.55	0.00E+00
69090	Ascc1	activating signal cointegrator 1 complex subunit 1	-1.55	0.00E+00
15931	Ids	iduronate 2-sulfatase	-1.54	5.30E-03
14874	Gstz1	glutathione transferase zeta 1 (maleylacetoacetate isomerase)	-1.54	6.60E-03
242736	Pramef8	PRAME family member 8	-1.54	5.40E-03
13178	Dck	deoxycytidine kinase	-1.54	4.20E-03
16431	Itm2a	integral membrane protein 2A	-1.54	7.10E-03
13057	Cyba	cytochrome b-245, alpha polypeptide	-1.54	5.00E-03
58238	Fam181b	family with sequence similarity 181, member B	-1.53	0.00E+00
66948	Acad8	acyl-Coenzyme A dehydrogenase family, member 8	-1.53	9.10E-03
66204	Acyp1	acylphosphatase 1, erythrocyte (common) type	-1.53	0.00E+00
12729	Clns1a	chloride channel, nucleotide-sensitive, 1A	-1.53	1.60E-03
13170	Dbp	D site albumin promoter binding protein	-1.53	5.00E-04
27364	Srr	serine racemase	-1.53	7.00E-04
75104	Mmd2	monocyte to macrophage differentiation-associated 2	-1.53	6.00E-03
80914	Uck2	uridine-cytidine kinase 2	-1.53	6.80E-03
22762	Zfpm2	zinc finger protein, multitype 2	-1.53	3.20E-03
70998	Phf6	PHD finger protein 6	-1.53	2.60E-03
66834	Acot13	acyl-CoA thioesterase 13	-1.52	9.70E-03
13180	Pcbd1	pterin 4 alpha carbinolamine dehydratase/dimerization cofactor of hepatocyte nuclear factor 1 alpha (TCF1) 1	-1.52	1.00E-04
65973	Asph	aspartate-beta-hydroxylase	-1.52	1.00E-04
11416	Slc33a1	solute carrier family 33 (acetyl-CoA transporter), member 1	-1.52	3.40E-03
319953	Ttll1	tubulin tyrosine ligase-like 1	-1.52	1.30E-03
71767	Tysnd1	trypsin domain containing 1	-1.52	1.00E-04
66291	Smim8	small integral membrane protein 8	-1.52	2.00E-04
24058	Sigirr	single immunoglobulin and toll-interleukin 1 receptor (TIR) domain	-1.52	4.00E-04
209018	Vps8	vacuolar protein sorting 8 homolog (S. cerevisiae)	-1.52	0.00E+00
242125	Mab21l3	mab-21-like 3 (C. elegans)	-1.52	3.80E-03
56046	Uqcc1	ubiquinol-cytochrome c reductase complex chaperone, CBP3 homolog (yeast	-1.51	0.00E+00
19057	Ppp3cc	protein phosphatase 3, catalytic subunit, gamma isoform	-1.51	0.00E+00
118451	Mrps2	mitochondrial ribosomal protein S2	-1.51	3.40E-03
108105	B3gnt5	UDP-GlcNAc:betaGal beta-1,3-N-acetylglucosaminyltransferase 5	-1.51	1.00E-04
20444	St3gal2	ST3 beta-galactoside alpha-2,3-sialyltransferase 2	-1.51	1.10E-03
227580	C1ql3	C1q-like 3	-1.51	0.00E+00
27494	Amot	angiomotin	-1.51	7.70E-03
26466	Zfp260	zinc finger protein 260	-1.51	9.10E-03

Table 32 continued

67429	Nudcd1	NudC domain containing 1	-1.51	6.50E-03
327747	Mettl24	methyltransferase like 24	-1.51	2.00E-04
27386	Npas3	neuronal PAS domain protein 3	-1.51	0.00E+00
27052	Aoah	acyloxyacyl hydrolase	-1.51	1.50E-03
70357	Kcnip1	Kv channel-interacting protein 1	-1.5	6.30E-03
17068	Ly6d	lymphocyte antigen 6 complex, locus D	-1.5	6.30E-03
109077	Ints5	integrator complex subunit 5	-1.5	5.00E-04
68038	Chid1	chitinase domain containing 1	-1.5	1.10E-03
13616	Edn3	endothelin 3	-1.5	4.20E-03
19335	Rab23	RAB23, member RAS oncogene family	-1.5	6.90E-03
78802	Ttc30a1	tetratricopeptide repeat domain 30A1	-1.5	4.10E-03
21843	Tial1	Tia1 cytotoxic granule-associated RNA binding protein-like 1	-1.5	2.00E-04
11836	Araf	v-raf murine sarcoma 3611 viral oncogene homolog	-1.5	0.00E+00
73296	Rhobtb3	Rho-related BTB domain containing 3	-1.5	6.00E-04
11441	Chrna7	cholinergic receptor, nicotinic, alpha polypeptide 7	-1.5	3.90E-03
74254	Gpn1	GPN-loop GTPase 1	-1.5	2.10E-03
72899	Macrod2	MACRO domain containing 2	-1.5	1.60E-03
74013	Rftn2	raftlin family member 2	-1.5	9.00E-04
78689	Naa35	MAK10 homolog, amino-acid N-acetyltransferase subunit, (S. cerevisiae)	-1.5	3.00E-04
55943	Stx8	syntaxin 8	-1.5	0.00E+00
102182	Prmt10	protein arginine methyltransferase 10 (putative)	-1.5	0.00E+00
13593	Ebf3	early B-cell factor 3	-1.5	3.20E-03
52163	Camk1	calcium/calmodulin-dependent protein kinase I	-1.49	2.00E-04
170728	Rtn4ip1	reticulon 4 interacting protein 1	-1.49	0.00E+00
56305	Pitpnb	phosphatidylinositol transfer protein, beta	-1.49	2.80E-03
13121	Cyp51	cytochrome P450, family 51	-1.49	8.40E-03
67405	Nts	neurotensin	-1.49	2.70E-03
11610	Agtrap	angiotensin II, type I receptor-associated protein	-1.49	3.40E-03
252864	Dusp15	dual specificity phosphatase-like 15	-1.49	3.00E-04
71902	Cand1	cullin associated and neddylation disassociated 1	-1.49	4.90E-03
12444	Ccnd2	cyclin D2	-1.49	1.10E-03
654824	Ankrd37	ankyrin repeat domain 37	-1.49	5.30E-03
15374	Hn1	hematological and neurological expressed sequence 1	-1.49	9.20E-03
51810	Hnrnpu	heterogeneous nuclear ribonucleoprotein U	-1.49	2.00E-03
12972	Cryz	crystallin, zeta	-1.49	9.40E-03
27385	Magel2	melanoma antigen, family L, 2	-1.48	1.60E-03
54711	Plagl2	pleiomorphic adenoma gene-like 2	-1.48	0.00E+00
12567	Cdk4	Cyclin-dependent kinase 4	-1.48	4.30E-03
233799	Acsm2	acyl-CoA synthetase medium-chain family member 2	-1.48	4.20E-03
14702	Gng2	guanine nucleotide binding protein (G protein), gamma 2	-1.48	3.90E-03
407790	Ndufa4l2	NADH dehydrogenase (ubiquinone) 1 alpha subcomplex, 4-like 2	-1.48	4.00E-04
68554	Cebpzos	CCAAT/enhancer binding protein (C/EBP), zeta, opposite strand	-1.48	0.00E+00
111175	Pecr	peroxisomal trans-2-enoyl-CoA reductase	-1.48	1.00E-04
12593	Cdyl	chromodomain protein, Y chromosome-like	-1.48	5.00E-04
66882	Bzw1	basic leucine zipper and W2 domains 1	-1.48	3.10E-03

Table 32 continued

218454	Lhfpl2	lipoma HMGIC fusion partner-like 2	-1.48	6.40E-03
14886	Gtf2i	general transcription factor II I	-1.48	6.90E-03
268566	Gphn	gephyrin	-1.47	6.00E-04
22059	Trp53	transformation related protein 53	-1.47	1.40E-03
13990	Smarcad1	SWI/SNF-related, matrix-associated actin-dependent regulator of chromatin, subfamily a, containing DEAD/H box 1	-1.47	3.00E-04
12447	Ccne1	cyclin E1	-1.47	8.50E-03
66249	Pno1	partner of NOB1 homolog (S. cerevisiae)	-1.47	3.00E-04
545428	Ccdc141	coiled-coil domain containing 141	-1.47	0.00E+00
19076	Prim2	DNA primase, p58 subunit	-1.46	2.50E-03
66870	Serbp1	serpine1 mRNA binding protein 1	-1.46	9.60E-03
12663	Chml	choroideremia-like	-1.46	0.00E+00
171170	Mbnl3	muscleblind-like 3 (Drosophila)	-1.46	5.00E-04
66614	Gpatch4	G patch domain containing 4	-1.46	7.10E-03
105670	Rcbtb2	regulator of chromosome condensation (RCC1) and BTB (POZ) domain containing protein 2	-1.46	0.00E+00
72135	Pygo1	pygopus 1	-1.46	9.70E-03
13612	Edil3	EGF-like repeats and discoidin I-like domains 3	-1.46	9.00E-04
12715	Ckm	creatine kinase, muscle	-1.46	2.00E-04
57264	Retn	resistin	-1.46	7.00E-03
621603	Aldh3b2	aldehyde dehydrogenase 3 family	-1.46	9.90E-03
108011	Ap4e1	adaptor-related protein complex AP-4, epsilon 1	-1.46	0.00E+00
67669	l7Rn6	lethal, Chr 7, Rinchik 6	-1.45	1.30E-03
18559	Pctp	phosphatidylcholine transfer protein	-1.45	1.90E-03
67005	Polr3k	polymerase (RNA) III (DNA directed) polypeptide K	-1.45	5.00E-04
69792	Med6	mediator of RNA polymerase II transcription, subunit 6 homolog (yeast)	-1.45	3.10E-03
50493	Txnrd1	thioredoxin reductase 1	-1.45	7.00E-04
12393	Runx2	runt related transcription factor 2	-1.45	2.50E-03
74782	Glt8d2	glycosyltransferase 8 domain containing 2	-1.45	9.80E-03
110920	Hspa13	heat shock protein 70 family, member 13	-1.45	2.10E-03
58244	Stx6	syntaxin 6	-1.45	8.90E-03
20204	Prrx2	paired related homeobox 2	-1.45	3.00E-04
109006	Ciapin1	cytokine induced apoptosis inhibitor 1	-1.45	1.50E-03
50530	Mfap5	microfibrillar associated protein 5	-1.45	2.20E-03
12180	Smyd1	SET and MYND domain containing 1	-1.45	9.00E-04

Table 33: Upregulated genes in inversin-depleted renal epithelial cells

Gene ID	Gene Symbol	Protein Name	Fold change/ NTC	*P*-value
72948	Tppp	tubulin polymerization promoting protein	21.78	0
20652	Soat1	sterol O-acyltransferase 1	7.6	0
68528	Smim6	small integral membrane protein 6	5.71	0
16840	Lect1	leukocyte cell derived chemotaxin 1	5.37	0
56863	Cldn9	claudin 9	5.19	0
75320	Etnk1	ethanolamine kinase 1	4.31	0
68236	Gtsf1l	gametocyte specific factor 1-like	3.91	0.0034
107503	Atf5	activating transcription factor 5	3.9	0
104681	Slc16a6	solute carrier family 16 (monocarboxylic acid transporters), member 6	3.21	0
74096	Hvcn1	hydrogen voltage-gated channel 1	3.2	0
1E+08	Six3os1	SIX homeobox 3, opposite strand 1	3.06	0.0143
14755	Pigq	phosphatidylinositol glycan anchor biosynthesis, class Q	2.94	0
80797	Clca2	chloride channel calcium activated 2	2.91	0
237847	Rtn4rl1	reticulon 4 receptor-like 1	2.89	0
67269	Agtpbp1	ATP/GTP binding protein 1	2.86	0.0299
67859	Cysrt1	cysteine rich tail 1	2.85	0.0135
224813	Lrrc73	leucine rich repeat containing 73	2.83	0.0213
12978	Csf1r	colony stimulating factor 1 receptor	2.76	0
23967	Osr1	odd-skipped related 1 (Drosophila)	2.76	0
58180	Hic2	hypermethylated in cancer 2	2.68	0
18104	Nqo1	NAD(P)H dehydrogenase, quinone 1	2.49	0
17470	Cd200	CD200 antigen	2.44	0.0013
23956	Neu2	neuraminidase 2	2.41	0
22762	Zfpm2	zinc finger protein, multitype 2	2.4	0
83814	Nedd4l	neural precursor cell expressed, developmentally down-regulated gene 4-like	2.37	0
53868	Rab25	RAB25, member RAS oncogene family	2.37	0
16581	Kifc2	kinesin family member C2	2.36	0.0014
210789	Tbc1d4	TBC1 domain family, member 4	2.3	0
52906	Ahi1	Abelson helper integration site 1	2.29	0
27494	Amot	angiomotin	2.28	0
19201	Pstpip2	proline-serine-threonine phosphatase-interacting protein 2	2.28	0.0343
246277	Csad	cysteine sulfinic acid decarboxylase	2.27	0
225187	Ankrd29	ankyrin repeat domain 29	2.26	3.00E-04
214505	Gnptg	N-acetylglucosamine-1-phosphotransferase, gamma subunit	2.26	0
53951	Gpatch11	G patch domain containing 11	2.26	0.0074
13423	Dnase2a	deoxyribonuclease II alpha	2.25	0
210982	Gltscr1l	GLTSCR1-like	2.24	0

Table 33 continued

17904	Myl6	myosin, light polypeptide 6, alkali, smooth muscle and non-muscle	2.24	0
68877	Maf1	MAF1 homolog (S. cerevisiae)	2.23	0.0049
54393	Gabbr1	gamma-aminobutyric acid (GABA) B receptor, 1	2.21	0
226751	Cdc42bpa	CDC42 binding protein kinase alpha	2.18	0.0013
83679	Pde4dip	phosphodiesterase 4D interacting protein (myomegalin)	2.17	0
108075	Ltbp4	latent transforming growth factor beta binding protein 4	2.16	0
71687	Tmem25	transmembrane protein 25	2.16	0.0084
63830	Kcnq1ot1	KCNQ1 overlapping transcript 1	2.15	0
105638	Dnph1	2'-deoxynucleoside 5'-phosphate N-hydrolase 1	2.14	0
16439	Itpr2	inositol 1,4,5-triphosphate receptor 2	2.13	0
16598	Klf2	Kruppel-like factor 2 (lung)	2.13	0
237930	Ttll6	tubulin tyrosine ligase-like family, member 6	2.13	0
67516	Kctd4	potassium channel tetramerisation domain containing 4	2.11	0.0052
14670	Gnl1	guanine nucleotide binding protein-like 1	2.09	0
74309	Osbp2	oxysterol binding protein 2	2.09	0.0057
109689	Arrb1	arrestin, beta 1	2.08	0
16600	Klf4	Kruppel-like factor 4 (gut)	2.07	0
66237	Atp6v1g2	ATPase, H+ transporting, lysosomal V1 subunit G2	2.05	0
237860	Ssh2	slingshot homolog 2 (Drosophila)	2.04	0
24132	Zfp53	zinc finger protein 53	2.02	0
68597	Ccdc167	coiled-coil domain containing 167	2.01	1.00E-04
13518	Dst	dystonin	2.01	0
68614	Letmd1	LETM1 domain containing 1	1.99	0
64657	Mrps10	mitochondrial ribosomal protein S10	1.99	0.0268
216445	Arhgap9	Rho GTPase activating protein 9	1.98	0.0285
17299	Mettl1	methyltransferase like 1	1.98	0
237336	Tbpl1	TATA box binding protein-like 1	1.98	0
12322	Camk2a	calcium/calmodulin-dependent protein kinase II alpha	1.97	0.0124
214854	Neurl3	neuralized homolog 3 homolog (Drosophila)	1.97	0
242022	Frem2	Fras1 related extracellular matrix protein 2	1.96	0
76071	Jakmip1	janus kinase and microtubule interacting protein 1	1.96	0
53627	Porcn	porcupine homolog (Drosophila)	1.96	0
224826	Ubr2	ubiquitin protein ligase E3 component n-recognin 2	1.96	0
22700	Zfp40	zinc finger protein 40	1.96	0
329165	Abi2	abl-interactor 2	1.95	0
64898	Lpin2	lipin 2	1.95	0
18803	Plcg1	phospholipase C, gamma 1	1.95	0
52830	Pnrc2	proline-rich nuclear receptor coactivator 2	1.95	0.029
71567	Mcm9	minichromosome maintenance complex component 9	1.94	0
81630	Zbtb22	zinc finger and BTB domain containing 22	1.94	0
110532	Adarb1	adenosine deaminase, RNA-specific, B1	1.93	0
11980	Atp8a1	ATPase, aminophospholipid transporter (APLT), class I, type 8A, member 1	1.93	0
12364	Casp12	caspase 12	1.93	0
58231	Stmnd1	stathmin domain containing 1	1.93	0.0029
215690	Nav1	neuron navigator 1	1.92	0
20539	Slc7a5	solute carrier family 7 (cationic amino acid transporter, y+ system), member 5	1.92	0

Table 33 continued

108995	Tbc1d10c	TBC1 domain family, member 10c	1.92	6.00E-04
71718	Telo2	TEL2, telomere maintenance 2, homolog (S. cerevisiae)	1.92	0
73822	Mfsd12	major facilitator superfamily domain containing 12	1.91	0
72886	Ccdc94	coiled-coil domain containing 94	1.9	0
19725	Rfx2	regulatory factor X, 2 (influences HLA class II expression)	1.89	0
52466	Slc46a1	solute carrier family 46, member 1	1.89	0
99681	Tchh	trichohyalin	1.87	0
16529	Kcnk5	potassium channel, subfamily K, member 5	1.86	0
269610	Chd5	chromodomain helicase DNA binding protein 5	1.85	2.00E-04
53621	Cnot4	CCR4-NOT transcription complex, subunit 4	1.85	0
20425	Shmt1	serine hydroxymethyltransferase 1 (soluble)	1.85	0
73582	Camkmt	calmodulin-lysine N-methyltransferase	1.84	0
15081	H3f3b	H3 histone, family 3B	1.84	1.00E-04
76137	Mcur1	mitochondrial calcium uniporter regulator 1	1.84	0
381695	N4bp2l2	NEDD4 binding protein 2-like 2	1.84	0.0053
241289	Ppp1r26	protein phosphatase 1, regulatory subunit 26	1.84	0
22084	Tsc2	tuberous sclerosis 2	1.84	0
106585	Ankrd12	ankyrin repeat domain 12	1.83	0
97112	Nmd3	NMD3 homolog (S. cerevisiae)	1.83	1.00E-04
20743	Sptbn2	spectrin beta, non-erythrocytic 2	1.83	0
75547	Akap13	A kinase (PRKA) anchor protein 13	1.82	0
223527	Eny2	enhancer of yellow 2 homolog (Drosophila)	1.82	0
72039	Mccc1	methylcrotonoyl-Coenzyme A carboxylase 1 (alpha)	1.82	0
233066	Syne4	spectrin repeat containing, nuclear envelope family member 4	1.82	2.00E-04
104806	Fancm	Fanconi anemia, complementation group M	1.81	0.0098
18011	Neurl1a	neuralized homolog 1A (Drosophila)	1.81	0.0071
53320	Folh1	folate hydrolase 1	1.8	0
78656	Brd8	bromodomain containing 8	1.79	5.00E-04
50766	Crim1	cysteine rich transmembrane BMP regulator 1 (chordin like)	1.79	2.00E-04
170755	Sgk3	serum/glucocorticoid regulated kinase 3	1.79	0
78830	Slc25a12	solute carrier family 25 (mitochondrial carrier, Aralar), member 12	1.79	1.00E-04
52430	Echdc2	enoyl Coenzyme A hydratase domain containing 2	1.78	0
16993	Lta4h	leukotriene A4 hydrolase	1.78	8.00E-04
72462	Rrp1b	ribosomal RNA processing 1 homolog B (S. cerevisiae)	1.78	0
74741	C2cd5	C2 calcium-dependent domain containing 5	1.77	0
12722	Clca1	chloride channel calcium activated 1	1.77	4.00E-04
240041	Zfp945	zinc finger protein 945	1.77	0
105504	Exoc5	exocyst complex component 5	1.76	0
330671	B4galnt4	beta-1,4-N-acetyl-galactosaminyl transferase 4	1.75	0
19647	Rbbp6	retinoblastoma binding protein 6	1.75	0
74011	Slc25a27	solute carrier family 25, member 27	1.75	6.00E-04
94089	Trim7	tripartite motif-containing 7	1.75	0
105785	Kdelr3	KDEL (Lys-Asp-Glu-Leu) endoplasmic reticulum protein retention receptor 3	1.74	0.0022
14536	Nr6a1	nuclear receptor subfamily 6, group A, member 1	1.74	0

Table 33 continued

68799	Rgmb	repulsive guidance molecule family member B	1.74	0
320226	Ccdc171	coiled-coil domain containing 171	1.73	7.00E-04
76917	Flywch2	FLYWCH family member 2	1.73	0
76500	Ip6k2	inositol hexaphosphate kinase 2	1.73	0
101706	Numa1	nuclear mitotic apparatus protein 1	1.73	1.00E-04
93759	Sirt1	sirtuin 1	1.73	0
224648	Uhrf1bp1	UHRF1 (ICBP90) binding protein 1	1.73	2.00E-04
80892	Zfhx4	zinc finger homeodomain 4	1.73	0
103406	Zfr2	zinc finger RNA binding protein 2	1.73	0
76863	Dcun1d5	DCN1, defective in cullin neddylation 1, domain containing 5 (S. cerevisiae)	1.72	0
29857	Mapk12	mitogen-activated protein kinase 12	1.72	0
106583	Scaf8	SR-related CTD-associated factor 8	1.72	0
67062	Slc25a53	solute carrier family 25, member 53	1.72	0
223922	Atf7	activating transcription factor 7	1.71	0.0161
26889	Cln8	ceroid-lipofuscinosis, neuronal 8	1.71	0.0084
72514	Fgfbp3	fibroblast growth factor binding protein 3	1.71	0
22038	Plscr1	phospholipid scramblase 1	1.71	8.00E-04
18845	Plxna2	plexin A2	1.71	1.00E-04
56468	Socs5	suppressor of cytokine signaling 5	1.71	0
12005	Axin1	axin 1	1.7	0
70772	Ggnbp1	gametogenetin binding protein 1	1.7	0.0281
66467	Gtf2h5	general transcription factor IIH, polypeptide 5	1.7	0
76781	Mettl4	methyltransferase like 4	1.7	0
338367	Myo1d	myosin ID	1.7	0
70439	Taf15	TAF15 RNA polymerase II, TATA box binding protein (TBP)-associated factor	1.7	0
11727	Ang	angiogenin, ribonuclease, RNase A family, 5	1.69	0
72029	Cnpy3	canopy 3 homolog (zebrafish)	1.69	0
50758	Fbxl17	F-box and leucine-rich repeat protein 17	1.69	3.00E-04
56516	Rbms2	RNA binding motif, single stranded interacting protein 2	1.69	0
100201	Tmem64	transmembrane protein 64	1.69	0
217333	Trim47	tripartite motif-containing 47	1.69	0
68789	Trmt61b	tRNA methyltransferase 61B	1.69	0
214150	Ago3	argonaute RISC catalytic subunit 3	1.68	0.00E+00
238123	Cog5	component of oligomeric golgi complex 5	1.68	0
20463	Cox7a2l	cytochrome c oxidase subunit VIIa polypeptide 2-like	1.68	0
12946	Cr1l	complement component (3b/4b) receptor 1-like	1.68	1.00E-04
211446	Exoc3	exocyst complex component 3	1.68	0
109801	Glo1	glyoxalase 1	1.68	0
22196	Ube2i	ubiquitin-conjugating enzyme E2I	1.68	0
77048	Cep83	centrosomal protein 83	1.67	0
70291	Mkrn2os	makorin, ring finger protein 2, opposite strand	1.67	0
20185	Ncor1	nuclear receptor co-repressor 1	1.67	0
72057	Phf10	PHD finger protein 10	1.67	0
51796	Srrm1	serine/arginine repetitive matrix 1	1.67	0.0035
69539	Trnp1	TMF1-regulated nuclear protein 1	1.67	0
11512	Adcy6	adenylate cyclase 6	1.66	0

Table 33 continued

11842	Arf3	ADP-ribosylation factor 3	1.66	0.0072
12915	Atf6b	Activating transcription factor 6 beta	1.66	0
73739	Cby1	chibby homolog 1 (Drosophila)	1.66	1.00E-04
56149	Grasp	GRP1 (general receptor for phosphoinositides 1)-associated scaffold protein	1.66	0
19250	Ptpn14	protein tyrosine phosphatase, non-receptor type 14	1.66	0
225027	Srsf7	serine/arginine-rich splicing factor 7	1.66	0
97503	Vwa7	von Willebrand factor A domain containing 7	1.66	0.0184
432486	Gnptab	N-acetylglucosamine-1-phosphate transferase, alpha and beta subunits	1.65	0
68537	Mrpl13	mitochondrial ribosomal protein L13	1.65	0
72193	Scaf11	SR-related CTD-associated factor 11	1.65	0
57908	Zfp318	zinc finger protein 318	1.65	0
193742	Abhd16a	abhydrolase domain containing 16A	1.64	0
67723	Cep83os	centrosomal protein 83, opposite strand	1.64	0
66978	Luc7l	Luc7 homolog (S. cerevisiae)-like	1.64	0
216154	Med16	mediator complex subunit 16	1.64	0
56716	Mlst8	MTOR associated protein, LST8 homolog (S. cerevisiae)	1.64	0
100273	Osbpl9	oxysterol binding protein-like 9	1.64	0
170719	Oxr1	oxidation resistance 1	1.64	0
22643	Zfp101	zinc finger protein 101	1.64	5.00E-04
240120	Zfp119b	zinc finger protein 119b	1.64	0
66548	Adamtsl5	ADAMTS-like 5	1.63	0.0026
233115	Dpy19l3	dpy-19-like 3 (C. elegans)	1.63	0
71436	Flrt3	fibronectin leucine rich transmembrane protein 3	1.63	0.0013
259277	Klk8	kallikrein related-peptidase 8	1.63	0
17356	Mllt4	myeloid/lymphoid or mixed-lineage leukemia (trithorax homolog, Drosophila); translocated to, 4	1.63	0
56409	Nudt3	nudix (nucleotide diphosphate linked moiety X)-type motif 3	1.63	0
19326	Rab11b	RAB11B, member RAS oncogene family	1.63	0
20662	Sos1	son of sevenless homolog 1 (Drosophila)	1.63	1.00E-04
22687	Zpr1	ZPR1 zinc finger	1.63	0.0014
16800	Arhgef2	rho/rac guanine nucleotide exchange factor (GEF) 2	1.62	0
18218	Dusp8	dual specificity phosphatase 8	1.62	0.0044
225055	Fbxo11	F-box protein 11	1.62	0
14910	Gt(ROSA)26Sor	gene trap ROSA 26, Philippe Soriano	1.62	0
16576	Kif7	kinesin family member 7	1.62	0.0051
17762	Mapt	microtubule-associated protein tau	1.62	0
13340	Slc29a2	solute carrier family 29 (nucleoside transporters), member 2	1.62	1.00E-04
12268	C4b	complement component 4B (Chido blood group)	1.61	0.0011
218210	Nup153	nucleoporin 153	1.61	6.00E-04
70335	Reep6	receptor accessory protein 6	1.61	0
66353	Riiad1	regulatory subunit of type II PKA R-subunit (RIIa) domain containing 1	1.61	0.0145

Table 33 continued

74355	Smchd1	SMC hinge domain containing 1	1.61	0
75956	Srrm2	serine/arginine repetitive matrix 2	1.61	0
11736	Ankfy1	ankyrin repeat and FYVE domain containing 1	1.6	0.0069
320162	Cep95	centrosomal protein 95	1.6	0.0014
224907	Dus3l	dihydrouridine synthase 3-like (S. cerevisiae)	1.6	0
16855	Lgals4	lectin, galactose binding, soluble 4	1.6	9.00E-04
17760	Map6	microtubule-associated protein 6	1.6	0.0022
240087	Mdc1	mediator of DNA damage checkpoint 1	1.6	0
18854	Pml	promyelocytic leukemia	1.6	0.0013
208292	Zfp871	zinc finger protein 871	1.6	0
229776	Cdc14a	CDC14 cell division cycle 14A	1.59	0
14885	Gtf2h4	general transcription factor II H, polypeptide 4	1.59	0
109241	Mbd5	methyl-CpG binding domain protein 5	1.59	0.0042
239985	Arid1b	AT rich interactive domain 1B (SWI-like)	1.58	0
12611	Cebpg	CCAAT/enhancer binding protein (C/EBP), gamma	1.58	0
319158	Hist1h4i	histone cluster 1, H4i	1.58	0
67042	Ift27	intraflagellar transport 27	1.58	0
240354	Malt1	mucosa associated lymphoid tissue lymphoma translocation gene 1	1.58	7.00E-04
320878	Mical2	microtubule associated monooxygenase, calponin and LIM domain containing 2	1.58	0.0081
114716	Spred2	sprouty-related, EVH1 domain containing 2	1.58	1.00E-04
69020	Zfp707	zinc finger protein 707	1.58	0.0031
67006	Cisd2	CDGSH iron sulfur domain 2	1.57	1.00E-04
224897	Dpp9	dipeptidylpeptidase 9	1.57	0
98053	Gtf2f1	general transcription factor IIF, polypeptide 1	1.57	0
67429	Nudcd1	NudC domain containing 1	1.57	0.0038
71365	Pdss2	prenyl (solanesyl) diphosphate synthase, subunit 2	1.57	0.0163
224893	Zfp959	zinc finger protein 959	1.57	2.00E-04
71361	Aifm2	apoptosis-inducing factor, mitochondrion-associated 2	1.56	0
11772	Ap2a2	adaptor-related protein complex 2, alpha 2 subunit	1.56	0
56724	Cript	cysteine-rich PDZ-binding protein	1.56	0
66590	Farsa	phenylalanyl-tRNA synthetase, alpha subunit	1.56	0.0063
11692	Gfer	growth factor, erv1 (S. cerevisiae)-like (augmenter of liver regeneration)	1.56	0
68304	Kdelc2	KDEL (Lys-Asp-Glu-Leu) containing 2	1.56	0
213760	Prepl	prolyl endopeptidase-like	1.56	0
56438	Rbx1	ring-box 1	1.56	1.00E-04
20194	S100a10	S100 calcium binding protein A10 (calpactin)	1.56	0
109552	Sri	sorcin	1.56	0
30056	Timm9	translocase of inner mitochondrial membrane 9	1.56	0
224836	Usp49	ubiquitin specific peptidase 49	1.56	0
106618	Wdr90	WD repeat domain 90	1.56	2.00E-04
78795	Armc9	armadillo repeat containing 9	1.55	0
268936	Brpf3	bromodomain and PHD finger containing, 3	1.55	0
384009	Glipr2	GLI pathogenesis-related 2	1.55	0.0111
80718	Rab27b	RAB27B, member RAS oncogene family	1.55	0
226781	Slc30a10	solute carrier family 30, member 10	1.55	0
68166	Spire1	spire homolog 1 (Drosophila)	1.55	1.00E-04

Table 33 continued

20383	Srsf3	serine/arginine-rich splicing factor 3	1.55	0
72322	Xpo5	exportin 5	1.55	0
233058	Zfp420	zinc finger protein 420	1.55	9.00E-04
226747	Ahctf1	AT hook containing transcription factor 1	1.54	0
73242	Atat1	alpha tubulin acetyltransferase 1	1.54	0
70686	Dusp16	dual specificity phosphatase 16	1.54	0.0065
72508	Rps6kb1	ribosomal protein S6 kinase, polypeptide 1	1.54	2.00E-04
63856	Taf8	TAF8 RNA polymerase II, TATA box binding protein (TBP)-associated factorq	1.54	0
110960	Tars	threonyl-tRNA synthetase	1.54	0
211660	Cspp1	centrosome and spindle pole associated protein 1	1.53	2.00E-04
239667	Dip2b	DIP2 disco-interacting protein 2 homolog B (Drosophila)	1.53	0.0171
75219	Dusp18	dual specificity phosphatase 18	1.53	0
246179	Fktn	fukutin	1.53	0
77480	Kidins220	kinase D-interacting substrate 220	1.53	1.00E-04
26416	Mapk14	mitogen-activated protein kinase 14	1.53	0
17181	Matn2	matrilin 2	1.53	0.0038
214742	Rcor3	REST corepressor 3	1.53	0
21843	Tial1	Tia1 cytotoxic granule-associated RNA binding protein-like 1	1.53	0
72515	Wdr43	WD repeat domain 43	1.53	0
15458	Hpx	hemopexin	1.52	0.0072
67733	Itgb3bp	integrin beta 3 binding protein (beta3-endonexin)	1.52	0.0171
74127	Krt80	keratin 80	1.52	0
382793	Mtx3	metaxin 3	1.52	0
330260	Pon2	paraoxonase 2	1.52	0.0071
19386	Ranbp2	RAN binding protein 2	1.52	0
66855	Tcf25	transcription factor 25 (basic helix-loop-helix)	1.52	3.00E-04
102791	Tcta	T cell leukemia translocation altered gene	1.52	0
68915	Vars2	valyl-tRNA synthetase 2, mitochondrial (putative)	1.52	0
21769	Zfand3	zinc finger, AN1-type domain 3	1.52	0
66136	Znrd1	zinc ribbon domain containing, 1	1.52	0
215748	Cnksr3	Cnksr family member 3	1.51	0
55936	Ctps2	cytidine 5'-triphosphate synthase 2	1.51	2.00E-04
13110	Cyp2j6	cytochrome P450, family 2, subfamily j, polypeptide 6	1.51	2.00E-04
56809	Gmeb1	glucocorticoid modulatory element binding protein 1	1.51	0.0031
15193	Hdgfrp2	hepatoma-derived growth factor, related protein 2	1.51	0
93730	Lztfl1	leucine zipper transcription factor-like 1	1.51	0
14924	Magi1	membrane associated guanylate kinase, WW and PDZ domain containing 1	1.51	0
18207	Nthl1	nth (endonuclease III)-like 1 (E.coli)	1.51	3.00E-04
214968	Sema6d	sema domain, transmembrane domain (TM), and cytoplasmic domain, (semaphorin) 6D	1.51	0.02
72895	Setd5	SET domain containing 5	1.51	0
73836	Slc35b2	solute carrier family 35, member B2	1.51	0.0041
20744	Strbp	spermatid perinuclear RNA binding protein	1.51	1.00E-04
109115	Supt3	suppressor of Ty 3	1.51	0
60532	Wtap	Wilms tumour 1-associating protein	1.51	0

Table 33 continued

68270	Dnaaf1	dynein, axonemal assembly factor 1	1.5	0.0399
74559	Elovl7	ELOVL family member 7, elongation of long chain fatty acids (yeast)	1.5	0
71927	Itfg1	integrin alpha FG-GAP repeat containing 1	1.5	1.00E-04
80877	Lrba	LPS-responsive beige-like anchor	1.5	0
17776	Mast2	microtubule associated serine/threonine kinase 2	1.5	1.00E-04
56462	Mtch1	mitochondrial carrier homolog 1 (C. elegans)	1.5	0
20683	Sp1	trans-acting transcription factor 1	1.5	0
72726	Tbcc	tubulin-specific chaperone C	1.5	0.0017
79263	Trim39	tripartite motif-containing 39	1.5	0
68767	Wash	WAS protein family homolog	1.5	0.0038
268933	Wdr24	WD repeat domain 24	1.5	0
77264	Zfp142	zinc finger protein 142	1.5	0.0278
240064	Zfp799	zinc finger protein 799	1.5	0
108058	Camk2d	calcium/calmodulin-dependent protein kinase II, delta	1.49	2.00E-04
13640	Efna5	ephrin A5	1.49	0
78878	Ftx	Ftx transcript, Xist regulator (non-protein coding)	1.49	0.0101
94353	Hmgn3	high mobility group nucleosomal binding domain 3	1.49	0
15382	Hnrnpa1	heterogeneous nuclear ribonucleoprotein A1	1.49	5.00E-04
16661	Krt10	keratin 10	1.49	0
56758	Mbnl1	muscleblind-like 1 (Drosophila)	1.49	0.0288
17685	Msh2	mutS homolog 2 (E. coli)	1.49	6.00E-04
320111	Prr18	proline rich 18	1.49	0.0252
19296	Pvt1	plasmacytoma variant translocation 1	1.49	0
215445	Rab11fip3	RAB11 family interacting protein 3 (class II)	1.49	4.00E-04
242585	Slc35d1	solute carrier family 35 (UDP-glucuronic acid/UDP-N-acetylgalactosamine dual transporter), member D1	1.49	2.00E-04
68268	Zdhhc21	zinc finger, DHHC domain containing 21	1.49	0
27410	Abca3	ATP-binding cassette, sub-family A (ABC1), member 3	1.48	0
11855	Arhgap5	Rho GTPase activating protein 5	1.48	1.00E-04
12211	Birc6	baculoviral IAP repeat-containing 6	1.48	0
109880	Braf	Braf transforming gene	1.48	0
12607	Cebpz	CCAAT/enhancer binding protein zeta	1.48	0
432508	Cpsf6	cleavage and polyadenylation specific factor 6	1.48	7.00E-04
70069	H1fnt	H1 histone family, member N, testis-specific	1.48	0.0045
78651	Lsm6	LSM6 homolog, U6 small nuclear RNA associated (S. cerevisiae)	1.48	0
66414	Ndufa12	NADH dehydrogenase (ubiquinone) 1 alpha subcomplex, 12	1.48	2.00E-04
18027	Nfia	nuclear factor I/A	1.48	0.0088
71175	Nipbl	Nipped-B homolog (Drosophila)	1.48	0
18195	Nsf	N-ethylmaleimide sensitive fusion protein	1.48	0.013
18515	Pbx2	pre B cell leukemia homeobox 2	1.48	0
319518	Pdpr	pyruvate dehydrogenase phosphatase regulatory subunit	1.48	0.0161
14083	Ptk2	PTK2 protein tyrosine kinase 2	1.48	0
380714	Rph3al	rabphilin 3A-like (without C2 domains)	1.48	0
20084	Rps18	ribosomal protein S18	1.48	2.00E-04
108077	Skiv2l	superkiller viralicidic activity 2-like (S. cerevisiae)	1.48	0

Table 33 continued

59033	Slc4a8	solute carrier family 4 (anion exchanger), member 8	1.48	0.0131
69434	Snhg10	small nucleolar RNA host gene 10	1.48	0
67023	Use1	unconventional SNARE in the ER 1 homolog (S. cerevisiae)	1.48	0.0111
237898	Usp32	ubiquitin specific peptidase 32	1.48	9.00E-04
54194	Akap8l	A kinase (PRKA) anchor protein 8-like	1.47	1.00E-04
75415	Arhgap12	Rho GTPase activating protein 12	1.47	0
102545	Cmtm7	CKLF-like MARVEL transmembrane domain containing 7	1.47	0.0011
77996	Cutal	cutA divalent cation tolerance homolog-like	1.47	0
13367	Diap1	diaphanous homolog 1 (Drosophila)	1.47	2.00E-04
71916	Dus4l	dihydrouridine synthase 4-like (S. cerevisiae)	1.47	1.00E-04
107508	Eprs	glutamyl-prolyl-tRNA synthetase	1.47	0.0027
12695	Inadl	InaD-like (Drosophila)	1.47	0
23849	Klf6	Kruppel-like factor 6	1.47	0.0019
76890	Memo1	mediator of cell motility 1	1.47	7.00E-04
18771	Pknox1	Pbx/knotted 1 homeobox	1.47	4.00E-04
20907	Stx1a	syntaxin 1A (brain)	1.47	0
237500	Tmtc3	transmembrane and tetratricopeptide repeat containing 3	1.47	0
22215	Ube3a	ubiquitin protein ligase E3A	1.47	8.00E-04
235574	Atp2c1	ATPase, Ca++-sequestering	1.46	0
66371	Chmp4c	charged multivesicular body protein 4C	1.46	1.00E-04
59079	Erbb2ip	Erbb2 interacting protein	1.46	1.00E-04
67529	Fgfr1op2	FGFR1 oncogene partner 2	1.46	0
53618	Fut8	fucosyltransferase 8	1.46	1.00E-04
328329	Mast4	microtubule associated serine/threonine kinase family member 4	1.46	1.00E-04
67245	Peli1	pellino 1	1.46	4.00E-04
83946	Phip	pleckstrin homology domain interacting protein	1.46	0
56194	Prpf40a	PRP40 pre-mRNA processing factor 40 homolog A (yeast)	1.46	0.0051
77300	Raph1	Ras association (RalGDS/AF-6) and pleckstrin homology domains 1	1.46	0.0012
71340	Riok1	RIO kinase 1 (yeast)	1.46	1.00E-04
216161	Sbno2	strawberry notch homolog 2 (Drosophila)	1.46	0
72198	Skiv2l2	superkiller viralicidic activity 2-like 2 (S. cerevisiae)	1.46	0.0078
20536	Slc4a3	solute carrier family 4 (anion exchanger), member 3	1.46	7.00E-04
72238	Tbc1d5	TBC1 domain family, member 5	1.46	0
194388	Tet3	tet methylcytosine dioxygenase 3	1.46	0.039
216810	Tom1l2	target of myb1-like 2 (chicken)	1.46	0.0019
22409	Wnt10a	wingless-type MMTV integration site family, member 10A	1.46	0
66894	Wwp2	WW domain containing E3 ubiquitin protein ligase 2	1.46	7.00E-04
22666	Zbtb14	zinc finger and BTB domain containing 14	1.46	3.00E-04
231866	Zfp12	zinc finger protein 12	1.46	4.00E-04
105841	Dennd3	DENN/MADD domain containing 3	1.45	0

Table 33 continued

14073	Faah	fatty acid amide hydrolase	1.45	0
76522	Lsm8	LSM8 homolog, U6 small nuclear RNA associated (S. cerevisiae)	1.45	0
67045	Riok2	RIO kinase 2 (yeast)	1.45	0
59009	Sh3rf1	SH3 domain containing ring finger 1	1.45	0
329584	Slc2a4rg-ps	Slc2a4 regulator, pseudogene	1.45	0
213773	Tbl3	transducin (beta)-like 3	1.45	1.00E-04
67226	Tmem19	transmembrane protein 19	1.45	8.00E-04
68327	Tsr3	TSR3 20S rRNA accumulation	1.45	1.00E-04
225049	Ttc7	tetratricopeptide repeat domain 7	1.45	0
218914	Wapal	wings apart-like homolog (Drosophila)	1.45	0
328801	Zfp414	zinc finger protein 414	1.45	7.00E-04
224691	Zfp472	zinc finger protein 472	1.45	0
77652	Zfp955a	zinc finger protein 955A	1.45	0

Table 34: Downregulated genes in inversin-depleted renal epithelial cells

Gene ID	Gene Symbol	Protein Name	Fold change/ NTC	*P*-value
105638	Dph3	diphthamine biosynthesis 3	-1.45	0
67456	Ergic2	ERGIC and golgi 2	-1.45	0
14391	Gabpb1	GA repeat binding protein, beta 1	-1.45	0
225887	Ndufs8	NADH dehydrogenase (ubiquinone) Fe-S protein 8	-1.45	2.00E-04
21679	Tead4	TEA domain family member 4	-1.45	0.0011
21898	Tlr4	toll-like receptor 4	-1.45	0
66058	Tmem176a	transmembrane protein 176A	-1.45	0
56224	Tspan5	tetraspanin 5	-1.45	0.0234
109711	Actn1	actinin, alpha 1	-1.46	0
12443	Ccnd1	cyclin D1	-1.46	0
13636	Efna1	ephrin A1	-1.46	0
14872	Gstt2	glutathione S-transferase, theta 2	-1.46	4.00E-04
15510	Hspd1	heat shock protein 1 (chaperonin)	-1.46	0
19139	Prps1	phosphoribosyl pyrophosphate synthetase 1	-1.46	0
226043	Cbwd1	COBW domain containing 1	-1.47	2.00E-04
211151	Churc1	churchill domain containing 1	-1.47	0
66573	Dzip1	DAZ interacting protein 1	-1.47	2.00E-04
20135	Rrm2	ribonucleotide reductase M2	-1.47	0.0077
229782	Slc35a3	solute carrier family 35 (UDP-N-acetylglucosamine (UDP-GlcNAc) transporter), member 3	-1.47	0
387524	Znrf2	zinc and ring finger 2	-1.47	0
50883	Chek2	checkpoint kinase 2	-1.48	1.00E-04
17951	Naip5	NLR family, apoptosis inhibitory protein 5	-1.48	0
244668	Sipa1l2	signal-induced proliferation-associated 1 like 2	-1.48	0.0178
66757	Adat2	adenosine deaminase, tRNA-specific 2	-1.49	0
26905	Eif2s3x	eukaryotic translation initiation factor 2, subunit 3, structural gene X-linked	-1.49	6.00E-04
69270	Gins1	GINS complex subunit 1 (Psf1 homolog)	-1.49	0.003
67441	Isoc2b	isochorismatase domain containing 2b	-1.49	0.0056
17304	Mfge8	milk fat globule-EGF factor 8 protein	-1.49	0
18472	Pafah1b1	platelet-activating factor acetylhydrolase, isoform 1b, subunit 1	-1.49	0
219189	Vwa8	von Willebrand factor A domain containing 8	-1.49	0.0033
320924	Ccbe1	collagen and calcium binding EGF domains 1	-1.5	1.00E-04
106143	Cggbp1	CGG triplet repeat binding protein 1	-1.5	1.00E-04
69605	Lnp	limb and neural patterns	-1.5	2.00E-04
68043	N6amt2	N-6 adenine-specific DNA methyltransferase 2 (putative)	-1.5	0
67916	Ppap2b	phosphatidic acid phosphatase type 2B	-1.5	0
57259	Tob2	transducer of ERBB2, 2	-1.5	0.0086
66622	Ubr7	ubiquitin protein ligase E3 component n-recognin 7 (putative)	-1.5	2.00E-04
66884	Appbp2	amyloid beta precursor protein (cytoplasmic tail) binding protein 2	-1.51	1.00E-04
70640	Dcp2	DCP2 decapping enzyme homolog (S. cerevisiae)	-1.51	0.008
16400	Itga3	integrin alpha 3	-1.51	0.0037

Table 34 continued

14489	Mtpn	Myotrophin	-1.51	0
17919	Myo5b	myosin VB	-1.51	0
66566	Ntpcr	nucleoside-triphosphatase, cancer-related	-1.51	0
70974	Pgm2l1	phosphoglucomutase 2-like 1	-1.51	0
225845	Pla2g16	phospholipase A2, group XVI	-1.51	0.0352
59069	Tpm3	tropomyosin 3, gamma	-1.51	0
20402	Zfp106	zinc finger protein 106	-1.51	0
11975	Atp6v0a1	ATPase, H+ transporting, lysosomal V0 subunit A1	-1.52	0
66121	Chchd1	coiled-coil-helix-coiled-coil-helix domain containing 1	-1.52	0
12848	Cops2	COP9 (constitutive photomorphogenic) homolog, subunit 2 (Arabidopsis thaliana)	-1.52	0
14423	Galnt1	UDP-N-acetyl-alpha-D-galactosamine:polypeptide N-acetylgalactosaminyltransferase 1	-1.52	1.00E-04
54426	Hgfac	hepatocyte growth factor activator	-1.52	0
15357	Hmgcr	3-hydroxy-3-methylglutaryl-Coenzyme A reductase	-1.52	0
56428	Mtch2	mitochondrial carrier homolog 2 (C. elegans)	-1.52	0.0089
17777	Mttp	microsomal triglyceride transfer protein	-1.52	0.0063
56309	Mycbp	c-myc binding protein	-1.52	0.0032
18187	Nrp2	neuropilin 2	-1.52	1.00E-04
109785	Pgm3	phosphoglucomutase 3	-1.52	1.00E-04
19712	Rest	RE1-silencing transcription factor	-1.52	0
319322	Sf3b2	splicing factor 3b, subunit 2	-1.52	0
236920	Stard8	START domain containing 8	-1.52	0
110208	Pgd	phosphogluconate dehydrogenase	-1.53	0.0044
13555	E2f1	E2F transcription factor 1	-1.54	0.0378
74386	Rmi1	RMI1, RecQ mediated genome instability 1, homolog (S. cerevisiae)	-1.54	0
20778	Scarb1	scavenger receptor class B, member 1	-1.54	0
15205	Hes1	hairy and enhancer of split 1 (Drosophila)	-1.55	0
20350	Sema3f	sema domain, immunoglobulin domain (Ig), short basic domain, secreted, (semaphorin) 3F	-1.55	3.00E-04
53413	Exoc7	exocyst complex component 7	-1.56	0
27418	Mkln1	muskelin 1, intracellular mediator containing kelch motifs	-1.56	0
68095	Ociad1	OCIA domain containing 1	-1.56	9.00E-04
224454	Zdhhc14	zinc finger, DHHC domain containing 14	-1.56	0
112407	Egln3	egl-9 family hypoxia-inducible factor 3	-1.57	0
17873	Gadd45b	growth arrest and DNA-damage-inducible 45 beta	-1.57	0
57342	Parva	parvin, alpha	-1.57	0.0141
67010	Rbm7	RNA binding motif protein 7	-1.57	0
209773	Dennd2a	DENN/MADD domain containing 2A	-1.58	0
66234	Msmo1	methylsterol monoxygenase 1	-1.58	0
72333	Palld	palladin, cytoskeletal associated protein	-1.58	0.0092
69178	Snx5	sorting nexin 5	-1.58	0
59025	Usp14	ubiquitin specific peptidase 14	-1.58	0
21452	Tcn2	transcobalamin 2	-1.58	6.00E-04
229900	Gbp7	guanylate binding protein 7	-1.59	0.0196

Table 34 continued

52014	Nus1	nuclear undecaprenyl pyrophosphate synthase 1 homolog (S. cerevisiae)	-1.59	0
76073	Pcgf5	polycomb group ring finger 5	-1.59	0
21752	Tert	telomerase reverse transcriptase	-1.59	0.0113
54343	Atf7ip	activating transcription factor 7 interacting protein	-1.6	0
18616	Peg3	paternally expressed 3	-1.6	2.00E-04
80890	Trim2	tripartite motif-containing 2	-1.6	0.0091
12448	Ccne2	cyclin E2	-1.61	0.0011
13433	Dnmt1	DNA methyltransferase (cytosine-5) 1	-1.61	0.0013
320878	Mis18bp1	MIS18 binding protein 1	-1.61	8.00E-04
18451	P4ha1	procollagen-proline, 2-oxoglutarate 4-dioxygenase (proline 4-hydroxylase), alpha 1 polypeptide	-1.61	0
64009	Syne1	spectrin repeat containing, nuclear envelope 1	-1.61	0
114606	Tle6	transducin-like enhancer of split 6, homolog of Drosophila E(spl)	-1.61	0.0039
80914	Uck2	uridine-cytidine kinase 2	-1.61	0
108000	Cenpf	centromere protein F	-1.62	0.0042
14569	Gdi2	guanosine diphosphate (GDP) dissociation inhibitor 2	-1.62	0
14873	Gsto1	glutathione S-transferase omega 1	-1.62	0
20973	Syngr2	synaptogyrin 2	-1.62	0
170938	Zfp617	zinc finger protein 617	-1.62	0
12331	Cap1	CAP, adenylate cyclase-associated protein 1 (yeast)	-1.63	0
12530	Cdc25a	cell division cycle 25A	-1.63	5.00E-04
13361	Dhfr	dihydrofolate reductase	-1.63	1.00E-04
207781	C2cd2	C2 calcium-dependent domain containing 2	-1.64	0.0198
108645	Mat2b	methionine adenosyltransferase II, beta	-1.64	0
17535	Mre11a	meiotic recombination 11 homolog A (S. cerevisiae)	-1.64	0
52615	Suz12	suppressor of zeste 12 homolog (Drosophila)	-1.64	0
13121	Cyp51	cytochrome P450, family 51	-1.65	0
16881	Lig1	ligase I, DNA, ATP-dependent	-1.65	0
14156	Fen1	flap structure specific endonuclease 1	-1.66	0
16151	Ikbkg	inhibitor of kappaB kinase gamma	-1.66	0.0023
57296	Psmd8	proteasome (prosome, macropain) 26S subunit, non-ATPase, 8	-1.66	0
17387	Mmp14	matrix metallopeptidase 14 (membrane-inserted)	-1.67	0
20439	Siah2	seven in absentia 2	-1.67	0.0018
20911	Stxbp2	syntaxin binding protein 2	-1.67	0
241525	Ypel4	yippee-like 4 (Drosophila)	-1.67	0.0067
54447	Asah2	N-acylsphingosine amidohydrolase 2	-1.68	0
52276	Cdca8	cell division cycle associated 8	-1.68	0.0066
237082	Nxt2	nuclear transport factor 2-like export factor 2	-1.68	0
12633	Cflar	CASP8 and FADD-like apoptosis regulator	-1.69	0
23881	G3bp2	GTPase activating protein (SH3 domain) binding protein 2	-1.69	0
14841	Gsg2	germ cell-specific gene 2	-1.69	0.0022
229317	Eif2a	eukaryotic translation initiation factor 2A	-1.7	0
234593	Ndrg4	N-myc downstream regulated gene 4	-1.7	0
114643	Oas1c	2'-5' oligoadenylate synthetase 1C	-1.7	0
20873	Plk4	polo-like kinase 4	-1.7	1.00E-04
67771	Arpc5	actin related protein 2/3 complex, subunit 5	-1.71	0

Table 34 continued

231999	Plekha8	pleckstrin homology domain containing, family A (phosphoinositide binding specific) member 8	-1.71	0.0024
64929	Scel	Sciellin	-1.71	0
56524	Mpp6	membrane protein, palmitoylated 6 (MAGUK p55 subfamily member 6)	-1.72	0
21335	Tacc3	transforming, acidic coiled-coil containing protein 3	-1.72	0.0058
66805	Tspan1	tetraspanin 1	-1.72	0
16835	Ldlr	low density lipoprotein receptor	-1.73	0
19272	Ptprk	protein tyrosine phosphatase, receptor type, K	-1.74	0
20133	Rrm1	ribonucleotide reductase M1	-1.74	1.00E-04
76044	Ncapg2	non-SMC condensin II complex, subunit G2	-1.75	5.00E-04
67963	Npc2	Niemann-Pick type C2	-1.75	0.0016
72065	Rap2c	RAP2C, member of RAS oncogene family	-1.75	0
108912	Cdca2	cell division cycle associated 2	-1.76	0.0097
58186	Rad18	RAD18 homolog (S. cerevisiae)	-1.76	2.00E-04
66309	Tmem128	transmembrane protein 128	-1.76	0
229841	Cenpe	centromere protein E	-1.77	0.0049
13116	Cyp46a1	cytochrome P450, family 46, subfamily a, polypeptide 1	-1.77	0.0204
26384	Gnpda1	glucosamine-6-phosphate deaminase 1	-1.77	0
17750	Mt2	metallothionein 2	-1.77	2.00E-04
107358	Tm9sf3	transmembrane 9 superfamily member 3	-1.77	0
74747	Ddit4	DNA-damage-inducible transcript 4	-1.78	0
68735	Mrps18c	mitochondrial ribosomal protein S18C	-1.78	0
94190	Ophn1	oligophrenin 1	-1.78	0
66395	Ahnak	AHNAK nucleoprotein (desmoyokin)	-1.79	0
236930	Ercc6l	excision repair cross-complementing rodent repair deficiency complementation group 6 like	-1.79	0.0017
53381	Prdx4	peroxiredoxin 4	-1.79	0
100678	Psph	phosphoserine phosphatase	-1.79	0
17436	Me1	malic enzyme 1, NADP(+)-dependent, cytosolic	-1.8	0
94219	Cnnm2	cyclin M2	-1.81	0
70355	Gprc5c	G protein-coupled receptor, family C, group 5, member C	-1.81	1.00E-04
71978	Ppp2r2a	protein phosphatase 2, regulatory subunit B, alpha	-1.81	0
12649	Chek1	checkpoint kinase 1	-1.82	1.00E-04
14200	Fhl2	four and a half LIM domains 2	-1.82	0
66387	Nudt8	nudix (nucleoside diphosphate linked moiety X)-type motif 8	-1.82	0
21384	Tbx15	T-box 15	-1.82	0.0013
66929	Asf1b	anti-silencing function 1B histone chaperone	-1.84	0.005
23834	Cdc6	cell division cycle 6	-1.84	5.00E-04
66197	Cks2	CDC28 protein kinase regulatory subunit 2	-1.84	0
69823	Fyttd1	forty-two-three domain containing 1	-1.84	0
15366	Hmmr	hyaluronan mediated motility receptor (RHAMM)	-1.84	0.026
404710	Iqgap3	IQ motif containing GTPase activating protein 3	-1.84	8.00E-04
53322	Nucb2	nucleobindin 2	-1.84	0
18974	Pole2	polymerase (DNA directed), epsilon 2 (p59 subunit)	-1.84	1.00E-04
70472	Atad2	ATPase family, AAA domain containing 2	-1.85	0

Table 34 continued

97484	Cog8	component of oligomeric golgi complex 8	-1.85	0.0262
224014	Fgd4	FYVE, RhoGEF and PH domain containing 4	-1.86	7.00E-04
56349	Net1	neuroepithelial cell transforming gene 1	-1.86	0
20878	Aurka	aurora kinase A	-1.87	0.0071
15945	Cxcl10	chemokine (C-X-C motif) ligand 10	-1.87	0.0111
13360	Dhcr7	7-dehydrocholesterol reductase	-1.87	0
15525	Hspa4	heat shock protein 4	-1.87	0
68332	Sdhaf1	succinate dehydrogenase complex assembly factor 1	-1.87	0
71703	Armcx3	armadillo repeat containing, X-linked 3	-1.88	0
18140	Uhrf1	ubiquitin-like, containing PHD and RING finger domains, 1	-1.88	0.004
192156	Mvd	mevalonate (diphospho) decarboxylase	-1.89	0
72584	Cul4b	cullin 4B	-1.9	0
101401	Adamts9	a disintegrin-like and metallopeptidase (reprolysin type) with thrombospondin type 1 motif, 9	-1.91	0
68631	Cryl1	crystallin, lambda 1	-1.91	0
67608	Narf	nuclear prelamin A recognition factor	-1.91	0
93732	Acox2	acyl-Coenzyme A oxidase 2, branched chain	-1.92	0
26886	Cenph	centromere protein H	-1.93	2.00E-04
80986	Ckap2	cytoskeleton associated protein 2	-1.93	0.0073
140486	Igf2bp1	insulin-like growth factor 2 mRNA binding protein 1	-1.93	1.00E-04
66442	Spc25	SPC25, NDC80 kinetochore complex component, homolog (S. cerevisiae)	-1.93	0.008
170459	Stard4	StAR-related lipid transfer (START) domain containing 4	-1.93	0
18186	Nrp1	neuropilin 1	-1.94	0
20460	Stil	Scl/Tal1 interrupting locus	-1.94	8.00E-04
100637	N4bp2l1	NEDD4 binding protein 2-like 1	-1.96	0
18611	Pea15a	phosphoprotein enriched in astrocytes 15A	-1.96	0
20855	Stc1	stanniocalcin 1	-1.96	3.00E-04
14793	Cdca3	cell division cycle associated 3	-1.97	0.0072
237436	Gas2l3	growth arrest-specific 2 like 3	-1.97	0.0073
15958	Ifit2	interferon-induced protein with tetratricopeptide repeats 2	-1.97	0
21938	Tnfrsf1b	tumor necrosis factor receptor superfamily, member 1b	-1.97	0
319554	Idi1	isopentenyl-diphosphate delta isomerase	-1.98	0
433904	Ociad2	OCIA domain containing 2	-1.98	0
18107	Nmt1	N-myristoyltransferase 1	-1.99	0
217325	Llgl2	lethal giant larvae homolog 2 (Drosophila)	-2.01	0
68209	Rnaseh2c	ribonuclease H2, subunit C	-2.02	0
20877	Aurkb	aurora kinase B	-2.03	0.0018
72391	Cdkn3	cyclin-dependent kinase inhibitor 3	-2.03	0.0167
58231	Stk4	serine/threonine kinase 4	-2.03	0
107568	Wwp1	WW domain containing E3 ubiquitin protein ligase 1	-2.03	0.0013
240641	Kif20b	kinesin family member 20B	-2.04	0
11306	Abcb7	ATP-binding cassette, sub-family B (MDR/TAP), member 7	-2.05	0
12367	Casp3	caspase 3	-2.06	0
12450	Ccng1	cyclin G1	-2.06	0

Table 34 continued

60530	Fignl1	fidgetin-like 1	-2.06	0
12534	Cdk1	cyclin-dependent kinase 1	-2.07	7.00E-04
272551	Gins2	GINS complex subunit 2 (Psf2 homolog)	-2.07	0.001
68014	Zwilch	zwilch kinetochore protein	-2.07	3.00E-04
22256	Ung	uracil DNA glycosylase	-2.08	0
231070	Insig1	insulin induced gene 1	-2.09	0
12189	Brca1	breast cancer 1	-2.1	0.0016
60411	Cenpk	centromere protein K	-2.11	2.00E-04
15901	Id1	inhibitor of DNA binding 1	-2.12	0
68298	Ncapd2	non-SMC condensin I complex, subunit D2	-2.12	5.00E-04
19361	Rad51	RAD51 homolog	-2.12	0
77630	Prdm8	PR domain containing 8	-2.15	0
20197	S100a3	S100 calcium binding protein A3	-2.15	0.007
14137	Fdft1	farnesyl diphosphate farnesyl transferase 1	-2.16	0
20198	S100a4	S100 calcium binding protein A4	-2.16	0.0097
11777	Ap3s1	adaptor-related protein complex 3, sigma 1 subunit	-2.17	0
17217	Mcm4	minichromosome maintenance deficient 4 homolog (S. cerevisiae)	-2.17	0
277414	Trp53i11	transformation related protein 53 inducible protein 11	-2.17	0
230145	Galnt12	UDP-N-acetyl-alpha-D-galactosamine:polypeptide N-acetylgalactosaminyltransferase 12	-2.18	0
18817	Plk1	polo-like kinase 1	-2.19	0.006
67196	Ube2t	ubiquitin-conjugating enzyme E2T (putative)	-2.19	3.00E-04
15201	Hells	helicase, lymphoid specific	-2.2	0
52076	Tmem38b	transmembrane protein 38B	-2.2	0
20893	Bhlhe40	basic helix-loop-helix family, member e40	-2.22	0
67177	Cdt1	chromatin licensing and DNA replication factor 1	-2.22	0
233406	Prc1	protein regulator of cytokinesis 1	-2.24	2.00E-04
51944	Knstrn	kinetochore-localized astrin/SPAG5 binding	-2.25	0.0028
74143	Opa1	optic atrophy 1	-2.25	0
52033	Pbk	PDZ binding kinase	-2.25	2.00E-04
67629	Spc24	SPC24, NDC80 kinetochore complex component, homolog (S. cerevisiae)	-2.27	0.0019
110920	Hspa13	heat shock protein 70 family, member 13	-2.29	0
21973	Top2a	topoisomerase (DNA) II alpha	-2.29	4.00E-04
73804	Kif2c	kinesin family member 2C	-2.31	0.0024
12442	Ccnb2	cyclin B2	-2.32	0.0026
20856	Stc2	stanniocalcin 2	-2.32	0.0066
110196	Fdps	farnesyl diphosphate synthetase	-2.33	0
20708	Serpinb6b	serine (or cysteine) peptidase inhibitor, clade B, member 6b	-2.33	0
73710	Tubb2b	tubulin, beta 2B class IIB	-2.33	0
224143	Poglut1	protein O-glucosyltransferase 1	-2.36	0
224116	Muc20	mucin 20	-2.37	0
76123	Gpsm2	G-protein signalling modulator 2 (AGS3-like, C. elegans)	-2.4	0.0283
16551	Kif11	kinesin family member 11	-2.4	0.0037
21814	Tgfbr3	transforming growth factor, beta receptor III	-2.44	0
227929	Cytip	cytohesin 1 interacting protein	-2.45	0

Table 34 continued

72415	Sgol1	shugoshin-like 1 (S. pombe)	-2.45	0.0057
11799	Birc5	baculoviral IAP repeat-containing 5	-2.46	0.0124
17279	Melk	maternal embryonic leucine zipper kinase	-2.47	0.0013
219114	Ska3	spindle and kinetochore associated complex subunit 3	-2.47	0.0182
56150	Mad2l1	MAD2 mitotic arrest deficient-like 1	-2.49	3.00E-04
52570	Ccdc69	coiled-coil domain containing 69	-2.51	0.0025
12615	Cenpa	centromere protein A	-2.54	0.0032
14866	Gstm5	glutathione S-transferase, mu 5	-2.54	0
18005	Nek2	NIMA (never in mitosis gene a)-related expressed kinase 2	-2.55	0.0078
54725	Cadm1	cell adhesion molecule 1	-2.56	0
208628	Kntc1	kinetochore associated 1	-2.61	1.00E-04
14677	Gnai1	guanine nucleotide binding protein (G protein), alpha inhibiting 1	-2.63	0
215387	Ncaph	non-SMC condensin I complex, subunit H	-2.63	5.00E-04
106347	Ildr1	immunoglobulin-like domain containing receptor 1	-2.67	1.00E-04
22418	Wnt5a	wingless-type MMTV integration site family, member 5A	-2.68	0
12428	Ccna2	cyclin A2	-2.7	0
16348	Invs	Inversin	-2.7	0
72107	Dscc1	defective in sister chromatid cohesion 1 homolog (S. cerevisiae)	-2.71	0
14182	Fgfr1	fibroblast growth factor receptor 1	-2.71	0
17829	Muc1	mucin 1, transmembrane	-2.72	0
70887	Dmrtc1a	DMRT-like family C1a	-2.76	0.0032
72119	Tpx2	TPX2, microtubule-associated protein homolog (Xenopus laevis)	-2.77	8.00E-04
69706	Lrr1	leucine rich repeat protein 1	-2.8	2.00E-04
17984	Ndn	Necdin	-2.8	0
56742	Psrc1	proline/serine-rich coiled-coil 1	-2.81	0
108907	Nusap1	nucleolar and spindle associated protein 1	-2.83	0.0012
192193	Edem1	ER degradation enhancer, mannosidase alpha-like 1	-2.84	0
54392	Ncapg	non-SMC condensin I complex, subunit G	-2.84	0.0137
241230	St8sia6	ST8 alpha-N-acetyl-neuraminide alpha-2,8-sialyltransferase 6	-2.85	0
17345	Mki67	antigen identified by monoclonal antibody Ki 67	-2.91	0.0173
94040	Clmn	Calmin	-2.92	0.0028
76843	Dtl	denticleless homolog (Drosophila)	-2.95	0
20750	Spp1	secreted phosphoprotein 1	-2.95	0
107995	Cdc20	cell division cycle 20	-2.97	0.0018
74107	Cep55	centrosomal protein 55	-2.99	6.00E-04
12728	Clcn5	chloride channel 5	-3.02	0
15953	Ifi47	interferon gamma inducible protein 47	-3.06	1.00E-04
66977	Nuf2	NUF2, NDC80 kinetochore complex component, homolog (S. cerevisiae)	-3.12	0.0232
26357	Abcg2	ATP-binding cassette, sub-family G (WHITE), member 2	-3.13	0
27384	Akr1c13	aldo-keto reductase family 1, member C13	-3.13	0
12236	Bub1b	budding uninhibited by benzimidazoles 1 homolog, beta (S. cerevisiae)	-3.13	0.0037
110033	Kif22	kinesin family member 22	-3.18	0.0013

Table 34 continued

12452	Ccng2	cyclin G2	-3.2	0
17215	Mcm3	minichromosome maintenance deficient 3 (S. cerevisiae)	-3.24	0
20617	Snca	synuclein, alpha	-3.33	0
17076	Ly75	lymphocyte antigen 75	-3.34	0
17218	Mcm5	minichromosome maintenance deficient 5, cell division cycle 46 (S. cerevisiae)	-3.41	0
16477	Junb	jun B proto-oncogene	-3.46	0
20419	Shcbp1	Shc SH2-domain binding protein 1	-3.49	1.00E-04
19274	Ptprm	protein tyrosine phosphatase, receptor type, M	-3.52	0
16420	Itgb6	integrin beta 6	-3.53	0
20349	Sema3e	sema domain, immunoglobulin domain (Ig), short basic domain, secreted, (semaphorin) 3E	-3.53	0
21987	Tpd52l1	tumor protein D52-like 1	-3.53	0
319468	Ppm1h	protein phosphatase 1H (PP2C domain containing)	-3.54	0.001
76400	Pbp2	phosphatidylethanolamine binding protein 2	-3.55	1.00E-04
67849	Cdca5	cell division cycle associated 5	-3.61	0
53416	Stk39	serine/threonine kinase 39	-3.61	0
12876	Cpe	carboxypeptidase E	-3.64	0
240638	Slc16a12	solute carrier family 16 (monocarboxylic acid transporters), member 12	-3.71	0
68612	Ube2c	ubiquitin-conjugating enzyme E2C	-3.8	0.0065
12235	Bub1	budding uninhibited by benzimidazoles 1 homolog (S. cerevisiae)	-3.93	0.005
353211	Prune2	prune homolog 2 (Drosophila)	-3.94	0
21853	Timeless	timeless circadian clock 1	-4.13	7.00E-04
235534	Pxylp1	2-phosphoxylose phosphatase 1	-4.21	0
71778	Klhl5	kelch-like 5	-4.32	0
76131	Depdc1a	DEP domain containing 1a	-4.53	0.0033
219228	Pcdh17	protocadherin 17	-4.63	0
19362	Rad51ap1	RAD51 associated protein 1	-4.79	0
210027	Slc35f3	solute carrier family 35, member F3	-4.83	0
21877	Tk1	thymidine kinase 1	-5.08	0.0045
21825	Thbs1	thrombospondin 1	-5.31	0
53614	Reck	reversion-inducing-cysteine-rich protein with kazal motifs	-5.51	0
70385	Spdl1	spindle apparatus coiled-coil protein 1	-5.78	0.0034
16574	Kif5c	kinesin family member 5C	-6.27	0
16007	Cyr61	cysteine rich protein 61	-6.39	0
18452	P4ha2	procollagen-proline, 2-oxoglutarate 4-dioxygenase (proline 4-hydroxylase), alpha II polypeptide	-9.91	1.00E-04
22634	Plagl1	pleiomorphic adenoma gene-like 1	-10.04	0
18973	Pole	polymerase (DNA directed), epsilon	-11.57	0
19876	Robo1	roundabout homolog 1 (Drosophila)	-22.63	0
18798	Plcb4	phospholipase C, beta 4	-32.41	0
16979	Lrrn1	leucine rich repeat protein 1, neuronal	-98.96	0

VITA

NALINI H. KULKARNI

EDUCATION:

Ph.D. Department of Biology, Purdue University, Indianapolis, IN., Graduation May 2017

Master of Science, Botany, Bharathiar University, India, Graduation, May 1989

Bachelor of Science, Biology and Chemistry, Osmania University, India, Graduation, May 1985

PROFESSIONAL EXPERIENCE:

2012 October-Present: Research Scientist, Biotechnology Discovery Research, Lilly Research Labs, Indianapolis, IN 46285

2006 June-2012 September: Associate Senior Biologist, Lilly Research Labs, Indianapolis, IN. Identification and application of bio-products (proteins and antibodies) for the treatment of musculoskeletal diseases, in particular, osteoporosis, osteoarthritis and cartilage repair.

2002 June-2006 June: Asst. Senior Biologist, Lilly Research Labs, Indianapolis, IN. Target identification and validation for osteoporosis and osteoarthritis, application and translation of genomic technologies to pre-clinical biomarker discovery and validation for bone/OA, drug mechanism of action.

1995 February-2002 May: Research Specialist, Dept. of Zoology, North Carolina State University, Raleigh, NC 27695. Molecular and biochemical aspects of olfaction.

1991 February-1994 October: Senior Research Assistant, Naylor Dana Institute, Valhalla, NY-10595: Development of molecular markers (biomarkers) for the early detection and chemoprevention of colon cancer in animal models. Detection of mutations in *ras* oncogenes, P^{53} tumor suppressor gene and also the expression of *ras* P^{21} and P^{53} proteins.

1989 August-1991 February: Research Assistant, Naylor Dana Institute, Valhalla, NY. Development of intermediate biomarkers for the early detection of colon cancer sponsored by National Cancer Institute.

PROFESSIONAL MEMBERSHIP:

2015-Present: Member of the American Physiological Society

2015-Present: Advisory committee representative for the Cell and Molecular Physiology Section Steering Committee (Junior Trainee), American Physiological Society

PUBLICATIONS

Kulkarni NH, Smith RC, Blazer-Yost BL (2017) Loss of inversin decreases transepithelial sodium transport in mouse renal cells. *AJP Cell Physiology* (under revision)

Kulkarni NH, Smith RC, Wei T, Blazer-Yost BL (2017) Pathway analyses of kidney transcriptome from *inv/inv* mice with polycystic kidney disease reveal altered cellular processes and sodium transport. In preparation

Kulkarni NH, Wei T, Han B, Schreiweis MA, Brune KA, Christopher TA, Wolos JA, Harvey A, Sterchi DL, Gitter BD, Chandrasekhar S, Martin TJ, Bryant HU, Ma YL, Mitchell P G, Hale JE, Onyia JE (2010) Tri-partite relationships between bone, cartilage and adipogenic changes contribute to bone loss. *J Bone and Res* 22: S1; S78

Gooi JH, Pompolo S, Karsdal SM, Kulkarni NH, McAhren SH, B Han B, Onyia JE, Ho PWM, Gillespie MT, Quinn JMW, Martin TJ, Sims NA (2010) Calcitonin attenuates the anabolic effect of PTH in young rats by rapid upregulation of sclerostin expression. *Bone 46 (6): 1486-97*

Kulkarni NH, Wei T, Zeng QQ, Helvering LM, Lin X, Lawrence F, Huang S, Hale L, Cole H W, Chambers MG, Lin C, Harvey A, Ma YL, Cain RL, Leigh-Oskins J, Carozza MA, McKinley DD, Hu T, Miles RR, Ryan TP, Onyia JE, Mitchell PG (2010) Analysis of early changes in the articular cartilage transcriptome reveals new pathways associated with joint degeneration in the rat meniscal tear model of osteoarthritis. *Osteoarthritis Cartilage 18(7): 992-1000*

Wei T, Geiser AG, Qian HR, Su C, Helvering LM, Kulkarni NH, Shou J, N'Cho M, Bryant HU, and Onyia JE (2007) DNA microarray data integration by ortholog gene analysis revealed potential molecular mechanisms of estrogen-dependent growth of human uterine fibroids. *BMC Womens Health 2; 7:5*

Kulkarni NH, Wei T, Kumar A, Dow E, Stewart T, Shou J, Ncho M, Halladay DL, Engler T, Martin TJ, Bryant HU, Ma YL, Liu M, Onyia JE (2007) Changes in osteoblast, chondrocyte, and adipocyte lineages mediate the bone anabolic actions of PTH and small molecule GSK-3 inhibitor. *J Cellular Biochem-102:1504-18*

Schreiweis M, Butler JP, Kulkarni NH, Kneirman MD, Higgs RE, Halladay DL, Onyia JE, Hale JE (2006) A proteomic analysis of adult rat bone reveals the presence of cartilage/chondrocyte markers: *J Cell Biochem*-101(2):466-476, 2007

Kulkarni NH, Onyia JE, Zeng QQ, Liu M., Halladay DL, Frolik CA, Engler T, Wei T, Kriauciunas A, Martin TJ, Sato M, Bryant HU, Ma YL (2006) An orally bioavailable GSK3α/β dual inhibitor increases markers of cellular differentiation *in vitro* and bone mass i*n vivo. J. Bone and Min. Res. 21: 910-920*

Shou J, Dotson C, Qian HR, We T, Lin C, Lawrence F, N'cho M, Kulkarni NH, Bull CM, Gelbert LM, Onyia JE (2005) An optimized blood cell profiling method for genomic biomarker discovery using high density microarray. *Biomarkers 10 (4): 310-20*

Kulkarni NH, Halladay DL, Miles RR, Frolik CA, Galvin RJS, Martin TJ, Gillespie MT, Onyia JE (2005) Effect of parathyroid hormone on Wnt signaling pathway in bone. *J. Cellular Biochem 95: 1178-1190*

Helvering LM, Liu R, Kulkarni NH, Wei T, Chen P, Huang S, Lawrence F, Halladay DL, Miles RR, Ambros EM, Sato M, Ma YL, Frolik CA, Dow ER, Bryant HU, Onyia JE (2005) Expression profiling of rat femur revealed suppression of bone formation gene by treatment with alendronate and estrogen but not raloxifene. *Molecular Pharmacology 68*: 1225-1238

Wei T, Liao B, Ackermann BL, Jolly RA, Eckstein JA, Kulkarni NH, Helvering LM, Goldstein KM, Shou J, Estrem S, Ryan TP, Colet JM, Thomas CE, Stevens JL, Onyia JE (2005) A data-driven analysis approach for biomarker discovery using molecular profiling technologies. *Biomarkers 10: 153-172*

Onyia JE, Helvering LM, Gelbert L, Wei T, Huang S, Chen P, Dow E, Maran A, Zhang M, Lotinun S, Lin X, Halladay DL, Miles RR, Kulkarni NH, Ambrose EM, Ma YL, Frolik CA, Sato M, Bryant HU, Turner RT (2005) Molecular profile of catabolic versus anabolic treatment regimens of parathyroid hormone (PTH) in rat bone: An analysis by DNA microarray. *J. Cellular Biochem 95: 403-418*

Anholt RRH, Dilda CA, Chang S, Fanara J, Kulkarni NH, Ganguly I, Rollmann SM, Kamdar KP, Mackay TFC (2003) The genetic architecture of odor-guided behavior in *Drosophila*: epistasis and transcriptome. *Nature Genetics 35: 180-184*

Kulkarni NH, Yamamoto A, Robinson KO, Mackay TFC, Anholt RRH (2002) The DSC1 sodium channel, encoded by the *smi60E* locus, contributes to odor-guided behavior in *Drosophila melanogaster*. *Genetics 161*: *1507-1516*

Anholt RRH, Fanara JJ, Fedorowicz GM, Ganguly I, Kulkarni NH, Mackay TFC Rollmann S (2001) Functional genomics of odor-guided behavior in *Drosophila melanogaster*. *Chem. Senses 26: 215-22*

Kulkarni NH, Karavanich CA, Atchley WR, Anholt RRH (2000) Characterization and differential expression of a human gene family of olfactomedin-related proteins. *Genet. Res. 76: 41-50*

Kulkarni NH, and Reddy BS (1994) Inhibitory effect of *Bifidobacterium longum* cultures on the azoxymethane-induced aberrant crypt foci formation and fecal β-glucuronidase. *Proc. Soc. Exper. Biol. Med., 207: 278-283*

Singh J, Rao CV, Kulkarni NH, Simi B, Reddy BS (1994) Molecular markers as intermediate end-points in chemoprevention of colon cancer: Modulation of *ras* activation by sulindac and phenyhexylisothiocyanate during colon carcinogenesis. *Int. J. Oncology, 5:1009-1018*

Singh J, Kulkarni NH, Kelloff G, Reddy BS (1994) Modulation of azoxymethane-induced mutational activation of *ras* protooncogenes by chemopreventive agents in colon. *Carcinogenesis, 15: 1317-1323*

Rao CV, Desai D, Simi B, Kulkarni NH, Amin S, Reddy BS (1993) Inhibitory effect of caffeic acid esters on axoxymethane-induced biochemical changes and aberrant crypt foci formation in rat colon. *Cancer Research, 53: 4182-4188*

Kulkarni NH, Zang E, Kelloff G, Reddy BS (1992) Effect of chemopreventive agents, piroxicam and D-L-α-difluromethylornithine on intermediate biomarkers of colon carcinogenesis. *Carcinogenesis, 13: 995-1000*

Reddy BS, Rivenson A, Kulkarni NH, Upadhyaya P, El-bayoumy K (1992) Chemoprevention of colon carcinogenesis by the synthetic organoselenium compound 1,4-phenylenebis(methylene) selenocyanate. *Cancer Research, 52: 5635-5640*

Reddy BS, Tokumo K, Kulkarni NH, Aliga C, Kelloff G (1992) Inhibition of colon carcinogenesis by prostaglandin synthesis inhibitors and related compounds. *Carcinogenesis, 13: 1019-1023*

PLATFORM TALKS:

Kulkarni NH (2016) Loss of inversin contributes to cystic renal disease through effects on ion transport. Lilly Research Labs, Grand Rounds Seminar, August 24, Indianapolis, IN

Kulkarni NH (2016) Renal Cystic Diseases: Pathway analyses of kidney transcriptome from *inv/inv* mice reveal altered cellular processes and decreased sodium transport. *11th International Congress Cell Volume Regulation and Fluid Homeostasis, August 15-18, Chicago, IL*

Kulkarni NH (2015) Inversin modulates transepithelial ion transport in renal epithelial cells. Biological Transport Meeting, June 21-24, Sponsored by *American Physiological Society* Lake Cumberland, KY

Kulkarni NH (2014) Renal Cystic Diseases: Current understanding of inversin in type II nephronophthisis. Biological Transport Meeting, June 8-10, Sponsored by *American Physiological Society,* Lake Cumberland, KY

Kulkarni NH (2007) Tri-partite relationships between bone, cartilage and adipogenic changes contribute to bone loss. *ASBMR September 16-19, 2007,* Honolulu, Hawaii

Kulkarni NH (2004) An orally bioavailable GSK3 α/β/ dual inhibitor increases markers of cellular differentiation *in vitro* and bone mass *in vivo. JBMR Vol 19 Suppl 1, S57 2004,* Seattle, WA

Kulkarni NH (2004) Gene expression profile separates different classes of bone therapies, the anabolics and antiresorptives and is associated with increase in bone mass. *The 33rd Annual Midwest Connective Tissue Workshop, Case Western University School of Medicine,* Sept 10-11 2004, Cleveland, OH

PRESENTATIONS AT PROFESSIONAL MEETINGS:

Kulkarni NH, Smith RC, Wei T, Blazer-Yost BL (2016) Pathway analyses of kidney transcriptome from *inv/inv* mice with polycystic kidney disease reveal altered cellular processes and sodium transport. *FASEB J. 30: 1224.26*

Kulkarni NH, Smith RC, Blazer-Yost BL (2015) Inversin modulates transepithelial ion transport in mouse renal cells. *FASEB J. 29:844.8*

Kulkarni NH, Patrick JS, Butler JP, Schreiweis M, Wei T, Higgs RE, Knierman MD, Gelfanova V, Halladay DL, Ganji G, Ma YL, Martin TJ, Bryant HU, Hale JE, Onyia JE (2006) Serum proteomics identify orosomucoid as a putative bone anabolic marker. *ASBMR September 15-19, Philadelphia, PA*

Wei T, Kulkarni NH, Zeng QQ, Helvering LM, Lin X, Lawrence F, Huang S, Cole HW, Chambers MG, Lin C, Harvey A, Ma YL, Cain RL, Leigh-Oskins J, Carozza MA, McKinley DD, Onyia JE, Mitchell PG (2006) Transcriptional profiling of articular cartilage from both a rat surgical model of osteoarthritis and from human osteoarthritic patients: potential involvement of cholesterol biosynthesis in the development of osteoarthritis. *ACR meeting, November 10-15, Washington, DC*

Kulkarni NH, Wei T, Schreiweis M, Brune K, Christopher T, Wolos J, Harvey A, Chandrasekhar S, Carozza M, Engler T, Martin TJ, Bryant HU, Ma YL, Mitchell PG, Hale JE, Onyia JE. (2006) Chondrogenic Markers are Expressed and Regulated in Bone and Correlate with Bone Mass. *Osteoarthritis Research Society International (OARSI) meeting Prague, Czech Republic*

Kulkarni NH, Wei T, Kumar A, Dow E, Stewart T, Shou J, Ncho M, Halladay DL, Engler T, Martin TJ, Bryant HU, Ma YL, Liu M, Onyia JE (2005) Changes in Osteoblast, Chondrocyte, and Adipocyte Lineages Mediate the Bone Anabolic Actions of PTH and Small Molecule GSK3 Inhibitor. (F437) *ASBMR, September 23-27, Nashville, TN*

Kulkarni NH, Gelbert L, Zhang M, Bemis K, Maran A, Lin X, Li Q, Mishra S, Halladay DL, Wei T, Chandrasekhar S, Frolik CA, Sato M, Helvering LM, Turner R, Dow E, Adams C, Lawrence F, Miles RR, Huang S, Chen P, Ma YL, Bryant HU, Onyia JE (2004) Gene expression profile identifies different classes of bone therapies: PTH, Alendronate and SERMs. *European Calcified Tissue Society meeting, Vol: 74, supp 1 2004, page 304 S124. Nice, France*

Kulkarni NH, Halladay DL, Miles RR, Frolik CA, Galvin RJS, Fuson TR, Martin TJ, Onyia JE (2003) Wnt signaling Pathway: A target for PTH action in bone and bone cells. *ASBMR meeting (F451) Plenary poster, Minneapolis, MN*

Anholt RRH, Dilda CA, Chang S, Fanara J, Kulkarni NH, Ganguly I, Rollmann SM, Kamdar KP, Mackay TFC (2003) The genetic architecture of odor-guided behavior in Drosophila. *Society of Neuroscience meeting, November 8-12, New Orleans, LA*

Kulkarni NH, Mackay TFC, Anholt RRH (2001) The DSC1 sodium channel, encoded by the smi60E locus, regulates olfactory sensitivity in *Drosophila melanogaster*. *42nd Annual Drosophila research conference (801C), March 21-25, Washington DC*

Anholt R, Kulkarni NH, Fedorowicz G, Ganguly I, Mackay TFC (2000) Functional genomics of odor-guided behavior. *Ann. meeting of the Assoc. for chemorecep. Sci. April 26-30, Sarasota FL*

Fedorowicz G, Kulkarni NH, Roote J, Ashburner M, Mackay T, Anholt RRH (1999) Disruption of the gene encoding a Dyrk2 homologue causes olfactory impairment in *Drosophila melanogaster*. *40th Annual Drosophila Research Conference, March 24-28, Bellevue, WA*

Kulkarni NH, Buczkowska G, Mackay TFC, Anholt R. R. H. (1997) Molecular cloning of *smell-impaired* genes that affect odor-guided behavior in *Drosophila melanogaster*. *International symposium on olfaction and taste XII and Achems XIX, San Diego, CA*

Kulkarni NH, Nuzhdin SV, Mackay TFC, Anholt RRH (1996) Characterization of *smell-impaired genes* of *Drosophila melanogaster*. *XVIII Ann. meeting of chemorecep. Sci. 156: 39, Sarasota FL*

Kulkarni NH, Mackay TFC, Anholt RRH (1996) Characterization of *smell-impaired* genes that affect odor-guided behavior in *Drosophila melanogaster.* A workshop conference focusing on the molecular biology of sensory systems and the adaptive response. *Sponsored by the U. S. Army Research Office*

Singh J, Kulkarni NH, Reddy BS (1994) Simple and sensitive one-step enriched PCR analysis of K-*ras* mutations as intermediate biomarkers in chemoprevention of colon cancer. *Proc. Am. Assoc. for cancer Res., 35: 3705*

Rao CV, Desai D, Simi B, Kulkarni NH, Amin S, Reddy BS (1993) Inhibitory effect of chemopreventive caffeic acid esters on modulation of azoxymethane-induced early events and aberrant crypt foci formation in rat colon. *Proc. Am. Assoc. for Cancer Res., 34: 986*

Singh J, Kulkarni NH, Reddy BS (1991) Effect of chemopreventive agents on intermediate biomarkers of colon carcinogenesis. *Proc. Am. Assoc. for Cancer Res., 32: 748*